

**STEADY-STATE ISOMETRIC CONTRACTILE
PROPERTIES OF CULTURED STRANDS OF
NEONATAL RATTUS NORVEGICUS (SPRAGUE-
DAWLEY STRAIN) CARDIAC MUSCLE**

CENTRE FOR NEWFOUNDLAND STUDIES

**TOTAL OF 10 PAGES ONLY
MAY BE XEROXED**

(Without Author's Permission)

ARUNACHALAM CHOCKALINGAM



STEADY-STATE ISOMETRIC
CONTRACTILE PROPERTIES OF CULTURED STRANDS OF
NEONATAL RATTUS NORVEGICUS
(SPRAGUE-DAWLEY STRAIN)
CARDIAC MUSCLE

BY



ARUNACHALAM CHOCKALINGAM, B.E., M.S.©

A THESIS SUBMITTED IN PARTIAL FULFILLMENT
OF THE REQUIREMENTS FOR THE DEGREE OF
DOCTOR OF PHILOSOPHY

FACULTY OF MEDICINE
MEMORIAL UNIVERSITY OF NEWFOUNDLAND
FALL, 1982

ST. JOHN'S, NEWFOUNDLAND

CANADA

ABSTRACT

Although the mechanical properties of cardiac muscle have been studied in various preparations, no direct measurement of isometric tension has been made at the cellular level. In this study, cultured strands of neonatal rat cardiac muscle were attached to a microgramme force transducer, using a non-traumatic method to obtain direct measurement of isometric tension.

The isometric mechanical properties of the cultured myocardial strands were studied during spontaneous and electrically-stimulated contractions at different lengths, temperatures and rates of stimulation. Steady-state inotropic and chronotropic responses to independent manipulation of external ionic concentration of K^+ , Ca^{++} and Na^+ as well as simultaneous manipulation of Na^+ and Ca^{++} were studied. Cholinergic and adrenergic receptor response was characterized using appropriate pharmacologic agonists and antagonists.

The basic mechanical properties observed included length-tension relationship, force-frequency response and effects of temperature. Total amount of strand stretch required to describe the complete length-tension relationship was only $\pm 1\%$ of the optimum length, L_{max} ;

suggesting that cultured strands are stiffer than adult rat papillary muscle. Repeating length-tension measurements in the same strand showed an absence of hysteresis. All other mechanical properties were similar to those observed for intact adult rat papillary muscle. Spontaneous contraction rate was influenced by K^+ and Na^+ , while Na^+ and Ca^{++} influenced contractility. The interaction between Na^+ and Ca^{++} was very striking; the observations were consistent with the function of a sodium-calcium exchange carrier. The strand was shown to possess cholinergic muscarinic receptors, which regulate only spontaneous rate and beta-adrenergic receptors which regulate both rate and contractility.

Thus, in the strand, functional properties of various regions of the heart are represented in a single preparation. The physiological characteristics were highly reproducible between and within strand preparations. Except for the fact that the strand is fragile and de-differentiated, it represents an accurate model for myocardial physiology and offers some important advantages for investigation of cellular physiology and the influence of ionic and drug manipulations on its basic physiology.

DEDICATION

In memory of my father
Mr. SP. Arunachalam Chettiar.
He was a victim of heart attack
in his early forties.

ACKNOWLEDGEMENTS

I express my deep sense of gratitude to my thesis advisors Dr. Michael Toll and Dr. Ted Hoekman for their long and patient help. I am grateful to Dr. Toll for being instrumental for the initiation of this project and providing me the opportunity to work on it. His continued valuable advice and critical comments formed a very useful part of my training. Dr. Hoekman has been a continuous source of insight and his help I found particularly congenial. I can never forget his readiness at all times to discuss problems and offer encouraging comments. I owe a very special intellectual debt to both of them.

My special thanks also go to Dr. Martin Tweeddale, member of my supervisory committee, who spent long hours in expanding my biological knowledge and read the manuscript with a critical eye. I am very grateful to him indeed for the criticisms and helpful suggestions.

My deepest debt, a debt I can never repay, I owe to Dr. Aldrich, Dean of Graduate studies, who made this all possible by his understanding and help. His continued support has been both an inspiring and indispensable element in my success.

My graduate studentship in the Faculty of Medicine became possible through the efforts of Dr. Aldrich and willingness of Dr. Cox, Dean of Medicine. I am grateful to both of them for their continued interest in my progress.

I recall my pleasant association with Dr. Graham Burke while he was at Memorial and the help he gave me in expanding my knowledge of cardiac physiology particularly tissue culturing.

Needless to say this work would not have been possible without the financial aid received which helped me to go through the graduate program. Fellowship support was generously provided by the Dean of Graduate Studies Memorial University and the Canadian Heart Foundation Traineeship Program. Supplementary financial aid was provided through Teaching Assistantship by the Faculty of Engineering and Research Assistantship from the grants of Drs. Toll, Hoekman, Tweeddale, Cox and Fodor. To all these people and the Canadian Heart Foundation I am specially grateful.

I express my warm appreciation to Medical Audio-Visual and ETV photography for the preparation of prints and photographs of my illustrations.

I acknowledge gratefully the help given by Mr. Nitin Joglekar and Ms. Rachel Roberts in proof reading this manuscript. I thank them for all their time and devotion given to the preparation of the manuscript. Finally, I express my thanks to my wife Shakuntala for the understanding and moral support she has shown during the course of my graduate study.

Portions of this thesis have been previously published:

Chockalingam, A., Toll, M.O. and Hoekman, T.B. 1980.
Characteristics of cultured strands. Proc. Can.
Fed. Biol. Soc. 23: 101.

Chockalingam, A., Toll, M.O. and Hoekman, T.B. 1980.
Length-tension and Force-frequency properties of
cultured heart muscle strands.
Physiologist 23: 118.

Toll, M.O. and Chockalingam, A. 1980. A new method of
measuring the isometric tension of cultured heart
muscle strands. Physiologist 23: 118.

Toll, M.O. and Chockalingam, A. 1981. Direct myocardial
measurements of cultured strands of cardiac muscle.
Presented at THE E.H. WOOD SYMPOSIUM, Mayo Clinic,
Rochester, MN. Aug 28-29, 1981.

TABLE OF CONTENTS

	Page
ABSTRACT	ii
DEDICATION	iv
ACKNOWLEDGEMENTS	v
TABLE OF CONTENTS	viii
LIST OF TABLES	xiv
LIST OF ILLUSTRATIONS	xv
LIST OF ABBREVIATIONS	xxii
I INTRODUCTION	1
1.1 MECHANICAL PROPERTIES OF THE HEART MUSCLE.....	3
1.1.1 Isometric Tension Development as a Function of Muscle Length.....	3
1.1.1.1 Length active-tension relation in terms of sarcomere lengths.....	7
1.1.2 Isometric Tension Development as a Function of Rate of Repetitive Contractions..	10
1.1.3 Spontaneous Contraction Frequency and Isometric Tension as a Function of Temperature.....	11
1.2 THE RESPONSE OF HEART MUSCLE TO IONIC MANIPULATIONS.....	13
1.3 EFFECT OF DRUGS ON MYOCARDIAL CONTRACTILITY.....	20
1.4 CULTURED HEART MUSCLE CELLS AS A MODEL OF MYOCARDIUM.....	23
1.5 PROBLEM AND ITS SIGNIFICANCE.....	31

	Page
II MATERIALS AND METHODS.....	34
2.1 CULTURE CHAMBER PREPARATION.....	35
2.2 CULTURED HEART MUSCLE STRAND - THE BIOLOGICAL PREPARATION.....	41
2.3 STRAND FORMATION.....	43
2.4 EXPERIMENTAL ENVIRONMENT.....	46
2.5 FORCE TRANSDUCER.....	47
2.6 TEMPERATURE CONTROL SYSTEM.....	48
2.7 ELECTRICAL STIMULATION.....	53
2.8 RECORDING ARRANGEMENT.....	56
2.9 PERFUSION FLUIDS.....	59
2.9.1 Standard Solution.....	59
2.9.2 SBSS With Varying Concentrations of Ions.....	59
2.9.3 Drug Solutions.....	61
2.10 PERFUSION SYSTEM.....	63
2.11 STRAND SUSPENSION.....	67
2.11.1 Suspension Apparatus.....	67
2.11.2 Strand Selection.....	71
2.11.3 Suspension Procedures.....	71

	Page
III RESULTS.....	78
3.1 STRAND DEVELOPMENT.....	79
3.2 EXCITABILITY OF THE STRAND - STRENGTH-DURATION RESPONSE.....	83
3.3 LENGTH-TENSION RELATIONSHIP.....	91
3.4 EFFECTS OF TEMPERATURE ON SPONTANEOUSLY CONTRACTING STRANDS.....	96
3.4.1 Relationship Between Temperature and Spontaneous Contraction Rate.....	96
3.4.2 Relationship Between Temperature and Isometric Tension.....	99
3.4.3 Relationship Between Temperature and Rate of Rise of Tension.....	99
3.4.4 Relationship Between Temperature and Time to Peak Tension.....	104
3.5 FORCE-FREQUENCY (FF) RESPONSE.....	104
3.5.1 Force-Frequency Relationship at Constant Temperature (25 °C) in Culture Medium.....	104
3.5.2 Force-Frequency Relationship at Different Temperatures in Culture Medium.....	105
3.6 FLUID EXCHANGE CHARACTERISTICS OF THE CULTURE CHAMBER.....	114
3.7 THE INFLUENCE OF EXTRACELLULAR POTASSIUM ION CONCENTRATION.....	115
3.7.1 The Relationship Between Potassium Concentration and Spontaneous Contraction Rate.....	115
3.7.2 Influence of $[K^+]_o$ Upon the Force-Frequency Response.....	119

	Page
3.8 INFLUENCE OF EXTRACELLULAR CALCIUM ION CONCENTRATION.....	122
3.8.1 Calcium Dose-Action Relationship.....	122
3.8.2 Isometric Responses at $[Ca^{++}]_o < 1.0 \times 10^{-6} M$	123
3.8.3 Influence of $[Ca^{++}]_o$ on the Force-Frequency Response.....	135
3.8.4 The Influence of Temperature on Calcium - Force-Frequency Response.....	138
3.9 INFLUENCE OF EXTRACELLULAR SODIUM ION CONCENTRATION.....	138
3.9.1 Influence of Varied $[Na^+]_o$ on the Rate and Strength of Spontaneous Contraction.....	141
3.9.2 Analysis for Possible Errors Introduced by Substitution of Choline for Sodium.....	144
3.9.3 Analysis of the Relationship Between $[Na^+]_o$ and Contractile Parameters.....	148
3.10 INFLUENCE OF SIMULTANEOUS MANIPULATION OF EXTRACELLULAR SODIUM AND CALCIUM UPON RATE AND STRENGTH OF CONTRACTION.....	153
3.11 PHARMACOLOGICAL RESPONSES.....	170
3.11.1 Drug Solutions.....	170
3.11.2 Effects of Acetylcholine.....	170
3.11.3 Effects of Atropine.....	178
3.11.4 Effects of Phenylephrine.....	178
3.11.5 Effects of Isoproterenol.....	179
3.11.6 Effects of Propranolol.....	184

	Page
IV DISCUSSION.....	185
4.1 CULTURED STRAND - BIOLOGICAL PREPARATION.....	186
4.1.1 Strand Morphology.....	186
4.1.2 Spontaneous Contraction Rate.....	189
4.1.2.1 Relationship with age.....	189
4.1.2.2 Effect of strand suspension.....	190
4.2 MECHANICAL PROPERTIES OF THE STRAND PREPARATION..	192
4.2.1 Length-Tension (LT) Relationship.....	192
4.2.1.1 Characteristics of the strands in the culture medium, during spontaneous contraction.....	192
4.2.1.2 Strand characteristics during electrical stimulation.....	198
4.2.1.3 Strand characteristics in the SBSS.....	200
4.2.2 Force-Frequency (FF) Relationship.....	201
4.2.3 Influence of Temperature.....	204
4.2.3.1 Effects of temperarure on spontaneously contracting strands.....	204
4.2.3.2 Effects of temperature on electrically stimulated strands.....	208
4.3 THE EFFECTS OF CATION MANIPULATION ON CONTRACTILITY.....	210
4.3.1 The Influence of Extracellular Potassium Concentration on the Contractile Responses...	211

	Page
4.3.2 The Influence of Extracellular Calcium Concentration on the Contractile Responses...	213
4.3.2.1 The relation between $[Ca^{++}]_o$ and the force-frequency relationship.....	224
4.3.3 The Influence of Extracellular Sodium Concentration on the Contractile Responses...	225
4.3.4 The Effects of Simultaneous Manipulations of $[Ca^{++}]_o$ and $[Na^+]_o$ on the Contractility of Cultured Strands.....	230
4.3.5 Characterization of Pharmacological Responses of the Myocardial Strand Preparation.....	234
4.3.5.1 Adrenergic receptor properties.....	234
4.3.5.2 Cholinergic receptor properties.....	239
4.3.6 The Interaction of K^+ , Na^+ , Ca^{++} Ions Regulation and Adrenergic and Cholinergic Receptors in Cultured Cardiac Muscle Strands...	241
V SUMMARY AND CONCLUSIONS.....	249
5.1 SUMMARY.....	250
5.2 CONCLUSIONS.....	254
BIBLIOGRAPHY	257
APPENDICES.....	283
I MYOCARDIAL TISSUE CULTURING TECHNIQUES.....	284
II THE MICROGRAMME FORCE TRANSDUCER.....	320
III CONSTANT CURRENT STIMULATOR.....	339
IV BACK-OFF AMPLIFIER AND DIFFERENTIATOR CIRCUITS...	342
V SOLUTION EXCHANGE CHARACTERISTICS OF THE PERFUSION SYSTEM.....	346

LIST OF TABLES

	Page
TABLE I Composition of Culture Medium and the Standard Balanced Salt Solution (SBSS).....	62
TABLE II Comparison of Length-Tension Relationship in Six Cultured Strands of Cardiac Muscle During Spontaneous and Electrically Driven Contractions.....	94
TABLE III Influence of Temperature on the Force-Frequency Relationship in Suspended Cultured Cardiac Muscle Strands.....	111
TABLE IV Contractile Parameters of Spontaneously Contracting Strands at Different Temperatures.....	206

LIST OF ILLUSTRATIONS

		Page
Fig. 2.1	Various stages in the preparation of the culture chamber used to grow cultured myocardial strand preparations.....	37
Fig. 2.2	A cross sectional view of the chamber showing the relative positions of glass microspheres and their mode of attachment on the palladium strips.....	40
Fig. 2.3	A schematic diagram of the inverted stage microscope and television (TV) projection system.....	45
Fig. 2.4	A line drawing showing mechanical components of the microgramme force transducer.....	50
Fig. 2.5	Two views of the heating unit used to regulate the temperature of the culture chamber.....	52
Fig. 2.6	A block diagram showing the relationship between the components used for electrical stimulation.....	55
Fig. 2.7	A silver/silver chloride (Ag/AgCl) electrode used for electrical stimulation of the suspended cultured myocardial strands.....	58
Fig. 2.8	A schematic diagram of the perfusion system used in this study, including the photo-detector utilized for flow calibration.....	66
Fig. 2.9	A diagram of the suction micropipette assembly used for suspension of strands....	70

	Page	
Fig. 2.10	Two stages in the preparation of a glass microtool, used to remove the strand from the palladium strip during strand suspension.....	70
Fig. 2.11	Diagrammatic representation of procedures followed in suspension of cultured cardiac muscle strands.....	73
Fig. 2.12	The overall experimental arrangement used in the study of contractility of the cultured myocardial strands.....	77
Fig. 3.1.	Gross morphological features of strand formation.....	81
Fig. 3.2	The relation between the strand age (in days) plotted versus spontaneous contraction rate (in contractions per minute).....	85
Fig. 3.3	Strength-duration curve obtained from spontaneously contracting myocardial strands under suspension.....	87
Fig. 3.4	Criteria used to select the optimal values for the stimulation of the strand preparation.....	90
Fig. 3.5	High speed tracings of isometric tension records obtained from a strand contracting spontaneously at different lengths.....	93
Fig. 3.6	The length-tension relationship obtained by combining data from spontaneously contracting cultured myocardial strands....	93

	Page
Fig. 3.7	The relationship between the spontaneous contraction rate and temperature before and after strand suspension..... 98
Fig. 3.8	A 3-dimensional plot relating Peak isometric tension, Rate of spontaneous contraction and Temperature..... 101
Fig. 3.9	Influence of temperature on the rate of rise of tension (+dP/dt) and time to peak tension obtained from six spontaneously contracting strands..... 103
Fig. 3.10	Force-Frequency relationship of the strands suspended in the culture medium..... 107
Fig. 3.11	Influence of temperature on the Force-Frequency relationship..... 109
Fig. 3.12	The relationship between the stimulus frequency required for peak isometric tension (f_F) and temperature..... 113
Fig. 3.13	The influence of extracellular potassium concentration, $[K^+]_o$, upon the rate of spontaneous contraction and isometric tension developed by the strand preparation..... 116
Fig. 3.14	The relationship between external potassium concentration, $[K^+]_o$, and the spontaneous contraction rate of cultured myocardial strands..... 118
Fig. 3.15	The influence of external potassium concentration, $[K^+]_o$, upon the force-frequency relationship..... 121

Fig. 3.16	The calcium dose-action relationship in spontaneously contracting cultured myocardial strands.....	125
Fig. 3.17	The relationship between maximal rate of rise of tension, (dP/dt), and external calcium concentration, $[Ca^{++}]_o$, in spontaneously contracting cultured cardiac muscle strands.....	127
Fig. 3.18	The relationship between isometric tension and time of exposure to low external calcium concentration (1.0×10^{-6} M) following transfer from varying high initial concentrations.....	129
Fig. 3.19	Representative records of isometric tension responses during calcium washout in a spontaneously contracting cultured myocardial strand.....	132
Fig. 3.20	The relationship between the time to reach zero tension upon exposure to 1.0×10^{-6} M $[Ca^{++}]_o$ and initial $[Ca^{++}]_o$	134
Fig. 3.21	The relationship between the time to reach steady-state isometric tension and $[Ca^{++}]_o$ in spontaneously contracting myocardial strands transferred from 1.0×10^{-6} M to a higher calcium concentration.....	134
Fig. 3.22	The influence of $[Ca^{++}]_o$ on the force-frequency relationship in cultured myocardial strands.....	137
Fig. 3.23	Influence of temperature upon the stimulus frequency required for maximal isometric tension (f_F) in cultured myocardial strands in culture medium and SBSS.....	140

Fig. 3.24	The influence of varying external sodium concentration, $[\text{Na}^+]_o$, upon the contractility of the cultured myocardial strands.....	143
Fig. 3.25	The influence of choline substitution for sodium on contractility of the cultured myocardial strands.....	147
Fig. 3.26	The relationship between external sodium concentration, $[\text{Na}^+]_o$, and steady-state isometric tension in spontaneously contracting cultured myocardial strands....	150
Fig. 3.27	The relation between external sodium concentration, $[\text{Na}^+]_o$, and maximal rate of contraction (dP/dt) in spontaneously contracting myocardial strands.....	152
Fig. 3.28	The relationship between time to peak tension and external sodium concentration, $[\text{Na}^+]_o$, in spontaneously contracting cultured cardiac muscle strands.....	155
Fig. 3.29	The relationship between spontaneous contraction rate (min^{-1}) and external sodium concentration, $[\text{Na}^+]_o$, in spontaneously contracting cultured cardiac muscle strands.....	157
Fig. 3.30	The influence of simultaneous manipulation of external sodium and calcium concentrations upon contraction rate and isometric tension in spontaneously contracting myocardial strands.....	160
Fig. 3.31	Comparison of the effects of exposure to low $[\text{Na}^+]_o$ in standard and zero $[\text{Ca}^{++}]_o$ upon isometric tension in spontaneously contracting cultured myocardial strands.....	163

Fig. 3.32	The influence of external calcium concentration, $[Ca^{++}]_o$, on steady-state and transient isometric tension responses during exposure to standard and low external sodium concentrations, $[Na^+]_o$	166
Fig. 3.33	The dose-action relationship between isometric tension and external calcium concentration, $[Ca^{++}]_o$, during exposure to standard and low sodium concentrations, $[Na^+]_o$	169
Fig. 3.34	The influence of acetylcholine (ACh) and atropine upon the rate of spontaneous contraction and contractility of cultured myocardial strands under suspension.....	173
Fig. 3.35	The dose-response relationship between spontaneous contraction rate and isometric tension and acetylcholine (ACh) concentration; interaction with atropine...	175
Fig. 3.36	The influence of ACh upon the force-frequency relationship in cultured cardiac muscle strands.....	177
Fig. 3.37	The influence of isoproterenol upon the contractility of cultured myocardial strands.....	181
Fig. 3.38	The influence of isoproterenol, ISO, upon rate and tension development in cultured cardiac muscle strands.....	183
Fig. 4.1	The relationship between calcium washout and isometric tension in cultured myocardial strands.....	220

Fig. 4.2 The contraction rate-corrected dose-isometric tension relationship in cultured myocardial strands responding to isoproterenol (ISO) and propranolol (prop). 238

Fig. 4.3 A schematic representation of possible mechanisms regulating the major ions involved in the contractility of cultured myocardial strands..... 243

LIST OF ABBREVIATIONS

ACh	:	Acetylcholine
Ag/AgCl	:	Silver/silver chloride
AP	:	Action potential
AT	:	Active tension
ATP	:	Adenosine triphosphate
ATPase	:	Adenosine triphosphatase
BSS	:	Balanced salt solution
cAMP	:	Cyclic adenosine monophosphate
Ca ⁺⁺	:	Calcium ion
dP/dt	:	Rate of rise of tension
FBS	:	Fetal bovine serum
FF	:	Force-frequency response
f _F	:	Stimulus frequency at which FF curve peaked
HCl	:	Hydrochloric acid
Hz	:	Herz, cycles per second
ISO	:	Isoproterenol
I _{Ca}	:	Slow inward calcium current
I _K	:	Potassium current
I _{Na}	:	Fast inward sodium current
I _{Rh}	:	Rheobase current
K ⁺	:	Potassium ion
LT	:	Length-tension relationship

L_0	:	Length at which neither resting nor active tension was present in the cardiac muscle preparation.
L_{max}	:	Length at which maximum AT occurred
M	:	Mole
MEM	:	Minimum essential medium
mM	:	millimole
mm	:	millimetre
ms	:	millisecond
mV	:	millivolt
min^{-1}	:	per minute
mM l^{-1}	:	millimoles per litre
N	:	Newton
Na^+	:	Sodium ion
Na-Ca	:	Sodium-calcium
NaCl	:	Sodium chloride
NaHCO_3	:	Sodium bicarbonate
O.D.	:	Outer diameter
P	:	Isometric tension or force
PEP	:	Phenylephrine
PLL	:	Phase-locked loop
pw	:	Pulse width
P_{FF}	:	Peak tension observed in the FF response
P_{max}	:	Peak isometric tension

P_{NCa}	:	Peak isometric tension observed in the calcium dose-response curve (at 5 mM $[\text{Ca}^{++}]_o$)
R	:	Spontaneous rate of contraction
RMP	:	Resting membrane potential
RT	:	Resting tension
SA node	:	Sinoatrial node
SBSS	:	Standard balanced salt solution
SD.	:	Standard deviation
SR	:	Sarcoplasmic reticulum
T	:	Temperature
t_e	:	Equilibration time
t_p	:	Time to peak tension
t_w	:	Wash-out time
μA	:	microamperes
μm	:	micrometre
μN	:	micro Newton
$[]_i$:	intracellular concentration of the ion concerned
$[]_o$:	extracellular concentration of the ion concerned

CHAPTER - I
INTRODUCTION

Ever since William Harvey discovered the role of the heart in blood circulation in 1628, understanding the intricacies of its function has been of major interest to physiologists. The present level of understanding of the myocardial function is made possible by the constant dedicated work of a large number of investigators in this field.

The heart is a complex arrangement of muscles, blood vessels and fibrous tissues designed to pump blood. This present investigation is focused on the contractility of cardiac muscle at the cellular level.

In order to summarize the current knowledge of the contractile properties of heart muscle, this chapter is divided into four major sections: (1) mechanical properties, (2) the response to ionic manipulations, (3) the effects of drugs on the contractility of myocardial muscle strips, and (4) a review of the properties of cultured (explanted) heart muscle cells.

1.1 MECHANICAL PROPERTIES OF THE HEART MUSCLE

Two different experimental conditions are commonly used to study contractility in isolated muscle strips: isometric or isotonic contraction. For isometric experiments the muscle length does not change; only internal shortening occurs. In isotonic experiments the muscle is allowed to shorten against a constant load. It is generally accepted that the mechanical properties of the muscle are represented by the active and passive forces that occur when the muscle is stimulated.

This investigation deals with a restricted aspect of this type of analysis; the isometric contractile properties of isolated heart muscle cells. The mechanical properties described here include: isometric tension development as a function of (1) muscle length; (2) rate of contraction; and (3) temperature.

1.1.1 Isometric Tension Development as a Function of Muscle Length

Ernest Starling introduced the concepts underlying his "law of the heart" in the Arris and Gale lecture (1897), and subsequently a wealth of information on the heart as a muscle and, in turn, as a pump was accumulated. Seventeen years later Starling and his colleagues presented

quantitative results obtained under controlled conditions (Patterson, Piper and Starling, 1914), which served as the basis for their definition of the law of the heart:

".....the mechanical energy set free on the passage from the resting to the contracting state depends on the length of the muscle fibers."

Over the next four decades, Starling's law remained controversial. The work of Sarnoff and Berglund (1954), constructing ventricular function curves in open chest anesthetized dogs, supported the Starling mechanism. Rushmer (1955) pointed out that cardiac responses predicted from Starling's law were not present in intact conscious dogs, since they were modified by neurogenic and circulatory reflex mechanisms.

However, explaining the physiology of the Starling mechanism in whole heart is cumbersome because of the complex geometry of the heart. In the nineteen-fifties, important mechanical properties of the skeletal muscle, such as the length-tension relationship (Abbott and Wilkie, 1953), were accurately defined. Using the approaches which had been successful in understanding skeletal muscle contractile physiology, Abbott and Mommaerts (1959) described the analogous behaviour for cat papillary muscle in vitro. These investigators showed qualitative similarities of the mechanical properties of cardiac muscle

(papillary muscle as well as trabeculae carneae) to those of skeletal muscle preparations. They also pointed out the significant differences between cardiac and skeletal muscle preparations. Both cardiac and skeletal muscles showed a similar pattern of tension responses (both having active and passive tension) with change in muscle length and a similar decrease in shortening velocity with increasing isotonic load. However, the relationship between active and passive forces was qualitatively different in cardiac muscle and the amount of active force generated by the cardiac muscle was significantly lower.

Ten years later, Sonnenblick and his co-workers repeated and expanded the experiments of Abbott and Mommaerts by comparing the length tension curves for a skeletal (frog sartorius) and a heart (cat papillary) muscle. The differences in tension development for these muscles, as described by Spiro and Sonnenblick (1964), are as follows:

In cardiac muscle, resting tension (RT) is present at all lengths above L_0 (the length at which active tension (AT) was almost zero) whereas in the skeletal muscle, resting tension is first observed in the neighbourhood of L_{max} (the length at which peak active tension occurred). In both muscles, active tension increases as the muscle is extended from L_0 to L_{max} and declines at lengths greater than L_{max} . These regions are referred to as the ascending

and descending limbs of the length-tension curves. The range of length-tension curves was reported to be $\pm 35\% L_{\max}$ in both types of muscles. When cardiac muscle is extended beyond L_{\max} , RT levels are greatly elevated (unlike skeletal muscle) while AT decreased markedly (Sonnenblick, Skelton, Spotnitz, and Feldman, 1973).

The magnitude of peak active tension developed by skeletal muscle was shown to be four times greater than that of cardiac muscle (0.235 N/mm^2 and 0.064 N/mm^2 respectively). This quantitative difference has been explained on the basis of the differing amounts of contractile proteins present in the two types of muscles (50% of cell mass in cardiac muscle Vs 90% in skeletal muscle) and the volume occupied by mitochondria (30% in cardiac muscle and negligible amount in skeletal muscle) (Fawcett and McNutt, 1969). In addition, it has been reported by Abbott (1971) that the papillary muscle has a spiral orientation, which may also affect the tension development.

The current understanding of the length-tension relationship in cardiac muscle was reviewed by Jewell (1977). A large body of evidence has shown that the active tension developed by the cardiac muscle is dependent upon the isometric length at the time of measurement.

In addition, the response to inotropic manipulation is also dependent upon the fiber length, a phenomenon Jewell has labelled as "length dependent activation".

1.1.1.1. Length active-tension relation in terms of sarcomere lengths

Both cardiac and skeletal muscles are striated. Thick and thin filaments overlap each other and the repeating band pattern is seen under electron microscopic (EM) studies (Spiro and Sonnenblick, 1964). The distance between two vertical dark dense lines, the Z-bands, is defined as one "sarcomere". In both types of muscles a change in length produces a change in the sarcomere band pattern and in the extent of overlapping between thick and thin filaments (Spiro and Sonnenblick, 1964).

A.F. Huxley and his coworkers (Gordon, Huxley and Julian, 1966) defined the relation between sarcomere length and isometric active tension in single frog skeletal muscle fiber using light microscopy techniques. Under normal conditions the length of the sarcomere is between 2.0 and 2.2 μm . If the sarcomere is either stretched beyond 2.2 μm , or shortened to produce a sarcomere length of less than 2.0 μm the developed tension falls. These changes in AT development were explained by the relative position of thick and thin filaments within the sarcomere, and their

cross-bridge formation. This relationship formed the basis of the "sliding filament" hypothesis (Huxley, 1965; Huxley, 1965a).

Similar electron microscopic sarcomere length-tension relationships have been shown in rat papillary muscle (Grimm, Katele, Kubota, and Whitehorn, 1970) and cat papillary muscle (Sonnenblick, Spiro, and Cottrell, 1963), using tissues fixed at known lengths according to the pre-determined length-tension curve. Pollack and Huntsman (1974) measured sarcomere lengths of very small papillary muscles in living rat hearts. They found the average length of the sarcomere in resting heart muscle to be about 2.2 μm .

Unlike skeletal muscle, shortening of cardiac muscle was not proportional to a similar shortening in its sarcomere lengths (Sonnenblick et al., 1963). In cardiac muscle no plateau of AT was observed and AT rather fell substantially with a 10% change in sarcomere length defining the sarcomere length-tension relationship over $\pm 10\%$ L_{max} (Sonnenblick and Skelton, 1974). It should be noted that there is a much smaller change in sarcomere length than in total muscle length over the range of the length-tension relationship. Similar values for sarcomere length changes were reported for rat papillary muscle

(Jewell, 1977) in a variety of preparations (skinned [membrane free] fibers, intact muscle and fibers fixed at different lengths).

Although the sarcomeres in skeletal and cardiac muscles are similar in structure, specialized differences exist which permit cardiac muscle to maintain length-dependent activation (Jewell, 1977) despite apparent optimal overlap of myofilaments (Sonnenblick and Skelton, 1974).

The cardiac sarcomeres resist overstretching; an extension of 20% L_{max} in muscle length produces only about 4-5% elongation in sarcomere length. Unlike skeletal muscle, reduction in tension in overstretched cardiac muscle can not be directly correlated with disengagement of the myofilaments (Braunwald, Ross and Sonnenblick, 1976). When cardiac muscle is stretched beyond the limits that can be tolerated by sarcomeres cellular damage occurs (Skelton, Spotnitz, Feldman, Serur, Mirsky and Sonnenblick, 1974).

Accordingly, (1) the stiffness of the passive elastic component does not permit diastolic sarcomere length to exceed 2.3 μm (about 5% L_{max}) and (2) the cardiac muscle is compliant enough so that the sarcomeres shorten during activation into that region of length-active tension curve (about -13% L_{max}) where the force falls as a function of sarcomere length during isometric contraction (Sonnenblick and Skelton, 1974).

1.1.2 Isometric Tension Development as a Function of Rate of Repetitive Contractions

Myocardial contractility is profoundly influenced by the rate of contraction. In isolated cardiac muscle preparations from a variety of species, tension has been shown to increase with increasing rate of contraction. For example, Bodem and Sonnenblick (1975) demonstrated a positive force-frequency relationship in rabbit and cat papillary muscles, at 30 °C, in the frequency range of 12-60 stimuli per minute. In 1902, Woodworth pointed out in whole heart preparations from dogs that tension magnitude decreases when the frequency of stimulation is increased beyond a certain level. This negative inotropic response seen at high frequencies of stimulation is often called the "Woodworth phenomenon".

In contrast with other mammalian species, even at relatively low frequencies (with respect to resting heart rate) rat heart muscle preparations show a prominent negative inotropic response with increasing rate of stimulation (Kelley and Hoffman, 1960; Benforado, 1958). Many investigators attributed this response to a lack of oxygen or glucose in the perfusing medium. However Langer and his co-workers (Blessa, Langer, Brady and Serena, 1970; Langer, 1978a) have shown that this peculiarity of rat

heart muscle is related to differences in the pattern of potassium ion movement during stimulation. In spite of these differences, the rats are widely used as experimental animals for the study of cardiac muscle because of their other positive aspects.

1.1.3 Spontaneous Contraction Frequency and Isometric Tension as a Function of Temperature

Temperature is an important parameter in studying the various physiological parameters of a muscle preparation. In general, cellular metabolic demands increase greatly with the body temperature; to meet these demands, the heart rate automatically increases. Temperature governs a number of physiological parameters. For example, ionic conductances and membrane potentials are functions of temperature. In the isolated heart, the rate of depolarization of the pacemaker potential is highly temperature dependant (Noble, 1979). Likewise, the increased spontaneous activity with temperature was demonstrated in isolated sheep Purkinje fibres (Weidman, 1956).

The effect of temperature on the contraction rate of mammalian (dog) heart was described by Martin (1883) and the effect on contractility by Langendorff and Nawrocki (1897). These investigators reported an increase in

contraction strength when cooled from 38 °C, attaining a maximum at 20 °C and then decreasing again with further lowering of temperature. Similar results have been reported since then by a number of investigators (Kruta, 1938; Blinks and Koch-weser, 1963; McLeod and Koch-weser, 1965; Kelly and Hoffman, 1960).

The strength of contraction in mammalian heart is also highly dependent upon the frequency of its spontaneous activity (Dale, 1930; Kruta, 1937; Rothberger and Sachs, 1938). The spontaneous frequency at which the maximal strength of contraction occurred was reported to be a function of temperature in guinea pig ventricle; maximum being at 20-22 °C (Kruta, 1938).

Thus the influence of temperature on myocardial contractility appears to consist of several components including changes on the physicommechanical properties of the myocardium as well as in the chemical reactions supplying energy for activation and relaxation of the contractile system (Sumbera, Kruta and Breveny, 1966). Changes in contractility may be a consequence of direct effects on the contractile proteins or related regulatory system, or may be caused by some secondary effects; e.g. in hypothermia, the content of Na^+ in the myocardium progressively decreases while that of K^+ increases (Spurr and Barlow, 1959), leading to an altered membrane

permeability, change in resting membrane potential and hence a change in rate of spontaneous activity.

The temperature dependence of biological processes is usually expressed by a parameter called Q_{10} , which is the ratio of the process concerned at two temperatures differing by 10°C (Prosser, 1973).

$$Q_{10} = (K_1 / K_2)$$

where K_1 and K_2 are the values of the variable at two different temperatures such that K_1 is 10°C above K_2 . If Q_{10} is greater than 1.0 the process is said to have a positive temperature coefficient while if Q_{10} is less than 1.0 the process has a negative temperature coefficient.

1.2 THE RESPONSE OF HEART MUSCLE TO IONIC MANIPULATIONS

In contrast to skeletal muscle cardiac muscle is highly dependent upon external calcium concentration, $[\text{Ca}^{++}]_o$ for tension development (Ringer 1883). However, in cardiac muscle electrical activity continues well after mechanical activity in the absence of $[\text{Ca}^{++}]_o$ (Locke and Rosenheim, 1907). The tension development in cardiac muscle is mediated by an excitation contraction coupling process with many similarities to that of skeletal muscle.

The cell membrane or sarcolemma of striated muscles (both skeletal and cardiac muscles) has a variety of functions. These include:

- (a) maintenance of intracellular ionic concentrations (high K^+ and low Na^+);
- (b) depolarization, with a rapid influx of Na^+ into the cell followed by an efflux of K^+ (and a slow but prolonged influx of Ca^{++} in cardiac muscle);
- (c) repolarization, during which the original resting state is recovered; and
- (d) propagation of this electrical event along the cell membrane.

The sarcolemma of cardiac muscle serves an important role in excluding $[Ca^{++}]_o$ from the resting cell when the intracellular calcium concentration, $[Ca^{++}]_i$, is very low and in actively extruding the Ca^{++} and Na^+ ions which enter the cell during the action potential (Schwartz, 1974).

A membrane potential arises due to the concentration gradient between intra- and extra-cellular ions, since the extracellular milieu is high in $[Na^+]$ and low in $[K^+]$ while the inside of the cell has a high $[K^+]$ and low $[Na^+]$. At rest the permeability to K^+ is high and that to Na^+ is low. Due to ionic concentration gradient the interior of the cell has a resting membrane potential (RMP) of -80 to -100 mV. This relationship is quantitatively described by the Goldman equation for electrochemical equilibrium.

Either pacemaker activity or electrical stimulation can initiate depolarization of the cell membrane. When this depolarization exceeds a critical level, known as the threshold level, the cell continues to depolarize spontaneously, to produce an action potential (AP) (which is quite different from that of a skeletal muscle).

During the action potential, a depolarizing current passes across the cell surface and penetrates the cell, presumably by way of the transverse tubular system. There are considerably fewer transverse tubules present in cardiac muscle than in skeletal muscle but they are larger in diameter and most likely have different electrical characteristics (Braunwald, Ross and Sonnenblick, 1967). Likewise cardiac muscle has less development of the sarcoplasmic reticulum (SR), an intracellular organelle which serves as a calcium depot, compared to skeletal muscle. In cardiac muscle the relationship between the transverse tubules and the SR is not so complex and well-defined as in skeletal muscle. When the action potential propagates along the cell, an influx of calcium as well as sodium leads to "activation" of the SR (Smith, 1966; Frossman and Girardier, 1970) and results in a graded release of free $[Ca^{++}]_i$ (Constantin and Taylor, 1973; Morad and Trautwein, 1968; Fabiato, Fabiato and Sonnenblick, 1971).

In general the wide variety of studies demonstrated that Na^+ , K^+ and Ca^{++} are the ions most critically involved in determining the electrical and contractile properties of cardiac muscle.

In cardiac muscle the alteration of extracellular K^+ can influence a variety of membrane properties (Noble, 1979; Katz, 1977); the mechanisms of these actions are not well understood. However, the simple and well understood action is its influence on the RMP. Increase in $[\text{K}^+]_o$ will cause a depolarized RMP (Noble, 1979) and hence will increase the spontaneous contraction rate. In addition, the repolarization of the cardiac AP is accelerated (Katz, 1977) and may have important consequences with respect to contractility.

External sodium influences both inotropic and chronotropic responses in cardiac muscle. Like potassium, changes in $[\text{Na}^+]_o$ directly alter the membrane potential (based on Goldman equation) and thus the rate of spontaneous contraction. The ratio of $[\text{Na}^+]_o$ to $[\text{Na}^+]_i$ also governs the rising phase or the upstroke and the duration of cardiac AP (Katz, 1977). With low $[\text{Na}^+]_o$, the rate of rise of AP is reduced, propagation velocity is reduced and the AP duration is increased. This permits larger amount of Ca^{++} to enter the cell. The effect of Ca^{++} on contractility and the influence of $[\text{Na}^+]_o$ on calcium exchange are discussed in the subsequent paragraphs.

The influence of $[Ca^{++}]_o$ is mainly inotropic. In skinned cardiac muscle a very low concentration of Ca^{++} (2.5×10^{-7} M), which is insufficient to activate the contractile materials in intact cardiac muscle, has been shown to trigger the release of a much larger amount of calcium from the SR (Fabiato et al., 1971). This free $[Ca^{++}]_i$ from the SR then activates the contractile system. This calcium-induced-calcium release has been termed "regenerative calcium release" (Ford and Podolsky, 1970; Fabiato et al., 1971). A similar mechanism does not seem to be present in the skeletal muscle under physiological conditions (Constantin and Taylor, 1973) probably because of its structural and functional differences. It is now clear that the major portion of free $[Ca^{++}]_i$ which activates cardiac muscle is stored inside the cell, presumably in the SR. In recent years, a number of investigators have shown evidence that mitochondria also act as a Ca^{++} storage site (Kubler and Shineborne, 1971; Scarpa and Graziotti, 1973; Lehninger, 1974). However, the mechanism of calcium handling by the mitochondria in heart muscle is still not clear.

The peak concentration of free calcium present during the contraction cycle is correlated with the influx of $[Ca^{++}]_o$ (this represents the synchrony with the triggered calcium mentioned earlier) which accompanies the AP (Morad and Goldman, 1973). The brief period of time during which

$[Ca^{++}]_i$ exceeds the threshold for activation of the contractile proteins is called the "active state" in cardiac muscle (Brady, 1968). This is analogous to that of skeletal muscle (Hill, 1949) but clearly is not identical. In cardiac muscle the calcium release and uptake mechanisms are quite different from those of skeletal muscle (Inesi, Ebashi and Watanabe, 1964; Inesi, 1973). Furthermore both duration and peak values of $[Ca^{++}]_i$ vary widely over the range of physiological conditions. Julian and Moss (1976) have suggested that some of the assumptions used in Hill's original definition of "active state" may not be valid and hence the term itself may not have the meaning initially intended. In addition, because of the important differences between skeletal and cardiac muscles there have been a longstanding recognition that active state in skeletal and cardiac muscles are not identical phenomena. The term "active state" has been chosen in this dissertation, despite its limitations, since no alternate term has been widely accepted which summarizes the excitation-contraction coupling events in cardiac muscle.

The calcium that entered the cell during the AP must exit through some energy dependent mechanism, since the concentration of Ca^{++} outside is greater than that inside. The involvement of sodium in cardiac calcium metabolism (the calcium-sodium exchange phenomenon) has been widely recognized (Luttgau and Niederggerke, 1958).

Katz (1975) has hypothesized that the calcium efflux coupled with sodium exchange mechanism involves a divalent negatively charged carrier (R^{2-}) which can bind either Na^+ or Ca^{++} inside or outside the sarcolemma. Accordingly, the concentration gradient for sodium across the sarcolemma acts as the driving force for calcium efflux. This passive inward sodium movement coupled with calcium efflux is in turn removed via the Na^+-K^+ coupled adenosine triphosphatase (ATPase), the "sodium pump" (Niedergerke, 1963).

The driving force of the Na^+ gradient allows the exchange carrier system to establish a calcium gradient described by the following equation:

$$\frac{[Ca^{++}]_i}{[Ca^{++}]_o} = \frac{[Na^+]_i^n}{[Na^+]_o^n}$$

In other words,
$$\frac{[Ca^{++}]_o}{[Na^+]_o^n} = \frac{[Ca^{++}]_i}{[Na^+]_i^n}$$

The number of sodium ions exchanged for each calcium ion remain a matter of controversy; some investigators feel that $n=2$ in the above equations (Katz, 1975; Langer 1977) while some feel that n is more than 2 (Horackova and Vassort, 1979a; Mullins, 1979).

When $[Ca^{++}]_o$ is held constant and $[Na^+]_o$ is reduced the carrier mediates an increased $[Ca^{++}]_i$. According to Katz's (1975) model, the initial effect of $[Na^+]_o$ reduction is to decrease the inward sodium movement and increase calcium influx. The level of $[Ca^{++}]_i$ increases until the sodium and calcium efflux matches the newly established influx values. Thus a new equilibrium is reached with an elevated $[Ca^{++}]_i$.

To summarize, the tension development by the cardiac contractile system, determined by the influx of $[Ca^{++}]_o$, is governed by: the extracellular $[Ca^{++}]$; the ratio $[Ca^{++}]_o / [Na^+]_o^n$ (Luttgau and Niedengerke, 1958; Horackova and Vassort, 1979a; Katz, 1975); and the amplitude and duration of the AP (Noble, 1974).

1.3 EFFECT OF DRUGS ON MYOCARDIAL CONTRACTILITY:

Various regions of the whole heart possess either cholinergic receptors (atria) or adrenergic receptors (ventricle) or both (Sino-Atrial node).

The possibility of neurohumoral transmission was first established unequivocally by the classic experiment of Otto Loewi in 1921. He demonstrated that the perfusion fluid collected from the perfused frog heart, during stimulation of parasympathetic (or vagal) nerves, contained a substance which he called "vagusstoff". When vagusstoff was

applied to a second perfused heart it imitated the effects of vagal stimulation (reduction in heart rate). Later, Loewi established the similarities between vagusstoff and acetylcholine (ACh) and also demonstrated that the vagal nerve endings contain ACh which was released during stimulation. The effect of ACh was shown to be at a "muscarinic" receptor since it was mimicked by muscarine and blocked by atropine.

Likewise, the stimulatory influence of the sympathetic nervous system on the heart was suggested by Langley as early as 1905. A year later, Dale (1906) described two types of adrenergic receptors which responded to the sympathetic neurotransmitter - excitatory and inhibitory. This dual adrenergic receptor concept was extended by Ahlquist (1948) when he studied the effects of six sympathetic stimulating drugs on a variety of adrenergic receptors. Two patterns were observed. The first pattern involved predominantly excitatory actions and phenylephrine was the most potent stimulant (Levy and Ahlquist, 1961). The second pattern involved primarily inhibitory actions but included cardiac stimulation of positive inotropic and chronotropic responses. In this case isoproterenol (or isoprenaline) was the most potent agonist. Based upon these differential effects two adrenergic receptor types were defined; alpha- and beta-receptors. At the beta-receptors isoproterenol was most active while adrenaline

and noradrenaline activate both alpha- and beta-receptors (adrenaline >> noradrenaline). Phenylephrine stimulates only alpha-receptors. Thus to identify the presence of adrenergic alpha- and beta- receptors in any preparation, phenylephrine and isoproterenol respectively are used as the classic test agents.

Both cholinergic (muscarinic) and adrenergic (both alpha and beta) receptors were reported to be present in whole-heart preparations from embryonic chick (McCarty, Lee, and Shideman, 1960) and neonatal mouse (Lane, Sastre, Law, and Salpeter, 1977) prior to innervation. During postnatal period, the cells of the heart differentiate, are innervated and receptors develop selectively in different regions of the heart (Friedman, 1972). Cultured cardiac myocytes prepared from either the embryonic chick (Ertel, Clarke, Chao, and Franke, 1971) or the neonatal mouse (Lane, et al., 1977) or rat (Ghanbari and McCarl, 1976), maintain the un-differentiated properties since they lack intrinsic nerve fibers (Jellinek, Sperelakis, Napolitano, and Cooper, 1968) and blood vessels, which appear to have an important trophic influence upon development.

1.4 CULTURED HEART MUSCLE CELLS AS A MODEL OF MYOCARDIUM

Development of simplified and reproducible methods for isolating and growing myocardial cells in culture made a marked revolution in understanding the physiology of the heart muscle and investigation of the mechanisms of action of many cardioactive drugs.

As early as 1910, Burrows initiated cell culture techniques by explanting fragments of chick hearts in clots of their own plasma. However, the first recorded maintenance of living myocardial cells appeared 20 years later (Goss, 1931) and was done using explants from rat embryos. Since then, many investigators have successfully isolated and grown myocardial cells from different species (e.g. chick embryos, Cavanaugh, 1955; new born rat, Harary and Farley, 1960; Kasten and Yip, 1974; and fetal mouse, Wildenthal, 1970). In the intervening period, tissue culture techniques were improved to produce a high yield of cultured myocardial cells (Cavanaugh, 1955; Kasten, 1971). Cultured cells in different forms have been prepared by various investigators; including single cell suspensions (Campbell, 1970; Goshima, 1973), monolayer cultures (Jongsma and van Rijn, 1972) and clustered cells in culture (Schanne, 1972; Schanne, Rivard and Doyon, 1975).

In the last decade attempts to isolate cell preparations from adult heart have had some success; these include preparations from frog (Tarr, Trank, Leiffer and Sheppard, 1979), rat (Brady, Tan and Ricchiuti, 1979) and mouse (Bloom, 1970). An excellent recent review by Schanne and Bkaily (1981) summarizes the state-of-the-art in cultured cardiac muscle cell preparations.

Explanted cells from various parts of the neonatal heart beat spontaneously (whole heart, Ghanbari and McCarl, 1976; Harary and Farley, 1960; atrial cells, Goshima, 1974; ventricular cells, Goshima, 1977). Such spontaneous activity is not found in normal ventricular cells in the intact heart of a newborn animal because the spontaneous rate in the atrial and conducting fibers are much higher and drive the ventricle at a rate that obscures any spontaneous activity within themselves. Spontaneous activity in explanted ventricular cells stems from a pacemaker potential which is not usually present under physiological conditions.

The basic morphology and the spontaneous beating activity of such cultured heart muscle cells are well documented (Harary and Farley, 1963; 1963a; Kasten, 1973). Harary and Farley observed that the rat heart cells in culture were dedifferentiated and appeared to have lost typical striations. However, spontaneous activity

persisted for up to 40 days. They also reported that when two isolated myocardial cells in culture came in contact, the spontaneous rate of contraction was determined by the faster cell. The spontaneous beating rate of cells or clusters increased non-linearly with temperature. Kasten (1973) reported that the yield of culture depends on the age of the rat used. He was able to culture beating heart cells from rats up to 10 days of age (similar to the experience of Harary and Farley, 1963) but the optimal age and highest yield was from 3-4 day old animals.

Ventricular cells in culture are not fully differentiated from the functional and morphological standpoint of view and are suitable for most experimental studies. The electrical properties such as resting membrane potential, action potential and maximum rate of depolarization have been studied by a number of investigators including a major contribution by Sperelakis and his associates using chick heart (Sperelakis, 1967; 1978; Sperelakis and Lehmkuhl, 1965; 1968; Sperelakis and Pappano, 1969; 1969a; Schanne et al., 1975). These investigators have shown that the electrical properties of the cultured cardiac cells resemble that of a normal intact myocardial cell preparation.

Indirect measurements of cultured cardiac cell contractility have been made using photoelectric methods for detecting cell movements (Boder, Harley and Johnson, 1971; Schanne, 1970; Okarma and Kalman, 1971; Thompson, Wilson, Schuette, Whitehouse and Nirenberg, 1973). Similar studies with small hearts in organ culture using a capacitance-sensitive method were reported (Wildenthal, Harrison, Templeton and Reardon, 1973). Although these methods reliably measure the rate of contraction, some workers (Wildenthal et al., 1973; Thompson et al., 1973) have used the rate of change of cell wall movement to provide an estimate of the unloaded velocity of contraction. Such interpretations do not provide accurate information about either force or velocity of contraction because of the complex geometry of the cells in culture. No direct measurements of force production in cultured cardiac cells have been reported. In single adult myocytes direct (Brady et al., 1979) and indirect (Tarr et al., 1979) measurements were made, but there were important limitations. Tarr and his colleagues evaluated only the resting tension while Brady's group measured unloaded active tension. In both cases the physiological condition of their cell preparations during measurement was questionable due to the nature of transducer attachment.

A large number of pharmacological studies have been carried out using cultured cardiac muscle cells (the type of preparation varies depending on the investigators). When the cultured cells were exposed to an appropriate concentration of isoproterenol, a sympathetic stimulant, the spontaneous beating activity was shown to increase (cultures derived from whole hearts of neonatal mice, Boder and Johnson, 1972; single and clustered mouse cardiocytes in culture, Lane et al., 1977). This response was similar to that of intact myocardium and was competitively blocked by propranolol, a beta-adrenergic blocking drug. While Lane et al. (1977) reported a stimulation of spontaneous beating rate by both phenylephrine and isoproterenol, suggesting the presence of both alpha- and beta-receptors, Ertel et al. (1971) could not elicit a response to phenylephrine in cultures derived from chick embryos.

In the presence of acetylcholine the beating rate decreased (cultures derived from whole heart of neonatal rats, Harary and Farley, 1960; ventricular chick embryo cells, Sperelakis and Pappano, 1969a; mouse myocytes, Lane et al., 1977) and was shown to be blocked by atropine. In adult tissues from a living animal cholinergic influence is not present, due to the cell differentiation. The presence of cholinergic response in cultured cells was attributed to the state of cell de-differentiation in vitro (Lane et al., 1977).

Even though the spontaneous activity of these cells in culture could be measured, they lacked a distinct striation pattern characteristic of cardiac muscle (Lieberman, Roggeveen, Purdy and Johnson, 1972). This prompted many investigators to consider developing techniques to produce a well-defined arrangement of cells in culture and several preparations resulted, including "threads" of contractile proteins (Crooks and Cooke, 1977). Using the principle of differential adhesion to an oriented substratum, two significant preparations were obtained. Halbert and associates (Halbert, Bruderer and Lin, 1971) cultivated myocardial cells on polystyrene sheets. Unfortunately, this technique produced non-homogeneous sheets of tissues with localised areas where spherical masses of cells were found. This did not lend itself easily to the study of directly measured contractile responses. In an ingenious way Lieberman et al. (1972) produced a thread-like preparation which they called "synthetic strands of cardiac muscle". Strands were formed by differential attachment of beating myocardial cells obtained from chick embryos to an oriented substratum (either a surface coated with collagen-agar or palladium metal strips on an agar surface). The ultrastructure of these strands shows an inner core of myocardial cells covered by an outer sheath of fibroblast-like cells (Purdy, Lieberman, Roggeveen and

Kirk, 1972). Well developed sarcomeres were seen under the electron microscope. This preparation is simple in geometry and free from nerves and blood vessels.

The electrical properties of this preparation have been recorded using microelectrode techniques. These include the transmembrane potential, propagated action potential (Lieberman, Kootsey, Johnson and Sawanobori, 1973) and cable properties of the cells in the strand (Lieberman, 1973). The passive electrical properties of the synthetic strands were shown to be similar to those of naturally occurring rabbit Purkinje fibers (Lieberman, Sawanobori, Kootsey and Johnson, 1975). Electrically these strands were reported to behave like a simple one-dimensional cable in which membrane impedance was described by a single resistor ($20.5 \times 10^3 \text{ ohms-cm}^2$) and a capacitor ($1.54 \mu\text{F-cm}^{-2}$) in parallel (Lieberman, 1973; Lieberman et al., 1975). The action potentials recorded from these strands, using microelectrode techniques, were shown to have the same configuration as those of adult mammalian Purkinje fibers and trabeculae carnea (Lieberman, Sawanobori, Shigeto and Johnson, 1975). These transmembrane potentials were rapidly abolished by tetrodotoxin (TTX), blocking the excitatory sodium current, in a manner similar to that observed in adult mammalian Purkinje fibers (Dudel, Peper, Rudel and Trautwein, 1967) and trabeculae carnea (Harrington and Johnson, 1973).

Although Lieberman and his associates characterized the electrical properties of this preparation very extensively, the mechanical properties have not been studied. Some attempts have been made to measure the contractile properties of the single adult myocytes (Tarr et al., 1979; Brady et al., 1979). But, there were severe limitations on their results caused by membrane damage which occurred when attached to the force transducer. It is not possible to directly measure the force generated by a single cell in culture because of its smaller size and the lack of space to provide an attachment site to a force transducer. The sensitivity of the force-transducers available is also a limiting factor. Lieberman's synthetic strands are suitable for measuring the isometric tension since they provide a uniform cylindrical mass of parallelly oriented cells, a pattern similar to that seen in isolated skeletal muscle preparation.

If the strand model is to be used to understand the cardiac physiology and the mechanisms of action of various cardioactive drugs, the preparation should be characterized for its mechanical properties and the influence of various extracellular ions. Its basic pharmacological properties should be assessed to see whether it is comparable (at least qualitatively, if not quantitatively) to that reported for intact isolated myocardial strips.

In the current research, cultured strands from newborn rat heart muscles were prepared in a manner similar to Lieberman's model, but with important modifications, so that the isometric tension could be measured directly. The isometric mechanical properties and the response of this preparation to various inotropic and chronotropic interventions including the classic neurotransmitters were characterized.

1.5 PROBLEM AND ITS SIGNIFICANCE

Although the mechanical properties of cardiac muscle have been studied in various preparations, (e.g. whole heart, Woodworth, 1902; isolated papillary muscle strips, Jewell, 1977; Toll, 1973), no direct measurement of isometric tension has been made for individual mammalian heart muscle cells.

The measurements reported for preparations such as papillary muscles or whole heart are modified by the presence of cell types other than myocytes and hence do not give direct evidence about myocardial cells. In an attempt to study the responses of myocardial cells alone, various investigators have used cardiac cells in culture (Boder et al., 1971; Schanne, 1970; Okarma and Kalman, 1971) or embryonic hearts in culture (Wildenthal et al, 1973).

The measurements reported for both cell and organ culture were indirect. With the cells changing in shape in three dimensions, it is very difficult to draw quantitative conclusions about the actual force generated (Toll, personal communication).

In this particular study, strands of cultured cardiac cells, prepared using a modification of Lieberman's techniques (Lieberman et al., 1972), were used to obtain direct measurements of isometric tension. Toll (1973) reported for cat papillary muscle, that diffusion limitation greatly complicates the analysis of inotropic responses to ionic manipulations. Because of the time required for concentration to equilibrate throughout the extracellular space after a solution change, the earliest response of the cell to the new concentration is not really observable in the papillary muscle preparation. Since the strand preparation is simple in geometry and very thin, diffusion limitations as discussed above should be reduced. Isometric tension produced by these strands was directly measured by a high sensitivity capacitance-type microgramme force transducer. A culture preparation technique was devised to provide a non-traumatic method of attachment to the force transducer.

The problems of cardiac muscle physiology outlined in this introduction provided the basic objectives of this study. They can be summarized as follows:

1) To measure the isometric tension produced in both spontaneously contracting and electrically stimulated cultured strands of cardiac muscle.

2) To characterize its isometric mechanical properties.

3) To observe steady-state inotropic and chronotropic response to manipulation of extracellular ionic concentrations.

4) To study the basic adrenergic and cholinergic pharmacological responses.

It is hoped that the results of these experiments will characterize the isometric steady-state contractile properties of the myocardial strand preparation and lay the groundwork for future examination of the underlying physiologic and pharmacologic mechanisms at the cellular level.

CHAPTER - II
MATERIALS AND METHODS

2.1 CULTURE CHAMBER PREPARATION

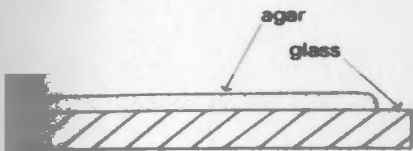
Myocardial cells were explanted and grown in a specially designed culture chamber to form thin strands. The different stages of culture chamber preparation are shown in Fig. 2.1.

A thin layer of 2% agar solution was spread over one side of a 45 X 50 mm, No. 1 glass coverslip (Fisher Scientific Co. Cat. #12-545H) and allowed to dry for 24 hours. Palladium lines (100 μ m wide and 10 mm long) were deposited over this using a mask and vacuum coating technique (Lieberman, et al., 1972). The cultured cells adhered differentially to a metallic substratum such as palladium (Carter, 1965) rather than to agar. As growth proceeds the cells form strands each of which overlies a narrow palladium line.

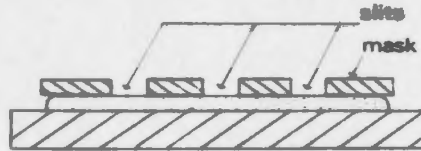
Fig. 2.1 Various stages in the preparation of the culture chamber used to grow cultured myocardial strand preparations.

(Figure, courtesy of Dr. M.O. Toll)

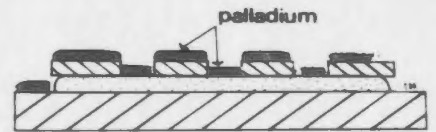
1 SPREAD THIN AGAR LAYER
OVER GLASS SUBSTRATE



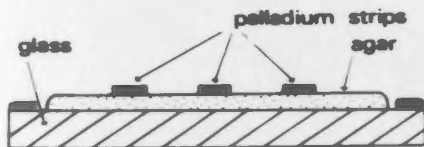
2 PLACE MASK WITH SLITS
OVER UNIT



3 DEPOSIT PALLADIUM METAL
OVER MASK USING
VACUUM COATING TECHNIQUES



4 REMOVE MASK LEAVING THIN
STRIPS OF PALLADIUM METAL
ON THE AGAR LAYER



5 COMPLETE HEART CELL
CULTURE CHAMBER



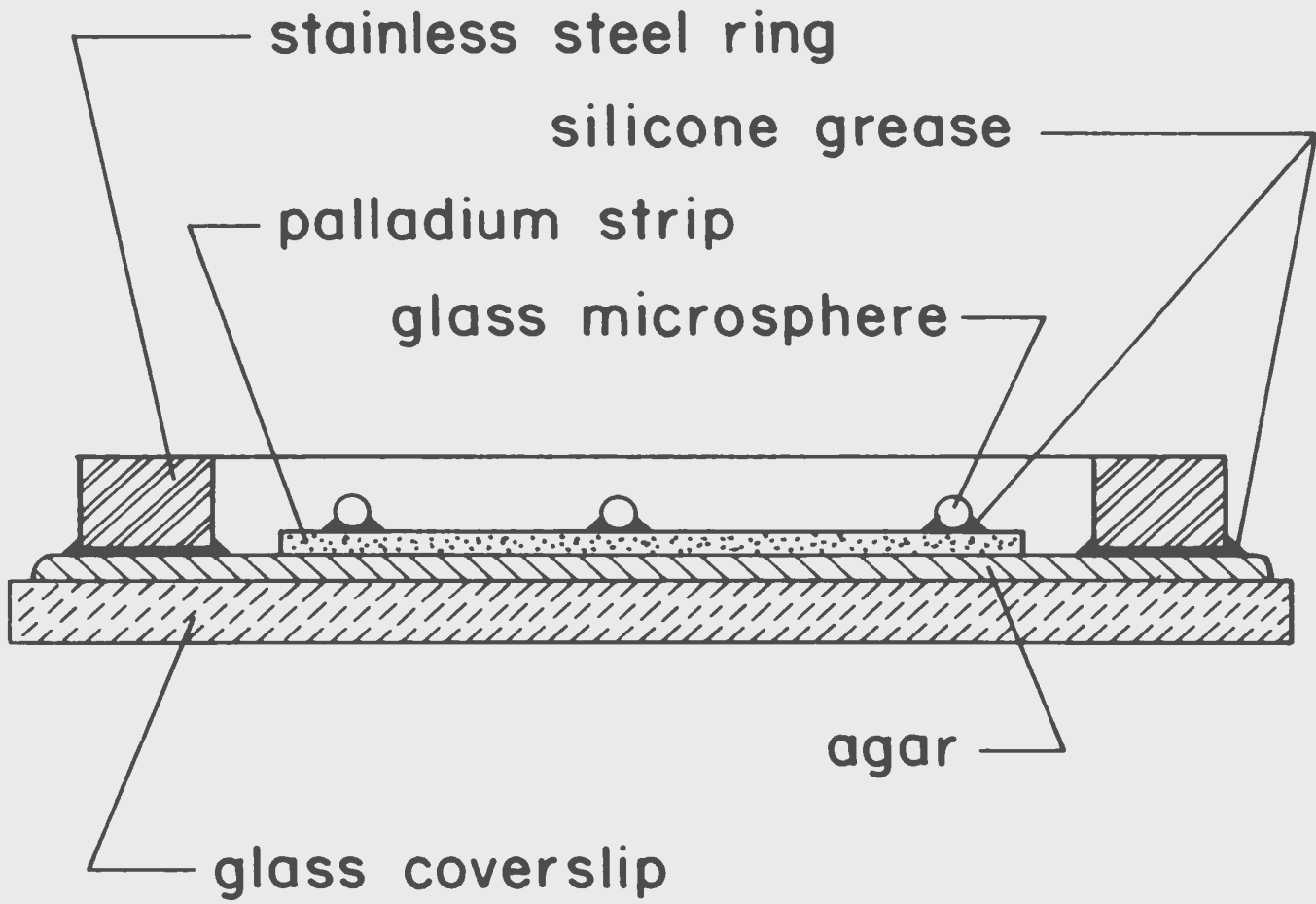
Since cultured cells also adhere to glass (Rappaport, Poole and Rappaport, 1960), 100 μm diameter glass microspheres were placed at intervals of approximately 3.5 mm apart along the length of the palladium lines. The microspheres act to terminate the strands and later serve as points of attachment to the force transducer. Microspheres were attached to the palladium lines with a minute amount of silicone grease, previously applied at the desired locations on the palladium strips. The technique of using microspheres was developed by Dr. M. O. Toll.

This specially prepared coverslip was sealed to the bottom of a 3 cm (outer diameter) stainless steel ring using a thin layer of silicone grease, thus forming the culture chamber. A cross-sectional view of the culture chamber showing the relative position of the microspheres is shown in Fig. 2.2.

A thin layer of silicone grease was applied to the top surface of the stainless steel ring which would serve as a sealing medium for a glass coverslip that covered the culture chamber. This assembly was then placed inside a plastic petridish and sealed with ethylene oxide sensitive tape. The petridishes were gas sterilised with ethylene oxide and allowed to remain in a ventilated area for 24-48 hours, before being used.

Fig. 2.2 A cross sectional view of the chamber showing the relative positions of glass microspheres and their mode of attachment on the palladium strips.

(Figure, courtesy of Dr. M.O. Toll)



When completed, each chamber contained seven palladium lines with 26 microspheres, allowing the potential development of 19 strands.

2.2 CULTURED HEART MUSCLE STRAND - THE BIOLOGICAL PREPARATION

The heart cell culture technique used was based on the method of Kasten (1972) as modified in our laboratory by G.H. Burke (private communication).

The ventricles from several 2-3 day old Sprague-Dawley rats were isolated under aseptic conditions, minced and disaggregated using multiple aliquots of a solution containing 25 mg of trypsin in 100 ml Hanks balanced salt solution (BSS) (Grand Island Biological Company (Gibco) product, Cat. # 310-4170) to which 2.5 ml HEPES buffer (Gibco product, Cat. # 845-1344) was added.

The cells were centrifuged at 100 X g for 5 minutes and resuspended in Eagle's minimum essential medium (MEM) (Gibco product, Cat. # 380-2370) supplemented with 10% fetal bovine serum (Flow Laboratories, Cat. # 29-101-54) and 1% PENSTREP (Gibco product, Cat. # 600-5740; equivalent to 60 $\mu\text{g ml}^{-1}$ penicillin G and 100 $\mu\text{g ml}^{-1}$ streptomycin sulphate). This resuspension procedure was repeated twice

more. The concentrations of major ions in the modified MEM were (mM l^{-1}): Na^+ , 136; K^+ , 6.5; Cl^- , 130; Ca^{++} , 1.48; and Mg^{++} , 0.83. p^{H} was 7.3.

After centrifugation and washing with MEM, the heart cells were poured into a culture flask (Fisher Scientific, Cat. # 10-126-1A) and incubated at $37\text{ }^{\circ}\text{C}$ for 90 minutes. This purifying step allowed fibroblasts and other cells to adhere to the surface of the flask, leaving the myocardial cells in suspension. This suspension of myocardial cells was poured off and a sample counted in a hemacytometer after addition of "trypan blue" dye. After counting the suspension was adjusted by dilution to a concentration of 1.5×10^5 cells ml^{-1} . Approximately 3 ml aliquots of this cell suspension were delivered into each culture chamber, covered by a glass coverslip and incubated at $37\text{ }^{\circ}\text{C}$ (complete details of the procedure of myocardial cell culturing are given in Appendix I).

After the first 24 hours of incubation, each culture chamber was examined under a microscope to ensure viability and the medium was changed. This procedure was then repeated every 48 hours.

2.3 STRAND FORMATION

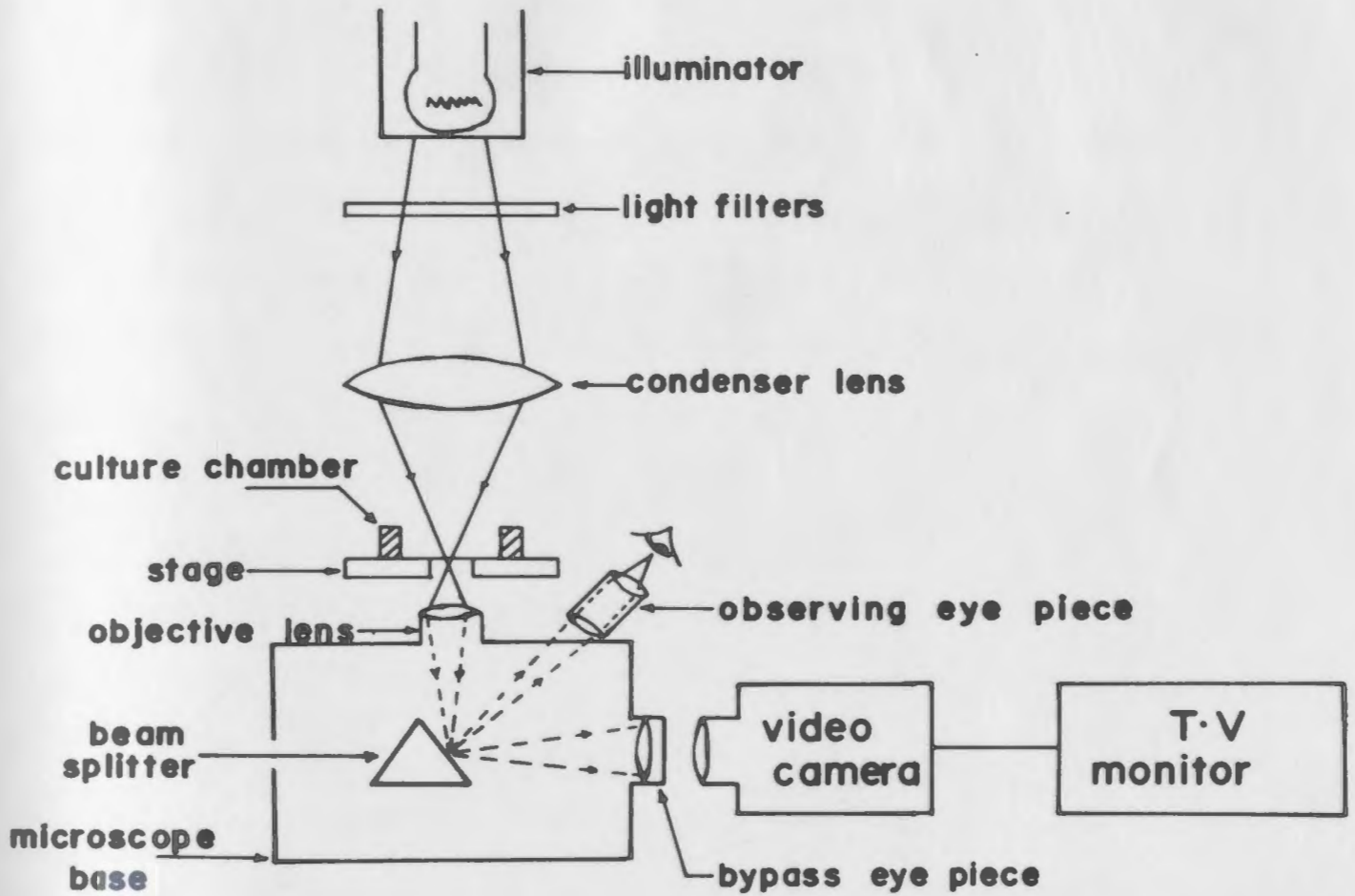
The strand development was monitored under a Nikon-M inverted microscope. The image was also projected on a television monitor using a Hitachi TV camera (model - HV 25B) attached to the bypass optical system of the microscope, as shown in Fig. 2.3. During microscopic observations, appropriate optical filters were placed between the light source and the culture chamber to eliminate the component wavelengths which produce heat and other lethal effects on the myocardial cells (Burke, private communication). A calibrated transparent grid-overlay, the same size as the TV monitor screen, was used in measurement of the myocardial strands. At 400X magnification, the width of the 30 cm TV screen was equal to 0.4 mm.

The strands were identified individually and were visualized on days 1, 2, 4, 6, 8, 10, 12 and 16. By use of the television monitoring apparatus, the distances between the microspheres and the portion of the distance between adjacent microspheres occupied by viable myocardial cells were measured.

Also on these days, the spontaneous beating rate of these strands was measured for a five minute period using a mechanical counter and a stop watch. From this the rate per minute was calculated.

Fig. 2.3 A schematic diagram of the inverted stage microscope and television (TV) projection system.

A television monitoring arrangement was used with the Nikon inverted light microscope to observe the strand formation on a day to day basis. The image of the sample on the microscope stage was magnified by the objective lens and split into two beams by a beam splitter. One beam was directed to the regular observing eyepiece while the other was directed to a by-pass eyepiece coupled to a television camera. Thus the preparation could be simultaneously observed directly through the microscope optics and on a television monitor.



2.4 EXPERIMENTAL ENVIRONMENT

In order to measure the microgramme forces generated by the cultured heart muscle strands a very sensitive force transducer was required. At this very high sensitivity, the output of the transducer could be affected by small mechanical vibrations, electrical noise and temperature fluctuations. All these problems were minimized by designing an isolated experimental environment.

A thick rubber tubing (2 cm outer diameter, 1 cm inner diameter and 65 cm in length) was spaced in a "zig-zag" arrangement on a sturdy table top with a dimension of 125 X 55 cm. A massive steel plate (123 kg; 125 X 75 X 1.25 cm in dimension) rested on top of the tubing. The mass of the steel plate and the cushioning effects of the rubber tubings effectively isolated the force transducer from the ambient vibrations which could affect its performance.

The experimental surface created by the steel plate was enclosed in a wooden frame (120 X 75 X 75 cm) lined with copper screening and 2.5 cm of expanded polystyrene. The copper screen and metal base were grounded. The inside of the box was illuminated by two incandescent lamps.

It was noted early in the project that power line voltage fluctuations interfered with experiments conducted during the day. To reduce such fluctuation effects,

subsequent experiments were carried out only in the late evening hours. (A suitable AC voltage regulator should minimize the line voltage fluctuations and permit experiments to be conducted at any time.)

2.5 FORCE TRANSDUCER

A microgramme force transducer (Toll, 1979a), consisting of a variable parallel plate capacitor and a phase-locked loop (PLL) circuit, was used to measure the force generated by the cultured cardiac strands. One capacitance plate was attached to a cantilever beam and the other was fastened to a fixed support.

The cantilever beam was made from a section of thin-walled hypodermic stainless steel tubing (24 gauge, type 304) and a glass micropipette (20 λ Yankee Disposable Micropet), of lengths 5.0 cm and 3.8 cm respectively with a 1.0 cm overlap. The tip of the glass micropipette was reduced to a diameter of about 60 μm using a micropipette puller and thermal polishing techniques (see Section 2.11.1). Suction was applied to this tip, through the transducer assembly and the composite beam.

The transducer assembly was mounted on a 'Prior' (code 22) micromanipulator which has a capability of precise movement in all three planes.

Over the desired range of operation (0-18,000 μg), there was a linear relationship between applied force and the output voltage. The electrical and mechanical specifications of the transducer were as follows:

force sensitivity	:	0.021	mv/ μg
displacement sensitivity	:	30.00	mv/ μm
compliance	:	0.0007	$\mu\text{m}/\mu\text{g}$
damping ratio	:	0.085	
resonant frequency	:	120	Hz

An overall view of this transducer is shown in Fig. 2.4 and its technical details (construction and calibration) are given in Appendix-II.

2.6 TEMPERATURE CONTROL SYSTEM

A specially designed temperature control system (Toll, 1979) was used to maintain the strands at constant temperature during experiments. The culture chamber was fitted into the circular opening in the heating unit, as shown in Fig. 2.5, which has the capacity for both simultaneous cooling and heating inputs. A constant flow of ice water was circulated continuously in tubular channel. The heating coil temperature within the assembly was regulated by a control system responding to a thermistor which monitored the temperature of the medium inside the culture chamber.

Fig. 2.4 A line drawing showing mechanical components of the microgramme force transducer.

This figure illustrates the physical arrangement of the parallel capacitor plates: one is fixed to the body of the transducer and the other is attached to a cantilever beam (a composite structure made of stainless steel and glass tubings) with a drop of molten wax. The capacitance plates were vacuum coated with aluminium and the connection to the phase-locked loop (PLL) circuit made by attaching wires to the plates with a drop of silver paint. The suction line is attached to the suction inlet which has a lumen continuous with a passage to the tip of the transducer's glass tube. The tip diameter of the glass tube was about 60 μm .

(Figure, courtesy of Dr. M.O. Toll)

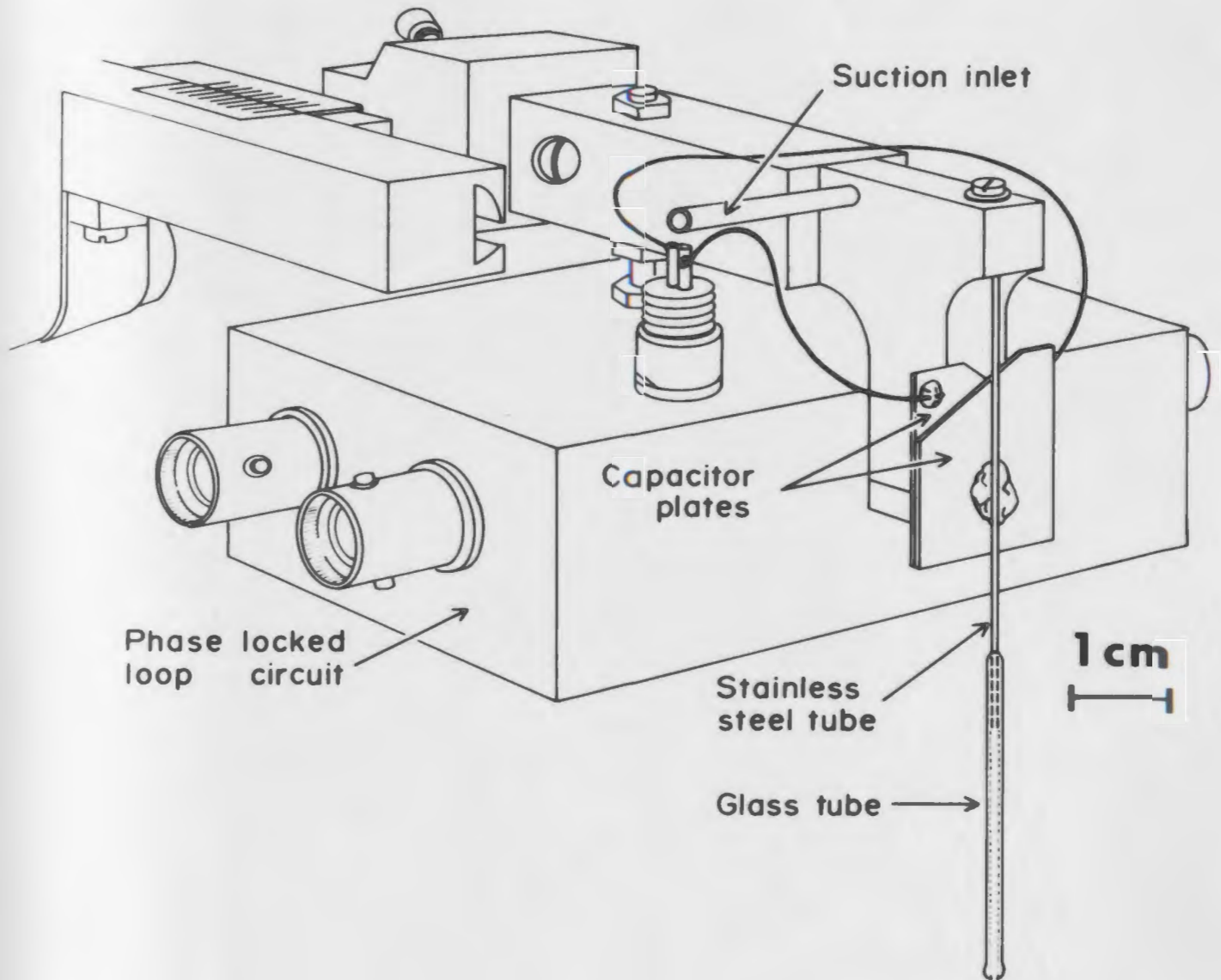
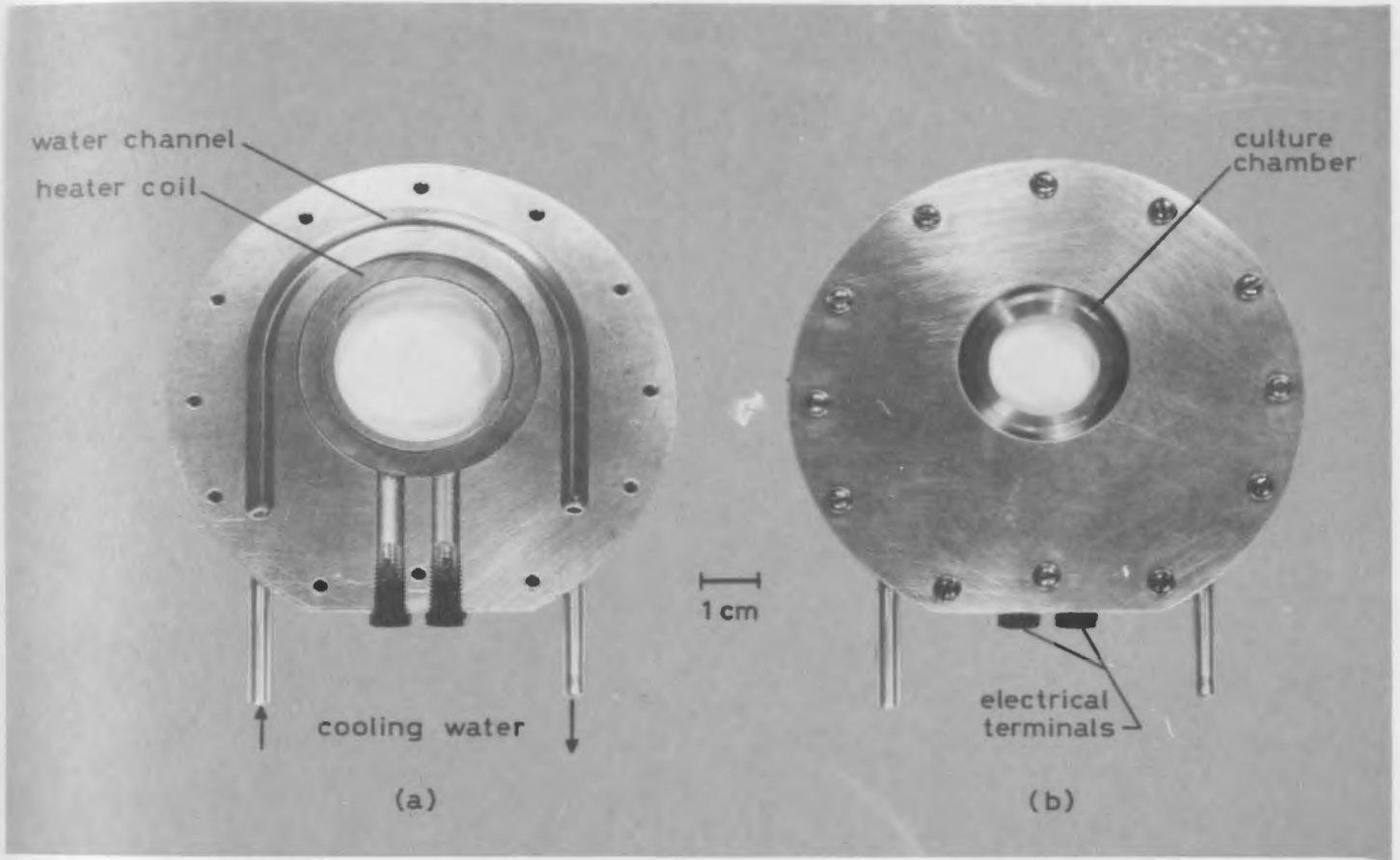


Fig. 2.5 Two views of the heating unit used to regulate the temperature of of the culture chamber.

(a) The top cover plate has been removed to show the cooling water channel and the heater coil arrangement.

(b) The assembled heater unit with a culture chamber in place.

(Photograph, courtesy of Dr. M. O. Toll)



The thermistor in the bath measured the temperature, which was compared to the set temperature in the control system, and the current to the heating coil was regulated accordingly.

Three experiments were carried out at 40 °C, but the strands were not viable at this higher temperature. Therefore experiments were limited to 37 °C and below. Because of design limitations of the system the lower temperature limit was 15 °C.

2.7 ELECTRICAL STIMULATION

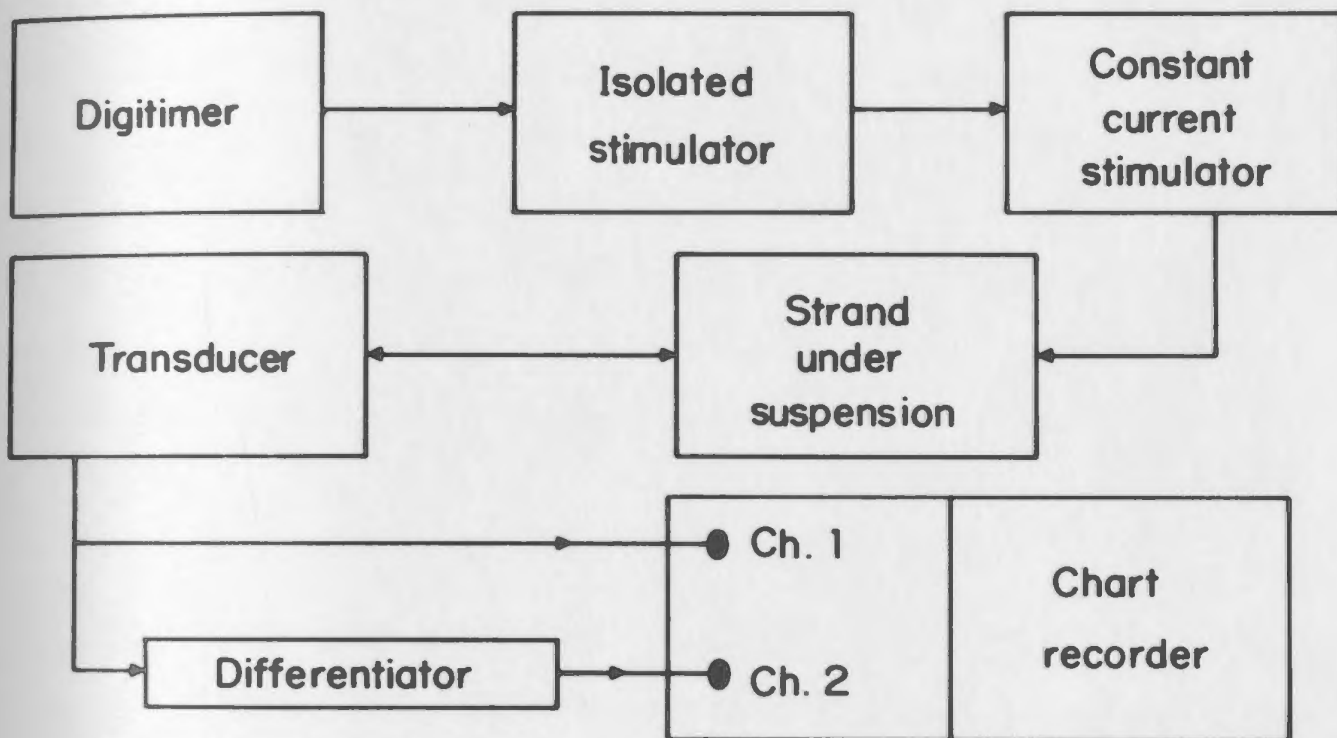
The general arrangement for electrical stimulation is shown in Fig. 2.6. The rate of stimulation was set by a Digitimer (Digitimer Limited, Model D4030); pulse width and amplitude were set by an isolated stimulator (Digitimer Limited, type 2533) with output pulses passed through a constant current stimulator (circuit shown in Appendix-III) to deliver constant-current rectangular pulses.

These pulses were applied to the strand by means of a Ag/AgCl electrode. This was made from a 0.254 mm diameter silver wire chlorided 5-8 mm from the tip. Some 1-2 mm of the tip was exposed, while the rest of the wire was tightly covered by a Teflon tubing of appropriate diameter. The other end of the silver wire was connected to a coaxial

Fig. 2.6 A block diagram showing the relationship between the components used for electrical stimulation.

The Digitimer set the rate of stimulation, while the isolated stimulator provided the rectangular pulses of different durations (ms) and intensities (Volts). These signals were passed through a constant current stimulator in which the voltage signal was transformed into a current signal (μA) with the same time course. Stimuli were applied to the suspended strand through an Ag/AgCl active electrode and a platinum return electrode placed on either side of the strand. Tension developed by the strand (P) was measured by the transducer and recorded on one channel of the chart recorder while its differential (dP/dt) was recorded on the other channel.

Ch1 and Ch2 refer to the channels 1 and 2 of the chart recorder.



cable. This arrangement was placed in a glass pipette. The diagrammatic representation of this electrode assembly is shown in Fig. 2.7.

Using a 'Prior' micromanipulator (code 20), the electrode was lowered into the culture chamber. The tip of the stimulating electrode was placed to one side of the strand under suspension, midway along its length and about 5 mm away from the strand. On the other side of the strand, a platinum wire of 0.254 mm diameter and 10 mm length was placed parallel to the length of the strand, 5 mm away from the strand. This served as the return electrode.

2.8 RECORDING ARRANGEMENT

The force sensitivity of the transducer was 0.021 mv/ μ g (see Section 2.5). In order to obtain an output of 1 mv/ μ g, a suitable amplifier circuit was developed (Appendix IV).

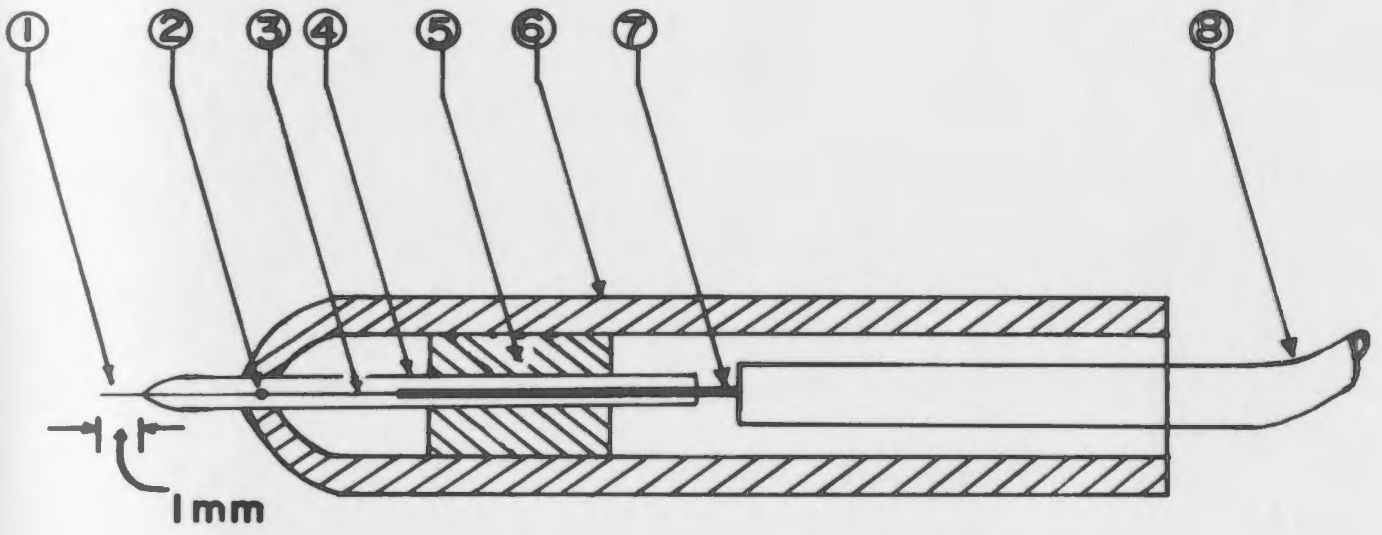
The amplified transducer output (P) and its differentiated form (dP/dt) were recorded with a 2-channel thermal stylus recorder (Hewlett-Packard HP-7702B) with paper speeds varying from 50 mm/sec to 2.5 mm/min. The gain sensitivity range was from 1 mV/div to 1000 mV/div.

Fig. 2.7 A silver/silver chloride (Ag/AgCl) electrode used for electrical stimulation of the suspended cultured myocardial strands.

The components of this electrode assembly are:

1. Ag/AgCl electrode tip.
2. Soldered joint between electrode wire and coaxial cable.
3. Bare center conductor.
4. 1.5 mm diameter glass micropipette.
5. Plastic heat shrink tubing to keep the micropipette in place.
6. 4.5 mm (O.D.) glass tubing with 1.0 mm wall thickness.
7. Insulated center conductor.
8. Shielded cable.

(diagram not to scale)



Each channel was calibrated initially with rectangular pulses of known amplitude. Once the gain and position settings were adjusted, they were left undisturbed until the end of the experiment.

2.9 PERFUSION FLUIDS

2.9.1 Standard Solution

The modified MEM in which the strands were grown contained fetal bovine serum (FBS). The presence of FBS made it difficult to selectively manipulate any one ion in the extracellular fluid. To overcome this problem, a standard balanced salt solution (SBSS) having the same pH and concentrations of major ions as those present in the culture medium was prepared, based on the methods of Hermsmeyer and Robinson (1977). The strands were viable in the SBSS for at least 24 hr and continued to contract spontaneously as they did in the culture medium.

2.9.2 SBSS With Varying Concentrations of Ions

The concentrations of extracellular calcium, potassium and sodium were manipulated by varying the concentration of a single ion at a time while maintaining the others at control concentrations. Extracellular calcium

concentration, $[Ca^{++}]_o$, was varied from 1.0×10^{-6} M to 5.0×10^{-2} M; extracellular potassium concentration, $[K^+]_o$, from 1 to 10 mM and that of sodium, $[Na^+]_o$, from 146.5 down to 40 mM.

The osmolarity of the SBSS was not disturbed when the concentration of calcium or potassium was altered in these ranges, hence no compensation was made when either of these ions were manipulated. To maintain the osmolarity, when $[Na^+]_o$ was lowered from the standard, 146.5 mM, an equimolar concentration of choline (choline chloride) was added to the solution to replace the sodium chloride. As a rule the sum of Na^+ and choline was kept equal to 146.5 mM. The pH of SBSS was adjusted with 0.1N HCl to match that of the usual culture medium (7.3).

The SBSS with a $[Ca^{++}]_o$ of 1.0×10^{-6} M and below was prepared using a calcium-EGTA (Ethylene Glycol-bis [B-amino ethyl ether] N,N'-Tetra Acetic acid, Sigma Chemical Co., Cat. # E-4378) buffer, adopting the methods described by Jewell and Reugg (1966). Calcium concentrations from 2.5×10^{-4} to 5.0×10^{-3} M were prepared by adding calcium chloride solutions of appropriate concentrations directly to the SBSS, at room temperature without additional buffers. For calcium chloride solutions of 1.0×10^{-2} M or

above, the calcium-free SBSS was heated gently over a Bunsen burner and a solution containing appropriate concentration of calcium chloride was added. The mixture was constantly stirred to avoid problems of precipitation. The pH was monitored during mixing. The concentration of the major ions present in the SBSS and in the culture medium were checked by chemical analysis using standard procedures. Table-I compares various ions present in both the culture medium and SBSS.

2.9.3 Drug Solutions

Various concentrations of acetylcholine (ACh), isoproterenol (ISO) and phenylephrine (PEP) were prepared using 0.1 N HCl. The ACh was prepared from crystalline acetylcholine chloride (Sigma Chemical Co., Cat. # A-6625); ISO from L-isoproterenol hydrogen chloride (1 [3",4'-dihydroxyphenyl] 2 -isopropylamino ethanol HCl; isopropylarterenol HCl) (Sigma Chemical Co., Cat.# I-5627); propranolol from DL-propranolol hydrogen chloride (1 - [isopropylamino]-3[1-Naphthyloxy]-2 Propanol HCl) (Sigma Chemical Co., Cat. # P-0884); PEP from L-Phenylephrine hydrogen chloride (Sigma Chemical Co., Cat. # P-6126); and atropine from atropine crystals (Sigma Chemical Co., Cat. # A-0132).

TABLE I

Composition of Culture Medium and
the Standard Balanced Salt Solution (SBSS)

<u>Ion/Compound</u>		<u>Culture Medium</u>	<u>SBSS</u>
Sodium, Na ⁺	mM l ⁻¹	136.0	146.5
Potassium, K ⁺	mM l ⁻¹	6.5	3.0
Chloride, Cl ⁻	mM l ⁻¹	130.0	136.8
Calcium, Ca ⁺⁺	mM l ⁻¹	1.48	1.5
Magnesium, Mg ⁺⁺	mM l ⁻¹	0.83	0.82
Dextrose/Glucose	mM l ⁻¹	5.0	5.5
p ^H		7.3	7.3
Fetal bovine serum, FBS.		10% Volume	-

2.10 PERFUSION SYSTEM

To study the steady-state inotropic and chronotropic responses of these strands at various extracellular concentrations of different ions, a perfusion system was designed. The objective was to provide a relatively rapid non-traumatic exchange of fluid in the experimental chamber.

The perfusion fluids from the reservoir were introduced into the culture chamber via a specially designed glass pipette input arm with "Technicon 0.0625 transmission tubing" running from the delta head of a Watson-Marlow MHRE-22 pump. The fluid from the chamber was removed by a specially designed glass tube and suction arrangement. This outlet glass tube has a small U-shaped end which was kept below the surface level of the fluid in the chamber. This arrangement eliminated any surface tension effects and maintained a constant fluid level in the chamber.

To determine the equilibration (t_e) and washout (t_w) times during solution change, a dye marker (thionin acetate, blue in colour; 3 ccs of dye mixed in 1 litre of distilled water) was introduced into the chamber through the perfusion system. The chamber was set up on a Wild M4A microscope stage. The microscope light passed through the chamber and was picked up by a photoconductive cell

(cadmium sulphide type; Clairex Electronics, type # CL-705 L/2). The response of the photo detector was proportional to the concentration and depth of the medium (dye) in the chamber and was recorded on a chart recorder. This experimental arrangement is shown in Fig. 2.8.

The t_e and t_w values were determined at different pump speed settings. When the strand was suspended and the flow experiments were done, the optimum flow rate was determined to be 2.56 ml min^{-1} . At lower flow rates the exchange time was very long and at higher flow rates the presence of turbulence caused the strand to break. At this value t_e was 45 sec and t_w was 50 sec for the exchange of the top 1.0 mm of fluid in the chamber. This perfusion system was suitable only for steady-state measurements because of the large t_e and t_w values. Technical details of the perfusion system are presented in Appendix-V.

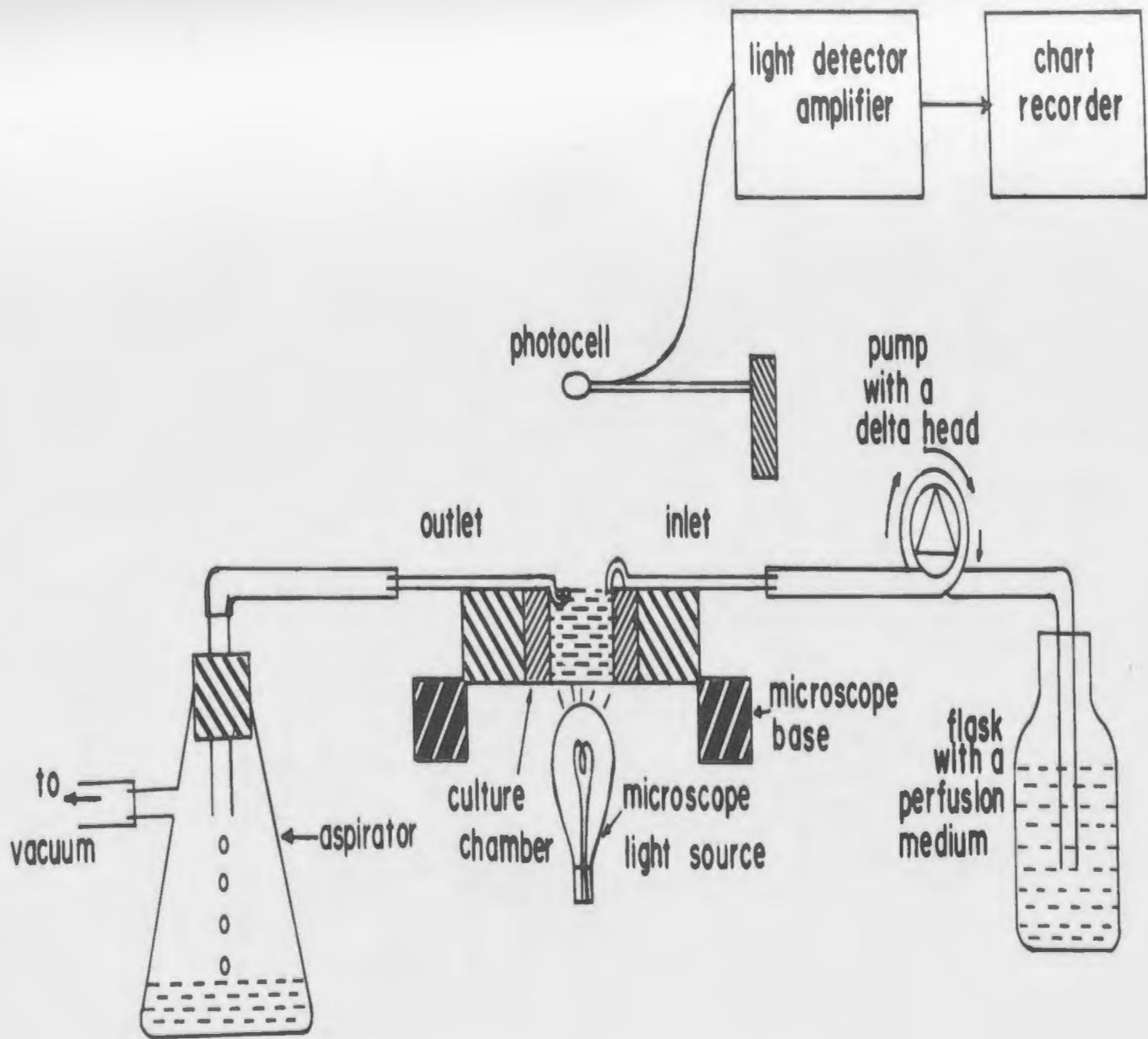
Whenever a new perfusion fluid was introduced the input lead was taken out of the current source reservoir and was placed in the new one. When switching between solutions an air bubble would enter the perfusion line; this served as an indicator of the arrival of the new solution at the culture chamber. The time taken for the fluid to reach the chamber from a given reservoir depended on the length and diameter of the input tube, the pump speed and the diameter of the exchange tubing at the delta

Fig. 2.8 A schematic diagram of the perfusion system used in this study, including the photo-detector utilized for flow calibration.

This arrangement was also used to determine the chamber-perfusion solution exchange characteristics

The perfusion solution from a flask (right-hand side) was introduced into the culture chamber by means of a pump with a delta head. The outlet glass tubing at the chamber had a small "U" shape. This arrangement prevented any surface tension effects at the meniscus and also maintained a constant fluid level. The inlet and outlet tubings just touched the top surface of the fluid in the chamber.

To characterize the perfusion system, light was transmitted from the bottom through a perfusion solution of the chamber (containing either water or a dye solution) and impinged on the photocell. The light intensity detected was inversely proportional to the dye concentration in the chamber. The fluid outlet was connected to an aspirator.



head of the pump. This time was observed to be 0.7 min in this experimental set-up and was accounted for in interpreting the chart records.

2.11 STRAND SUSPENSION

2.11.1 Suspension apparatus

In addition to the force transducer a suction arm and a glass microtool are necessary to suspend the strand. The techniques used to prepare these apparatus are described as follows:

Disposable micropipettes (20 λ Yankee Disposable Micropet, similar to those used for the force transducer) were used for the preparation of specially designed suction arms. Micropipettes were drawn into two pieces, one longer and one shorter, using a micropipette puller (Industrial Scientific Corp. Inc., N.Y. model MI) at the settings Coarse: 30, and fine: 30. The longer portion of a drawn micropipette was fire polished by briefly exposing the pulled end to the flame of a Bunsen burner while air was blown through the opposite end. This thermal polishing process continued until the tip was 60 μm in diameter and the surface was smooth.

The micropipette was then bent twice at an angle of 135° (Fig. 2.9), with the $60\ \mu\text{m}$ tip forming the end of the vertical limb. A suction line was attached to the horizontal limb. The horizontal limb was then fixed inside a glass tube, which both stabilized the micropipette and provided a convenient site for mounting on an instrument holder (having a ball and socket arrangement), and attached to a 'Narishige' model MM3 micromanipulator mounted on a rod with magnetic base. In this arrangement, the micropipette could be moved precisely in all three planes using the micromanipulator.

The glass microtool was prepared using a $10\ \lambda$ Yankee Disposable Micropet. At a high heat (micropipette puller settings were Coarse: 50, and fine: 60), exposed for a short duration (less than 1.0 s), the micropipette was pulled into two pieces. One of these pieces was pulled into a thinly-drawn flexible fiber, the tip diameter being of the order of $1\text{-}2\ \mu\text{m}$. At about 4-5 cm from the tip, the fiber was bent at an angle of 135° at a very low heat. A diagrammatic representation of this tool is shown in Fig 2.10. This tool was then attached to the rotating head of a 'Leitz' micromanipulator.

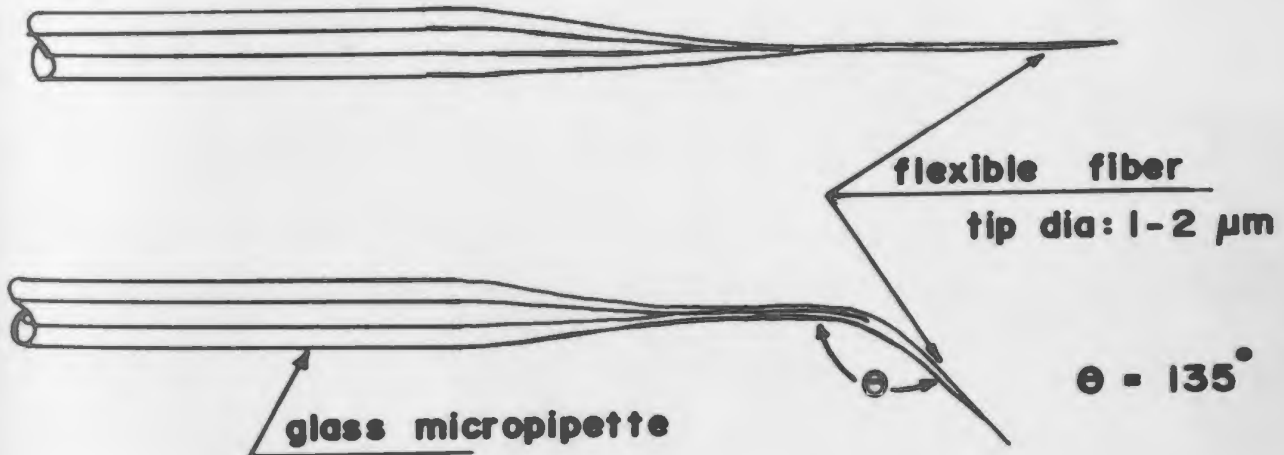
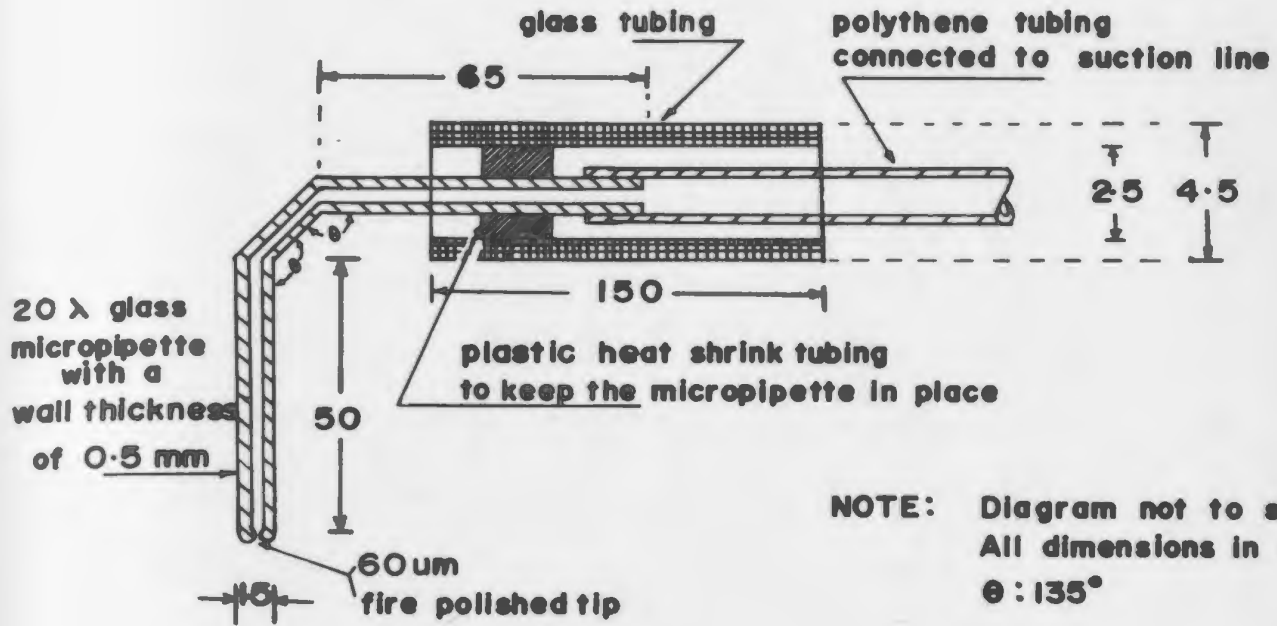
Fig. 2.9 A diagram of the suction micropipette assembly used for suspension of strands.

Various physical details of preparing a suction micropipette for use in suspending a strand is presented here. The tip diameter (about 60 μm) is critical; it should be smaller than the diameter of the glass microspheres (about 100 μm) terminating the cultured myocardial strands.

Fig. 2.10 Two stages in the preparation of a glass microtool, used to remove the strand from the palladium strip during strand suspension.

Stage 1: A glass micropipette was drawn into two pieces using a micropipette puller. The portion of the micropipette with a long thinly drawn end (about 1-2 μm tip diameter, flexible) was used to prepare the tool.

Stage 2: The flexible fiber, about 4-5 cm from the tip, was then bent at an angle of 135° at a very low heat.



2.11.2 Strand Selection

At an age of 6-12 days from the day of culturing, strands were viewed under a Nikon inverted microscope (Model M) at a magnification of 400X, to choose suitable specimens for suspension and for measurement of presuspension lengths. The primary selection criteria were that the strand should be complete between microspheres, contract spontaneously and have physical dimensions of at least 3.1 mm in length and 0.1 mm in width.

2.11.3 Suspension Procedures

When a suitable strand was identified, the top coverslip of the culture chamber was removed and the chamber fitted into the circular opening of the heater unit of the temperature control system (Fig. 2.5). This assembly was then fixed onto the stage of a Wild M4A microscope, with the temperature control sensing thermistor placed against the inner edge of the chamber. The strand suspension was performed during constant microscopic (Wild type M4A) observation, at a X20 magnification.

The various stages of strand suspension procedure are shown in Fig. 2.11.

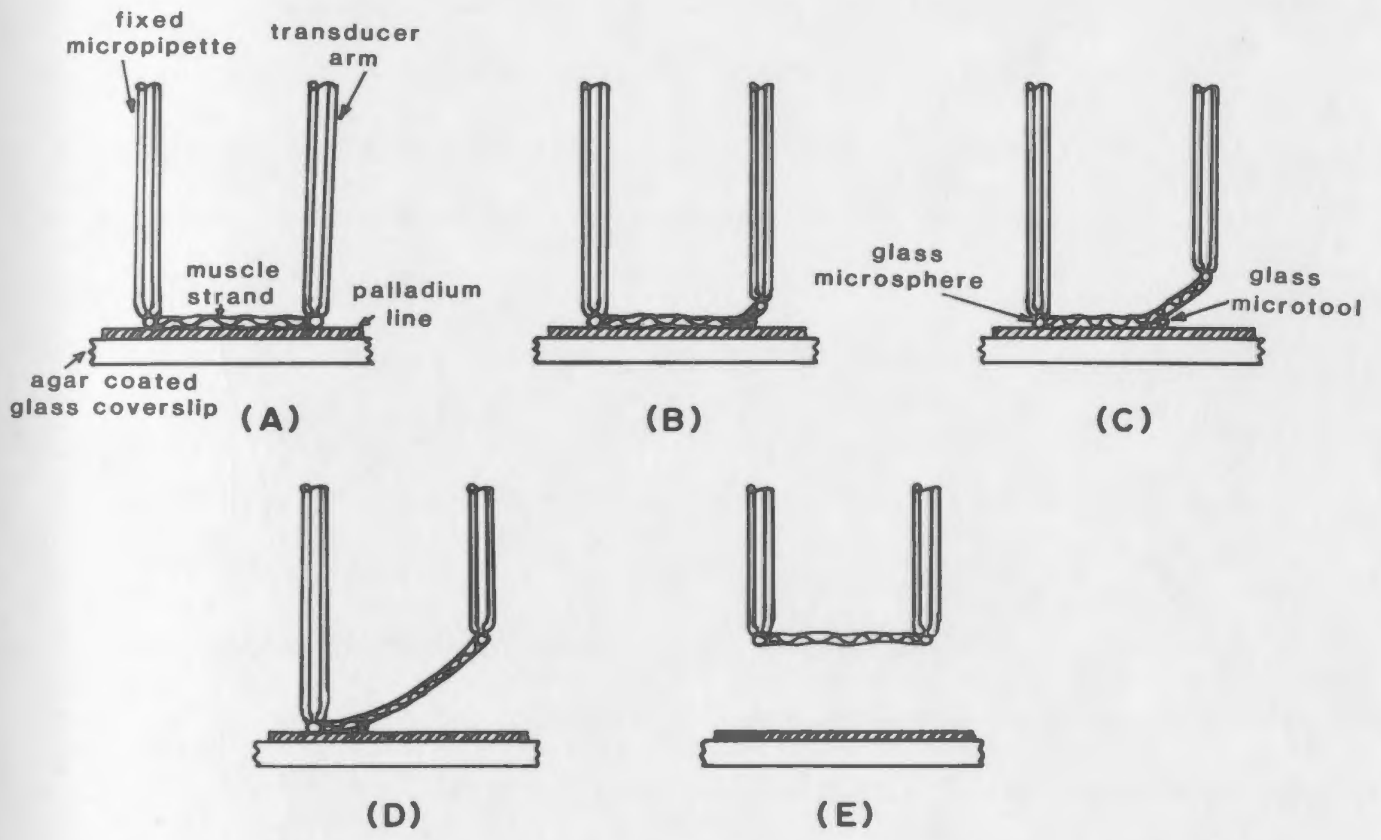
ig. 2.11 Diagrammatic representation of procedures followed in suspension of cultured cardiac muscle strands.

A: Transducer arm and fixed micropipette are placed just above the glass microspheres at the termini of the strand.

B: Suction is applied, the force transducer end slowly being lifted. The glass microtool is then carefully inserted under this end as shown. This initiates the process of scraping the strand from the palladium line.

C-D: Scraping process continues, the force transducer being slowly lifted.

E: With the strand completely removed from the palladium line, the fixed micropipette end is then lifted. The heights of both the transducer arm and the fixed micropipette above the base are adjusted so that the cultured myocardial strand is suspended horizontally in the top 1.0 mm of culture medium.



The equipment was adjusted to bring the tip of the suction arm and the tip of the force transducer into proximity to the two glass microspheres which identified the ends of the strand. With the help of a calibrated U-tube manometer the total suction at the tip of each micropipette was maintained at -52 mmHg. In order to suspend the myocardial strand in the culture medium, this negative pressure was applied to the micropipettes and the strand microspheres were sucked to their tips (step A, Fig. 2.11). Once the microspheres were picked up any strands extending (on either side of the experimental strand) beyond them were cut using a sharp glass micropipette.

The strand was disengaged from the palladium substratum with the help of the glass microtool. The microtool was slowly introduced to the vicinity of the strand and its flexible tip was carefully inserted below the microsphere attached to the force transducer (step B, Fig. 2.11). The tool was slowly moved along the strand to disconnect it from the palladium line (step C, Fig. 2.11). As the strand was loosened, the transducer was raised very gradually using the vertical vernier and the scraping process continued for the entire length of the strand (step D, Fig. 2.11). When the microtool finally passed

beneath the bottom surface of the distant microsphere, the fixed support was also raised carefully to match that of the transducer (step E, Fig. 2.11).

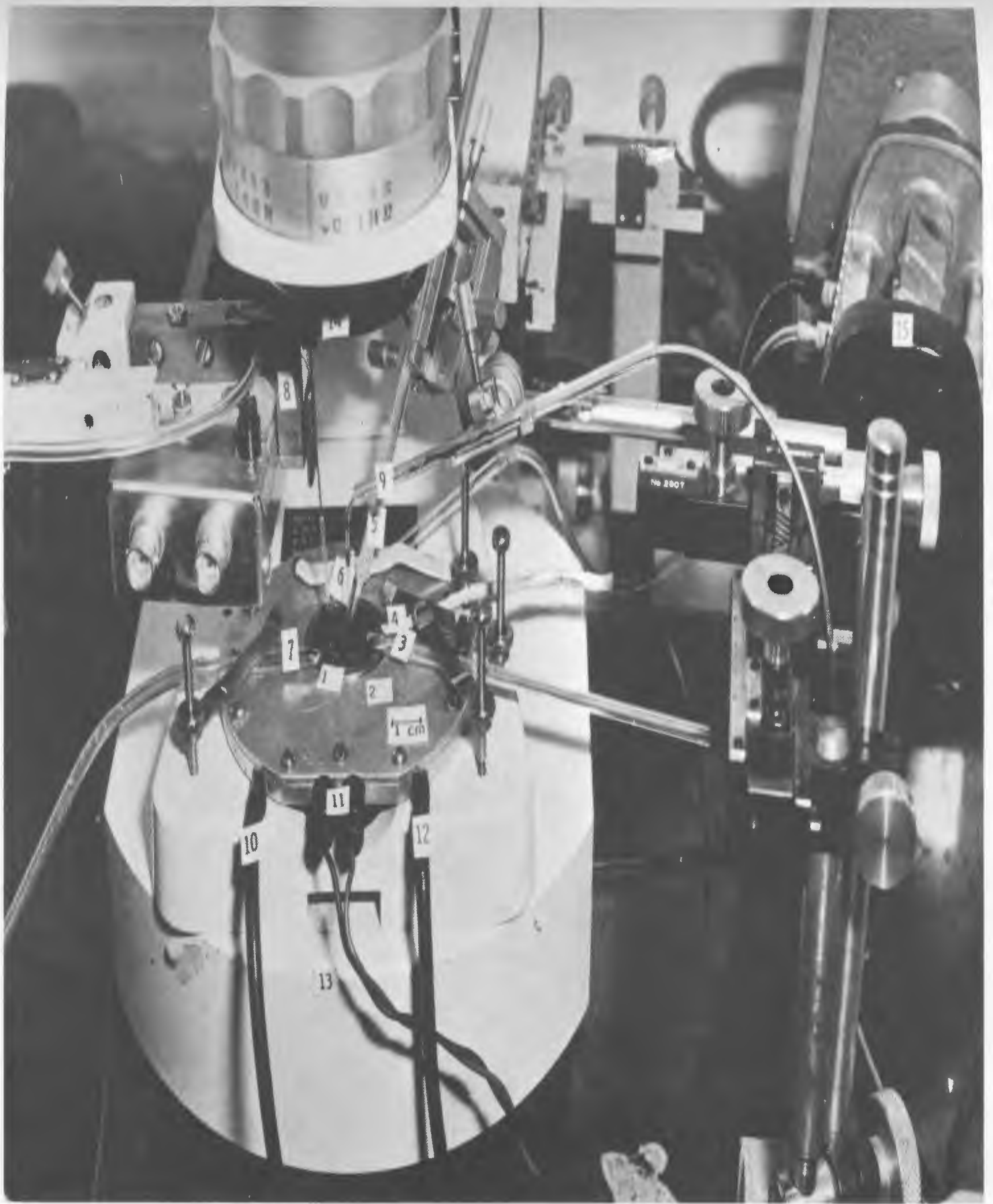
The freed strand was carefully raised from the chamber bottom and, using the two micromanipulators, was maneuvered until it was positioned horizontally in the centre of the chamber in the upper 1.0 mm of the culture medium. Finally, the distance between the microspheres was adjusted to match the measured presuspension length of the strand.

Fig. 2.12 shows the overall experimental arrangement.

ig. 2.12 The overall experimental arrangement used in the study of contractility of the cultured myocardial strands.

The various components of this arrangement are as follows:

1. Culture chamber.
2. Culture chamber heater unit.
3. Platinum return electrode.
4. Thermistor.
5. Ag/AgCl active stimulating electrode.
6. Perfusion system inlet.
7. Perfusion system outlet.
8. Isometric force transducer.
9. Fixed micropipette used for strand suspension.
10. Heater cooling water outlet.
11. Heater coil connections.
12. Heater cooling water inlet.
13. Illuminated microscope base.
14. Stereo zoom microscope.
15. Cooling fluid/perfusion pump.



CHAPTER - III

RESULTS

3.1 STRAND DEVELOPMENT

It was observed that within 24 hours of culturing, cardiac muscle cells flattened and attached to the palladium lines. At this time the isolated cardiac cells were usually elongated and spindle-shaped with a central nucleus. Occasionally two nuclei were seen in a cell. The myocardial cells aligned longitudinally along the palladium line, conforming to the principle of contact guidance (Ohara and Buck, 1979).

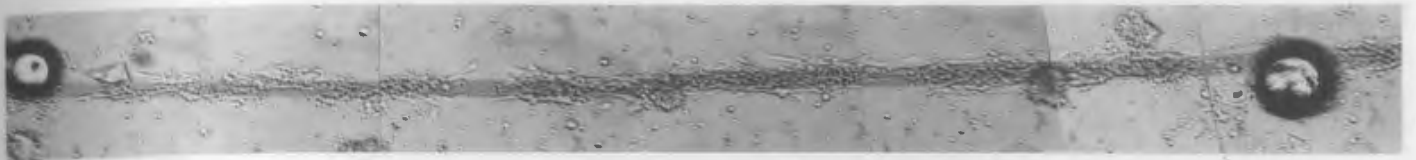
Clusters of cells formed at various points on the palladium lines and contracted spontaneously at independent rates. Similar clusters of cells grew around the glass microspheres. The force generated by these spontaneously contracting cells was sufficient to pull the microspheres from their original attachment spots making the strand appear to shrink with age. Fig. 3.1 shows the formation of one strand studied 2,4,6,8 and 16 days from the time of culturing. The patches of palladium line unoccupied by the myocardial cells on days 2 and 4 can be seen (Fig. 3.1).

Fig. 3.1. Gross morphological features of strand formation.

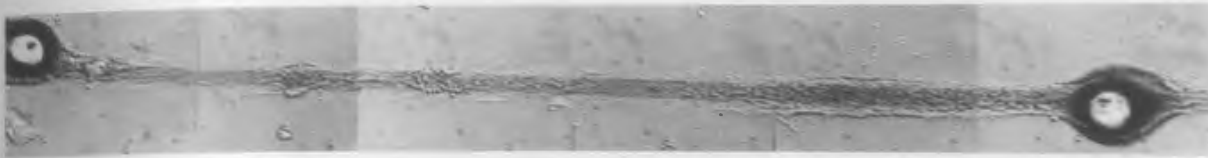
This sequence of photographs follow the changes in a single myocardial strand developing in culture, from day 2 to day 16. Myocardial cells aligned themselves along the palladium strip, forming patches of cells. Unoccupied portions of the palladium line between two microspheres were observed on day 2 and 4. From day 6 onward completed contracting myocardial strands were seen.

The "microsphere pulling effect" by the strand could be seen in these series of photographs. The microsphere on the right-hand side moved as the contractility of the strand developed and the length decreased.

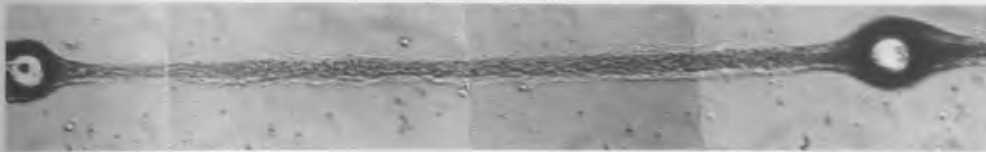
Note that the microspheres were completely encased by the cells forming the termination of the strand.



2 days



4 days



6 days



8 days



16 days

100 μ m

Complete strands were formed between the two microspheres by day 6 at which time all cells were contracting at the same rate. The strands remained intact, in a healthy state, and contracting spontaneously and synchronously up to 12-13 days of age. Around day 16, the strands began to disintegrate.

Fifty-six strands from different batches of culture were initially selected for sequential observation. All strands were complete between microspheres by day 6. All of them were still beating at day 12. Only 19 strands, out of 56, were viable at day 16 due to (a) the microsphere pulling effects which resulted in strand damage; (b) loss of some cultures because of bacterial infection and (c) the tendency for strands to stop beating after days 12-13. On the basis of these observations strands 6-12 days old were used for all further experimental studies.

A limited study of the strands using the electron microscope showed that the average strand was 5 cells wide (63 μm) and 1-2 cells (about 3 μm) thick. Most strands investigated had a length of 3.1 mm. Based on the observed dimensions of isolated cells, growing in culture, before strands were formed, minimal cell length was estimated to be approximately 60 μm . This value was used in estimating the number of cells present in a strand. Using a strand

width of 5 cells, a strand thickness of 1.5 cells and a mean cell length of 60 μm , the average strand (3.1 mm long) consisted of approximately 385 cells.

The very limited electron microscopy done on this preparation included only its cross-sectional examination. Hence, no unequivocal statements could be made about the presence or absence of organised contractile filaments.

The rate of spontaneous contraction was observed to decrease with age. Fig. 3.2 shows the rate of spontaneous contraction as a function of strand age, for 6 strands from different culture batches. By day 9, the rate of spontaneous contraction was $4 \pm 0.5 \text{ min}^{-1}$ (mean \pm S.D, $n=6$). It was also observed that each contraction was initiated at the same site in the strand and travelled along the entire length of the strand.

3.2 EXCITABILITY OF THE STRAND - STRENGTH-DURATION RESPONSE

The myocardial strand preparation was electrically excitable. When field stimulated a strength-duration relation was obtained as shown in Fig. 3.3. The response was a characteristic hyperbolic curve typical of that obtained from many other excitable tissues (Dudel, 1975).

Fig. 3.2 The relation between the strand age (in days) plotted versus spontaneous contraction rate (in contractions per minute).

Each data point represents the mean \pm standard deviation of values obtained from six strands observed over a period of 12 days at a regulated temperature of 25 °C. These observations demonstrate a progressive decrease in spontaneous contraction rate with increasing age of the strand in culture.

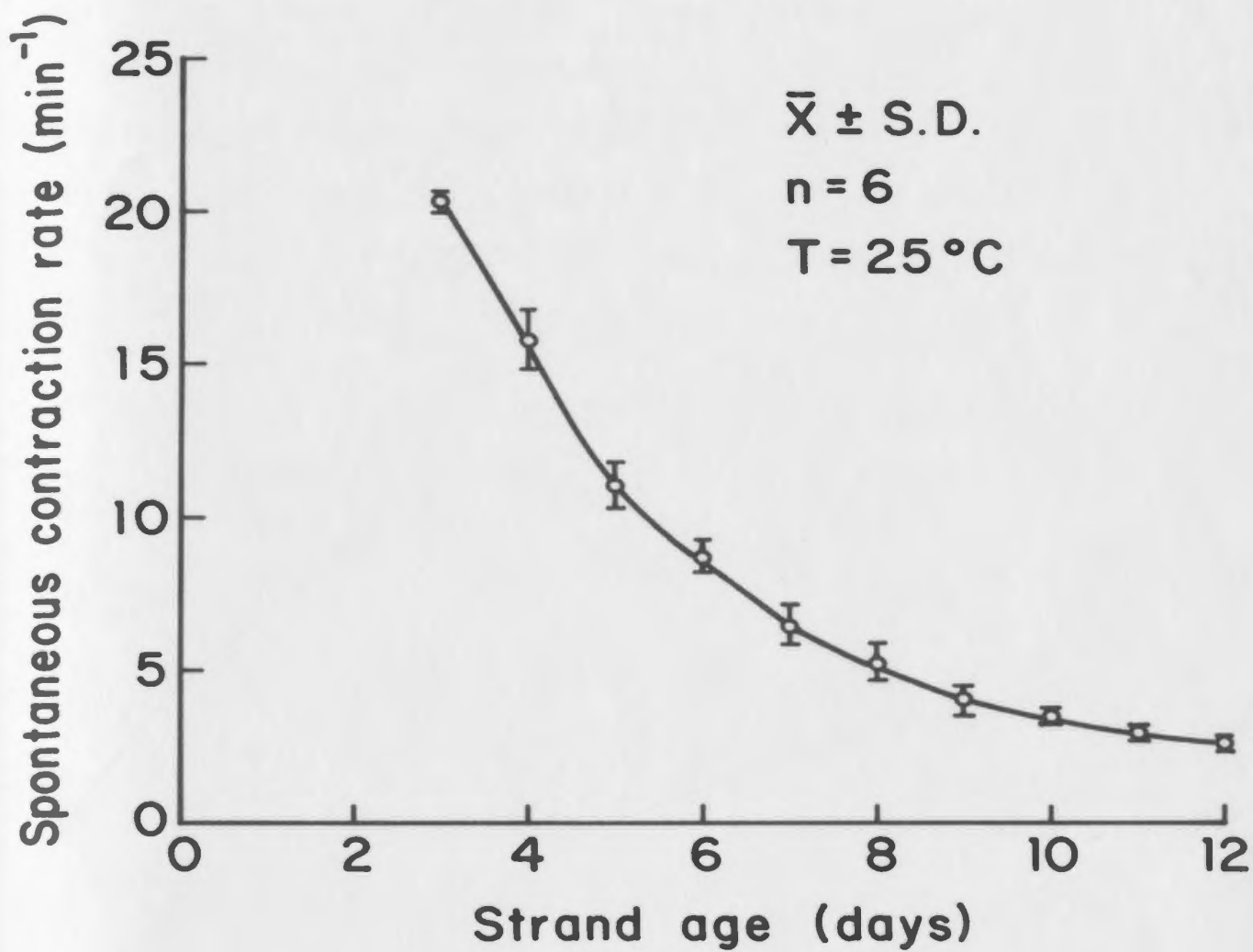
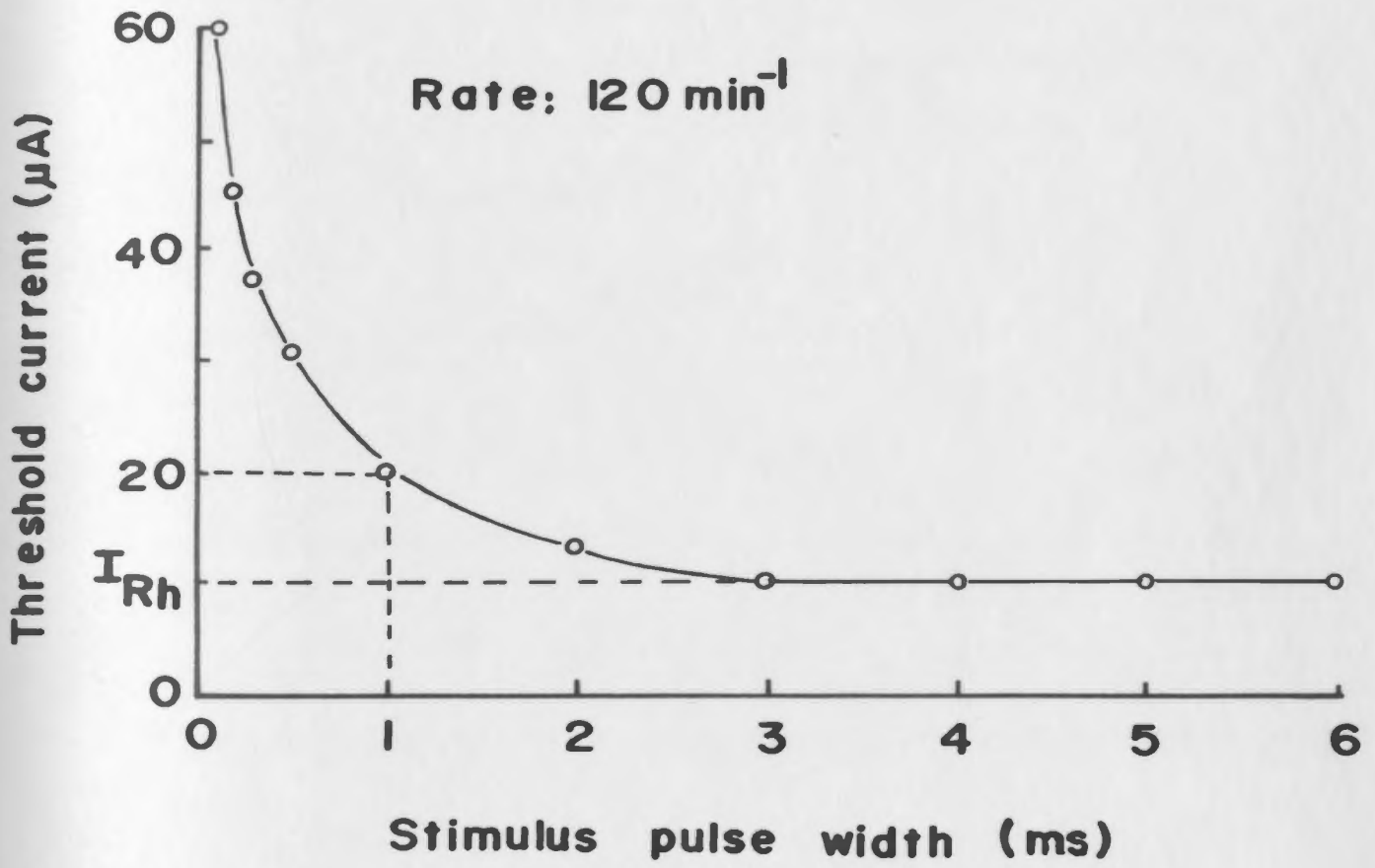


Fig. 3.3 Strength-duration curve obtained from spontaneously contracting myocardial strands under suspension.

Pulse width (duration) is plotted along the abscissa while the threshold current required to transform the rate of contraction of the strand from its spontaneous rate (73 min^{-1}) to the driven rate (120 min^{-1}) is plotted along the ordinate. Temperature of the bath was maintained at $25 \text{ }^\circ\text{C}$.

Optimal stimulus parameters are generally accepted to be the strength-duration pair on the curve identified at a current value of 2 X rheobase (I_{Rh}) ($20 \mu\text{A}$ and 1.0 ms).



The rheobase current for this preparation (I_{Rh}) from Fig. 3.3 is $10 \mu A$. In making an initial selection of a suitable stimulus strength and duration a current value, twice I_{Rh} (often known as chronaxie) and its corresponding duration were obtained from Fig. 3.3, as $20 \mu A$ and 1.0 ms (Grundfest, 1932).

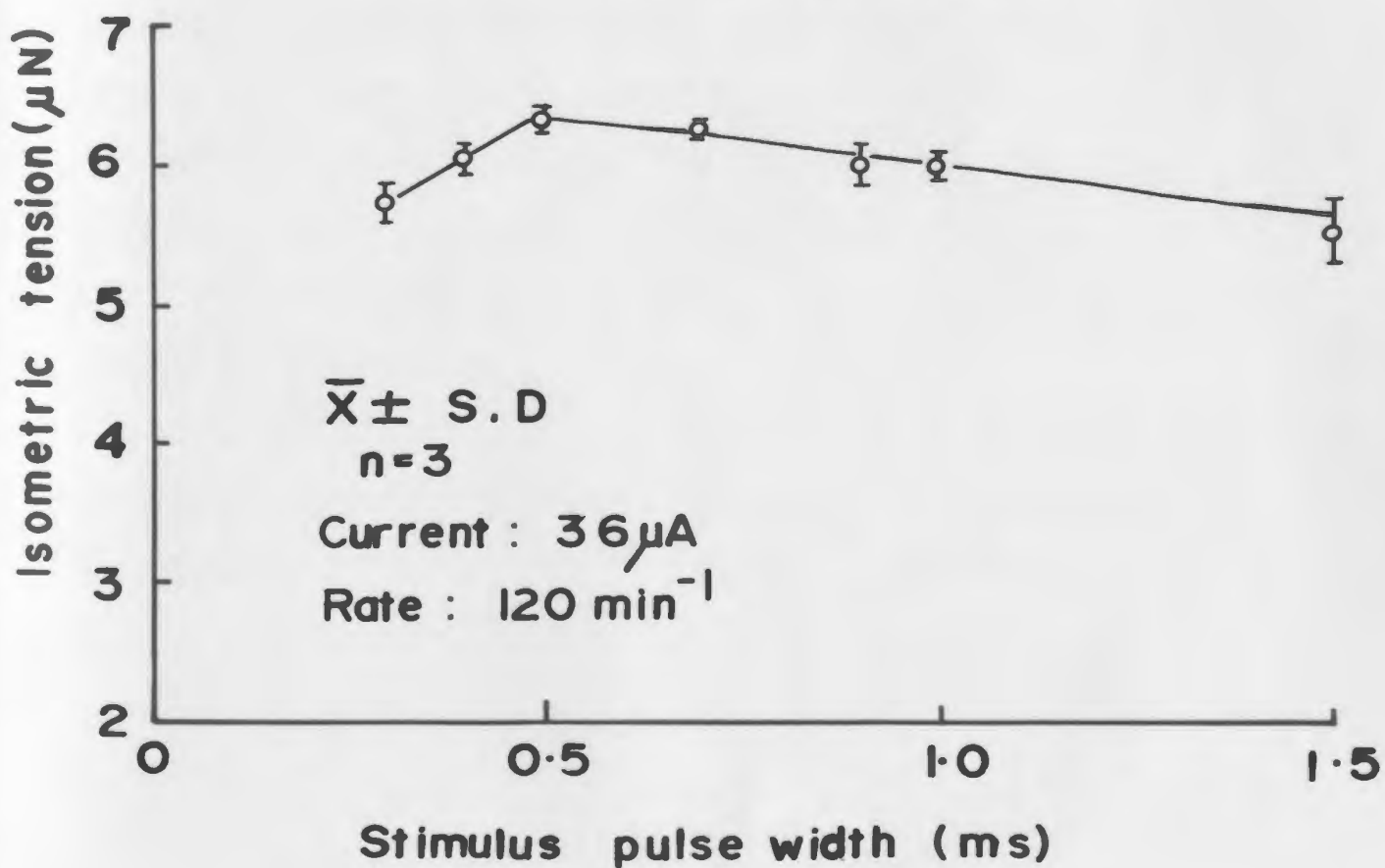
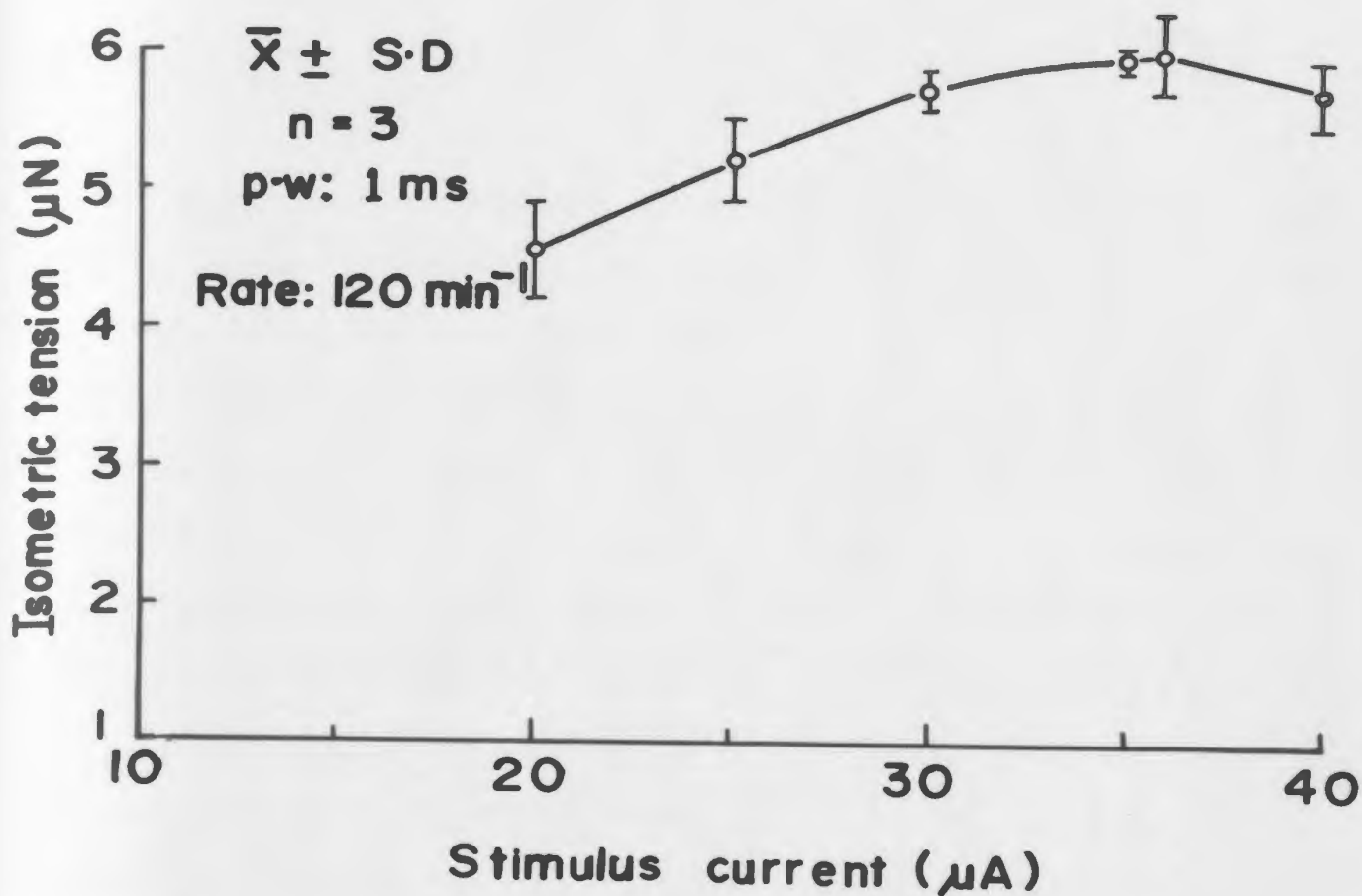
The active tension amplitudes obtained for various stimulus intensities when the suspended strands were stimulated at a rate of 120 min^{-1} with 1.0 ms pulses (obtained from Fig. 3.3) are shown in Fig. 3.4(a). Maximal tension occurred when the intensity was $36 \mu A$. The experiment was repeated with this stimulus intensity for different pulse widths. The resulting tension as a function of stimulus duration is plotted in Fig. 3.4 (b). It was observed that peak tension occurred at 0.5 ms pulse width for $36 \mu A$ intensity of stimulation. For values of current or duration greater than these values the amplitude of contraction was either unchanged or reduced in relation to the maximal tension values. The optimal stimulus parameter values were rounded off as 0.5 ms pulse width and $35 \mu A$ current. The optimal values of strength and duration determined in this way were used for all electrical stimulation experiments.

Fig. 3.4 Criteria used to select the optimal values for the stimulation of the strand preparation. The combinations of pulse width and stimulus current values that produced maximal isometric tension were considered to be the optimal stimulus parameters.

(a) Keeping the pulse width constant (1.0 ms, obtained from Fig. 3.3) and the rate of stimulation at 120 min^{-1} , stimulus current was varied and the isometric tension measured. Maximal tension occurred when the stimulus strength was $36 \mu\text{A}$.

(b) Keeping the stimulus strength (obtained from "a" above) at $36 \mu\text{A}$ and the stimulation rate at 120 min^{-1} , pulse width was varied. Peak tension occurred at 0.5 ms pulse width.

The optimal parameters for strength and duration were $36 \mu\text{A}$ and 0.5 ms; for convenience in setting the stimulator, $35 \mu\text{A}$ was used as an approximation.



3.3 LENGTH-TENSION RELATIONSHIP

While studying the LT relationship the strands were stretched and relaxed in 10 μm steps from 3.06 mm (L_0) to 3.13 mm. When strands were stretched beyond 3.13 mm, they broke. Typical isometric tension records from a single spontaneously contracting strand obtained at different lengths are shown in Fig. 3.5.

There was no significant difference (2-tailed paired t-test, $p > 0.2$) between the isometric tension recorded during stretching and shortening of either spontaneously contracting or electrically driven strands. Hence the isometric tension values at each strand length during stretching and shortening were averaged for each strand. A typical LT curve for 6 strands (mean \pm S.D) is shown in Fig. 3.6. The actual values for resting and active tensions at L_{max} were respectively $2.77 \pm 0.24 \mu\text{N}$ and $4.70 \pm 0.38 \mu\text{N}$ (mean \pm S.D, $n=6$). Maximum resting tension was $11.68 \pm 0.37 \mu\text{N}$.

Table II compares the LT relationship in the same strands when contracting spontaneously and during electrical stimulation (at a stimulus rate of 120 min^{-1}). During electrical stimulation the active tension increased by 10-20% but there was no change in the resting tension.

Fig. 3.5 High speed tracings of isometric tension records obtained from a strand contracting spontaneously at different lengths are presented. The panel labelled "0 μm " represents the resting strand length, L_0 . Each successive panel represents the response at $L_0 +$ the labelled increments in strand length. The two components of tension, resting (RT) and active (AT), are shown. The temperature of the bath was 22 °C.

Fig. 3.6 The length-tension relationship obtained by combining data from spontaneously contracting cultured myocardial strands. Each point represents the mean \pm standard deviation of measurements from 6 strands. The resting (RT), active (AT) and total (TT) tensions are plotted along the ordinate; tension values were normalized as a ratio with P_{max} , the maximum AT observed in each stand. Strand length, plotted on the abscissa, was normalized as $[(\text{actual length} - L_{\text{max}}) / L_{\text{max}}]$, where L_{max} is the length at which P_{max} occurred. L_0 is the length at which neither AT nor RT was present. The temperature of the bath was 22 °C.

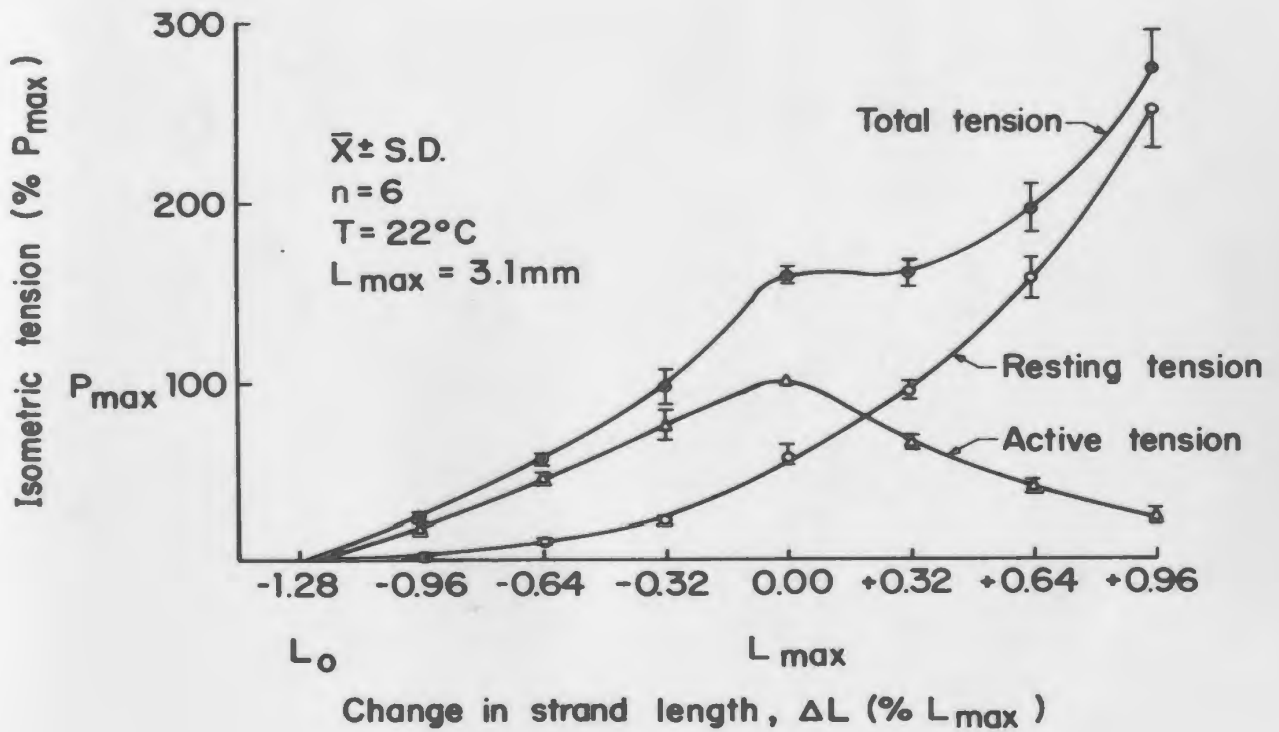
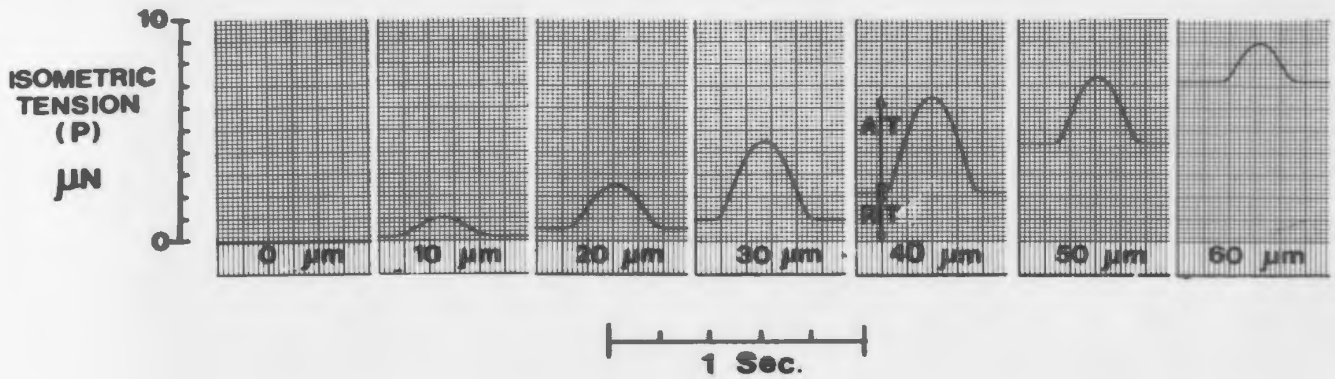


TABLE II

Comparison of Length-Tension Relationship in Six Cultured Strands of Cardiac Muscle During Spontaneous and Electrically Driven Contractions

Change in Strand Length (ΔL)	Resting Tension (RT)	Active Tension (AT)		Total Tension (TT)	
		Spontaneous	Stimulation	Spontaneous	Stimulation
% L_{\max}	% P_{\max}	% P_{\max}	% P_{\max}	% P_{\max}	% P_{\max}
-1.28	0,0 \pm 0,0*	0,0 \pm 0,0*	0,0 \pm 0,0*	0,0 \pm 0,0*	0,0 \pm 0,0*
-0.96	3,7 \pm 0,5	20,6 \pm 2,1	29,1 \pm 3,0	24,4 \pm 2,0	32,9 \pm 3,1
-0.64	12,4 \pm 1,1	44,5 \pm 2,8	58,5 \pm 10,1	56,9 \pm 3,7	71,3 \pm 11,5
-0.32	21,9 \pm 2,0	75,2 \pm 9,9	93,7 \pm 15,3	97,1 \pm 11,4	116,0 \pm 17,4
-0.00 (L_{\max})	59,0 \pm 5,1	100,0 \pm 0,0 (P_{\max})	118,8 \pm 11,6	159,0 \pm 5,1	180,6 \pm 16,5
+0.32	94,3 \pm 5,2	65,2 \pm 2,7	79,5 \pm 8,5	159,4 \pm 7,0	176,2 \pm 17,2
+0.64	155,9 \pm 12,3	41,1 \pm 1,6	52,7 \pm 6,4	197,0 \pm 13,6	211,7 \pm 24,5
+0.96	249,6 \pm 22,0	23,4 \pm 2,2	32,1 \pm 4,1	273,1 \pm 21,8	293,5 \pm 34,9

Spontaneous rate of contraction: $73 \pm 2,35 \text{ min}^{-1}$, L_{\max} of each strand was 3.1 mm.

* mean \pm S.D., n=6. Temperature: 22°C. Stimulation parameters: 35 μ A, 0,5 ms rectangular pulses at 120 min^{-1} .

The increase in active tension during electrical stimulation at a rate of 120 min^{-1} was statistically significant at all lengths above L_0 ($p < 0.01$, paired t-test).

To try and assess whether electrical stimulation altered the contractile response, the strands were exposed to SBSS having $3 \text{ mM } [K^+]_o$ which reduced the spontaneous contraction rate to 63 min^{-1} (see Section 3.7.1). When such strands were electrically stimulated at a rate of 73 min^{-1} (corresponding to the spontaneous contraction rate in the culture medium) the LT relationship was identical to that obtained in the same strands beating spontaneously in culture medium.

Similarly, in the presence of 10^{-4} M ACh (see Sec. 3.11.2), the spontaneous contraction rate dropped to 9 min^{-1} . When such strands were stimulated at 73 min^{-1} and the LT relation was studied, the resulting response was the same as that seen in Fig. 3.6. These experiments confirm that electrical stimulation did not alter the contractile properties but that the increase in active tension seen when strands were stimulated at 120 min^{-1} in normal culture medium is a consequence of the force-frequency relationship of this preparation (see Sec. 3.5).

3.4 EFFECTS OF TEMPERATURE ON SPONTANEOUSLY CONTRACTING STRANDS

3.4.1 Relationship Between Temperature and Spontaneous Contraction Rate

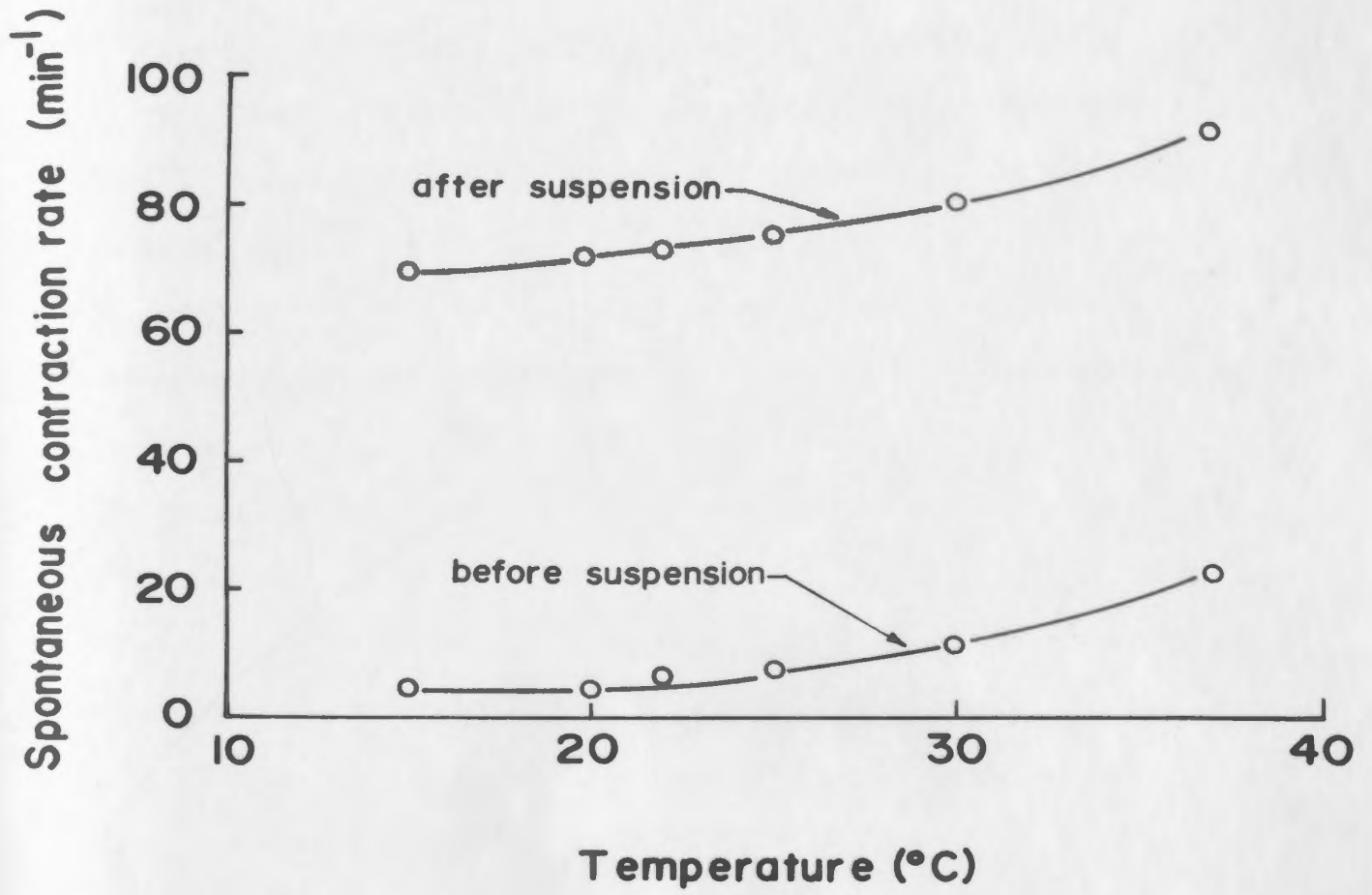
The unsuspended strands contracted at a basal rate of 6 min^{-1} , while still attached to the bottom of the culture chamber (vide section 3.3), at a chamber temperature of $22 \text{ }^{\circ}\text{C}$. This rate fell to 4 min^{-1} when the temperature was reduced to $15 \text{ }^{\circ}\text{C}$. As the temperature of the chamber was increased from 15 to $37 \text{ }^{\circ}\text{C}$ the rate of spontaneous contraction increased from 4 to 22 min^{-1} (see Fig. 3.7).

After suspension, the strand length was held at L_{max} . Suspension increased the spontaneous contraction rate to 69 min^{-1} at $15 \text{ }^{\circ}\text{C}$. As the temperature of the bath was increased from 15 to $37 \text{ }^{\circ}\text{C}$, the rate of contraction increased in a nonlinear manner to 91 min^{-1} (Fig. 3.7). These curves show that the spontaneous contraction after suspension was elevated at all temperatures compared to that of presuspension strands and that the change in rate with temperature is the same in both conditions.

Fig. 3.7 The relationship between the spontaneous contraction rate and temperature before and after strand suspension.

Spontaneous contraction rate is represented on the ordinate as contraction per minute and the temperature on the abscissa as °C. Each point represents the mean of two experiments; each strand was examined before and after suspension.

The rate of contraction "after suspension" was elevated at all temperatures compared to "before suspension".



3.4.2 Relationship Between Temperature and Isometric Tension

While the rate of contraction increased progressively with temperature over the entire range studied, the peak isometric active tension (P_{\max}) of the suspended strands increased progressively with temperature in the range of 15-20 °C, maintained a plateau in the range of 20-25 °C and decreased above 25 °C. The RT was not altered by temperature.

These data are presented in Fig. 3.8. Temperature (T) is represented on the X-axis; peak isometric tension (P_{\max}) on the Y-axis; and the spontaneous contraction rate (R) on the Z-axis.

From this figure it was concluded that the maximum contraction occurred at 25 °C. Therefore, all further studies not concerned with temperature relationships were carried out at a temperature of 25 °C.

3.4.3 Relationship Between Temperature and Rate of Rise of Tension

In Fig. 3.9 (a) the maximal rate of rise of tension, ($+dP/dt$), during spontaneous contraction is plotted as a function of temperature. It should be noted that at higher

Fig. 3.8 A 3-dimensional plot relating Peak isometric tension, Rate of spontaneous contraction and Temperature.

Temperature (T) in °C is represented on the X-axis; isometric tension (P_{\max}) (normalized as $\%P_{\max}$), on the Y-axis, and the spontaneous contraction rate (R) (in contractions per minute), on the Z-axis. Temperature Vs P_{\max} is defined by the X-Y plane, while temperature Vs spontaneous contraction rate is shown in the X-Z plane. Projection of these two curves in the Y-Z plane gives the relation between spontaneous contraction rate and P_{\max} . ($100\% P_{\max} = 5.51 \mu\text{N}$).

This represents the data compiled from one strand. However, the data was so reproducible that in effect this is a generalized relationship.

Isometric tension increased rapidly in the temperature range of 15-20 °C and between 20 and 25 °C the increment is smaller compared to that of 15-20 °C. Above 25 °C the isometric tension declined. Taking all three parameters - P_{\max} , R and T - into account, it was observed that the maximal tension occurred at 25 °C.

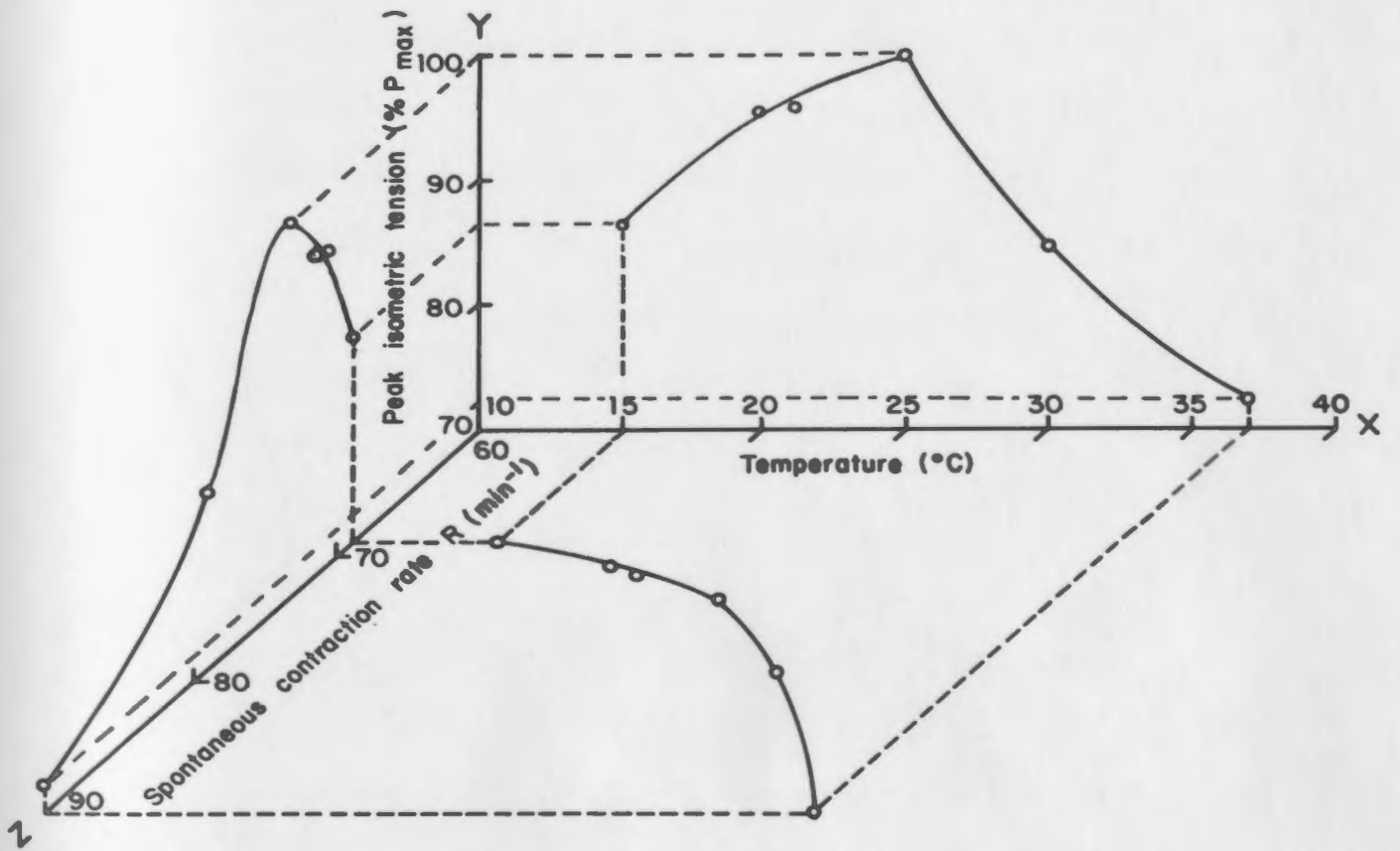
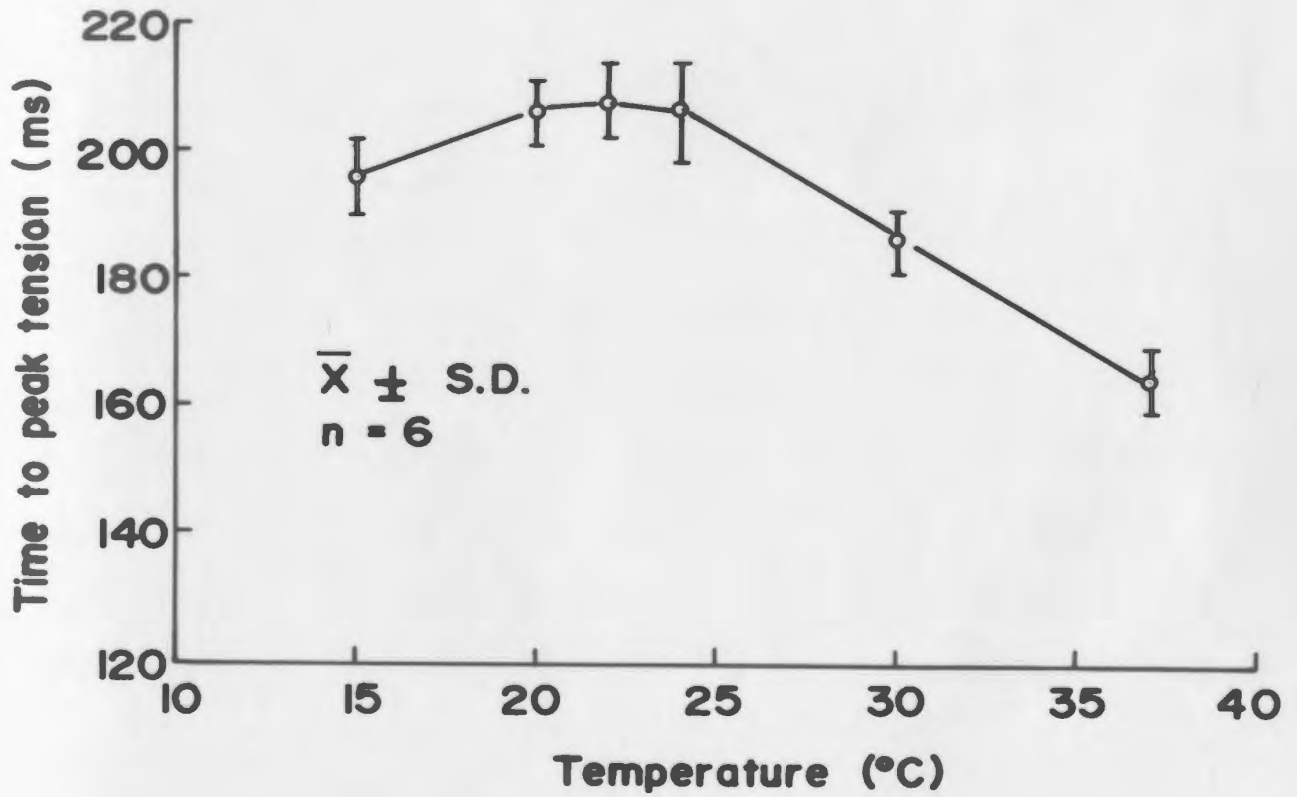
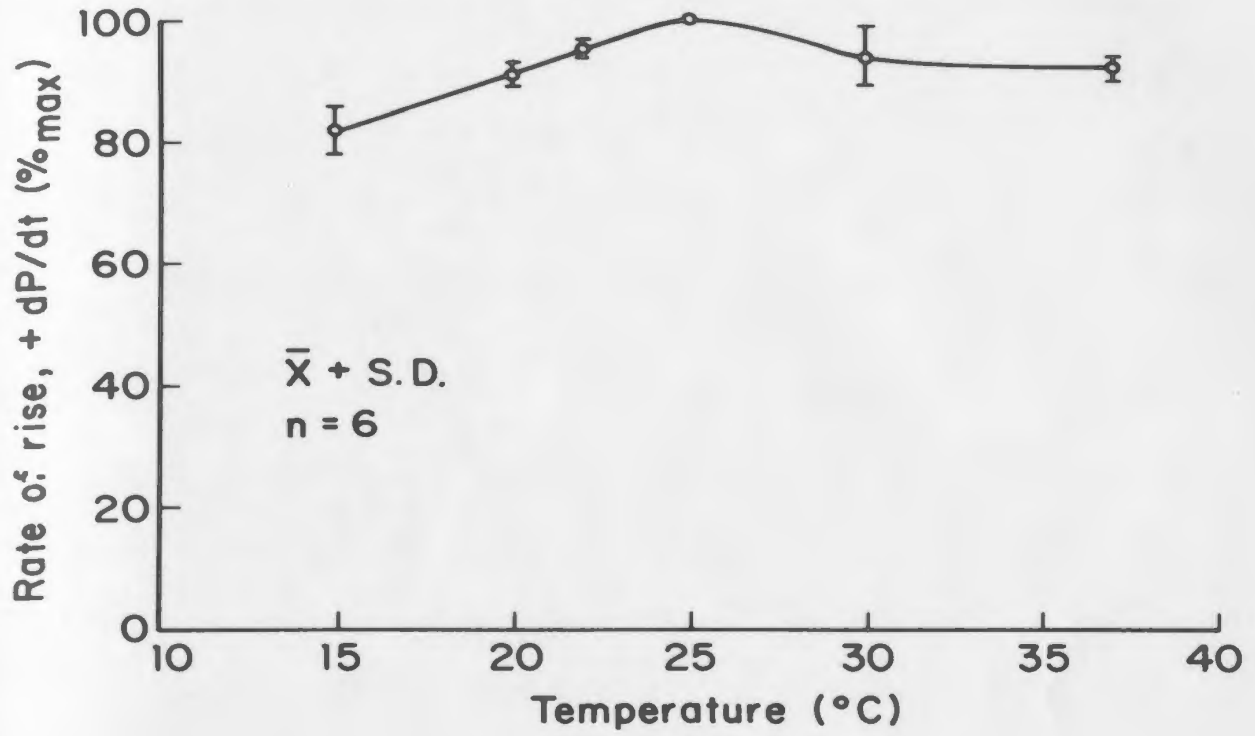


Fig. 3.9 Influence of temperature on the rate of rise of tension ($+dP/dt$) and time to peak tension obtained from six spontaneously contracting strands is illustrated.

(a) Rate of rise of tension is plotted on the ordinate as a percentage of maximum dP/dt . Temperature is plotted along the abscissa. The dP/dt increased with temperature in the range of 15-25 °C and thereafter was maintained at a nearly constant value. (The mean value of 100% dP/dt was $43.25 \mu\text{N sec}^{-1}$).

(b) Time to peak tension (in ms) is plotted along the ordinate, while temperature (in °C) is represented on the abscissa. Time to peak tension increased slightly with temperature in the range of 15-20 °C, maintained a plateau in the range of 20-25 °C and thereafter decreased rapidly.



temperatures (25 °C and above) the dP/dt did not show the prominent reduction that was apparent in the analysis of isometric tension (Fig. 3.8).

3.4.4 Relationship Between Temperature and Time to Peak Tension

Temperature modified the time to peak tension as illustrated in Fig. 3.9 (b). Time to peak tension increased linearly with temperature in the range of 15-20 °C, maintained a plateau in the range of 20-25 °C and decreased rapidly above 25 °C.

3.5 FORCE-FREQUENCY (FF) RESPONSE

3.5.1 Force-Frequency Relationship at Constant Temperature (25 °C) in Culture Medium

As mentioned in Section 3.3, the strands contracted spontaneously at a rate of 73 min^{-1} while suspended in the medium in which they were grown. To study the relation between isometric tension and the rate of contraction, strands were stimulated electrically, at rates from $75-240 \text{ min}^{-1}$, while being kept at a constant temperature of

25 °C and held at L_{\max} . The developed isometric tension was measured at each frequency. The frequency at which the FF curve peaked was also recorded for each experiment.

When developed tension, normalized as a percentage of the maximum tension value recorded (P_{FF}), was plotted as a function of stimulus frequency, the relation shown in Fig. 3.10 was observed. It was observed that the active tension increased progressively in the range of 75-90 min^{-1} , had a peak at 90 min^{-1} (f_F) and showed a negative inotropic response with increasing frequency above 90 min^{-1} . The resting tension was not affected by electrical stimulation.

3.5.2 Force-Frequency Relationship at Different Temperatures in Culture Medium

This procedure was repeated at different temperatures varying from 15-37 °C. At all temperatures the FF relation (Fig. 3.11 a) was qualitatively similar to that obtained at 25 °C, but there were important quantitative differences. It was found that the frequency at which maximum tension occurred (f_F) was temperature dependent. The peak tensions at 15-20 °C were comparatively lower than those for 25 °C at all frequencies as might have been expected from the results of Section 3.4. At 22-25 °C, the tension values

Fig. 3.10 Force-Frequency relationship of the strands suspended in the culture medium.

This figure illustrates the relationship between isometric tension and stimulus frequency in suspended strands observed at 25 °C. Isometric tension, represented as a percentage of maximum tension developed (P_{FF}), is plotted on the ordinate. Stimulus frequency is plotted on the abscissa. The portion of the curve between spontaneous contraction rate and the first stimulus frequency is connected by a dotted line.

Because of the spontaneous activity of the strand, it was not possible to study the relationship in the frequencies below the spontaneous rate of contraction.

The force-frequency relationship appears as a biphasic response, demonstrating a positive inotropic response from spontaneous rate up to about 90 min^{-1} and thereafter a negative inotropic response.

The solid circle with two way standard deviation represents the mean value of tension and spontaneous contraction frequency of five strands.

Mean value of 100% $P_{FF} = 7.11 \mu\text{N}$.

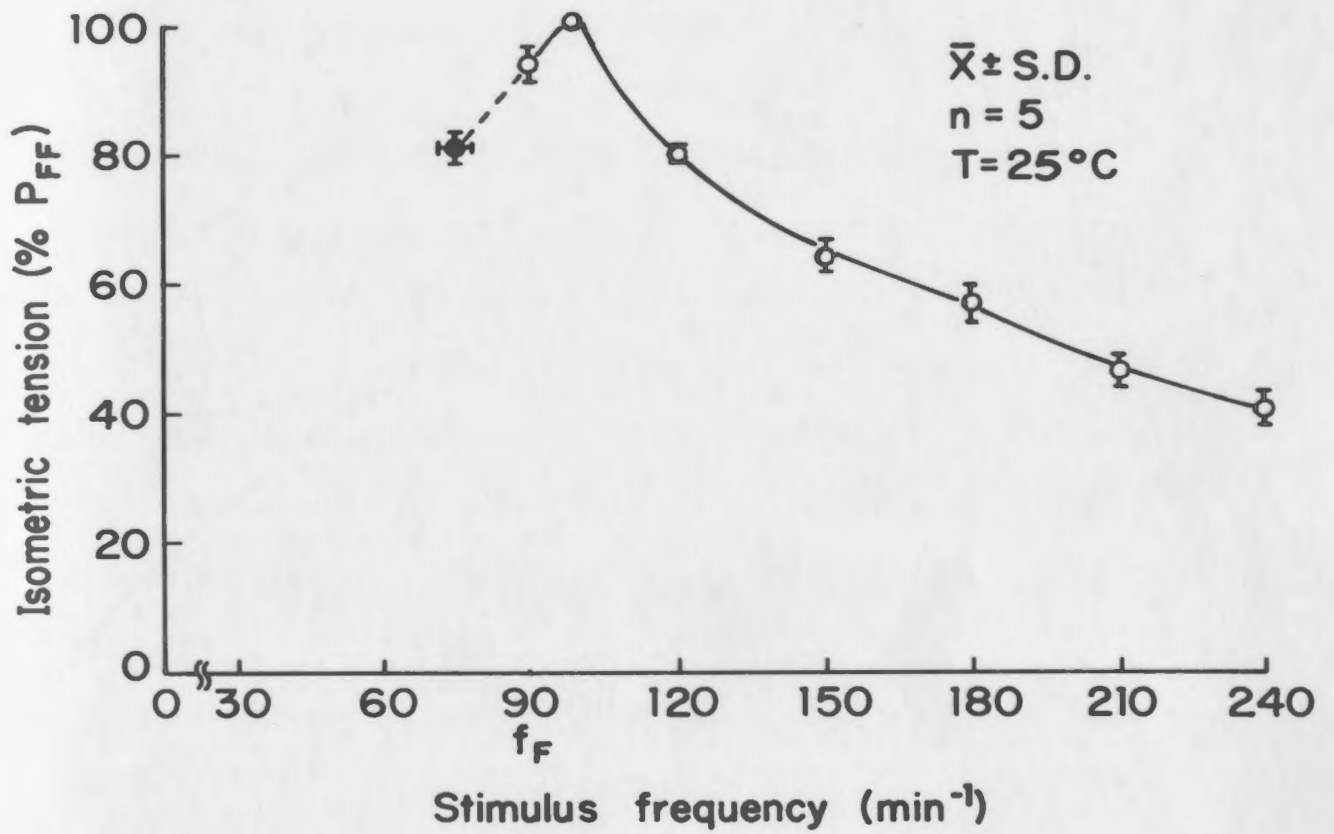
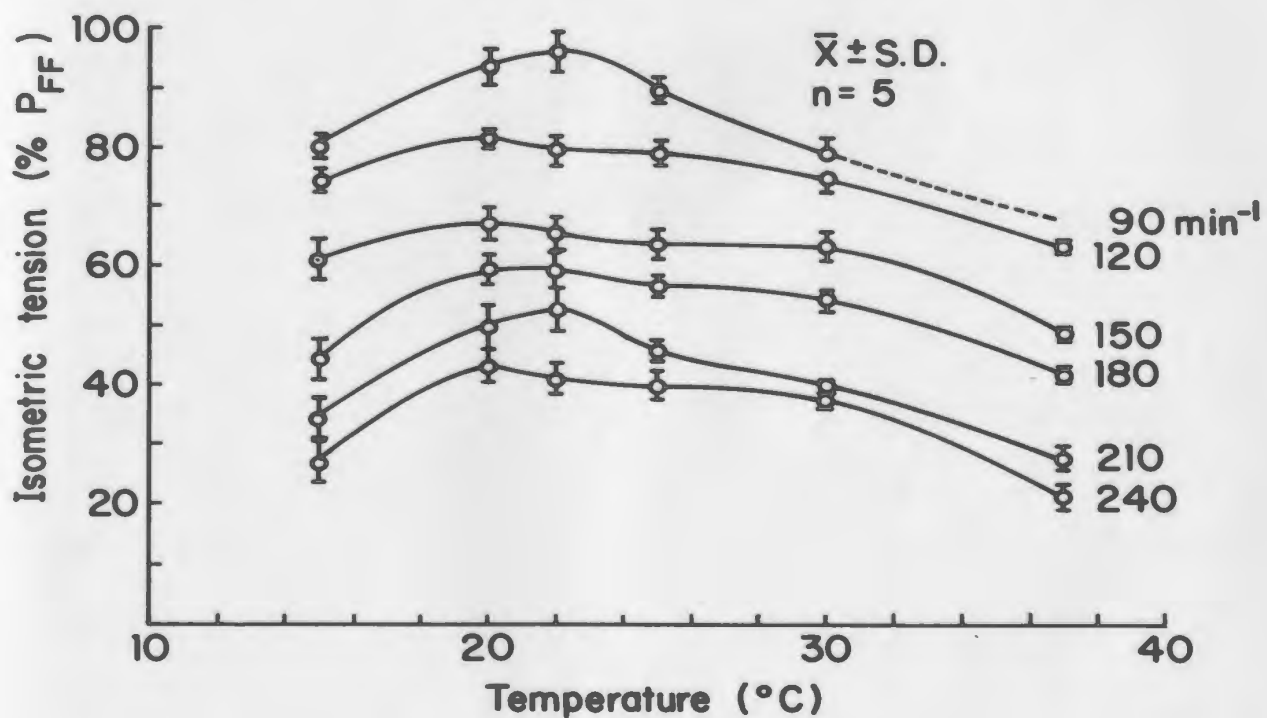
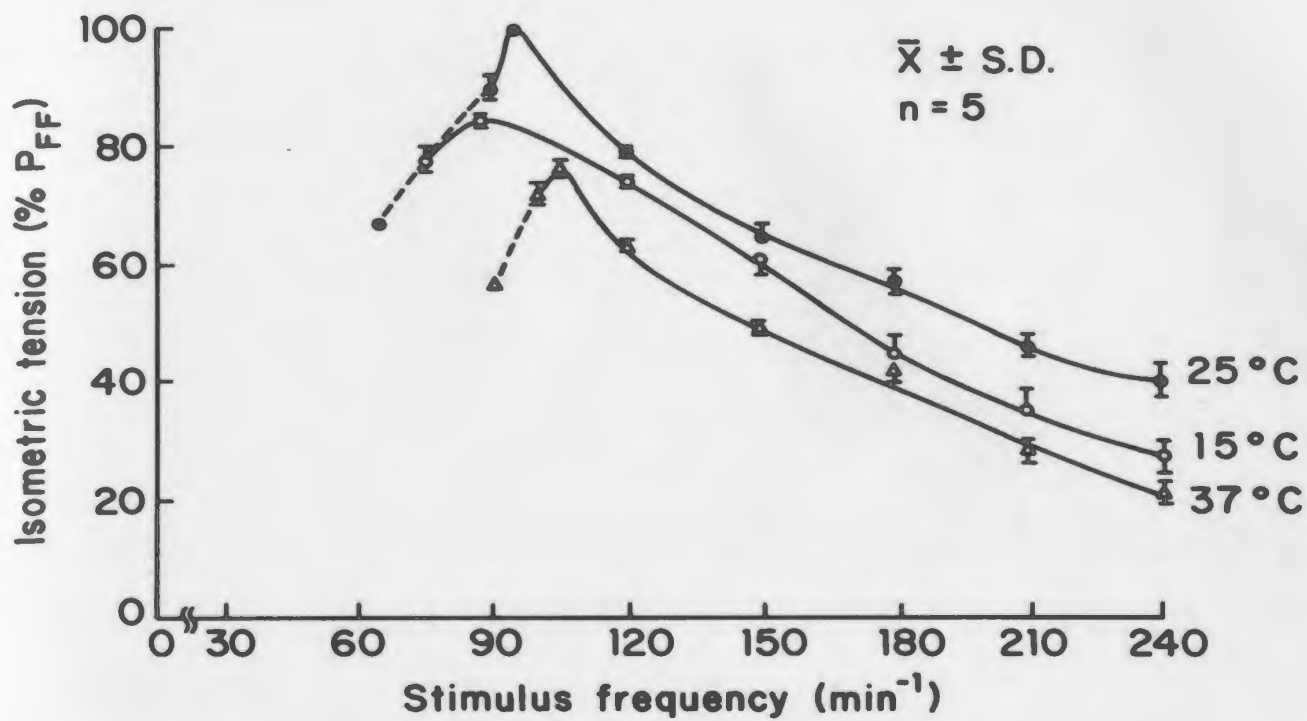


Fig. 3.11 Influence of temperature on the force-frequency relationship.

(a) Isometric tension is plotted on the Y-axis and the stimulus frequency on the X-axis for spontaneously contracting strands during electrical stimulation at three different temperatures.

The tension amplitudes are normalized as a percentage of maximal tension obtained for each strand in the entire family of temperature-force-frequency relationship. Each point is the mean \pm standard deviation of measurements from five strands. The force-frequency relationship at different temperatures were qualitatively similar to one another. The tension magnitudes at 25°C for all stimulus frequencies were greater than those at either 15°C or 37°C (Refer to Table-III for the complete data). Note that the frequency at which peak tension occurred appears to increase with increasing temperature.

(b) The same data is presented in a different form. Isometric tension is plotted versus temperature at different stimulus frequencies. At all frequencies of stimulation, tension increased in the temperature range of 15-20°C, maintained a plateau in the range of 20-25°C and decreased above 25°C. At stimulus rates of 75 and 90 min^{-1} the curves are incomplete, because the spontaneous contraction rate exceeded the driving rate at higher temperatures. Refer to Table III for complete data.



were equivalent, but decreased slowly as temperature increased to 37 °C. Table-III lists the tension magnitudes for all temperatures and frequencies studied.

Since maximum developed tension (P_{FF}) occurred at different frequencies for different strands, no single frequency ever had a mean value of 100% P_{FF} when the data was grouped. Fig. 3.11(a) shows the relation between percentage maximum developed tension (P_{FF}) and stimulus frequencies at different temperatures. Fig. 3.11 (b) illustrates the relation between percentage maximum tension (P_{FF}) and temperature at different stimulus frequencies above spontaneous contraction rates.

From Fig. 3.11 (b), it can be seen that maximum active tension occurred in the range of 20-25 °C at all frequencies, similar to that seen in Fig. 3.8. The observed maximum tension magnitudes occurred in the frequency range of 80-100 min^{-1} (f_F) with an apparent temperature dependence. Fig. 3.12 illustrates the linear relation between temperature and the frequency at which maximum tension developed (f_F).

Rate of rise of tension, ($+dP/dt$), increased with temperature at all frequencies. The time to peak tension was not altered in the range of 15-22 °C and decreased with further increase in temperature at all frequencies of stimulation.

TABLE III

Influence of Temperature on the Force-Frequency
Relationship in Suspended Cultured Cardiac Muscle Strands

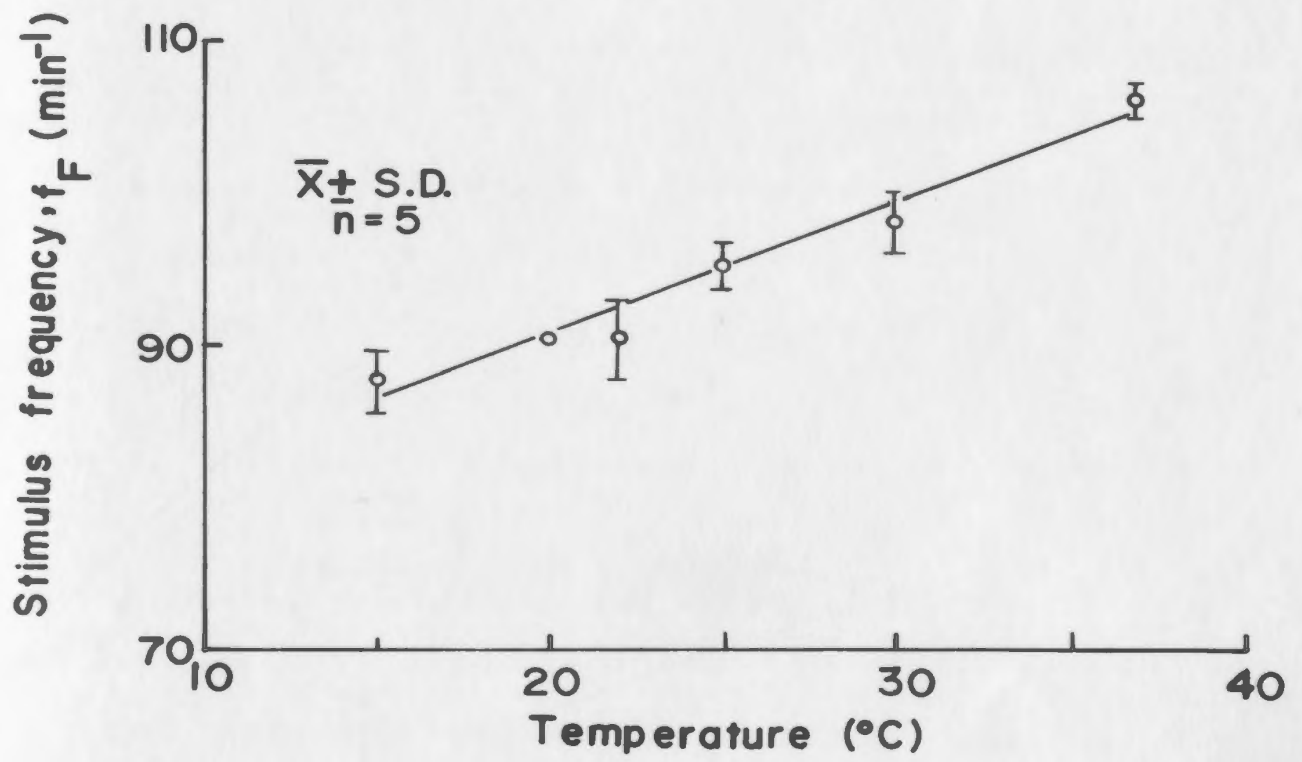
Stimulus frequency (min ⁻¹)	Amplitude of Active Tension (% P _{FF})					
	Temp: 15°C	20°C	22°C	25°C	30°C	37°C
75	78.2 ± 2.3	76.4 ± 2.1	84.1 ± 0.6	-	-	-
90	80.4 ± 1.7	93.5 ± 3.0	96.1 ± 2.2	93.7 ± 1.5	78.9 ± 2.8	-
120	74.1 ± 1.2	81.9 ± 1.1	79.6 ± 2.3	79.3 ± 0.8	75.0 ± 2.5	63.1 ± 0.9
150	61.2 ± 3.5	67.1 ± 2.7	65.5 ± 1.8	63.6 ± 2.5	63.3 ± 2.4	48.6 ± 1.1
180	44.3 ± 3.6	59.5 ± 2.5	59.5 ± 3.3	56.9 ± 1.5	54.6 ± 1.3	41.9 ± 1.5
210	34.5 ± 3.5	49.8 ± 3.7	52.6 ± 3.8	45.8 ± 1.9	40.1 ± 0.8	27.8 ± 2.0
240	27.1 ± 3.0	43.2 ± 2.8	40.9 ± 2.7	39.8 ± 2.6	37.6 ± 1.3	21.2 ± 2.2

111

Each data point represents the mean ± S.D., for 5 strands, held at L_{max}.

Fig. 3.12 The relationship between the stimulus frequency required for peak isometric tension (f_F) and temperature.

Stimulus frequency (f_F) expressed in contractions per minute is plotted on the ordinate; temperature is plotted on the abscissa. Each point is the mean \pm standard deviation from five strands suspended in the culture medium. There appears to be a linear relationship between f_F and temperature.



3.6 FLUID EXCHANGE CHARACTERISTICS OF THE CULTURE CHAMBER

With the chamber-perfusion arrangement used in this study equilibration and washout times were estimated to be about 45 s and 50 s respectively for the top 1.0 mm of the fluid in the chamber (Refer Sec. 2.10). Using a step-change in the input solution (from one concentration to another) as the input function and the mixing characteristics for equilibration or washout in the top 1.0 mm (which was found to be a ramp function) as the output function, the transfer function of the system was obtained using Hewlett-Packard Fourier Analyser Model 5451B. The transfer function indicated that the delay caused by the chamber was substantial and thus any dynamic analysis of isometric tension during solution changes were not valid (Refer Appendix-V).

With this in mind, the data obtained during the time when the concentration of a solution was changing can not be explained with any degree of confidence. However, the steady-state values or the responses of the strands occurring 3.0 min after a solution change (approximately 4 time constants) would represent the physiological properties of the strand. The discussion in the remainder of this thesis will be focussed on the steady-state responses to ionic manipulation even though the experimental records also contain the transients between two steady-state conditions.

3.7 THE INFLUENCE OF EXTRACELLULAR POTASSIUM ION CONCENTRATION

3.7.1 The Relationship Between Potassium Concentration and Spontaneous Contraction Rate

The spontaneous contraction rate of the suspended strands in the culture medium was $73 \pm 2 \text{ min}^{-1}$ (mean \pm S.D, n=6) at 25 °C. When the bathing medium was switched to SBSS the spontaneous rate decreased to $63 \pm 2 \text{ min}^{-1}$ (mean \pm S.D, n=5). Since the external potassium concentration was 6 and 3 mM in the culture medium and SBSS respectively, it appeared that lowering of $[\text{K}^+]_o$ resulted in a decrease in spontaneous rate of contraction.

Experiments were conducted at 25 °C, while $[\text{Ca}^{++}]_o$ and $[\text{Na}^+]_o$ were maintained at the standard values of 1.5 mM and 146.5 mM respectively. At the same time, external potassium concentration, $[\text{K}^+]_o$, was altered in the range of 1-10 mM. In these experiments, the spontaneous contraction rate varied directly with $[\text{K}^+]_o$. Actual high speed tracings at different values of $[\text{K}^+]_o$, obtained from a single strand, are shown in Fig. 3.13 while a plot of the $\log ([\text{K}^+]_o)$ Vs spontaneous contraction rate is shown in Fig. 3.14. From 1 to 2 mM, the rate remained constant at $57 \pm 1 \text{ min}^{-1}$ (mean \pm S.D, n=5); from 2 to 8 mM it

Fig. 3.13 The influence of extracellular potassium concentration, $[K^+]_o$, upon the rate of spontaneous contraction and isometric tension developed by the strand preparation.

All chart records shown were obtained from a representative spontaneously contracting strand during manipulation of $[K^+]_o$. Paired high- and low-speed records are shown for $[K^+]_o = 1, 3, 5, 8$ and 10 mM. The rate of spontaneous contraction increased with increasing $[K^+]_o$ while the amplitude of active tension or the level of resting tension was not affected by manipulation of $[K^+]_o$.

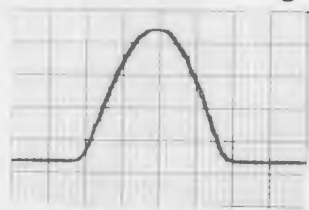
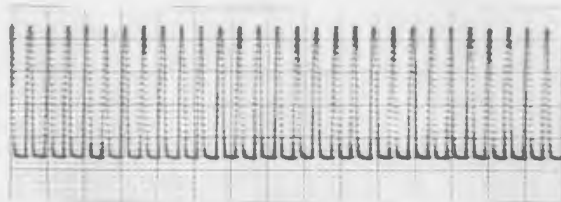
Isometric
tension
(μN)

4
0



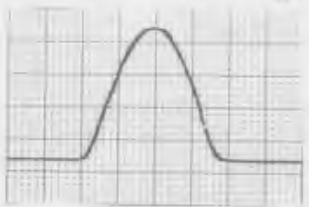
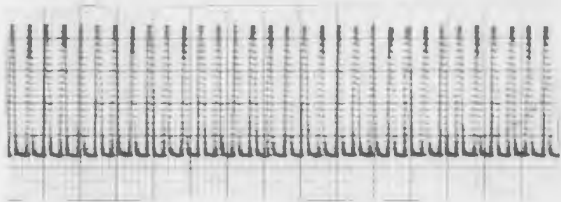
$[\text{K}^+]_o = 1 \text{ mM}$

rate : 58 min^{-1}



$[\text{K}^+]_o = 3 \text{ mM}$

rate : 64 min^{-1}



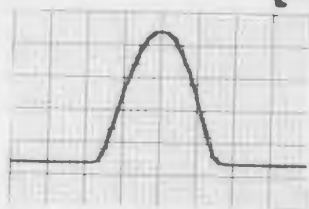
$[\text{K}^+]_o = 5 \text{ mM}$

rate : 71 min^{-1}



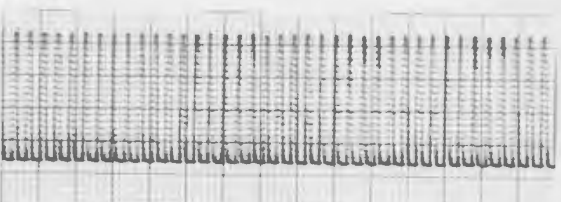
$[\text{K}^+]_o = 8 \text{ mM}$

rate : 74 min^{-1}



$[\text{K}^+]_o = 10 \text{ mM}$

rate : 79 min^{-1}



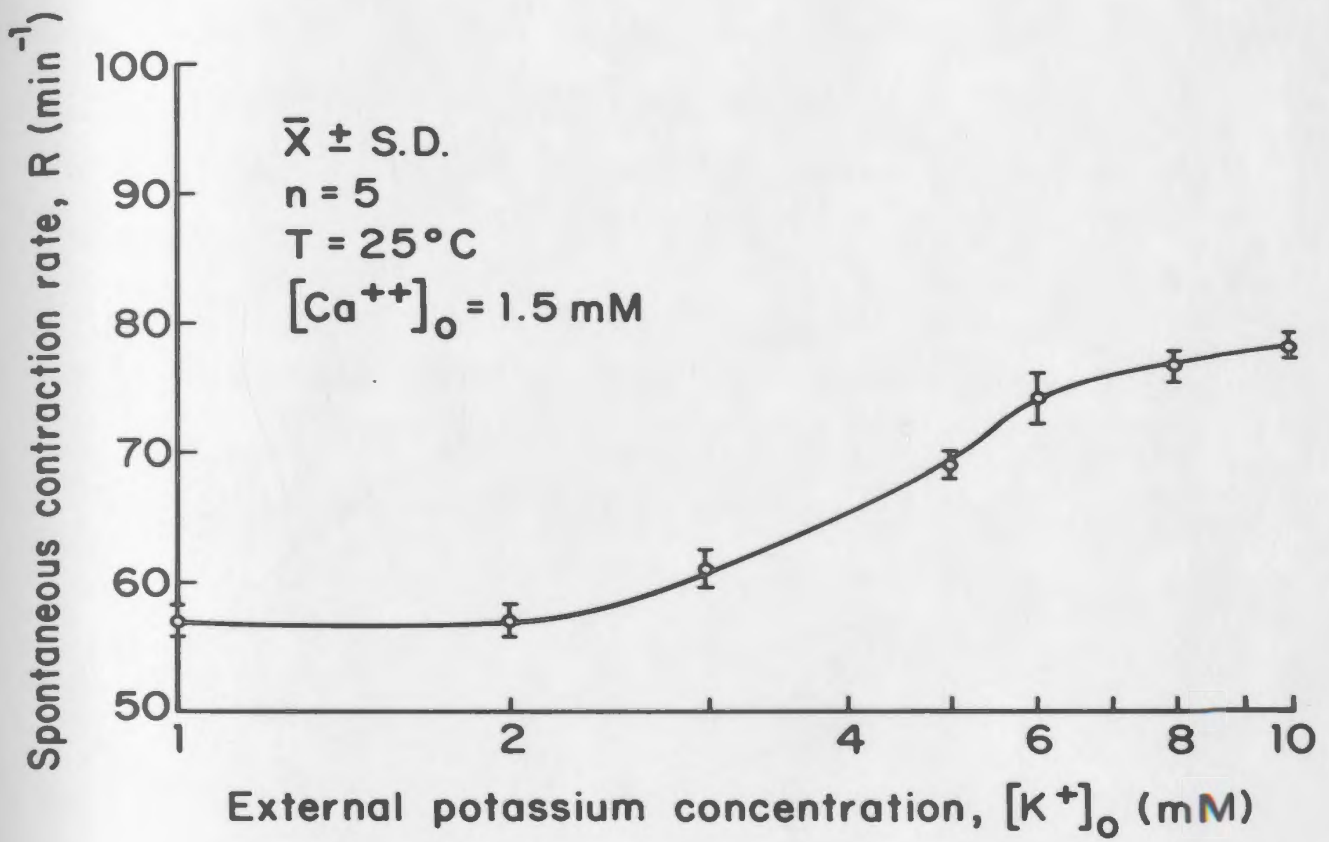
0.0 0.5
Time (sec)

0.0 0.5
Time (min)

Fig. 3.14 The relationship between external potassium concentration, $[K^+]_o$, and the spontaneous contraction rate of cultured myocardial strands is illustrated in this figure.

The logarithm of $[K^+]_o$ (in mM) is expressed on the abscissa while the spontaneous contraction rate (per minute) is plotted on the ordinate in linear scale. Each data point represents the mean \pm standard deviation of the response obtained from 5 different strands.

There appears to be a potassium dose-action relationship; spontaneous contraction rate increasing progressively with $[K^+]_o$.



increased from 57 to 77 min^{-1} ; and for $[\text{K}^+]_0$ greater than 8 mM it reached a plateau of $78 \pm 1.0 \text{ min}^{-1}$.

It should be noted that the rate in the SBSS with 6 mM $[\text{K}^+]_0$ was $74 \pm 1.5 \text{ min}^{-1}$ (mean \pm S.D, $n=5$). This agrees very well with the rate of $73 \pm 2.35 \text{ min}^{-1}$ recorded from the same strand in culture medium with the same $[\text{K}^+]_0$. Over the range studied, changes in $[\text{K}^+]_0$ did not alter either the amplitude of the active tension or the resting tension.

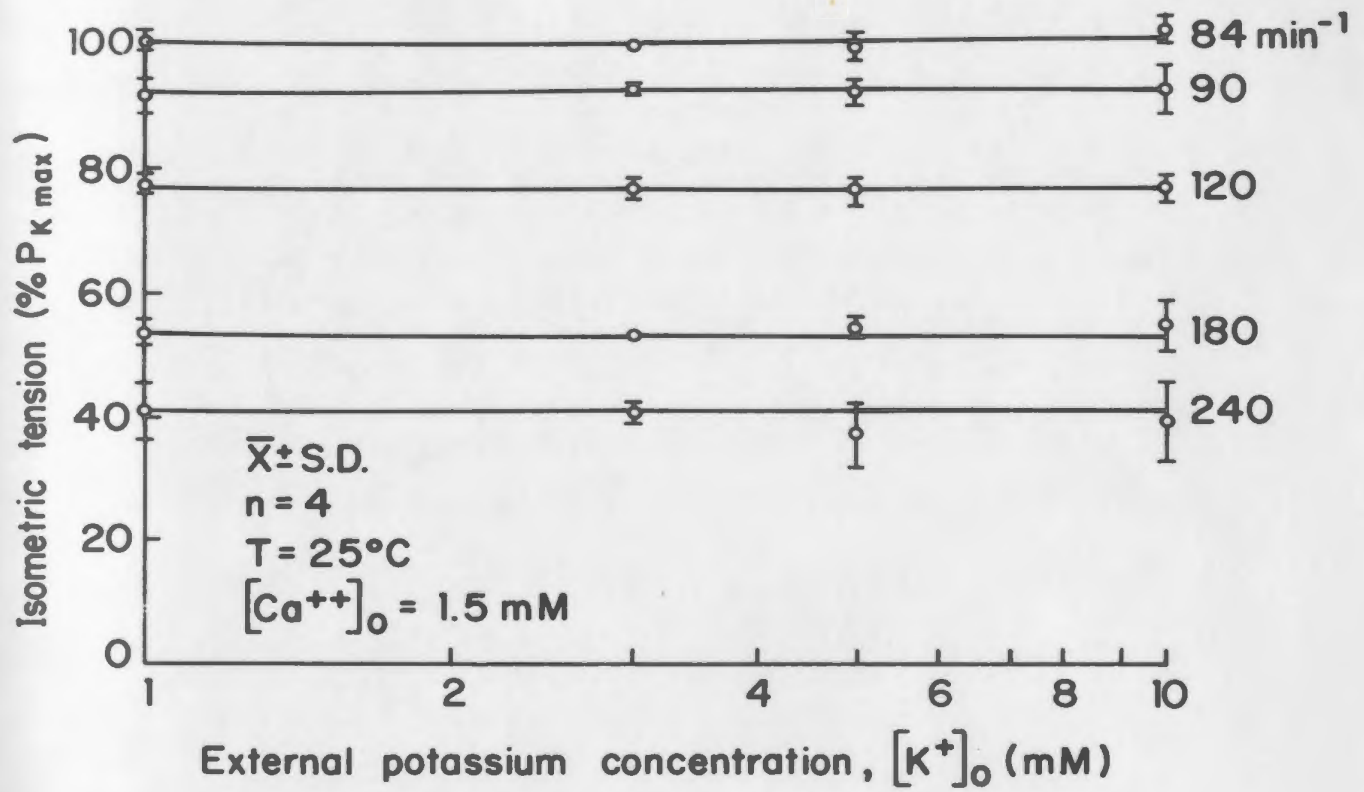
3.7.2 Influence of $[\text{K}^+]_0$ Upon the Force-Frequency Response

The force-frequency response of this preparation was studied at different $[\text{K}^+]_0$. Allowing for changes in the spontaneous contraction rate induced by changes in $[\text{K}^+]_0$, the FF responses for different $[\text{K}^+]_0$ were superimposable. Thus the FF curve obtained in normal culture medium (Fig. 3.10) is representative and unaffected by changes in $[\text{K}^+]_0$. Similarly, when active tension was plotted against $[\text{K}^+]_0$ at several constant frequencies, it was shown that active tension was independent of $[\text{K}^+]_0$ (see Fig. 3.15).

Fig. 3.15 The influence of external potassium concentration, $[K^+]_o$, upon the force-frequency relationship.

Isometric tension (ordinate) is plotted against the logarithm of $[K^+]_o$ (abscissa), for different stimulus frequencies. Tension values were normalized as a percentage of maximum force developed during the force-frequency study, $P_K \text{ max}$. Each data point represents the mean \pm standard deviation of the response obtained from 4 different strands.

The $[K^+]_o$ did not influence the inotropic response of the strand preparation.



3.8 INFLUENCE OF EXTRACELLULAR CALCIUM ION CONCENTRATION

Cardiac muscle depends on extracellular calcium for tension development (Ringer, 1883). To assess the dependency on $[Ca^{++}]_o$ in the strand model, the calcium concentration was manipulated using a continuous perfusion system, as described in Section 2.10. The concentrations of extracellular Na^+ and K^+ were kept constant at 146.5 mM and 3.0 mM respectively (as in SBSS).

3.8.1 Calcium Dose-Action Relationship

The SBSS had a normal $[Ca^{++}]_o$ of 1.5 mM (vide Table-I). The range of calcium concentrations studied was between 1.0×10^{-7} and 5.0×10^{-2} M. At calcium concentrations below 2.5×10^{-4} M, EGTA buffer (Jewell and Reugg, 1966) was used to obtain precise calcium concentrations.

To obtain the dose-response data, spontaneously beating strands (at a rate of 63 min^{-1}) at 25°C were held at L_{max} , and $[Ca^{++}]_o$ was varied by switching between reservoirs containing SBSS of different calcium concentrations. The order of concentration changes was randomized (using a random number table) with periodic switching to SBSS to verify the control values.

Once the isometric active tension amplitude had stabilized at its new value, contractile parameters were measured. Fig. 3.16 shows the semi-logarithmic plot of a calcium dose-action curve, obtained from 6 different strands. The threshold dose was about 1.0×10^{-5} M; the response was nonlinear in the range of 1.0×10^{-5} - 5.0×10^{-4} M. In the range of 5.0×10^{-4} - 5.0×10^{-3} M the response appeared as a straight line when plotted semi-logarithmically, reaching a peak response ($P_{\text{N}Ca}$) at 5.0×10^{-3} M. Above this concentration the tension decreased slightly with increasing calcium concentration.

The rate of rise of tension, ($+dP/dt$), for the same preparations showed a response similar to that of active tension (Fig.3.17).

3.8.2 Isometric Responses at $[Ca^{++}]_o < 1.0 \times 10^{-6}$ M

The equilibrium steady-state isometric active tension was zero at calcium concentrations of 1.0×10^{-6} M and below (Fig.3.16). Upon switching solutions, the time required to reach steady-state (zero tension) at 1.0×10^{-6} M was considerably longer than that at higher concentrations.

Fig. 3.18 illustrates the time course of tension response when switching to 1.0×10^{-6} M $[Ca^{++}]_o$ from various higher concentrations. Within the first 3-4 min

Fig. 3.16 The calcium dose-action relationship in spontaneously contracting cultured myocardial strands.

Isometric tension (ordinate) is plotted against the logarithmic concentration of external calcium, $[Ca^{++}]_o$ (abscissa). Tension amplitudes were normalized as a percentage of maximum response obtained (at 5.0×10^{-3} M $[Ca^{++}]_o$), called $P_{N\text{Ca}}$. Threshold for tension generation occurred at 1.0×10^{-5} M. The relation increased progressively up to 5.0×10^{-3} M, where tension peaked; at higher concentrations there was a slight decrease in tension. Between 5.0×10^{-4} and 5.0×10^{-3} M, the semi-logarithmic dose-action plot was a good approximation of a straight line.

Each data point denotes the mean \pm standard deviation of tension responses obtained from 6 different strand preparations.

(100% $P_{N\text{Ca}} = 6.27 \pm 0.52$ μN , mean \pm standard deviation, $n=6$)

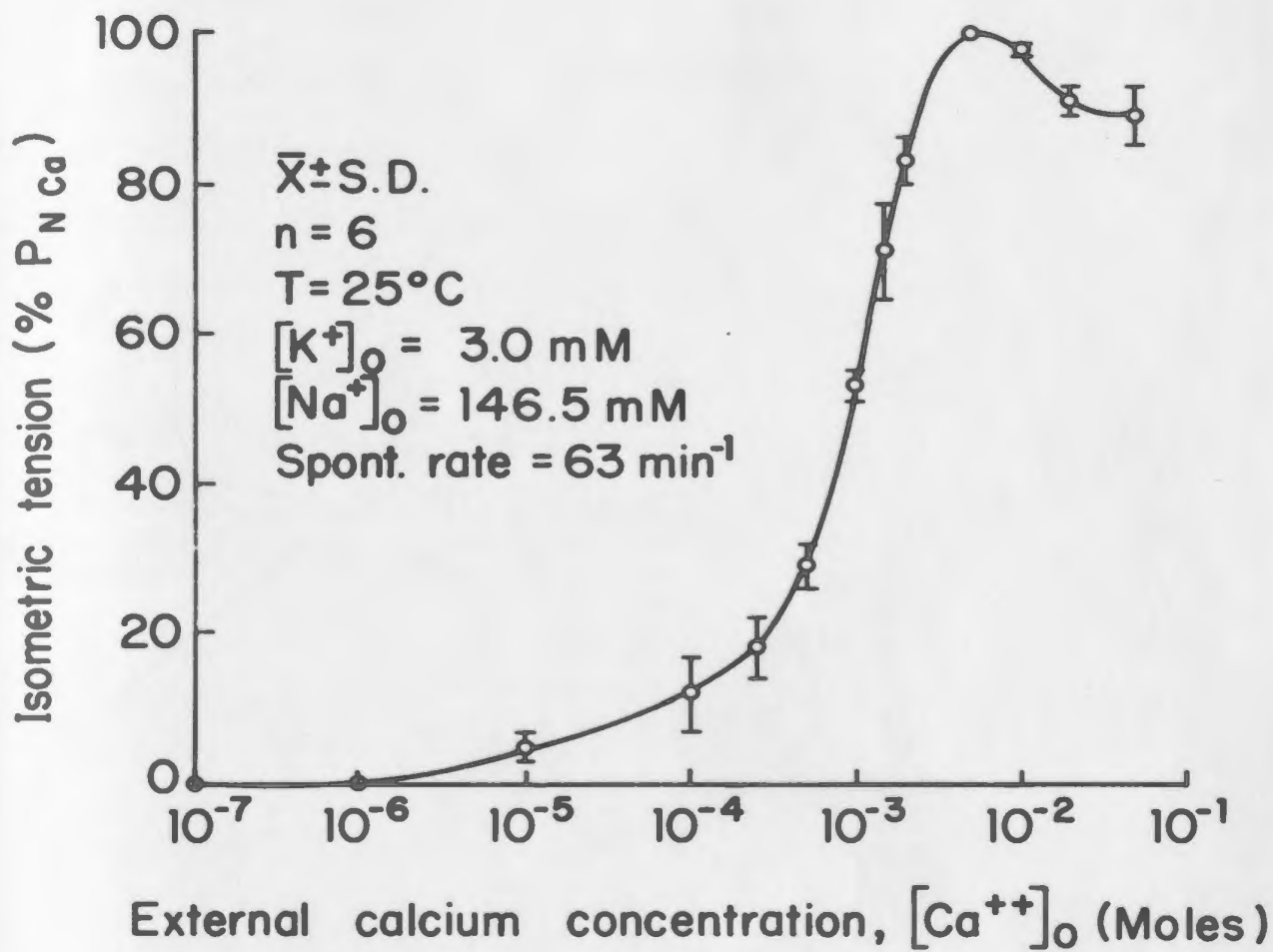


Fig. 3.17 The relationship between maximal rate of rise of tension, (dP/dt), and external calcium concentration, $[Ca^{++}]_o$, in spontaneously contracting cultured cardiac muscle strands.

Rate of rise of tension is plotted on the ordinate and the logarithm of $[Ca^{++}]_o$ on the abscissa. The dP/dt values were normalized with respect to the maximum value obtained at 5.0×10^{-3} M $[Ca^{++}]_o$. Each data point represents the mean \pm standard deviation of the values obtained from 6 strands.

This relationship is similar to that seen between isometric tension and $[Ca^{++}]_o$, (Fig. 3.16).

(100% max = $38.5 \pm 4.35 \mu\text{N sec}^{-1}$, mean \pm standard deviation, n=6)

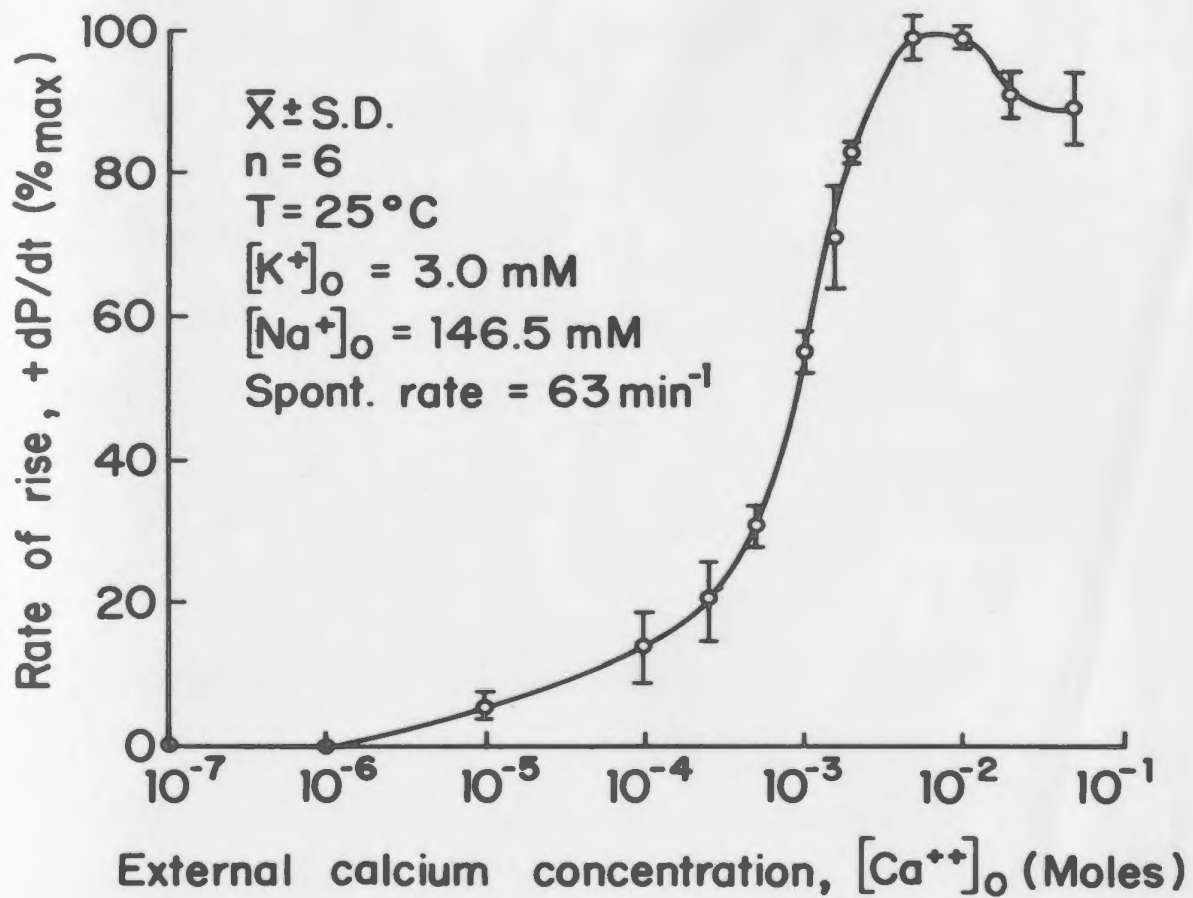
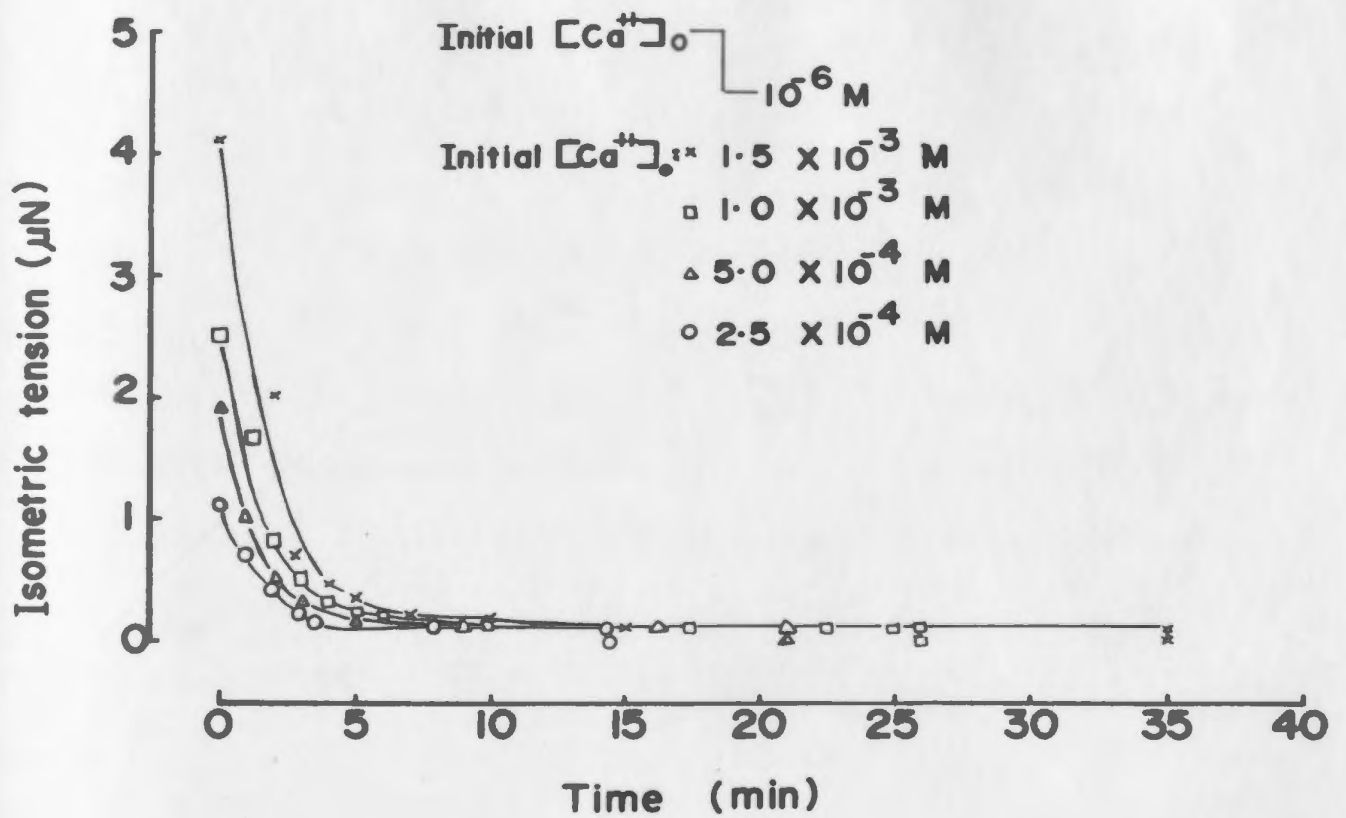


Fig. 3.18 The relationship between isometric tension and time of exposure to low external calcium concentration (1.0×10^{-6} M) following transfer from varying high initial concentrations.

Isometric tension in μN is represented on the ordinate, elapsed time of exposure to the low calcium on the abscissa. The data presented is derived from a single strand; similar results were obtained from two other preparations. The perfusion medium was switched to a solution containing low $[\text{Ca}^{++}]_o$ (1.0×10^{-6} M) from four different initial concentrations (\times : 1.5×10^{-3} M; \square : 1.0×10^{-3} M; Δ : 5.0×10^{-4} M; \circ : 2.5×10^{-4} M).

The tension magnitudes decreased rapidly in the first 3-5 minutes to a very low value (about $0.1 \mu\text{N}$) and thereafter maintained a constant value for a longer period of time. Active tension disappeared abruptly as shown by either \times or Δ or \square or \circ . The time to reach zero tension increased as a direct proportion with increasing initial $[\text{Ca}^{++}]_o$.



the tension dropped to approximately 10% P_{NCa} and decreased very slowly over the next 10-35 minutes. Finally, the tension dropped to zero abruptly. Fig. 3.19 shows the actual tracings at different times after the perfusion medium was switched from 1.5×10^{-3} to 1.0×10^{-6} M.

The time to reach zero tension at 1.0×10^{-6} M depended upon the initial concentration from which it was switched. Fig. 3.20 plots initial concentration versus time taken to reach zero tension. When switched to 1.0×10^{-6} M from 1.0×10^{-4} M $[\text{Ca}^{++}]_0$, active tension was abolished in 5.5 minutes as compared to about 34.0 minutes when switched to 1.0×10^{-6} M from 1.5×10^{-3} M. At concentrations above 1.5×10^{-3} M, the time taken to reach zero tension remained constant at about 34.0 minutes.

Conversely, when the perfusates were returned to a higher concentration from 1.0×10^{-6} M, the time taken to reach a steady-state tension value depended upon the final concentration. Fig. 3.21 shows the relation between final concentration and time taken to reach steady-state active tension. At calcium concentrations greater than 1.5×10^{-3} M, the strands equilibrated very quickly, whereas at lower concentrations it took a longer time to reach steady-state.

From Figures 3.20 and 3.21 it appears that 1.5×10^{-3} M $[\text{Ca}^{++}]_0$ was a critical concentration, where a transition took place.

Fig. 3.19 Representative records of isometric tension responses during calcium washout in a spontaneously contracting cultured myocardial strand.

At the beginning of the trace the initial $[Ca^{++}]_o$ was 1.5×10^{-3} M. The arrow indicates the time at which the perfusion medium was replaced by one containing 1.0×10^{-6} M $[Ca^{++}]_o$. The time markers and the tension scales are indicated.

A : Both resting (RT) and active (AT) tensions are shown. Note that RT was not altered during $[Ca^{++}]_o$ manipulation. Within three minutes, the AT magnitudes decreased to a low steady-state active tension.

B : The reduced tension was maintained for a long time with very slow decrement. Note the doubling of amplification and base line shift for isometric tension. The RT was not altered.

C : A further doubling of amplification, otherwise a continuation. Same as B except for a scale change.

D : Continuation from C. Note that at 34.9 min the amplitude of spontaneous contractions disappeared abruptly and only the RT remained.

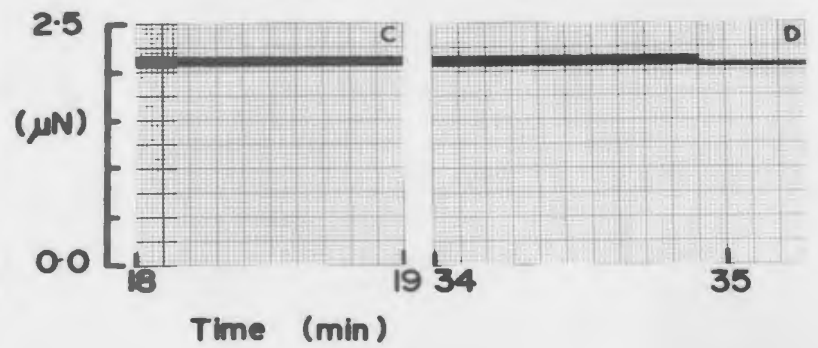
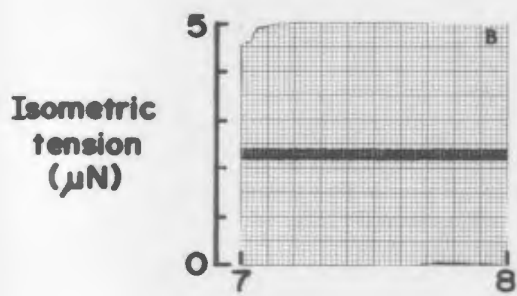
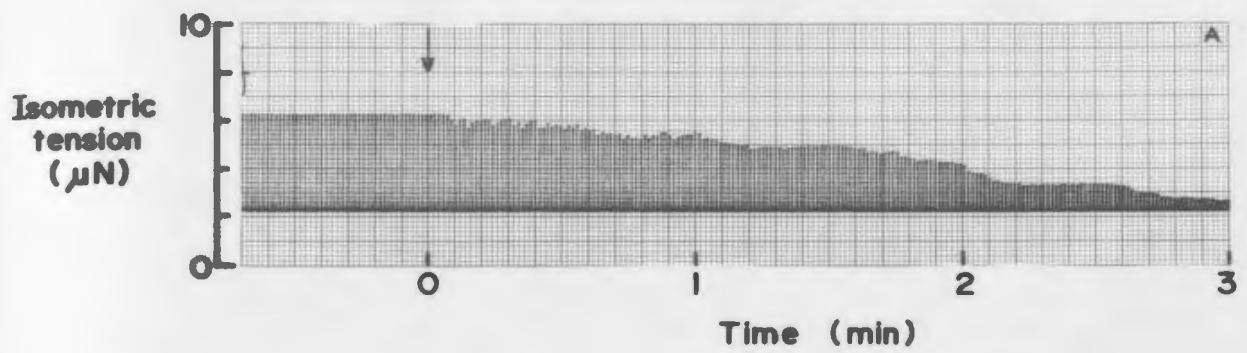


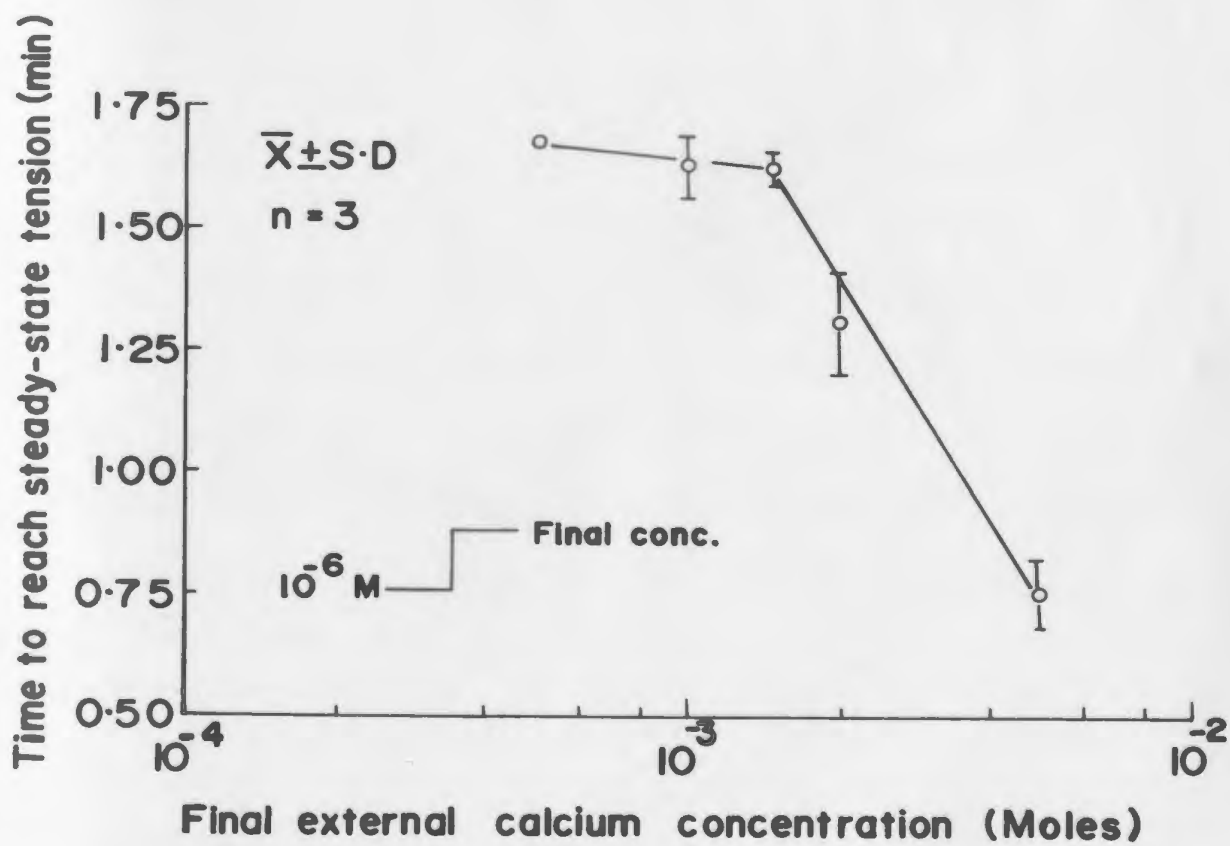
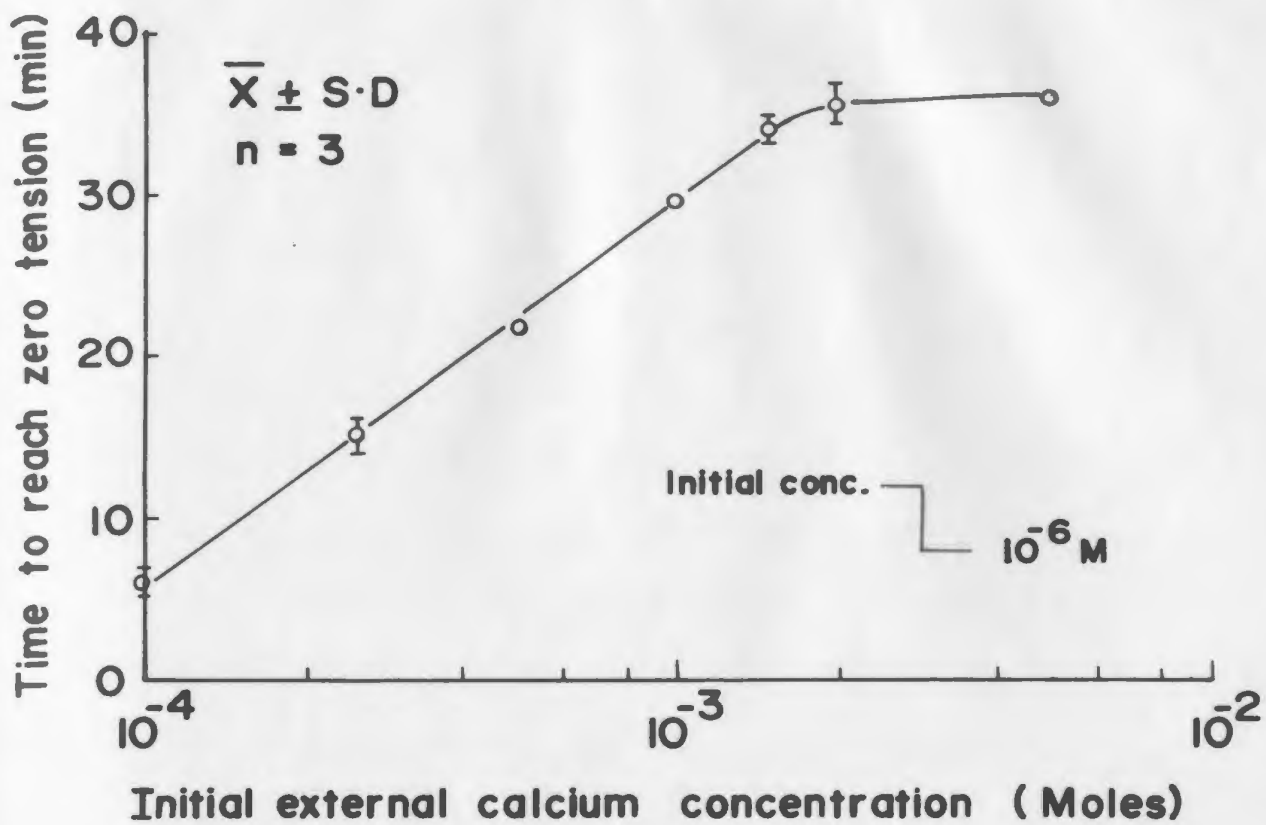
Fig. 3.20 The relationship between the time to reach zero tension upon exposure to 1.0×10^{-6} M $[\text{Ca}^{++}]_0$ and initial $[\text{Ca}^{++}]_0$.

Time to reach zero tension (in minutes) on the ordinate is plotted against the logarithm of initial $[\text{Ca}^{++}]_0$ (in Moles) on the abscissa. Each point represents the mean \pm standard deviation of the values from 3 preparations.

With low initial $[\text{Ca}^{++}]_0$, the strand reached zero tension quickly while higher initial $[\text{Ca}^{++}]_0$ caused longer time. Note that above 1.5×10^{-3} M, the time to reach zero tension attained an apparent plateau, a transition occurred at 1.5×10^{-3} M.

Fig. 3.21 The relationship between the time to reach steady-state isometric tension and $[\text{Ca}^{++}]_0$ in spontaneously contracting myocardial strands transferred from 1.0×10^{-6} M to a higher calcium concentration.

Time to reach steady-state tension (in minutes) on the ordinate is plotted versus the logarithm of the final $[\text{Ca}^{++}]_0$ on the abscissa. With increasing final $[\text{Ca}^{++}]_0$ values, the strand equilibrated faster. Note that the transition occurring at 1.5×10^{-3} M is analogous to that seen in Fig. 3.20.



3.8.3 Influence of $[Ca^{++}]_o$ on the Force-Frequency Response

The force-frequency response of this preparation at 25 °C was studied at different $[Ca^{++}]_o$, while $[Na^+]_o$ and $[K^+]_o$ were maintained at their standard levels (146.5 mM and 3 mM respectively).

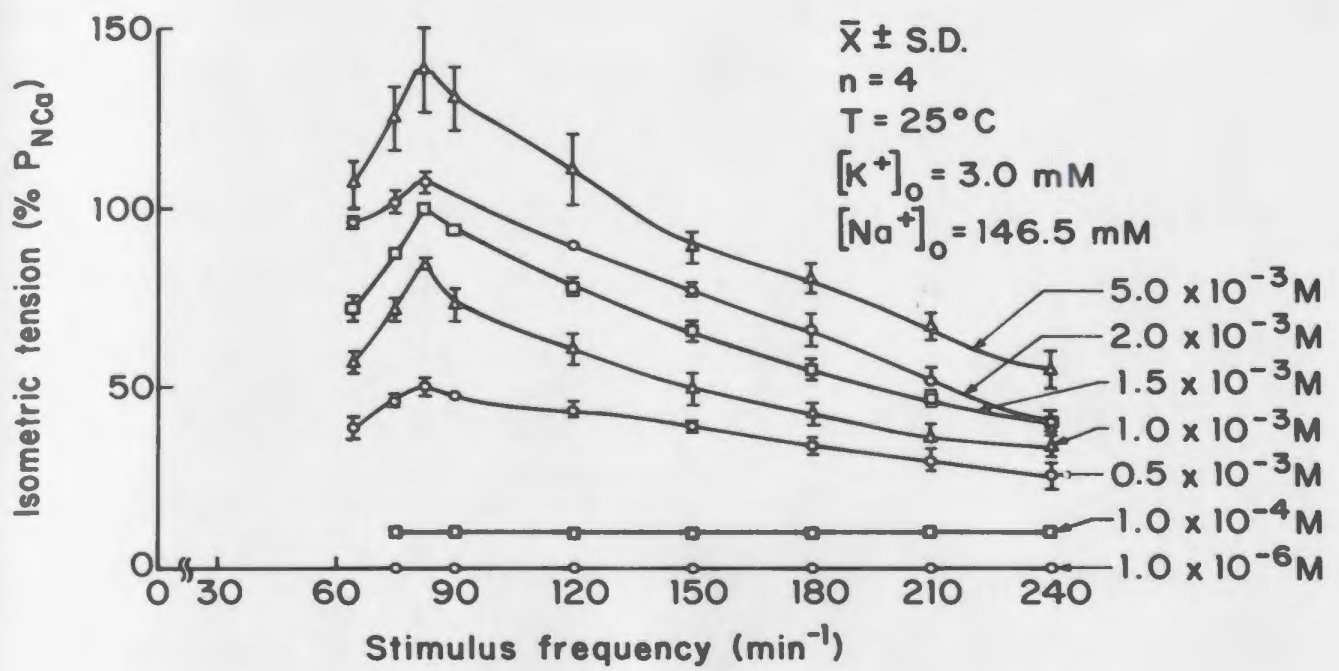
It was observed that at equilibrium, active tension was not developed at 1.0×10^{-6} M and below, even when strands were electrically stimulated. At higher values of $[Ca^{++}]_o$ the active tension was proportional to $[Ca^{++}]_o$ but remained constant at all frequencies of stimulation (Fig. 3.22). For values of $[Ca^{++}]_o$ equal to or greater than 0.5×10^{-3} M, the force-frequency response bore a general resemblance to that of Fig. 3.10. In the frequency range of 65 - 83 min^{-1} , the tension magnitudes increased, reaching a peak at $82 \pm 2.4 \text{ min}^{-1}$ (mean \pm S.D, n=4). Above this frequency, the tension amplitudes decreased with increasing stimulus frequencies. Throughout the experimental frequency range, isometric active tension was directly proportional to $[Ca^{++}]_o$ but the spontaneous contraction rate, the frequency at which the peak tension was developed and the resting tension were independent of $[Ca^{++}]_o$.

Fig. 3.22 The influence of $[Ca^{++}]_O$ on the force-frequency relationship in cultured myocardial strands.

Normalized isometric tension, $\%P_{N\text{Ca}}$, represented on the ordinate, is plotted versus stimulus frequency (min^{-1}) on the abscissa for seven different values of $[Ca^{++}]_O$ (5.0×10^{-3} M, 2.0×10^{-3} M, 1.5×10^{-3} M, 1.0×10^{-3} M, 0.5×10^{-3} M, 1.0×10^{-4} M and 1.0×10^{-6} M). $100\% P_{N\text{Ca}}$ represents the isometric tension developed during spontaneous contraction at 5.0×10^{-3} M $[Ca^{++}]_O$.

There was a roughly parallel decrement in the entire force-frequency relation with decreasing $[Ca^{++}]_O$, until 0.5×10^{-3} M. At this and all lower concentrations there was a qualitative change in the response, the frequency sensitivity was impaired and disappeared at 1.0×10^{-4} M. At a concentration of 1.0×10^{-6} M, no active tension was developed even with stimulation.

Each data point represents the mean \pm standard deviation of the value obtained from 4 different strands. Neither the spontaneous contraction rate, nor the frequency at which the force-frequency relation peaked (f_F), was influenced by the manipulation of $[Ca^{++}]_O$.



3.8.4 The Influence of Temperature on Calcium-Force-Frequency Response

The influence of temperature on the force-frequency relation at different calcium concentrations was similar to that seen in Section 3.5; temperature altered the frequency at which peak tension in the force-frequency response was seen (f_F). Fig 3.23 shows the relation between temperature and f_F , both in the culture medium, at $[Ca^{++}]_O = 1.5$ mM (same as Fig.3.12) and in SBSS with a $[Ca^{++}]_O$ of 5.0 mM. The temperature - f_F curves in the SBSS were identical at $[Ca^{++}]_O$ values greater than or equal to 1.0 mM.

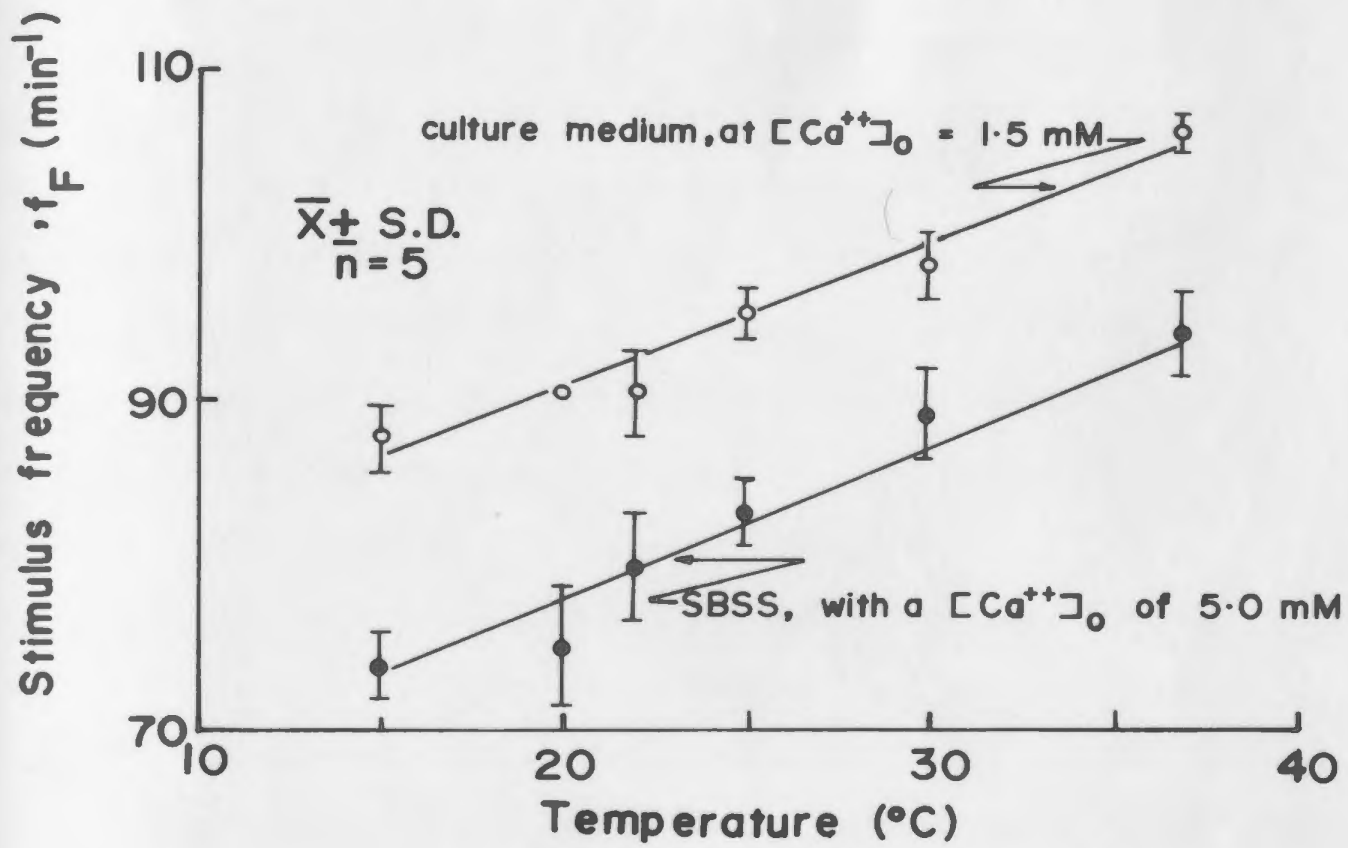
3.9 INFLUENCE OF EXTRACELLULAR SODIUM ION CONCENTRATION

Manipulation of extracellular sodium concentration, $[Na^+]_O$, alters the spontaneous contraction rate in any excitable tissue, and it has been observed by a number of investigators that sodium also changes the isometric tension developed by cardiac muscle (Luttgau and Niedergerke, 1958; Mullins, 1979; Horackova and Vassort, 1979). To observe whether sodium alters the inotropic and/or chronotropic properties of the cultured heart muscle strands, extracellular sodium was lowered from its standard value in the SBSS (146.5 mM) down to as low as 40 mM.

Fig. 3.23 Influence of temperature upon the stimulus frequency required for maximal isometric tension (f_F) in cultured myocardial strands in culture medium and SBSS.

Stimulus frequency, f_F , (min^{-1}) represented on the ordinate, is plotted versus temperature (in $^{\circ}\text{C}$), represented on the abscissa. Each point is the mean \pm standard deviation of the response from 5 different strands. The f_F value increased with increasing temperature, but remained unchanged for different $[\text{Ca}^{++}]_o$ when observed in SBSS. Since the curves obtained using other external calcium concentrations (1.0, 1.5 and 2.0 mM) were superimposable, only one set of values (corresponding to 5.0 mM, represented in closed circles) is shown.

Fig. 3.12 is reproduced here (open circles) for comparison. Except for the elevation in basal spontaneous rate due to the higher $[\text{K}^+]_o$ present in the culture medium, the temperature relation appears identical to that in SBSS.



3.9.1 Influence of Varied $[\text{Na}^+]_o$ on the Rate and Strength of Spontaneous Contraction

Unlike calcium and potassium which affected either the inotropic or chronotropic responses respectively, modification of $[\text{Na}^+]_o$ altered both the spontaneous rate and the strength of contraction of the suspended strands.

As $[\text{Na}^+]_o$ was reduced in the medium surrounding spontaneously contracting strands, no noticeable change was seen in the contractile response until $[\text{Na}^+]_o$ reached 100 mM when the rate of contraction decreased from 62 to 59 min^{-1} (Figures 3.24 & 3.29). When $[\text{Na}^+]_o$ was further reduced, the rate of contraction continued to drop and the active tension magnitudes began to increase dramatically, reaching a maximum at 55 mM. At this sodium concentration, the active tension was often as high as 300% of its control value (in SBSS).

When the sodium content of extracellular fluid was reduced from SBSS to any value below 100 mM (all other ions remaining at their standard concentrations), three distinct phases in the isometric tension response were seen. Within 1.0-1.5 minutes after the low sodium solution entered the chamber, AT amplitudes increased rapidly to a peak value and then decreased slowly over the next 1.5-3.0 minutes to a stable plateau of about 80-85% of the peak value. This steady-state level was maintained as long as the low sodium

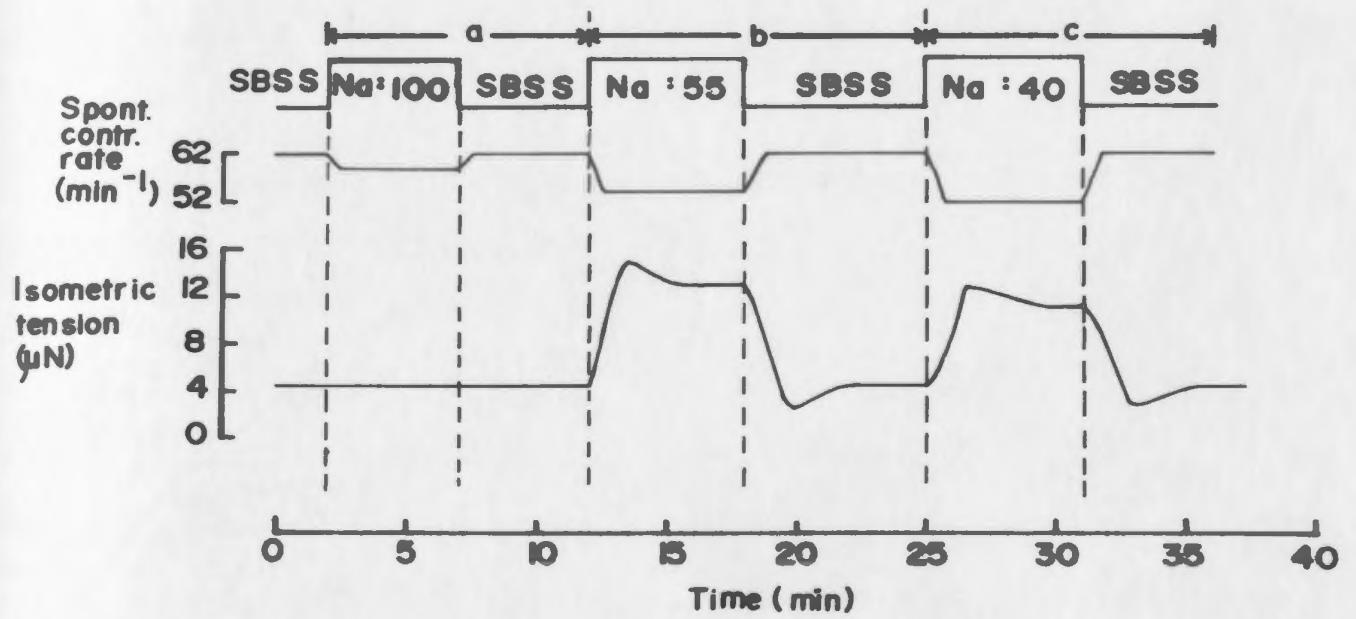
Fig. 3.24 The influence of varying external sodium concentration, $[\text{Na}^+]_o$, upon the contractility of the cultured myocardial strands.

A representative experiment is shown in this figure. The upper line indicates the timing for solution changes; the second line, the rate of spontaneous contraction (min^{-1}); and the third line, an envelope representing the tension peaks of the spontaneous isometric contractions (μN).

Panel a: Decreasing $[\text{Na}^+]_o$ to 100 mM resulted in a slight reduction in spontaneous contraction rate; isometric tension was not altered. Return to SBSS restored the control values.

Panel b: When $[\text{Na}^+]_o$ was lowered to 55 mM, contraction rate decreased further. Isometric tension magnitudes increased dramatically in the first 1.1-1.3 min, declined over the next 1.5 min, and thereafter maintained a potentiated steady-state level. Return to SBSS restored the contraction rate to control values within 0.5 min while tension dropped below the control value within 1.5 min. Tension returned to control levels within the next 2.0 minutes.

Panel c: The response to 40 mM $[\text{Na}^+]_o$ was qualitatively the same as in panel b.



solution was in the chamber. In contrast to these changes, the spontaneous rate of contraction changed within the first minute of switching to a new solution.

When the low sodium perfusate was replaced by SBSS, the tension values at first decreased below the control values for 1.0-2.0 minutes and then slowly returned to the control value. The spontaneous rate of contraction returned to the control value within the first minute of switching back to SBSS.

3.9.2 Analysis of Possible Errors Introduced by Substitution of Choline for Sodium

In the study of $[\text{Na}^+]_o$ investigators have substituted lithium, magnesium, choline, tris, (Luttgau and Niedrigerke, 1958; Schanne, Ruiz-Cereti, Payet and Deslauriers., 1979, Horackova and Vassort, 1979) or sucrose (Horackova and vassort, 1979) for Na^+ to maintain constant osmolarity. The most commonly used agents have been lithium, sucrose, and choline. Lithium produces either inotropic inhibition (at 1.0 mM Ca^{++}) or facilitation (at 4.0 mM Ca^{++}) (Luttgau, and Niedrigerke, 1958). Sucrose (Horackova and Vassort, 1979a) alters the steady-state tension following the potentiated tension response induced by low $[\text{Na}^+]_o$ perfusion, whereas choline did not modify any of the contractile parameters as seen in the strand

preparation, in cultured ventricular cells (Schanne, et.al., 1979), or in frog ventricular muscle strips (Luttgau and Niedengerke, 1958). Thus choline appears to be the ion of choice for replacing sodium.

To assess whether choline had any influence on contractility of the strands, the following experiments were carried out.

(i) First, control tension and rate values were measured in the SBSS. The perfusion fluid was then switched to a low sodium solution, 80 mM $[\text{Na}^+]_o$, with choline (66.5 mM) added to maintain osmolarity. The new rate and strength of contraction were measured and the solution changed back to SBSS. The envelope of peak isometric tension and spontaneous contraction rate are shown in Fig. 3.25 (panel a).

(ii) Next, additional choline was added, increasing the total concentration of choline to 101.5 mM (the concentration of choline needed to maintain osmolarity at a sodium concentration close to 45 mM). This solution was then introduced to the chamber and after the steady-state response was reached, the perfusate was switched back to SBSS (Fig. 3.25 panel b). The responses for the two different choline concentrations (with constant $[\text{Na}^+]_o$ at 80 mM) were identical.

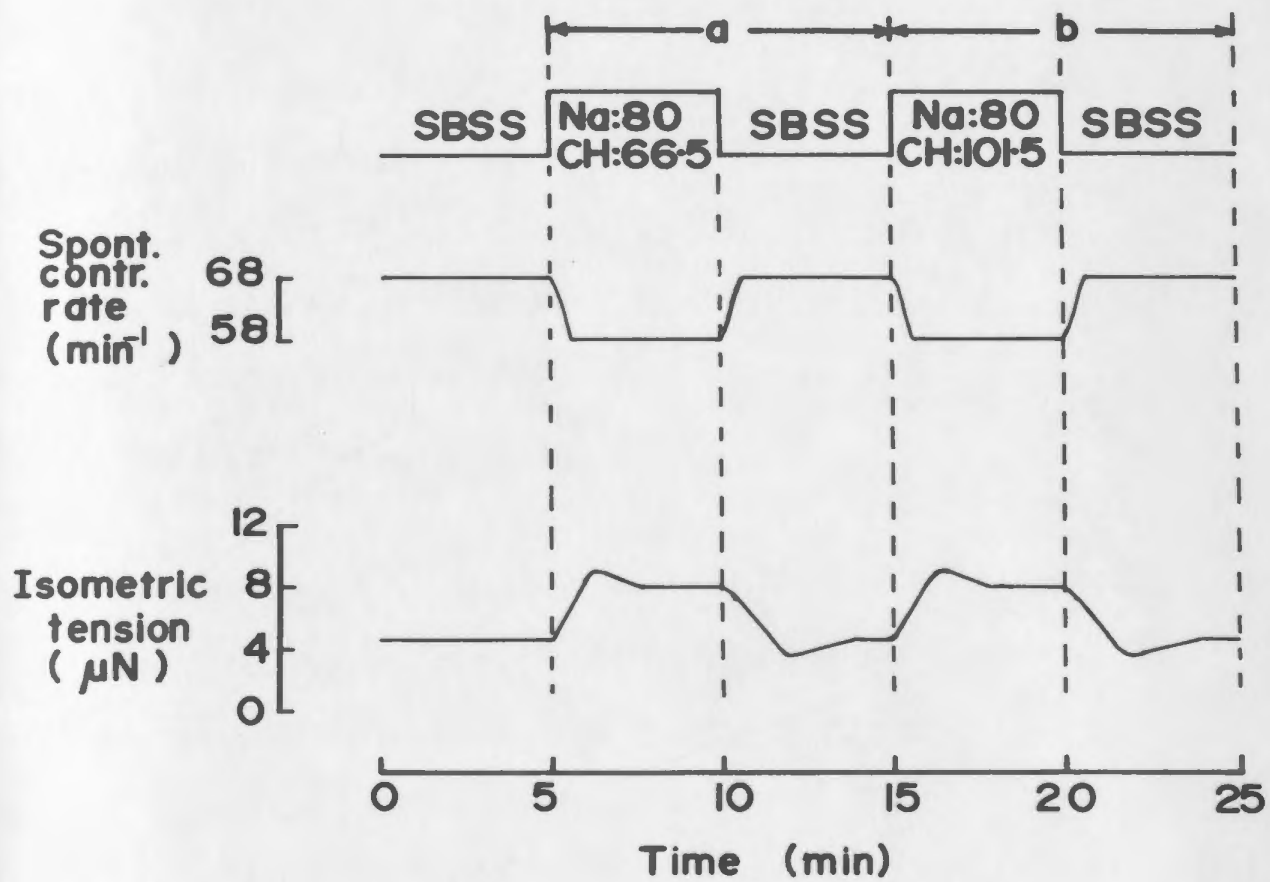
Fig. 3.25 The influence of choline substitution for sodium on contractility of the cultured myocardial strands.

Choline (CH) was substituted for Na^+ , during manipulation of $[\text{Na}^+]_o$, to maintain a constant osmolarity and electroneutrality.

Panel a: The combination of 80 mM $[\text{Na}^+]_o$ and 66.5 mM choline produced a decreased rate of contraction and an elevated steady-state isometric tension (similar to the results shown in Fig 3.24, panel b). Return to SBSS restored control values.

Panel b: Inclusion of an additional 35 mM of choline with 80 mM $[\text{Na}^+]_o$ increased choline concentration to 101.5 mM. The contractile response was identical to that seen with simple Na^+ replacement.

These results imply that choline replacement did not influence either the spontaneous rate of contraction or the isometric tension developed by the strand, but that these are consequence only of changes in $[\text{Na}^+]_o$.



Similarly, in the presence of SBSS ($\text{Na}^+ = 146.5 \text{ mM}$), the isometric tension produced by a suspended strand was $4 \mu\text{N}$ and the spontaneous contraction rate was 63 min^{-1} . When choline chloride (about 80 mM) was added to the SBSS, it was observed that neither isometric active tension, resting tension nor spontaneous rate of contraction of the strand was altered. Thus it appears that choline, in the concentrations required in these experiments, does not have a significant influence on either strength or rate of spontaneous contraction in these cardiac muscle strands.

3.9.3 Analysis of the Relationship Between $[\text{Na}^+]_o$ and Contractile Parameters

The steady-state isometric active tension is plotted versus $\log [\text{Na}^+]_o$ in Fig. 3.26. Isometric tension is inversely proportional to $[\text{Na}^+]_o$ in the range of $55\text{--}100 \text{ mM}$. When $[\text{Na}^+]_o$ was reduced below 55 mM , the AT amplitudes decreased from their peak value at 55 mM . The lowest $[\text{Na}^+]_o$ which gave useful and reproducible data was 40 mM ; below this the contractions became irregular and the strands broke.

The rate of rise of tension, $(+dP/dt)$, (Fig. 3.27) varied in a manner similar to that of isometric active tension.

Fig. 3.26 The relationship between external sodium concentration, $[\text{Na}^+]_o$, and steady-state isometric tension in spontaneously contracting cultured myocardial strands.

Isometric tension on linear scale, normalized as a percentage of (control) tension developed in standard balanced salt solution (SBSS) represented on the ordinate, is plotted against $[\text{Na}^+]_o$, expressed in log-units on the abscissa.

Each data point represents the mean \pm standard deviation of the values obtained from 5 different strand preparations.

Isometric tension exhibited an inverse relationship with $[\text{Na}^+]_o$ in the concentration range 55-100 mM; peak tension occurred at 55 mM. At concentrations below 55 mM tension magnitudes decreased slightly.

(100% $P_{\text{control}} = 4.40 \pm 0.16 \mu\text{N}$, mean \pm standard deviation, n=5)

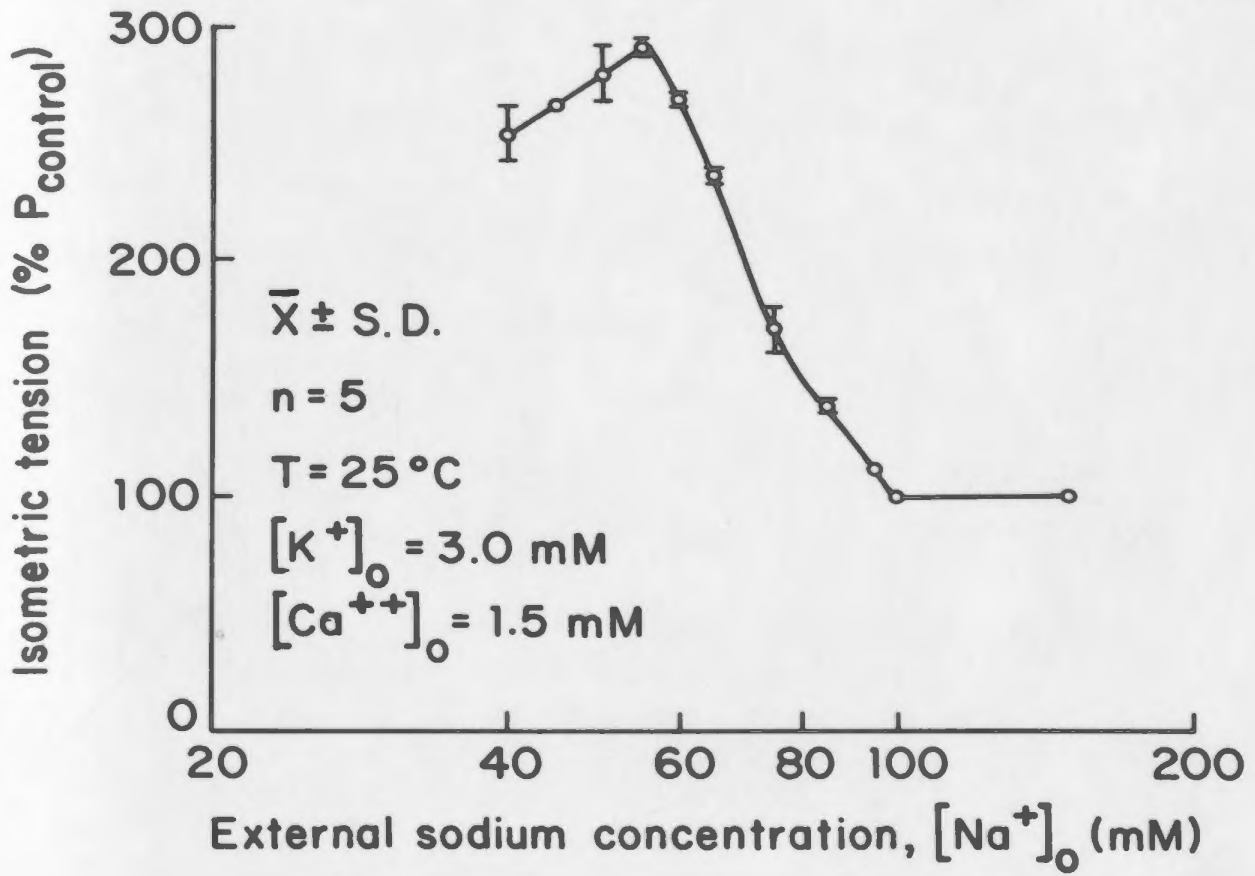
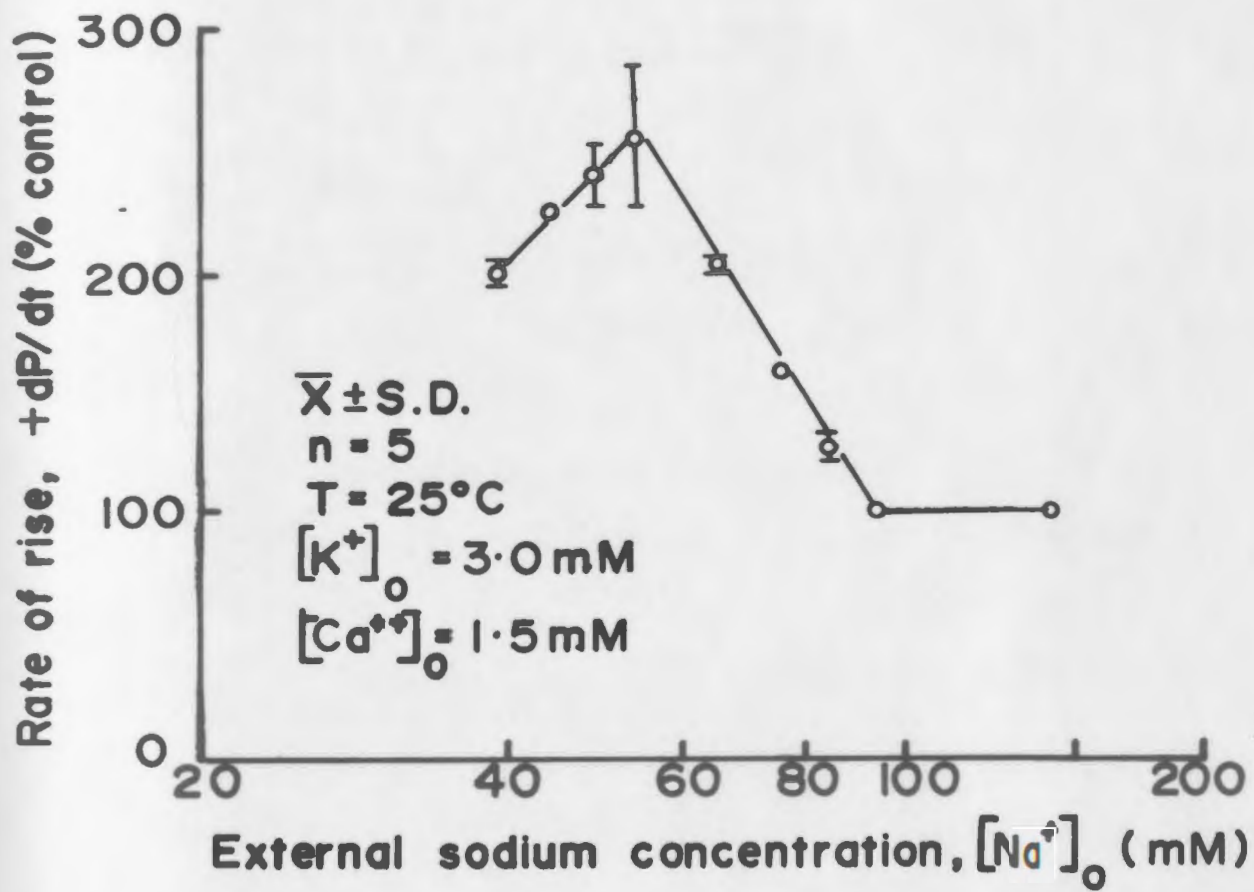


Fig. 3.27 The relation between external sodium concentration, $[\text{Na}^+]_o$, and maximal rate of contraction (dP/dt) in spontaneously contracting myocardial strands.

The dP/dt , normalized as a percentage of control dP/dt measured in standard balanced salt solution, represented on the ordinate is plotted against the logarithm of $[\text{Na}^+]_o$. Each point represents the mean \pm standard deviation of measurements from 5 different preparations.

This relationship is similar to that shown in Fig. 3.26 between isometric tension and $[\text{Na}^+]_o$.

(control value of $dP/dt = 30.83 \pm 4.07 \mu\text{N sec}^{-1}$, mean \pm standard deviation, $n = 5$)



The extracellular sodium also influenced the time course of tension development. The time to peak tension (t_p) varied inversely with $[\text{Na}^+]_o$ as shown in Fig. 3.28.

The chronotropic response varied directly with $[\text{Na}^+]_o$. In the concentration range of 40-100 mM, the relation between $[\text{Na}^+]_o$ and spontaneous contraction rate could be fitted by a semi-logarithmic curve according to the equation,

$$R = 35.0 + 5.25 \log [\text{Na}^+]_o \text{ min}^{-1}$$

as shown in Fig. 3.29. The correlation coefficient for this theoretical curve was 0.9794.

3.10 INFLUENCE OF SIMULTANEOUS MANIPULATION OF EXTRACELLULAR SODIUM AND CALCIUM UPON RATE AND STRENGTH OF CONTRACTION

It was shown in cardiac muscle fibers that the isometric tension was governed by both extracellular calcium and sodium ions (Horackova and Vassort, 1979; Luttgau and Niederggerke, 1958). Manipulation of either sodium or calcium resulted in a change in the contractile strength of the myocardial strands. In order to assess the influence of simultaneous manipulation of calcium and sodium upon the isometric contractile properties of the cultured heart muscle strands, the following experiments

Fig. 3.28 The relationship between time to peak tension and external sodium concentration, $[\text{Na}^+]_o$, in spontaneously contracting cultured cardiac muscle strands.

Time to peak tension, normalized as a percentage of control value in SBSS, (ordinate) is plotted against the logarithm of $[\text{Na}^+]_o$ (abscissa). Each point represents the mean \pm standard deviation of values from 5 different preparations. Points with no error bars indicate the absence of a significant deviation when these data values were normalized to their control values.

Time to peak tension showed an inverse relationship with $[\text{Na}^+]_o$. When $[\text{Na}^+]_o$ was lowered, time to peak tension increased.

(control value of time to peak tension, 100%, is 232 ± 18 ms, mean \pm standard deviation, $n=5$)

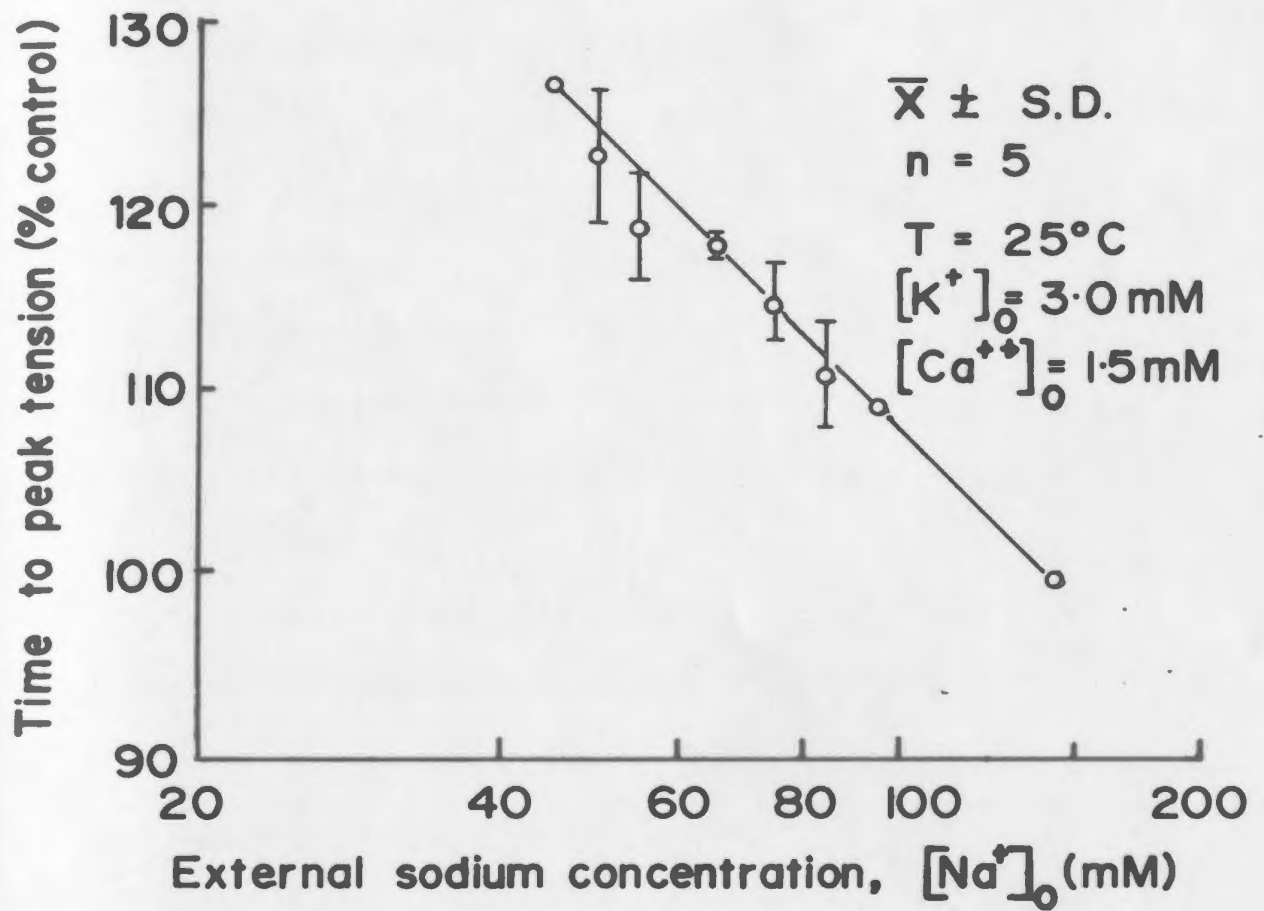
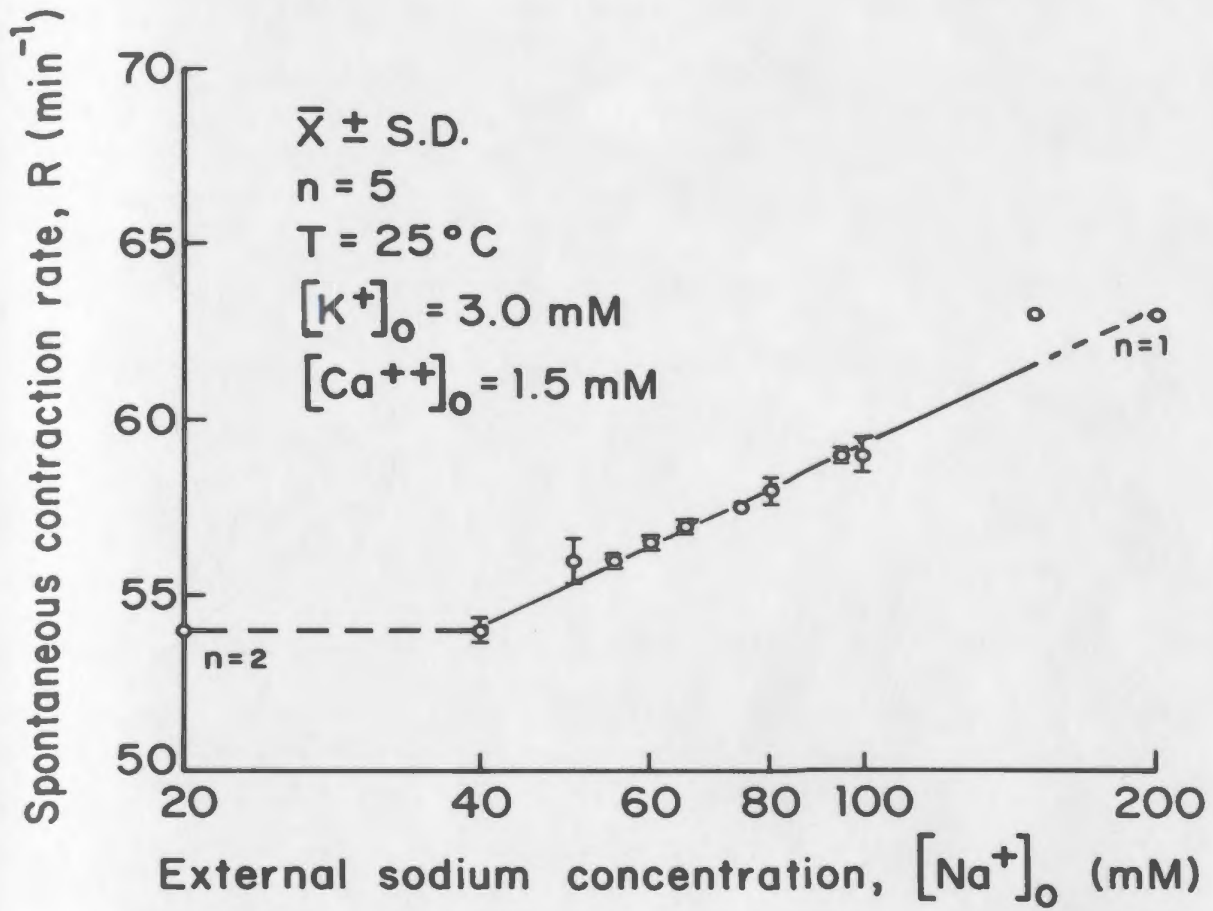


Fig. 3.29 The relationship between spontaneous contraction rate (min^{-1}) and external sodium concentration, $[\text{Na}^+]_o$, in spontaneously contracting cultured cardiac muscle strands.

Spontaneous contraction rate (min^{-1}), represented on a linear scale on the ordinate, is plotted against the logarithm of $[\text{Na}^+]_o$ on the abscissa. Each data point connected by the solid line represents the response obtained from 5 different preparations.

In the range of 40-146.5 mM the spontaneous contraction rate increased proportionally with $[\text{Na}^+]_o$.

Two strands were exposed to 20 mM $[\text{Na}^+]_o$ and developed an arrhythmic contraction pattern. One strand was exposed to 200 mM $[\text{Na}^+]_o$ and no change in rate of contraction from its control value was observed. Because of osmotic limitations, strands were not exposed above standard $[\text{Na}^+]_o$.



were performed. Both $[\text{Na}^+]_o$ and $[\text{Ca}^{++}]_o$ were manipulated, all other ions remained at their standard concentration. The SBSS was perfused intermittently to assure that the baseline conditions had not altered.

Experiment 1: In this experiment, the initial control values for tension and rate of contraction measured in the SBSS were $4.6 \mu\text{N}$ and 63 min^{-1} respectively. Keeping $[\text{Ca}^{++}]_o$ at its standard concentration of 1.5 mM , $[\text{Na}^+]_o$ was reduced from normal, 146.5 mM , to 80 mM . A few minutes after the strand reached a steady-state tension level, the strand was restored to the control tension with SBSS. Next, the strand was exposed to a solution containing low sodium (80 mM) and low calcium (1.0 mM) followed by SBSS and another perfusate containing lower calcium (0.5 mM) and low sodium (80 mM). The resulting rate of contraction and isometric tension profiles are plotted in Fig. 3.30, from which the following generalizations can be made:

- 1) The changes in rate (elevation in SBSS or depression in low sodium solution) are completed in less than 1.0 minute and are not affected by $[\text{Ca}^{++}]_o$.

- 2) Peak transient tensions in low $[\text{Na}^+]_o$ are unaffected by $[\text{Ca}^{++}]_o$ down to 0.5 mM .

- 3) At normal $[\text{Ca}^{++}]_o$, reducing $[\text{Na}^+]_o$ results in a tension plateau of about 85% peak tension. In low $[\text{Ca}^{++}]_o$ (less than 1.5 mM) solutions, low $[\text{Na}^+]_o$ abolishes the

Fig. 3.30 The influence of simultaneous manipulation of external sodium and calcium concentrations upon contraction rate and isometric tension in spontaneously contracting myocardial strands.

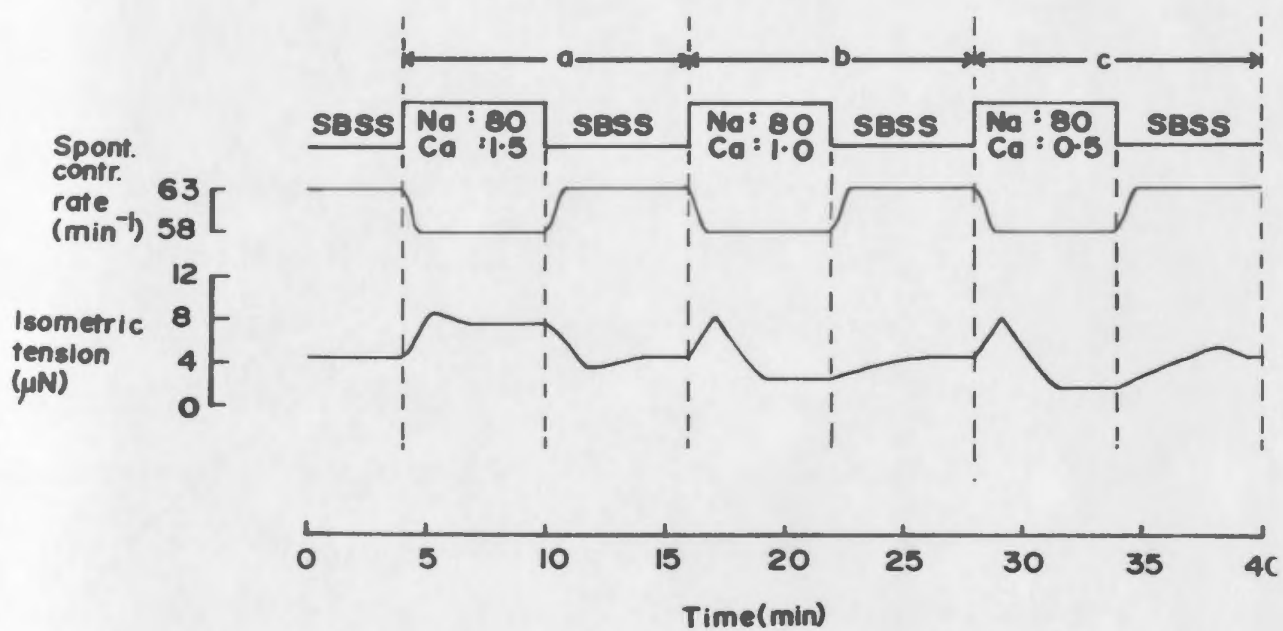
A representative record from an experiment is shown. The top line represents the time of solution changes with labels representing $[\text{Na}^+]_o$ and $[\text{Ca}^{++}]_o$ in mM. The second line with its calibration shows changes in spontaneous rate of contraction and the third line represents the envelope of tension peaks of isometric contractions.

Panel a: Sodium is reduced to 80 mM with the standard (1.5 mM) calcium; producing a response similar to that shown in Fig. 3.24.

Panel b: $[\text{Na}^+]_o$ is reduced to 80 mM and $[\text{Ca}^{++}]_o$ to 1.0 mM: peak isometric tension increased transiently, but rapidly decayed below control level to reach a new depressed steady-state level proportional to $[\text{Ca}^{++}]_o$. Upon return to the SBSS it took about 3 minutes to restore control tension; rate returned to control more quickly.

Panel c: $[\text{Na}^+]_o$ is reduced to 80 mM and $[\text{Ca}^{++}]_o$ to 0.5 mM; same as panel b, but the new steady-state tension level is further reduced compared with panel b.

These results show a high dependence on steady-state tension values and a relative independence of the early transient potentiation on $[\text{Ca}^{++}]_o$ during exposure to low $[\text{Na}^+]_o$.



potentiated steady-state tension response and depresses tension below the control to a value dependent upon $[Ca^{++}]_o$.

4) In normal $[Ca^{++}]_o$, (1.5 mM), recovery from low $[Na^+]_o$ is rapid and marked by an undershoot of reduced tension before control values are regained. In low $[Ca^{++}]_o$, such recovery is slow.

Experiment 2: As in experiment 1, initial control tension and rate were measured in SBSS, as shown in Fig.3.31. The response of the strand to low $[Na^+]_o$ (75 mM) and standard $[Ca^{++}]_o$ was measured and it was then returned to the SBSS. The strand was then perfused with a calcium free solution (5.0×10^{-4} M EGTA buffer) in the presence of low sodium. The strand was then exposed to the low sodium (75 mM), standard calcium (1.5 mM) solution (same as the initial control perfusate) to determine the response of the strand after exposure to calcium free medium (see Fig. 3.31).

From the results of this experiment, the following observations were made.

As shown in experiment 1, the spontaneous contraction rate was unaffected by $[Ca^{++}]_o$ and was proportional to $[Na^+]_o$. The rate of contraction reached its new value within 1.0 minute of switching.

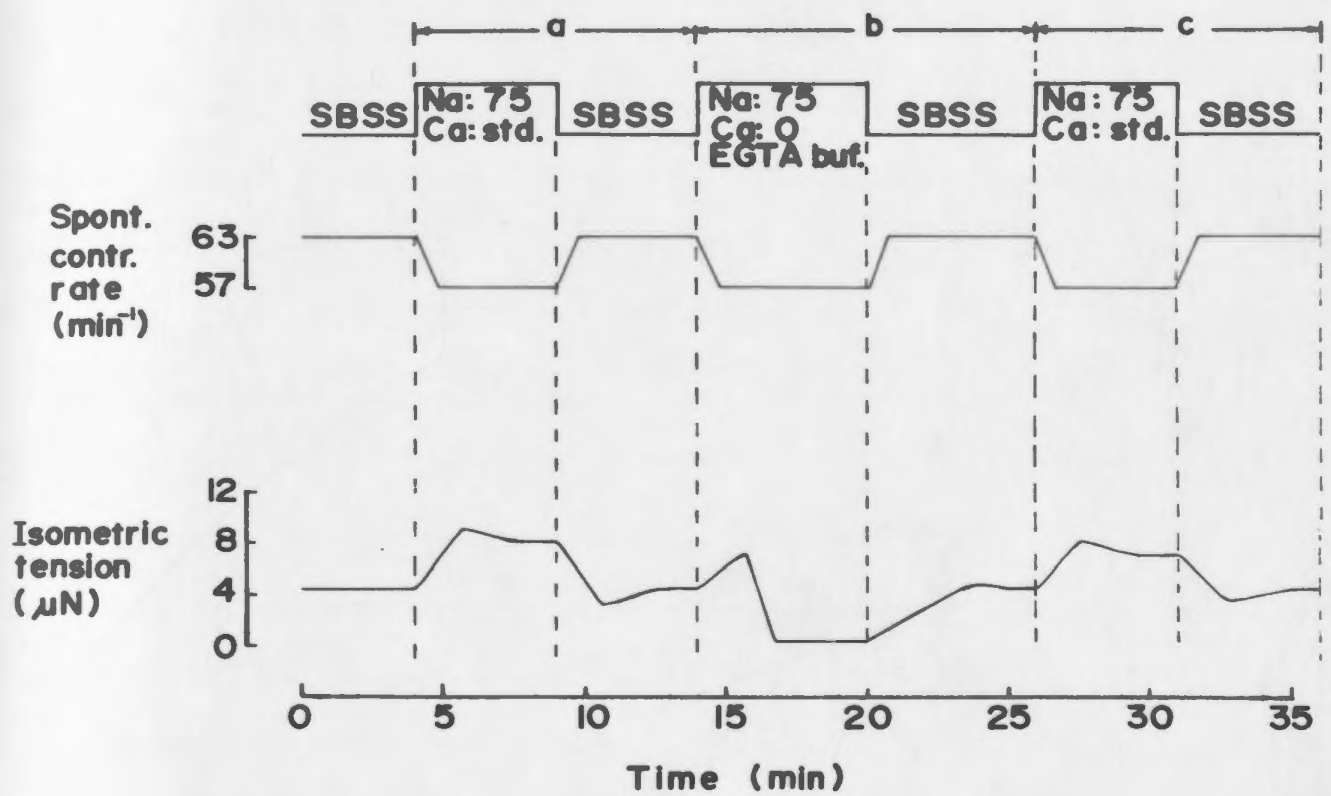
Fig. 3.31 Comparison of the effects of exposure to low $[\text{Na}^+]_o$ in standard and zero $[\text{Ca}^{++}]_o$ upon isometric tension in spontaneously contracting cultured myocardial strands.

A representative experiment is shown in which timing of solution changes, time course of rate of spontaneous contraction and time course of changes in peak isometric tension are presented.

Panel a: The strand is first exposed to low sodium (75 mM) and standard calcium (1.5 mM) and then returned to the SBSS. The characteristic pattern is seen with transient potentiation and steady-state potentiated tension, followed by transient undershoot before recovery to control tension on return to the SBSS.

Panel b: The exposure to low sodium (75 mM) and zero calcium concentration (in 5.0×10^{-4} M EGTA buffer) resulted in a transient potentiation followed by a rapid decline to (almost) zero tension. Return to SBSS resulted in a graded return to control tension with a small transient overshoot.

Panel c: Shows a second challenge with reduced sodium and standard calcium concentration; the response is very similar to that seen initially in panel a: the peak of the transient potentiation and the value of the steady-state plateau are slightly reduced, but the effects of exposure to zero calcium are largely quickly reversible.



The peak tension in low sodium was reduced by the calcium free perfusate and the steady-state tension was almost zero.

When returned to SBSS from low $[\text{Na}^+]_o$ calcium-free solution, the strand gradually regained control tension over a period of 4.0 minutes.

After exposing the strand to calcium-free medium, the inotropic effect of low $[\text{Na}^+]_o$ standard $[\text{Ca}^{++}]_o$ was qualitatively similar but quantitatively reduced in comparison to control treatment (the peak response was reduced by 11% and the steady-state tension response by 7.5%).

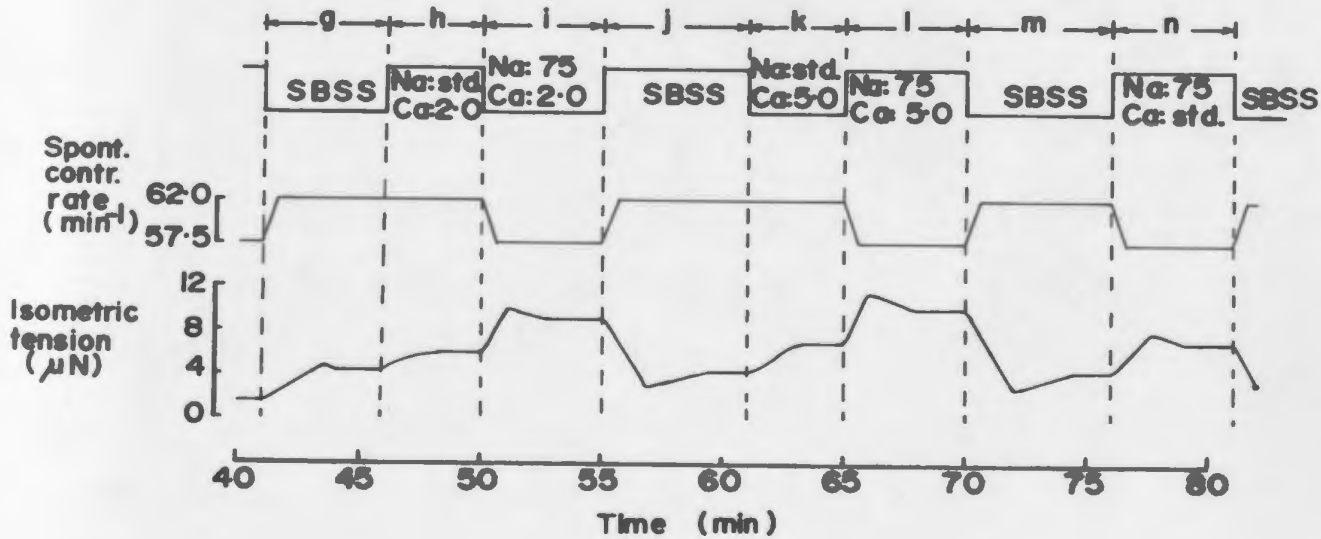
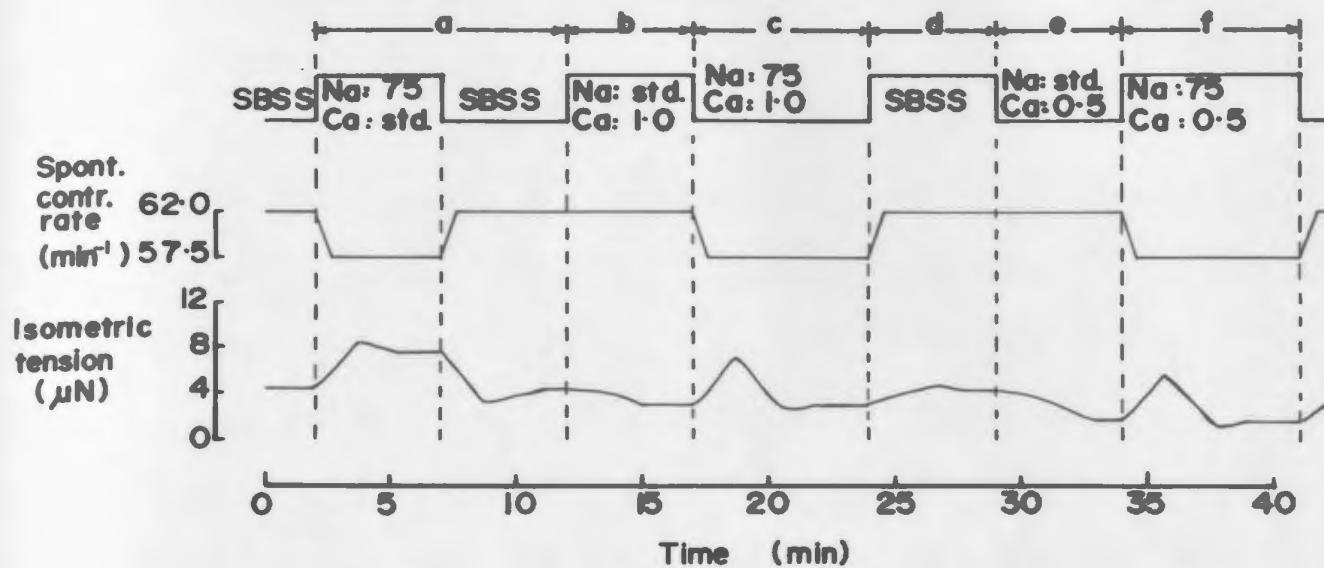
Experiment 3: In this experiment, after a control challenge of low-sodium (75 mM) and standard calcium (1.5 mM) (Fig. 3.32, panel a), the tension was first measured in SBSS and then in a modified calcium solution with standard sodium content. This was followed by a medium containing both low-sodium (75 mM) and the new $[\text{Ca}^{++}]_o$. In this way, the extracellular calcium and sodium ions were manipulated one after another. The perfusion sequence, corresponding rate of spontaneous contraction and isometric active tension developed by the strand are shown in Fig. 3.32.

Fig. 3.32 The influence of external calcium concentration, $[Ca^{++}]_o$, on steady-state and transient isometric tension responses during exposure to standard and low external sodium concentrations, $[Na^+]_o$.

A representative experiment is shown in which the strand was repeatedly exposed to a new $[Ca^{++}]_o$ in standard $[Na^+]_o$, then to reduced $[Na^+]_o$ (75 mM) in the same $[Ca^{++}]_o$ and finally returned to SBSS to reestablish the control rate and tension conditions before testing the next calcium concentration.

As shown in panels a through f, the transient potentiation of isometric tension by low $[Na^+]_o$ remains essentially unchanged at low $[Ca^{++}]_o$ but the steady-state potentiated tension disappears at concentrations below 1.5 mM.

At elevated $[Ca^{++}]_o$ both transient and steady-state potentiations are present (panels g through n). The increment over the elevated baseline tension produced by exposure to low $[Na^+]_o$ was nearly identical at 1.5, 2.0, and 5.0 mM $[Ca^{++}]_o$.



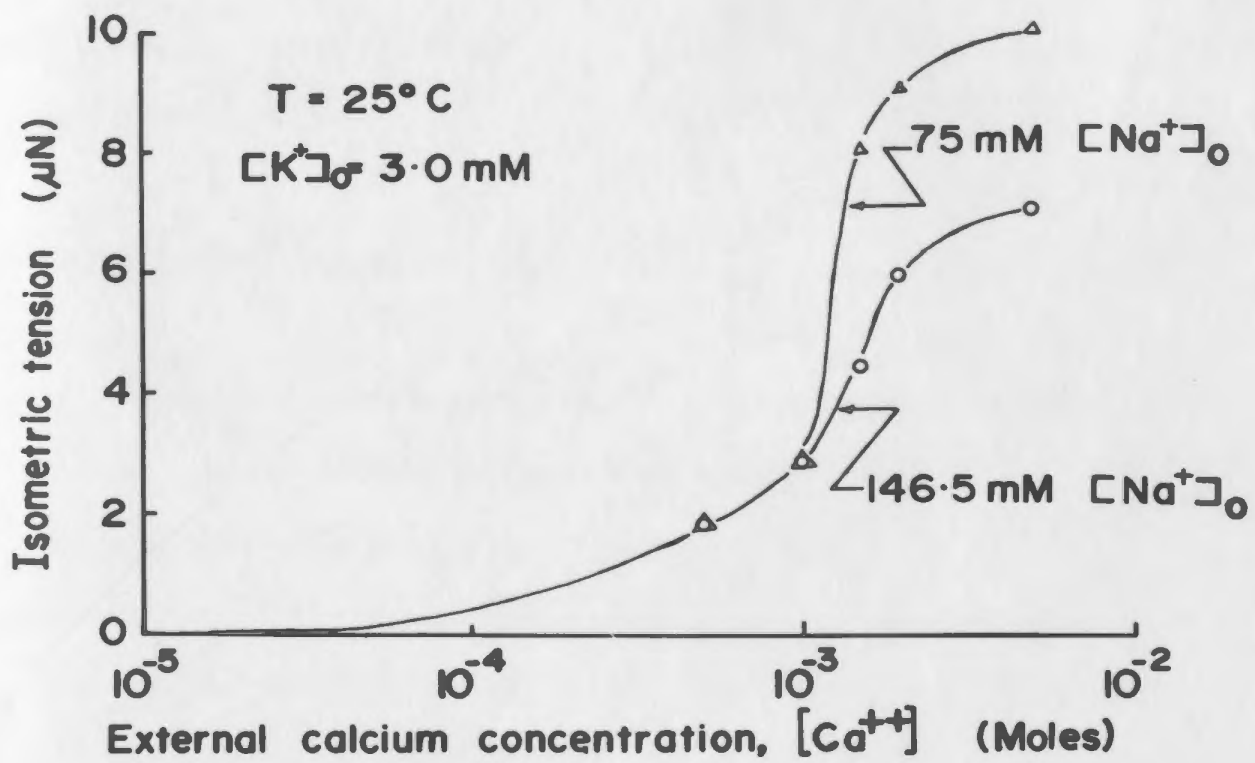
As before (refer experiment 1), the peak transient tensions in low $[\text{Na}^+]_o$ are not affected by $[\text{Ca}^{++}]_o$; the tension plateau following peak tension existed only for $[\text{Ca}^{++}]_o$ greater than or equal to 1.5 mM. In low $[\text{Ca}^{++}]_o$ (less than 1.5 mM), at a low-sodium concentration, the final steady-state tension is lower than the control level and is dependent upon $[\text{Ca}^{++}]_o$. When returned to the SBSS from low $[\text{Ca}^{++}]_o$ there was no prominent overshoot in tension. As in the other experiments, the spontaneous rate of contraction is governed solely by $[\text{Na}^+]_o$.

The steady-state tension response, following the transient peak, presented in Fig. 3.32 were analysed and plotted with respect to $\log [\text{Ca}^{++}]_o$ for normal (146.5 mM) and low $[\text{Na}^+]_o$ (75 mM) conditions (Fig 3.33). Not surprisingly the curve is identical to that of Fig. 3.16. At the reduced $[\text{Na}^+]_o$, the tension values at 5.0×10^{-4} M and 1.0×10^{-3} M $[\text{Ca}^{++}]_o$ were similar to those obtained in standard $[\text{Na}^+]_o$ (146.5 mM). The extension of the curve to values of $[\text{Ca}^{++}]_o$ below 5.0×10^{-4} M, was based on the data from the calcium dose-action curve (Fig. 3.16) with standard (146.5 mM) $[\text{Na}^+]_o$. Above 1.0×10^{-3} M $[\text{Ca}^{++}]_o$, low $[\text{Na}^+]_o$ potentiated the steady-state tension, but the $[\text{Ca}^+]_o$ at which maximal values of tension were recorded was the same at both $[\text{Na}^+]_o$.

Fig. 3.33 The dose-action relationship between isometric tension and external calcium concentration, $[Ca^{++}]_o$, during exposure to standard and low sodium concentrations, $[Na^+]_o$.

Isometric tension (μN) on the ordinate is plotted against the logarithm of $[Ca^{++}]_o$ on the abscissa for standard (146.5 mM, \bullet) and low (75 mM, \blacktriangle) $[Na^+]_o$. Up to 1.0×10^{-3} M, the curves were identical; above this value there was a dramatic change in steady-state tension magnitudes during low $[Na^+]_o$ exposure. This suggests that 1.5 mM $[Ca^{++}]_o$ is a critical threshold for operation of a system which will potentiate isometric tension.

The extension of the curve to values of $[Ca^{++}]_o$ below 5.0×10^{-4} , was based on the data from the calcium dose-action curve (Fig. 3.16) with standard $[Na^+]_o$.



3.11 PHARMACOLOGICAL RESPONSES

To characterize the pharmacological responsiveness of cultured heart cells, experiments were made with acetylcholine (ACh), phenylephrine (PEP) and isoproterenol (ISO), to identify the presence of cholinergic, alpha- or beta- sympathetic receptors respectively. Receptors were further identified with specific muscarinic- and beta-receptor blocking agents.

3.11.1 Drug Solutions

For different concentrations, appropriate volumes of the desired drug preparation were added to 100 ml SBSS and the bottles were labelled. When the the action of antagonists were studied either atropine or propranolol was added to SBSS, SBSS with ACh or SBSS with ISO to provide a final blocker concentration of 1.0×10^{-6} M.

3.11.2 Effects of Acetylcholine

When the strands were exposed to ACh, both the rate and strength of contraction decreased from their control levels in SBSS. The range of concentrations of ACh studied was between 1.0×10^{-7} and 1.0×10^{-1} M. Threshold

concentration occurred at 1.0×10^{-6} M and the responses saturated at 1.0×10^{-4} M.

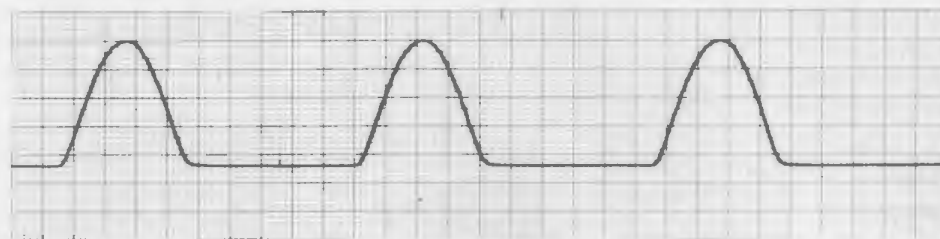
The rate of spontaneous contraction in the SBSS (control) and 1.0×10^{-4} M ACh were respectively, 63 and 9 min^{-1} . The high speed tracings obtained from one experiment show the control response, the effect of atropine alone, the effect of two different concentrations of ACh and the effect atropine upon the response to 5×10^{-4} M ACh (Fig. 3.34). The ACh log(dose)-response (chronotropic and inotropic) relationships are plotted in Fig. 3.35.

The tension amplitudes in 1.0×10^{-4} M ACh fell to approximately 40% of the control value. It was recognized that this apparent reduction in tension could be due to a corresponding reduction in spontaneous contraction rate. When the strands were stimulated at 63 min^{-1} in the presence of 1.0×10^{-4} M ACh, the tension amplitudes returned to the control values. The full range of stimulated contraction was examined and the force-frequency relation in the presence of 1.0×10^{-4} M ACh is plotted in Fig. 3.36. Except for low frequency values which could not be obtained under these conditions the curve is identical to that obtained in SBSS (Fig. 3.10).

Fig. 3.34 The influence of acetylcholine (ACh) and atropine upon the rate of spontaneous contraction and contractility of cultured myocardial strands under suspension.

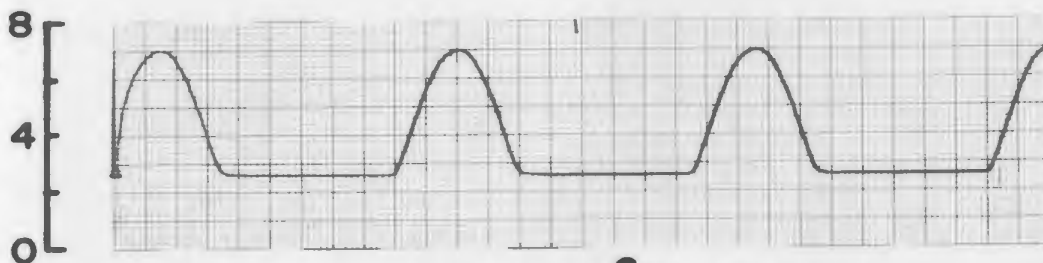
Representative high speed records obtained from a spontaneously contracting strand are shown during exposure to ACh and its competitive muscarinic antagonist atropine.

The upper trace illustrates the contraction response in the standard balanced salt solution (SBSS). The second trace documents the response of this strand to 1×10^{-6} M atropine; neither isometric tension nor the contraction rate was affected. Third and fourth traces demonstrate that both spontaneous contraction rate and the isometric tension were progressively depressed by exposure to increasing concentrations of ACh (5×10^{-6} and 5×10^{-4} M). In the last trace, the blocking action of atropine is illustrated (compare traces 4 and 5); rate and amplitude of contractions are restored to near control values in spite of the continued presence of ACh.



SBSS (rate: 63 min^{-1})

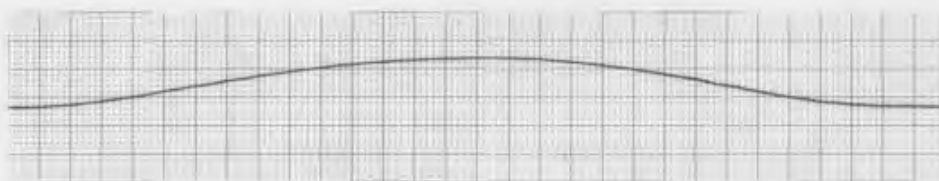
Isometric
tension
(μN)



$1 \times 10^{-6} \text{ M}$ Atropine
(rate: 63 min^{-1})



$5 \times 10^{-6} \text{ M}$ ACh (rate: 48 min^{-1})



$5 \times 10^{-4} \text{ M}$ ACh (rate: 10 min^{-1})



$1 \times 10^{-6} \text{ M}$ Atropine $5 \times 10^{-4} \text{ M}$ ACh
(rate: 57 min^{-1})

0 ————— |
Time (sec) |

Fig. 3.35 The dose-response relationship between spontaneous contraction rate and isometric tension and acetylcholine (ACh) concentration; interaction with atropine

(a) Spontaneous contraction rate, normalized as percentage control (without ACh), is plotted (ordinate) against the logarithm of ACh concentration, in moles (abscissa). As the concentration of ACh was increased above 1×10^{-6} M, the rate of spontaneous contraction decreased, reaching a maximal negative chronotropic state at 1×10^{-4} M; at this concentration the response was saturated. (100% = 63 min^{-1})

In the presence of 1×10^{-6} M atropine, the ACh induced reduction in spontaneous contraction rate was shifted by approximately 2.5 log units to the right. This illustrates the competitive antagonism by atropine at a muscarinic receptor.

(b) Isometric tension, represented as percentage control (ordinate) is plotted versus logarithm of ACh concentration (abscissa) with and without atropine. The ACh induced a negative inotropic response and atropine (1×10^{-6} M) acted as a competitive blocker. Threshold ACh concentration was 1×10^{-6} M as before and the final saturation level was 1×10^{-4} M. Atropine shifted the dose-response curve by approximately 2.5 log units to the right.

(100% control = $4.38 \pm 0.14 \mu\text{N}$, mean \pm S.D., $n=3$)

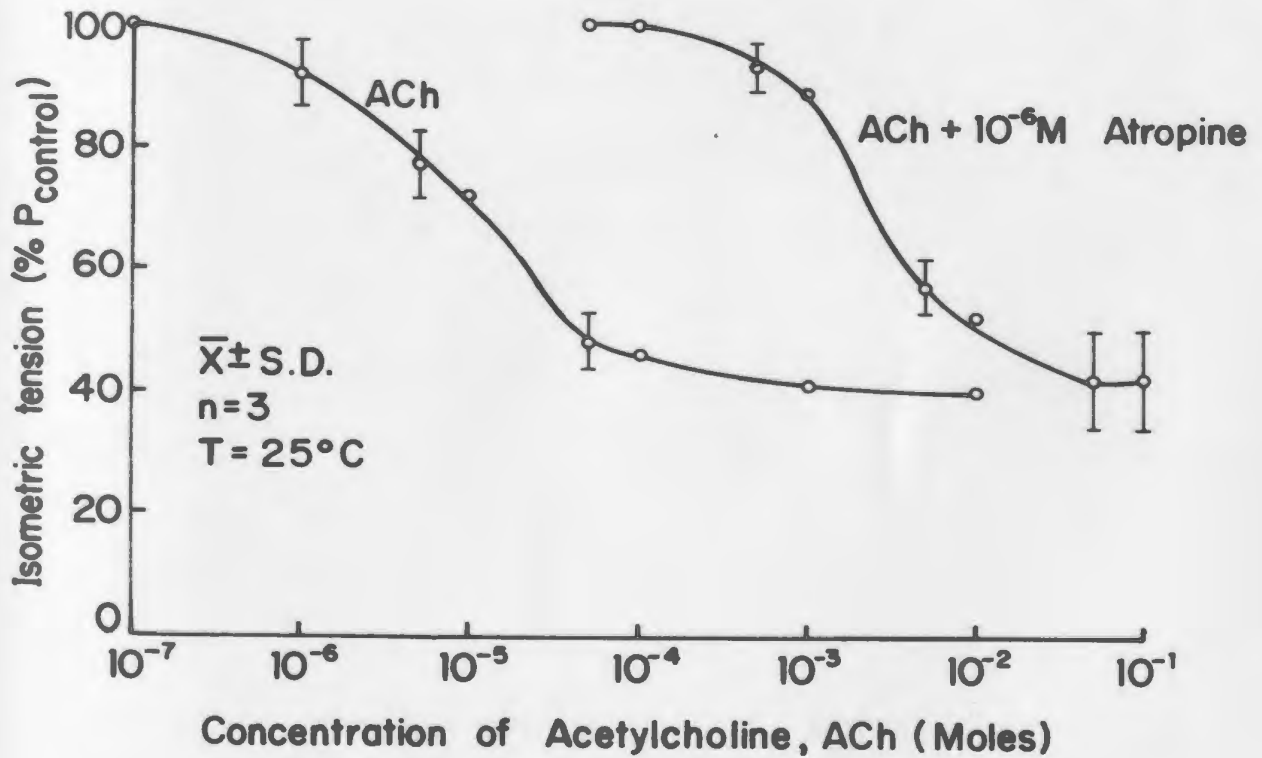
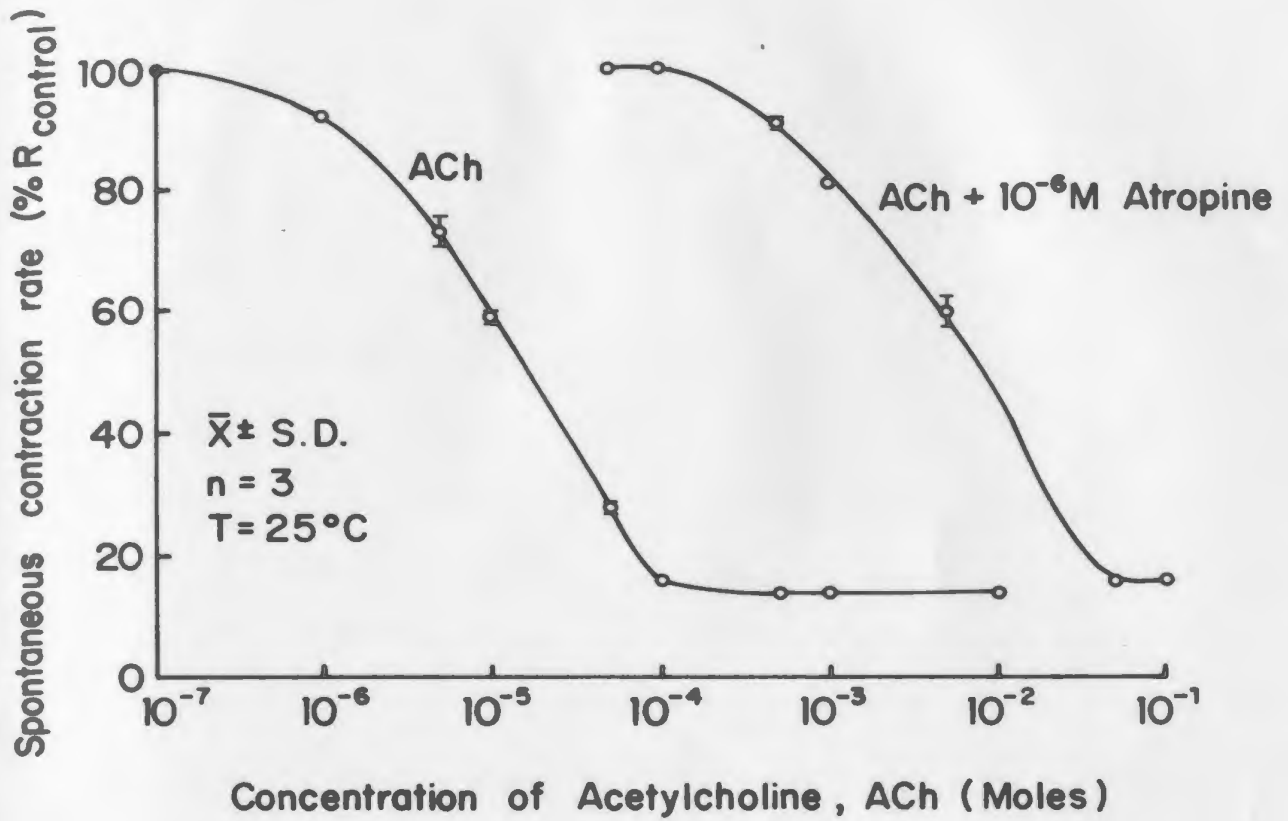
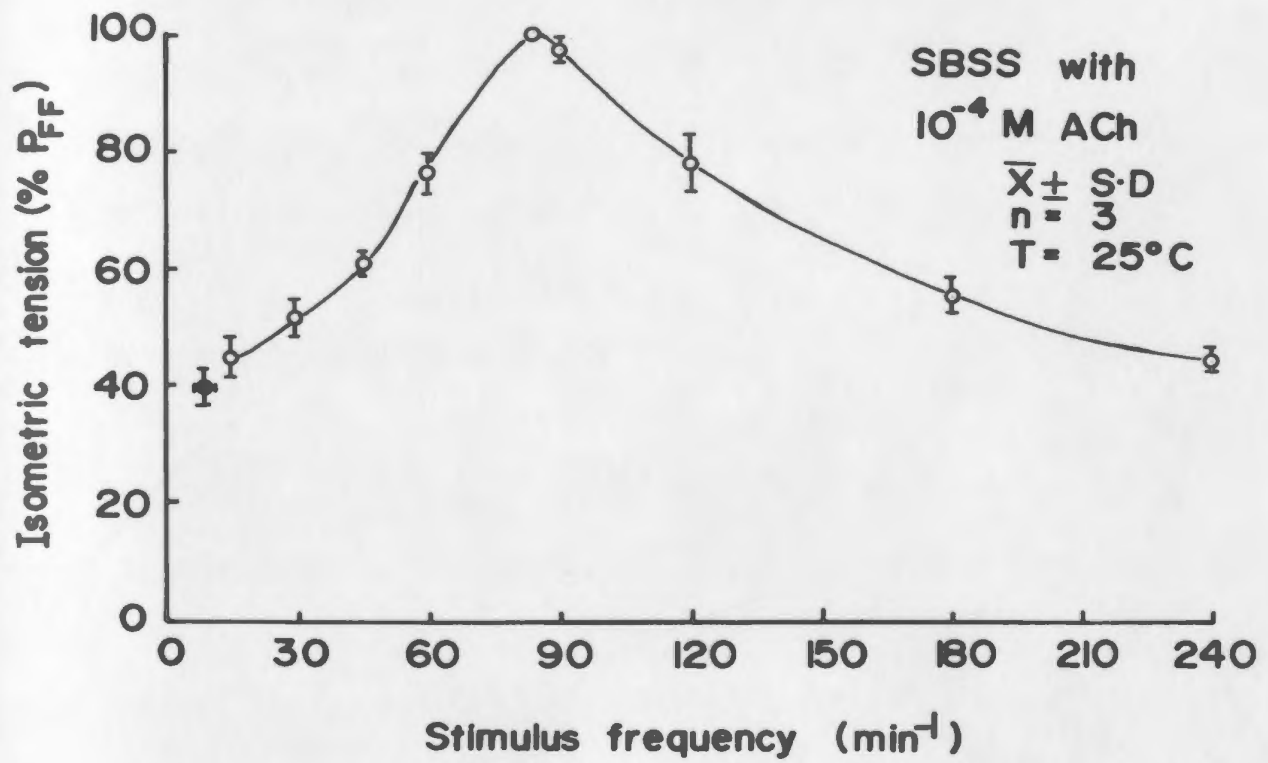


Fig. 3.36 The influence of ACh upon the force-frequency relationship in cultured cardiac muscle strands.

Normalized isometric tension (as percentage of the maximum tension developed in this study, $\%P_{FF}$) of the spontaneously contracting strands under suspension in a medium containing 1×10^{-4} M ACh, is plotted along the ordinate versus stimulus frequency (min^{-1}) represented along the abscissa. In the presence of 1×10^{-4} M ACh, both rate and tension dropped to very low values (9 min^{-1} and $40\% P_{FF}$). The strands were stimulated for force-frequency analysis beginning at 15 min^{-1} and the resulting response is presented. The solid circle with a two way standard deviation represents the mean value of tension and the spontaneous contraction frequency of the three strands. When the strands were stimulated at their natural spontaneous contraction frequency (in the absence of ACh), they regained their control tension magnitudes. The portion of the curve obtained for frequencies above 75 min^{-1} is identical to that of Fig. 3.10.

This demonstrates that ACh-induced negative inotropic response is a secondary effect, due to the reduction in spontaneous contraction frequency.



3.11.3 Effects of Atropine

When the strands were exposed to 1.0×10^{-6} M atropine (a muscarinic blocking agent) alone, there was no change in either the rate or force of contraction of the strands (Fig. 3.34).

However, in the presence of ACh, 1.0×10^{-6} M atropine blocked the responses of ACh competitively. This is demonstrated in Fig. 3.35 (a) and (b); both chronotropic and inotropic dose-response curves to ACh were shifted approximately by 2.5 log units to the right by atropine.

3.11.4 Effects of Phenylephrine

The alpha-adrenergic agonist, phenylephrine, at varying concentrations from 1.0×10^{-6} M to 1.0×10^{-1} M did not produce any change either in inotropic or in chronotropic responses of these strands. This experiment was repeated in three strands from three different batches of cultures and the results were the same. As the responses of these strands were not affected by phenylephrine, it was therefore concluded that they had no alpha adrenergic receptors.

3.11.5 Effects of Isoproterenol

These strands showed both a positive inotropic and chronotropic response to ISO, a beta-adrenergic agonist. The range of concentrations studied was between 1.0×10^{-8} M and 1.0×10^{-2} M.

The high speed tracings obtained from a single strand show the control response, response to 1.0×10^{-6} M propranolol, effect of 5.0×10^{-6} M and 5.0×10^{-5} M ISO and the interaction between propranolol and 5.0×10^{-5} M ISO (Fig. 3.37). When the data from four different strands were combined, the threshold response (both chronotropic and inotropic) occurred at a concentration of 5.0×10^{-7} M, reached a peak at 1.0×10^{-4} M and levelled off above this concentration, as shown in Fig. 3.38 (a) and (b). These graphs were normalized as a percentage of control values obtained (in SBSS). The peak tension was potentiated to approximately 360% of the control tension in SBSS. The spontaneous contraction rate increased from 63 min^{-1} (in SBSS) to about 180 min^{-1} in the presence of 1.0×10^{-4} M ISO.

Fig. 3.37 The influence of isoproterenol upon the contractility of cultured myocardial strands.

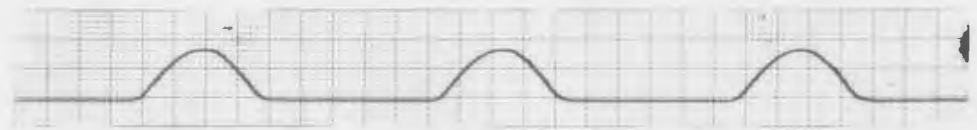
This series of representative traces was obtained from a strand preparation exposed to isoproterenol (ISO) and its competitive antagonist propranolol.

Trace 1 represents the control spontaneous contractions of the strand in SBSS.

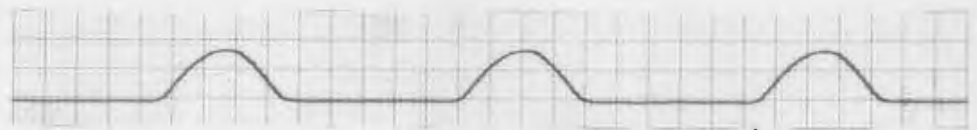
Trace 2 shows exposure to 1×10^{-6} M propranolol; no response was seen.

Traces 3 and 4 show the graded response to ISO at concentrations of 5×10^{-6} M and 5×10^{-5} M, indicating the increased rate of contractions and tension amplitudes.

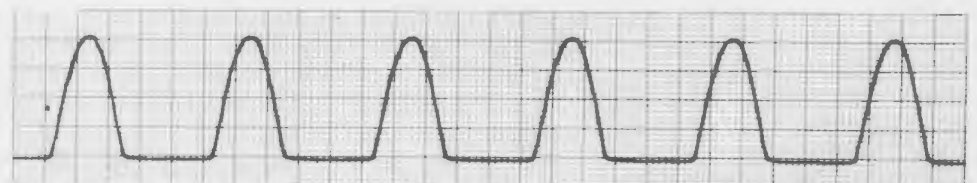
Trace 5 shows the blocking action of 1×10^{-6} M propranolol upon ISO induced positive inotropic and chronotropic responses (compare traces 4 and 5; the concentration of ISO is the same in both cases).



SBSS

(rate: 63 min^{-1}) $1 \times 10^{-6} \text{ M}$

Propranolol

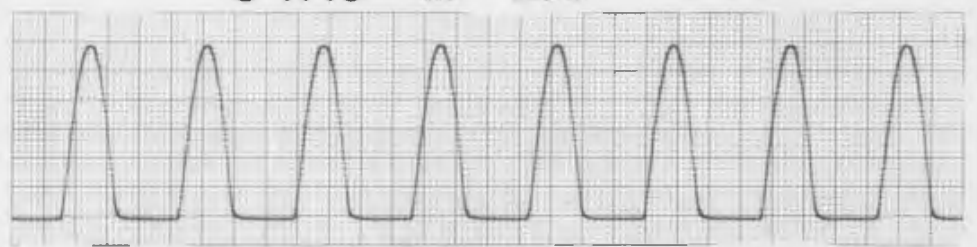
(rate: 63 min^{-1}) $5 \times 10^{-6} \text{ M}$

ISO

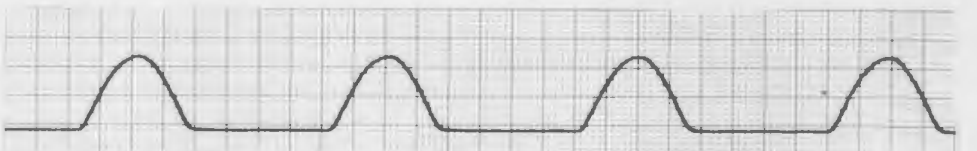
(rate: 120 min^{-1})

Isometric
tension
(μN)

20
10
0

 $5 \times 10^{-5} \text{ M}$

ISO

(rate: 167 min^{-1}) $1 \times 10^{-6} \text{ M}$

Propranolol

+ $5 \times 10^{-5} \text{ M}$ ISO(rate: 77 min^{-1})

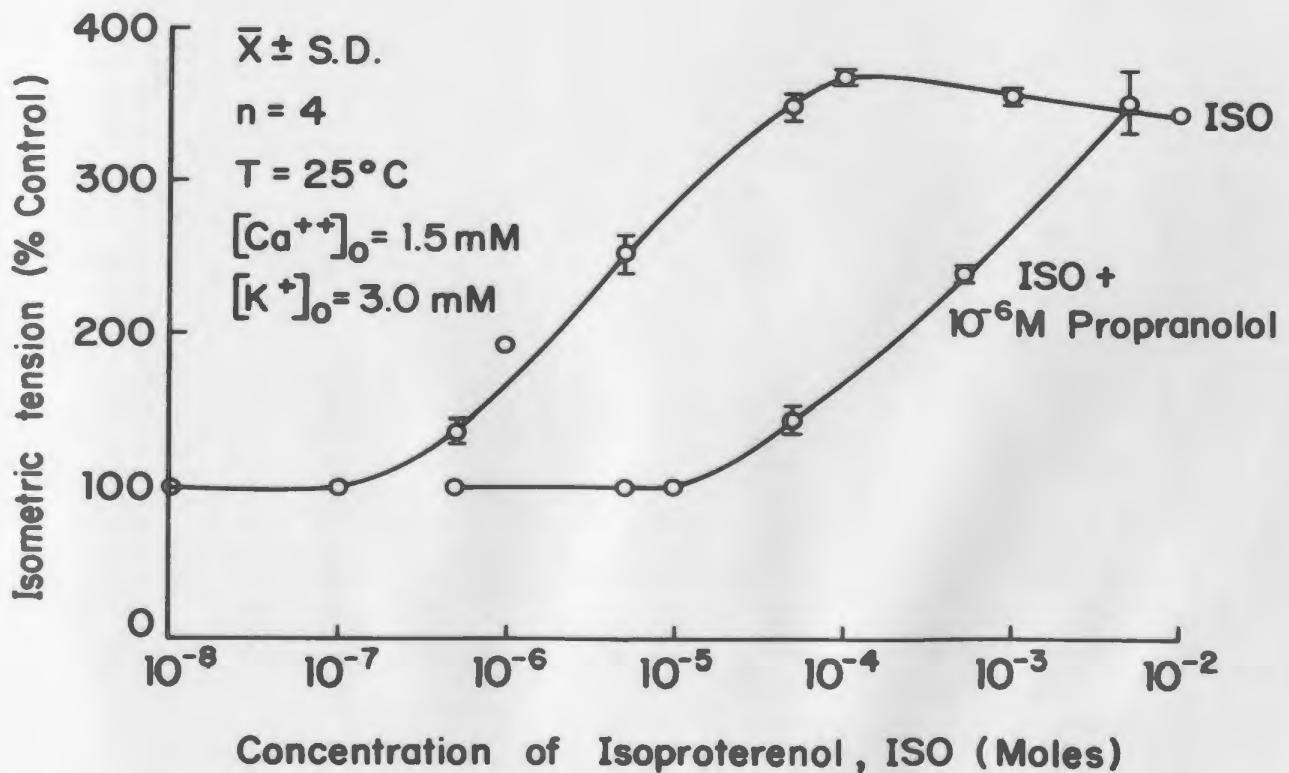
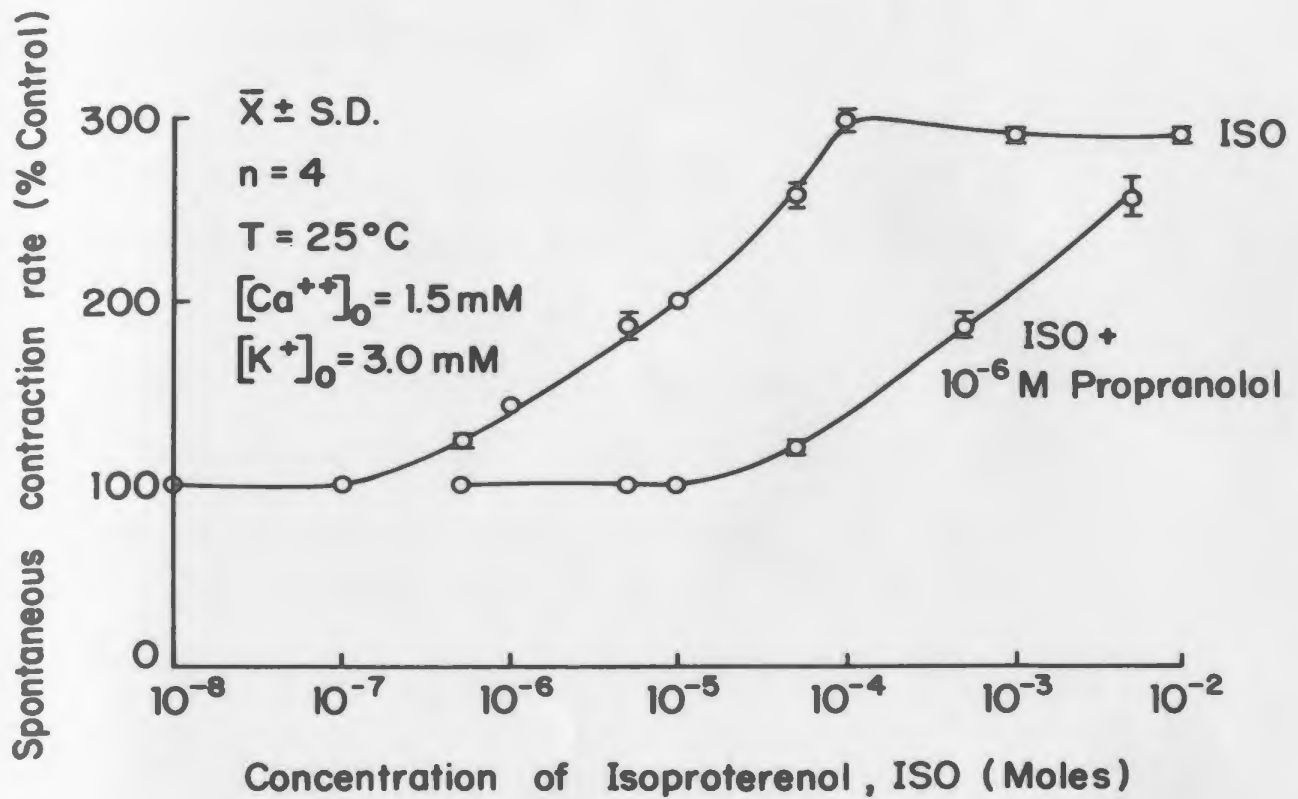
0 Time (sec) |

Fig. 3.38 The influence of isoproterenol, ISO, upon rate and tension development in cultured cardiac muscle strands.

Each data point in panels (a) and (b) represents the mean \pm standard deviation of the response obtained from 4 strands.

(a) Spontaneous contraction rate (normalized as a percentage with respect to its control value in the SBSS) is plotted along the ordinate while logarithmic concentration of ISO (in Moles) is plotted along the abscissa. The rate of contraction increased in the presence of ISO. The threshold dose was 5×10^{-7} M and the response reached a peak at 1×10^{-4} M; there was no significant change in rate at higher concentrations. In the presence of 1×10^{-6} M propranolol, a competitive antagonist for the beta-receptor, the ISO induced positive chronotropic response was shifted by about 2.0 log units to the right. This demonstrates the presence of beta-adrenergic receptors in the strands. (100% = 63 min^{-1}).

(b) Isometric tension (expressed as a percentage of control tension magnitude in SBSS) is plotted (ordinate) versus the logarithmic concentration of ISO. Threshold and peak concentrations were the same as for the chronotropic response. Propranolol shifted the dose-isometric tension response to the right by 2.0 log units. This confirms the presence of beta-adrenergic receptors in the spontaneously contracting cultured cardiac muscle strands which produce positive inotropic and chronotropic effects. (100% control = $4.38 \pm 0.13 \mu\text{N}$).



3.11.6 Effects of Propranolol

When the strands were exposed to 1.0×10^{-6} M propranolol, a non-selective beta-adrenergic blocking agent, there was no change in response (Fig. 3.37). However this concentration of propranolol competitively blocked both the positive inotropic and chronotropic responses elicited by ISO. As shown in Fig. 3.38 (a) and (b), the logarithmic dose-response curves were shifted in parallel by approximately 2 log units to the right, by propranolol.

CHAPTER - IV
DISCUSSION

4.1 CULTURED STRAND - BIOLOGICAL PREPARATION

4.1.1 Strand Morphology

Isolated single myocardial cells obtained from neonatal rats have different shapes, appearing either circular, elongated (spindle shaped), or trapezoidal (Norwood, Castaneda, and Norwood, 1980), depending on the age of the rats used for culturing (Burke, private communication). In this study, hearts were obtained from 2-3 day old rats and the cells used for culturing were usually elongated in shape and had a centrally located nucleus. They contracted along the long axis and aligned themselves parallel to and on the palladium lines, conforming to the principle of contact guidance (Harris, 1973; Carter, 1965; Ohara and Buck, 1979).

After 24 hours of culturing, neither Z-lines nor regularly arranged contractile proteins were observed in these strands when viewed with light microscopy. This is consistent with the observations of Kasten (1973) and Harary and Farley (1963), who reported that sarcomeres were not found in their cultured neonatal rat heart muscle cell preparation; but differs from the regularly arranged sarcomeres seen either in cultured strands of embryonic chick heart muscles (Purdy et al., 1972) or in cultures derived from adult rat heart muscle (Jacobson, 1977). In newborn rat heart ventricles trypsin is reported to digest myosin and disrupt the well organized myofibrils (Mark and Strasser, 1966; Mihalyi and Szent-Gyorgi, 1953), thus eliminating the usual precise organization of thick and thin filaments into sarcomeres. This suggests that the formation of a regular arrangement of contractile filaments in cultured cells is dependent upon species, age of the animal and the technique used for culturing.

It had been reported that sarcoplasmic reticulum (SR) and t-tubules were not well-developed in cultured myocardial cells (Legato, 1972; Zacchei and Caravita, 1972). The present study indicates that both SR and t-tubules are present in these cells at least in their functional form, though no morphological evidence is available. This hypothesis is based upon the following observations:

1. The strands were electrically excitable (Refer Sec. 3.2) implying the existence of a functional excitation-contraction mechanism. This is demonstrated by the classical hyperbolic strength-duration curves obtained for this preparation (Fig. 3.3) which have a shape similar to that of many other excitable tissues (Grundfest, 1932; Noble and Stein, 1966; Scott, 1973; Cooley and Dodge, 1966).

2. Manipulation of $[Ca^{++}]_o$ altered the strength of contraction (Fig. 3.16). The shape of the calcium dose-action curve obtained for this preparation was consistent with multicompartmental regulation of calcium access to the contractile proteins (Langer, 1978). In the intact papillary muscle preparation calcium kinetics is associated with morphologically identifiable sarcolemma, which has a unique calcium binding characteristics. It is also known that structures like the SR and mitochondria have calcium storage sites. but their role in the Ca^{++} movement is not clear. Although no morphological correlation has been performed the functional properties of the strands imply the presence of some morphological substrates analogous to those present in the intact cardiac muscle. This evidence also indicates that the cell membrane of the strand preparation is intact.

A detailed study of the morphology of this preparation, which is outside the scope of this investigation, might enable correlation between the structure of the strands and the quantitative measurements obtained for contractile parameters. A detailed electron microscopic study would provide the details of the morphology (specialised intracellular membrane system, physical orientation of the mitochondria and other structural factors known or suspected to be related to calcium ion transport) and, thus, suggest which of these factors may be more important to Ca^{++} regulation within the strand.

4.1.2 Spontaneous Contraction Rate

4.1.2.1 Relationship with age

As seen in Fig. 3.2, the spontaneous rate of contraction for the developing strands decreased with age. After one day of culturing, the spontaneous contraction rate was observed to be 24 min^{-1} . With increasing age, cells contacted their neighbours, forming a small group or section of the strand (Fig. 3.1). The resultant rate of contraction of these sections was lower than that of single cells one day old. When these segments fused to complete

a strand, the rate dropped still further. This observation appears to contradict the phenomenon reported by Harary and Farley (1963a), that when two contracting cells establish contact, they assume the rate of the cell with the higher frequency of contraction. Their observation was only for two cells when they came into contact. They have not reported what happened to this rate a few hours after contact, nor what happens when multiple cells are in prolonged contact, nor have they studied contraction rate as a function of culture age.

One possible factor may be that the spontaneous rate of contraction of an individual cell may decrease based upon the age of the donor animals. An attempt was made to observe the rate of contractions of isolated cells cultured from older rats. With the preparative techniques used in this study, culturing of adult rat heart cells was not successful. Hence the contribution, if any, of this sort of process to the decreased rate of contraction of the developing strand was not evaluated.

4.1.2.2 Effect of strand suspension

When the strand was suspended, the spontaneous contraction rate increased dramatically to about 73 min^{-1} at 25°C . One possible explanation for this increased rate in suspended strands may be related to the observations of

Martin and Rubin (1974) that cultured cells have a negative surface charge, which could be the mechanism for their attraction and alignment on metallic surfaces such as palladium lines. Electrical neutrality would exist at the junctions between the palladium lines and the cells of the strand. This electrical neutrality as well as the positive charge of the metal surface may influence the rate of contraction. Once the strand was freed from the palladium line and suspended in the medium, these cells might regain their intrinsic excitability and begin to contract spontaneously at a higher rate. The depression of spontaneous contraction rate associated with the metal appears to be confirmed indirectly by the observations of Schanne (1972). In his studies, using clusters of cultured neonatal rat ventricular cells grown in plastic culture dishes (no metal or agar surface) spontaneous contraction rate remained between 40 and 70 min^{-1} in the age range of 1-2 weeks.

Alternatively the possibility that the increased rate is due to injury potentials (Brady et al., 1979) induced by cell damage incurred while removing the strand from the palladium line during suspension must also be considered. This does not seem very likely because (1) this rate was sustained without modification for as long as three hours during experiments and (2) the basal rate was modifiable in a highly predictable fashion by temperature, ions and

neurotransmitters; e.g. 1.0×10^{-4} M ACh decreased the rate of contraction markedly, as seen in Fig. 3.35(a), and ISO increased the rate [see Fig. 3.38(a)]. If the increased rate on strand suspension were due to an injury at the strand surface, it would not be so stable and it seems unlikely that it would be susceptible to change in response to ionic manipulations and the classical neurotransmitters.

4.2 MECHANICAL PROPERTIES OF THE STRAND PREPARATION

4.2.1 Length-Tension (LT) Relationship

4.2.1.1 Characteristics of strands in the culture medium, during spontaneous contraction

The LT relationship of cultured strands (Fig. 3.6) was qualitatively similar to that of intact cardiac muscle (Spiro and Sonnenblick, 1964). Resting tension increased progressively at all lengths above L_0 and isometric active tension has an ascending and descending limb, similar to that of isolated adult Sprague-Dawley rat papillary muscle (Grimm and Whitehorn, 1968).

Since the thick and thin filaments were not identifiable in these strands (see Sec. 4.1.1), it is impossible to account for the LT relationship on the basis

of classical sliding filament hypothesis (Gordon et al., 1966). Correlation between morphology and function will require the contribution of some one possessing a sophisticated set of electron microscopic techniques operating in conjunction with carefully controlled physiological experiments.

In rat papillary muscle the length tension relationship was defined over length changes of about $\pm 25\% L_{\max}$ (Krueger and Pollack 1975). However the cultured strands prepared from neonatal rat hearts required length changes of only $\pm 1\% L_{\max}$ to define the full LT relationship (Fig. 3.6). This suggests that the strand is stiffer than papillary muscle. The observed difference in the range of length changes may be due to the structural differences between the two preparations. Intact papillary muscle contains both collagen and elastin fibres, as well as blood vessels in addition to the myocardial fibres. They also have a complex geometric arrangement (Abbott, 1971). All these factors tend to make the intact muscle more compliant. On the other hand, cultured strands are formed by the longitudinal arrangement of de-differentiated myocardial cells and probably some fibroblasts (Lieberman et al., 1972). One of the important modifications of Lieberman's technique, devised at Memorial University

(see Section 1I, appendix I) resulted in a substantial reduction in the fraction of fibroblasts remaining in the cultures. Hence, the fraction of strand consisting of fibroblasts is minimal.

In contrast to the skeletal muscle, where the correlation between sarcomere length changes and the LT relationship is direct, the parallel measurements for cardiac muscle are much less conclusive (Sonnenblick and Skelton, 1974). Rat papillary muscle, which required $\pm 25\% L_{\max}$ to define the LT relationship, had a corresponding change in sarcomere length of only $7\% L_{\max}$ in living muscle (using light diffraction method, Krueger and Pollack, 1975). A similar study using analysis of photomicrographs containing sarcomeres (Julian and Sollins, 1975) gave a value of 11%. The difference in the extent of shortening between the muscle and sarcomere lengths suggests the presence of a large series and parallel elastic components residing outside the contractile proteins. Experiments on skinned rat cardiac cells suggest the presence of a stiff intracellular structure (Fabiato and Fabiato, 1978) which may be associated with a high density elastic protein, known as "connectin" (Maruyama, Kimura, Kuroda and Handa, 1977; Matsubara and Maruyama, 1977). This demonstrates that the unique passive elasticity of cardiac muscle is based upon intracellular

structural properties. In the strand preparation, the absence of functional elastin, collagen and blood vessels and possibly the presence of connectin-like intracellular structure may both contribute to the observed reduced range of LT relationship.

Furthermore, the stiffness of the strand preparation can be analysed based upon the stress-strain relationship. The resting tension is due to the passive elastic property of the cardiac muscle (both intact muscle strip and strand). Since the cross section of the strand is known ($63 \mu\text{m} \times 3 \mu\text{m} = 0.189 \times 10^{-3} \text{mm}^2$), the resting tension values can be normalized as stress values ($\mu\text{N}/\text{mm}^2$). Likewise the strand stretches can be normalized with respect to initial length (L_0) to give strain values. This stress-strain data has been compared to that obtained from intact rat papillary muscle (Krueger and Pollack, 1975). The two stress-strain relationships were similar nonlinear functions, comparable to those seen in other biological preparation; they did not follow Hooke's law. The stress-strain relationship can be fitted by an exponential equation of the form

$$P = P_x (e^{kx} - 1) \quad \dots (4.1)$$

where P : Stress , N/mm^2

P_x : a constant, N/mm^2

k : elastic stiffness, N/mm^2

and x : strain.

This relation was also used in describing the stress-strain relationship in skeletal muscle (Hoekman, 1968).

For the strand preparation the constants of eq.(4.1) were $P_x = 6.8 \times 10^{-4} \text{ N/mm}^2$; and $k = 210.2 \text{ N/mm}^2$. The corresponding values for the intact rat papillary muscle (calculated from the data of Krueger and Pollack, 1975) were $P_x = 8.0 \times 10^{-4} \text{ N/mm}^2$; and $k = 14.11 \text{ N/mm}^2$. From this analysis the value of P_x is approximately the same in both preparations. Sonnenblick and his associates (Yeatman, Parmley and Sonnenblick, 1969) defined the slope of the stress-strain curve (k) as the "elastic stiffness". The elastic stiffness for the strand is about fifteen times greater than that of adult rat papillary muscle. This quantitatively confirms the apparent difference between the two preparations. There are two possible speculations: (1) the cardiac muscle obtained from a newborn animal is stiffer than that of an adult one (this was shown in a sheep model; Friedman, 1972). (2) the myocardial strand preparation obtained from culture is stiffer than the adult muscle. The influence of culture conditions on stiffness have not been defined except for the results of this dissertation.

One of the possible bases for the distinctive stiffness of the strand preparation could be the presence of non-contractile cells (such as fibroblasts) within the strand. They could cause a reduced range of length-active

tension relationship and a reduction in peak active tension if they constituted a large fraction of the cell population. The normalized cross-sectional active tension at L_{\max} computed from the data of Krueger and Pollack (1975) for intact adult rat papillary muscle was 0.123 N/mm^2 . The corresponding value for the strand preparation (0.026 N/mm^2) was about 20% of the adult. The cross-sectional tension in neonatal animal is smaller (about 50%) compared to that of adult (Friedman, 1972). Because the cells in the strands are even less differentiated than neonatal, it might be expected that the cross-sectional tension would be still lower. These comparisons suggest that the relative fraction of myocardial cells present in the strand is lower than that found in intact rat papillary muscle, but that the ratio of contractile to non-contractile cells is not dramatically different.

No significant hysteresis was observed in the LT relationship of the strands when stretched and allowed to shorten, unlike most other muscles (skeletal - frog sartorius - muscle, Hill, 1968; cardiac - cat papillary - muscle, Skelton et al., 1974). In both skeletal and cardiac muscle preparations, these investigators have shown that the repeat length-tension curves obtained after overstretching were uniformly shifted to the right and altered the position of L_{\max} . Electronmicrographs obtained from cardiac muscle, fixed at lengths 20% beyond L_{\max} ,

showed Z-line effacement sarcomere disruption and spotty areas of cell necrosis (Skelton et al., 1974). The absence of hysteresis observed in the strand preparation suggests that the electrical and mechanical continuity was maintained unchanged throughout the $\pm 1\% L_{\max}$ length change. In fact the small length change required for the full LT relationship may by itself account for the lack of hysteresis since it may be sufficiently small that no irreversible changes in elasticity or cell-to-cell relationships occurred during the measurements.

4.2.1.2 Strand characteristics during electrical stimulation

The peak isometric active tension of electrically stimulated strands (120 min^{-1}) increased relative to their spontaneous contraction amplitudes (Table - II) while the resting tension was not altered. The increase in active tension during electrical stimulation appears to be a frequency-mediated inotropic response produced by the stimulus rate of 120 min^{-1} (Refer Sec. 3.5). When tension amplitude is corrected using the force-frequency relation, the LT relationships for strands during spontaneous and electrically driven contractions are equivalent.

The rate of rise of tension, ($+dP/dt$), both during spontaneous and electrically driven contractions, varied with length changes in direct proportion with the isometric active tension developed by the strands at all lengths. This observation is consistent with increased maximal velocity of shortening as muscles were stretched from their maximally shortened lengths (L_0) to L_{max} as has been shown for cardiac (Sonnenblick, 1965a) and skeletal muscle (Bahler, Fales and Zierler, 1968).

Time to peak tension, t_p , did not change for different strand lengths. The length changes provide a scaling effect on the rate of active tension development; the amplitude of active tension increased as length approached L_{max} , dP/dt also increased and time to peak tension changed very little, similar to results obtained in isolated rat papillary muscle.

The two useful measurements, often referred by the muscle physiologists, in understanding the contractile dynamics are the velocity of shortening and the duration of the active state. Under isometric conditions, it is not possible to obtain direct measurements of either shortening velocity or the precise time course of contractile activation, because of the limitations of measurement techniques. However, one can estimate approximately these

values indirectly. The dP/dt is proportional to the maximum shortening velocity of the contractile materials. The duration of active state, in general proportional to the time to peak tension, is very crudely defined as the time during which the contractile material is maximally activated (Abbott and Mommaerts, 1959)

4.2.1.3 Strand characteristics in the SBSS

Length-tension relationship in SBSS was qualitatively similar to that of Fig. 3.6 for culture medium. There was a 10% reduction in active tension amplitude and a reduction in the spontaneous rate of contraction from 72 to 63 min^{-1} . The decrease in rate of contraction was due to lower $[K^+]_0$ present in the SBSS (Refer Fig. 3.20 b). When the strands were stimulated in the SBSS at a rate of 72 min^{-1} , the active tension magnitudes developed were equivalent to those in the culture medium. Thus the apparent reduction of active tension amplitudes in the SBSS was in reality a force - frequency effect (Refer Sec.3.5).

The shape of the LT relationships in the SBSS, while manipulating $[Ca^{++}]_0$, remained similar to that of Fig. 3.6. During calcium manipulation, the resting tension was not altered, but the magnitude of peak isometric active tension was directly proportional to the $[Ca^{++}]_0$ over the entire range of length studied.

4.2.2 Force-Frequency (FF) Relationship

When the strand was stimulated at 25°C, a biphasic force-frequency relationship was seen (Fig. 3.10). As frequency was increased from the spontaneous contraction rate to about 90 min⁻¹ active tension amplitude increased progressively to its maximal value (P_{FF}). At stimulus rates above this active tension amplitude decreased with increasing frequency. This result is consistent with the work of Woodworth (1902), who demonstrated the same phenomenon in intact dog heart. A biphasic FF relationship has also been reported by Henry (1975) for isolated papillary muscle from adult Sprague-Dawley rat hearts and by Benforado (1958) for adult rat ventricular muscle strips. The apparent differences between the frequencies at which the peak tension occurred in those preparations and that in this study may be accounted for by the differences in the preparations and techniques used. Henderson and associates (Henderson, Brutsaert, Parmley and Sonnenblick, 1969) reported a negative FF response in isolated rat papillary muscle strips. They attributed this characteristic to a decrease in contractility as reflected by a corresponding decrease in rate of rise of tension (dP/dt) and time to peak tension. These observations are consistent with those observed in the strand preparation, where the negative inotropic effect at high frequencies was accompanied by decreased dP/dt and t_p measurements.

There is considerable lack of consistency in the literature with regard to the FF relationship in rat heart preparations. Some investigators have reported a biphasic relation (Henry, 1975; Benforado, 1958) while others have reported only a negative inotropic response (Henderson et al., 1969) to increasing stimulus frequencies. The cultured cardiac muscle strands produced a biphasic FF relationship (Fig. 3.10)

The work of several investigators provides some insight as to the mechanisms that may be responsible for the biphasic FF response seen in rat in contrast to the positive inotropic response seen in other mammalian models. In cat and guinea pig increasing stimulus frequency causes an increase in time to peak tension and an increased loss of K^+ from the cytoplasm (Langer, 1968). Increased K^+ efflux results in a higher influx of Na^+ , which in turn leads to accumulation of Ca^{++} at the membranes, promoting increased tension (Buckley, Penefsky and Litwak, 1972). In contrast, no K^+ loss was observed with increasing stimulus frequencies in rat ventricles (Blessa et al., 1970). These investigators suggested that stimulation did not cause a lag in Na^+ pumping; hence there was no intracellular Ca^{++} accumulation and the positive inotropic effect associated with it in other species is absent in rat heart. The negative inotropic response at

higher frequencies may be a consequence of a constant rate of supply of contractile calcium combined with a progressively increasing demand for such calcium.

At higher frequencies of stimulation, the time to peak tension was shortened in isolated rat papillary muscle (Henderson et al., 1969); it was suggested that this resulted from a reduced duration of the active state. As a consequence, less calcium enters the cell during the contractile cycle and the amplitude of active tension is decreased. This evidence correlates with that from the strand preparation; time to peak tension increased directly with frequency up to 90 min^{-1} and thereafter decreased with further increases in frequency of stimulation (see Sec. 3.5.1).

The rather rapid spontaneous rate of contraction prevented a direct study of the FF relation at lower frequencies (below 73 min^{-1}) in the culture medium. Depression of the spontaneous rate by ACh allowed the range of FF assertion to be extended down to 9 min^{-1} . As seen in Fig. 3.36, in the presence of $1 \times 10^{-4} \text{ M ACh}$; active tension decreased dramatically. When this strand was stimulated at 72 min^{-1} (its spontaneous contraction rate in the culture medium), the active tension was identical to that observed for spontaneous contraction at that rate.

When the full frequency range ($10-240 \text{ min}^{-1}$) was studied in the presence of ACh, the portion of the curve which duplicated the frequency range possible without ACh was identical to results obtained in either the SBSS alone or the culture medium. This implies that experimental changes which cause a change in spontaneous rate alone, do not alter the contractile process except in accordance with the FF response.

4.2.3 Influence of Temperature

4.2.3.1 Effects of temperature on spontaneously contracting strands

Both the inotropic and chronotropic properties of the strands were temperature dependent as shown in Sec. 3.3. The rate of spontaneous contraction of the strands both before and after suspension increased progressively with temperature (Fig. 3.7). A similar phenomenon has been observed in cultured isolated single myocardial cells (Burke, G.H. private communication). Conversely, when the temperature was decreased the spontaneous contraction rate decreased in a manner similar to that reported for cultured chick embryonic heart cells (Koidl, Tritthart and Erkingen, 1980).

Isometric tension also increased progressively in the temperature range 15-20 °C, reaching a plateau in the range of 20-25 °C, and thereafter decreasing with further increases in temperature (Fig. 3.8). This is comparable to the data from the isolated heart muscle strips of adult Sprague-Dawley rats, where the isometric tension amplitudes were reported to be higher at 27 °C than at 37 °C (Kelly and Hoffman, 1960). Up to 25 °C the rate of rise of tension, ($+dP/dt$), of the strand increased with increasing temperature and thereafter was maintained or declined slightly (Fig. 3.9).

Table - IV lists contractile parameters computed from the data presented in Figures 3.7 to 3.9 at 10 °C temperature increments in the range of 15-35 °C. The Q_{10} values for lower (15-25 °C) and higher (25-35 °C) temperature ranges are computed.

The spontaneous rate of contractions has a Q_{10} value greater than 1.0 for both the temperature ranges (the two values are not significantly different) and thus it has a positive temperature coefficient for the entire temperature range. The variation of isometric tension (P_{max}) and the rate of rise of tension (dP/dt) with temperature are qualitatively similar (Figures 3.8 and 3.9 a). Both have a positive temperature coefficient ($Q_{10} > 1.0$) in the lower range and a negative temperature coefficient ($Q_{10} < 1.0$) in the higher range, with a transition occurring at 25 °C.

TABLE IV

Contractile Parameters of Spontaneously Contracting Strands at
Different Temperatures

Parameter	15 °C	25 °C	35 °C	Q ₁₀ low	Q ₁₀ high
Isometric tension (% max)	86	100	77	1.16	0.77
Spontaneous contraction rate (min ⁻¹)	69	74	88	1.07	1.19
dP/dt (% max)	82	100	92	1.22	0.92
time to peak tension (ms)	196	206	170	1.05	0.83

The Q_{10} values of these two parameters are nearly identical in the lower range, but that for the tension was notably lower than that for dP/dt in the higher temperature range.

Considering the rate of contraction, P_{\max} and $+dP/dt$ together, it appears that they may depend upon two different chemical processes which have different temperature-sensitive, rate-limiting steps. The positive temperature coefficient for the rate of contraction, throughout the entire temperature range studied, may indicate dependence on a pure "physical" process such as diffusion. In contrast, the tension appears to be mediated by two different processes, one with a positive temperature coefficient (in the temperature range of 15-25 °C) and the other with a negative temperature coefficient (in the range of 25-35 °C) with a transition occurring at 25 °C.

Interestingly, $+dP/dt$ seems to be mediated by a process which may reflect the combined effect of these two hypothetical processes. Above 25 °C, dP/dt has a temperature coefficient (0.92) that is roughly equivalent to the mean of that for tension and rate of contraction (0.98), resulting in a less negative temperature coefficient compared to that of isometric tension.

Temperature does not seem to alter either the resting tension or L_{\max} of the strand preparation, confirming the results obtained for intact papillary muscle (McLeod and Koch-Weser, 1965; Sonnenblick, 1974)

In the strand preparation, the time to peak tension, an index of active state duration, is longer in the temperature range of 20-25 °C than at higher temperatures (Fig. 3.9 b). In rat ventricular muscle at 27 °C, action potential duration and that of contraction were increased relative to values at 37 °C (Kelly and Hoffman, 1960). An increased duration of the action potential (AP) would facilitate entry of an increased amount of calcium during the plateau of the AP and $[Ca^{++}]_i$ would remain high for a longer period of time. This results in an increased active state duration with greater isometric tension.

4.2.3.2 Effects of temperature on electrically stimulated strands

The response of the strand during electrical stimulation was influenced by temperature in a manner similar to that observed for the spontaneous contraction. The force-frequency relationships obtained at all temperatures were qualitatively similar to one another. The Q_{10} values for all parameters at each frequency of stimulation were identical to those for spontaneous contraction. However, the frequency (f_F) at which the peak of force-frequency response occurred increased linearly with temperature (Fig. 3.12) and the Q_{10} value of f_F remained fairly constant over the entire temperature range (Q_{10} for 15-25 °C was 1.08 and that for 25-35 °C was 1.06).

Rate of rise of tension, (dP/dt), which reflects the velocity of shortening, increased progressively with temperature. The time to peak tension, which depends upon the active state duration as well as shortening velocity, was not altered until temperature reached 22 °C and then decreased nonlinearly with further increases in temperature (Refer Sec. 3.5.2). As a consequence, in the range of 15-22 °C, where time to peak tension was constant and dP/dt was increasing, tension amplitudes increased. Above 22 °C, even though the velocity of shortening continued to increase (as shown by dP/dt), the duration of the active state (as shown by time to peak tension) decreased in greater proportion, resulting in reduced tension development.

The maximum tension observed during force-frequency study is an interaction between the rate of shortening and the duration of the active state (both are variable with dependence on a number of factors including temperature). Thus when the frequency of stimulation is increased above its spontaneous rate, the closely spaced stimuli modify calcium release and uptake mechanisms resulting in potentiated contractile response.

With increasing temperatures, the rate of metabolism and chemical reactions controlling the shortening velocity are increased. However, the recovery process is also accelerated, resulting in a quicker restoration of calcium

involved in the contraction cycle (a shortening of the active state duration and a decrease in t_p). The decrease in the t_p was clearly seen at temperatures above 25 °C, in the strand preparation. At any given temperature, there will be an optimal frequency value for maximal tension development by the muscle, which is dependent upon the velocity of shortening and active state. The frequency at which maximal tension (P_{FF}) occurred during the force-frequency study increased with temperature due to the enhancement of the recovery processes by temperature. Thus with increasing temperature, f_F increased as seen in Fig. 3.12, because only with a shorter interstimulus period will baseline $[Ca^{++}]_i$ still be elevated when the next contractile cycle is initiated.

4.3 THE EFFECTS OF CATION MANIPULATION ON CONTRACTILITY

In the course of this study, K^+ , Na^+ and Ca^{++} concentrations in the SBSS were manipulated and the effects of these changes on the contractile functions of the suspended strands studied.

4.3.1 The Influence of Extracellular Potassium Concentration on the Contractile Responses

Manipulation of extracellular potassium ions altered only the spontaneous contraction rate, while the actual magnitude of AT remained constant (Fig. 3.13). When all other ions were held at standard concentrations (refer Table-I) and $[K^+]_o$ was manipulated, the membrane potential changes proportionally as predicted by the "constant field" theory of Goldman (1943) and Hodgkin and Katz (1949). An increase in $[K^+]_o$ will partially depolarize the membrane (Noble, 1979; Katz, 1977), raising the interspike membrane potential closer to the threshold. Assuming that the leakage conductances of the generator potential are unchanged, this leads to an increased rate of contraction. Opposite changes should occur when $[K^+]_o$ is reduced. This has been confirmed experimentally.

Using microelectrode techniques in cultured chick embryo heart cells, Lieberman (1967) observed a similar reduction in the spontaneous beating rate in low K^+ media. A reduction in spontaneous rate induced by low potassium was also reported for mammalian hearts (Gettes, Surawicz, and Shive, 1962; Watanabe, 1965).

Conversely, with low $[K^+]_o$, prolonged APs have been observed in cultured chick heart cells (Lieberman, 1967) and in mammalian cardiac muscle (Hoffman and Cranefield, 1960; Gettes et al., 1962; Watanabe, 1965). Thus the increased calcium influx due to the prolonged AP would compensate for the expected negative inotropic effect of decreased rate.

4.3.2 The Influence of Extracellular Calcium Concentration on the Contractile Responses

Over the entire range of calcium manipulation there was no significant change in the basal spontaneous contraction rate of the suspended myocardial culture strands. This is consistent with the reports on cultured embryonic chick ventricles (Barry, Pitzen, Protos and Harrison, 1975) and contradictory to the observations from clusters of cultured neonatal rat hearts (Schanne et al., 1975). This apparent difference in clusters of cardiac cells may be due either to the age of the cells (around 2 days) or to the difference in culture conditions.

The calcium dose-response curve obtained from this preparation (Fig.3.16) has a sigmoid shape typical of isolated cardiac muscle strips from frog ventricle (Chapman and Niedergerke, 1970), chicken and rabbit papillary or

trabecular muscle (Kitazawa, 1976; Ebashi, Kitazawa, Kohama, and van Eerd, 1978) and skinned cardiac cells obtained from adult rat ventricles (Fabiato and Fabiato, 1975).

While calcium dose-action curve from intact adult rat papillary muscle have also been reported (Forester and Mainwood, 1974), they were obtained over a very limited range of $[Ca^{++}]_o$ (1.0×10^{-4} - 2.5×10^{-3} M). Hence a direct comparison with the results for the myocardial strand preparation is not possible. In order to make quantitative comparisons, the best data available is from frog ventricular strips (Chapman and Niedergerke, 1970). In this preparation, the threshold response occurred at 1.0×10^{-3} M calcium. The dose-action curve when plotted semi-logarithmically had a straight line fit in the range of 2.0 - 5.0×10^{-3} M with a peak response at 5.0×10^{-3} M. The range of calcium concentration over which the (semi-logarithmic) calcium dose-action curve had a linear relationship in the strand preparation is analogous to these results. In the strand preparation the threshold occurred at 1.0×10^{-5} M. Thus it appears to be more responsive to low calcium concentrations. The detection of tension at the lower calcium concentration may be due to a higher sensitivity of the force transducer employed in this study, a smaller thickness of the strand preparation or the species' differences.

Fabiato and Fabiato (1975) demonstrated a calcium dose - action curve for skinned cardiac cells obtained from adult rat ventricles, in which the tension response had a linear (in semi-logarithmic plot) relationship with free calcium in the range of 6.0×10^{-7} - 3.0×10^{-6} M. It is not possible to make a direct quantitative comparison between the results obtained from the strand preparation and the work of Fabiato and Fabiato (1975), since their preparation was devoid of sarcolemma and their results are thus an index of intracellular calcium concentration. However, the dose-action curve for the strand is qualitatively comparable to that of skinned cardiac (Hibberd and Jewell, 1979; Fabiato and Fabiato, 1975; 1978) and skeletal (Endo, 1977) muscle preparations. In skinned preparations, where the cell membrane is removed, tension develops at very low calcium concentrations because it can act directly on the contractile proteins. The shift in the dose-action curve for the strand preparation by about three decades in concentration to the right of that of skinned cardiac cell preparation may be accounted for by the presence of intact membranes. This implies that even though a structural correlation with contractile filaments has not yet been made, functionally the response is typical of a contracting cardiac muscle.

The fall in tension observed at concentrations above 1.0×10^{-2} M may be due to local anesthetic membrane effects of high $[Ca^{++}]_o$ (Weidmann, 1955), similar to that seen in lobster giant axon (Hoekman and Dettbarn, 1972). High $[Ca^{++}]_o$ modifies the membrane properties of the cell by depressing the amplitude of action potential and changing the ionic conductance. An alternate possibility is that Ca^{++} affects the cyclic nucleotide system regulating contractility (Tada, Kirchberger, Iorio and Katz, 1975). Some of the critical enzyme reactions that are part of the contractile pathway (Winegrad and McClellan, 1979) show biphasic responses at different calcium concentrations. At low to moderate concentrations (intracellular free calcium ion concentration up to 1.0×10^{-7} M), calcium has a stimulatory effect, while increased $[Ca^{++}]_i$, (between 1.0×10^{-6} - 1.0×10^{-5} M) proportional to $[Ca^+]_o$, tends to produce inhibitory effects. This appears to be caused by a reduction in cyclic Adenosine monophosphate (cAMP) levels, mediated by the ability of elevated calcium to inhibit adenylate cyclase and to activate phosphodiesterase (Tada et al., 1975). In cultured chick embryonic heart cells a decrease in Ca^{++} influx at high $[Ca^{++}]_o$ have been reported (Fosset, Barry, Lenoir and Lazdunski, 1977). It is not clear from this data whether the decrease in calcium conductance at high $[Ca^{++}]_o$ is due to direct effects or a modification of enzyme systems that regulate calcium channels.

When $[Ca^{++}]_o$ was reduced to 1.0×10^{-6} M and below, tension developed by the strand disappeared (see Figures 3.16 and 3.19), indicating its extreme dependence on $[Ca^{++}]_o$. This was mirrored by the rapid restoration of contractility when $[Ca^{++}]_o$ was returned to control levels (see Fig. 3.21). If indeed the strand represents a good model for cardiac muscle, this would be expected since cardiac muscle differs from skeletal muscle, in its dependence on $[Ca^{++}]_o$ for tension development (Langer, 1973). This is because of the organizational differences between the two muscle types. Cardiac muscle depends on the sarcolemma as a major pathway for the transient introduction of Ca^{++} to contractile filaments (Chapman, 1971; Chapman and Tunstall, 1971).

Thus, in relation to external calcium levels, the strand preparation appears to be an accurate model of cardiac muscle both for membrane (Chapman and Niedergerke, 1970a) and contractile (Fabiato and Fabiato, 1975) properties.

An increase in $[Ca^{++}]_o$ increases both the velocity of shortening and the active state amplitude (Braunwald et al., 1976). This might account for the increase in dP/dt , which has been observed to be directly proportional to the amplitude of active tension (see Figures 3.17 and 3.16). Time to peak tension is determined by the interplay between the active state and the velocity

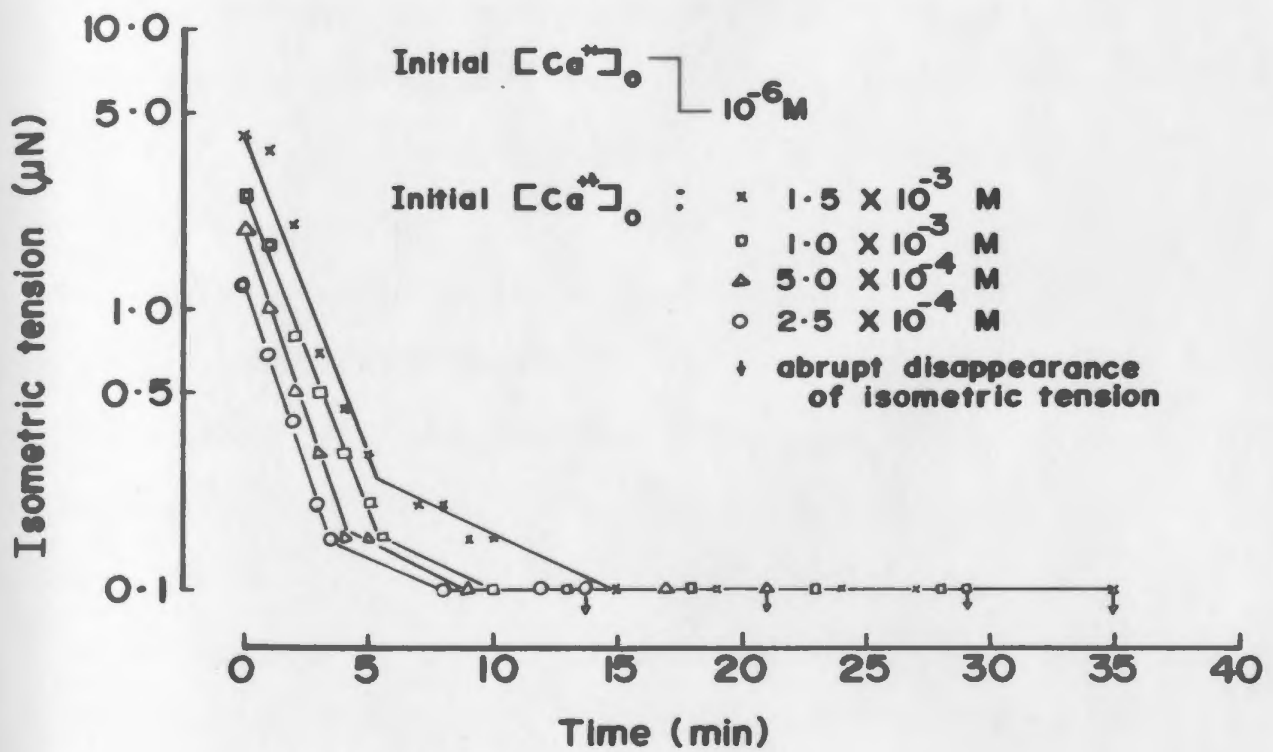
of shortening (Sonnenblick, 1967). It was observed that the extracellular calcium may influence both the duration and intensity of the active state. There appears to be a mechanism in the myocardium, which tends to maintain the same time to peak of active tension, irrespective of $[Ca^{++}]_o$. Because of the simultaneous increase in shortening velocity and the active state amplitude, a parallel prolongation of active state duration is not reflected in the time to peak tension measurements (Sonnenblick, 1965).

Calcium washout curves obtained by decreasing $[Ca^{++}]_o$ to 1.0×10^{-6} M (Fig. 3.18) can be broken down into three components. The data shown in Fig. 3.18 was replotted on a semi-logarithmic form (Fig. 4.1) to better define the decay of contractility. When the tension response, on the ordinate, is plotted on a logarithmic scale, it is evident from Fig. 4.1 that three phases in calcium washout are present for each of the initial concentrations from which the strand was switched to zero (or 1.0×10^{-6} M) calcium.

Analysis of the curves (using standard curve-fitting procedures) showed that they are parallel to one another. The first and second phases are very clearly exponential decays while the third phase appears as a constant tension of $0.1 \mu N$ maintained for a prolonged time with an abrupt disappearance. The time constants of phases 1 and 2 are

Fig. 4.1 The relationship between calcium washout and isometric tension in cultured myocardial strands.

Replot of Fig. 3.18. Isometric tension (μN) is represented on the ordinate on a logarithmic scale while the elapsed time (min) is on the abscissa as a linear scale. Reduction of $[\text{Ca}^{++}]_0$ to $1 \times 10^{-6} \text{ M}$ resulted in three phases of tension in calcium washout; each was a good approximation of a straight line on this semi-logarithmic plot. The lines derived from different initial $[\text{Ca}^{++}]_0$ were parallel to one another.



the same for all initial concentrations ($t_1 = 2.02$ min and $t_2 = 12.75$ min) but the initial amplitude and final time to reach zero tension are concentration dependent. The first phase with a smaller time constant (2.02 min) may represent the fluid exchange properties of the chamber-perfusion system. The value of this time constant is so similar to the fluid-equilibration time in the upper 2 mm of the chamber that it is impossible to distinguish whether there is another functional mechanism other than the simple mixing. The second slower phase with a larger time constant (12.75 min) may represent the depletion of membrane-bound calcium (Philipson and Langer, 1979). The third prolonged phase with a very small tension (0.1 μN) and then an abrupt decrease to zero tension after an extended period of time may represent an internal storage site for calcium. This prolonged small amplitude of tension reflects some physiological mechanism whereby there is a small amount of free calcium present. This calcium is abruptly turned off. Such a phenomenon has never been reported in the literature. One possible explanation for this observation may be the sensitivity of the transducer employed in this study, which is capable of measuring contractions as low as 0.1 μN (or 10 μg). The usual force transducers used by other investigators did not have such a high sensitivity and hence they could not detect the persistent low tension in the presence of external calcium

concentrations as low as 1.0×10^{-6} M. This unusual observation needs further investigation before any speculation as to its basis is possible. From Fig. 3.20, it appears that this internal calcium store has a limited capacity (it is saturable), since $[Ca^{++}]_o$ above 1.5 mM do not increase washout time. The amount of calcium in this pool is small (as reflected by its influence on the active tension amplitude) compared to the other calcium sources represented in the washout curves; most calcium involved in the contractile response appears to be membrane associated or extracellular, as is also the case for intact cardiac muscle (Langer, 1976; 1977; 1978).

Because of this fact, upon return to higher $[Ca^{++}]_o$ from 1.0×10^{-6} M, it is not unexpected that the strands develop steady-state tension in a very short time, since the restoration of $[Ca^{++}]_o$ and "recharging" the membrane binding sites are the critical events required.

An attempt can now be made to postulate the significance of different "functional" calcium compartments demonstrated by Ca^{++} washout in this preparation.

(1) Phase 1 of the washout curves most likely includes the extracellular calcium pool. Because of the slow response characteristics of the perfusion system it was not possible to accurately analyze any thing other than the steady-state conditions for the extracellular calcium pools.

(2) Phase 2 probably reflects the loss of calcium from cell membranes or tightly associated organelles such as "membrane cisternae" (Fawcett and McNutt, 1969) or the SR acting as a labile calcium storage, the content of which determines the inotropic state of the muscle (Allen, Jewell and Wood, 1976).

(3) Phase 3 or the prolonged low tension response is maintained by slowly exchangeable intracellular calcium reservoirs (mitochondria or other "deep" intracellular organelles).

A similar three calcium component system has been hypothesized by Chapman and Tunstall (1971) based upon data from frog auricle trabaculae. These authors propose a sequential release of calcium from (2) and (3) above, triggered by the calcium entering from the extracellular pool (1) during depolarization of the cell membrane. They visualized these three compartments in series as: (1) extracellular pool; (2) a storage site on the sarcolemmal inner surface; and (3) reservoirs in the sarcoplasm - possibly the SR or mitochondria.

The steady-state conditions of this investigation employing strand preparation appeared to be consistent with the above hypothesis. However, since an accurate determination of the dynamic relationship between $[Ca^{++}]_o$ and the strand response was not possible with this perfusion arrangement, the question still remains as to

whether changes in calcium concentration produced effects in serial fashion between the three compartments. An unequivocal resolution of this question might be obtained in a fast switching system in which $[Ca^{++}]_o$ very rapidly reaches equilibrium.

4.3.2.1 The relation between $[Ca^{++}]_o$ and the force-frequency relationship

Below 0.5 mM $[Ca^{++}]_o$, a force-frequency relation did not exist; tension amplitude was constant regardless of stimulus frequency (see Fig. 3.22). This concentration corresponds to the lower limit of the semi-logarithmic region seen in the calcium dose-action curve (Fig. 3.16). This suggests that at low $[Ca^{++}]_o$, a relatively small amount of calcium ions move across the sarcolemma during the contractile cycle. Thus a significant baseline intracellular calcium concentration, capable of producing potentiation during repetitive stimulation was not built up. The amount of calcium available for the contractile process may remain constant even at high frequencies due to a balance between increased baseline intracellular calcium concentration with increased stimulation frequency and shortened action potential duration which reduce Ca^{++} influx.

Between 0.5 mM and 5.0 mM, the typical biphasic force-frequency response (similar to Fig. 3.10) was observed. The rate of rise of tension and the tension amplitudes were greater with higher $[Ca^{++}]_o$. This finding is in agreement with the radioactive calcium experiments in which Teiger and Farah (1967; 1968) demonstrated that the rate of uptake of calcium was greater at high than low $[Ca^{++}]_o$.

The depression of tension amplitudes at higher frequencies of stimulation is similar to that discussed in section 4.2.2 (page 202).

4.3.3 The Influence of Extracellular Sodium Concentration on the Contractile Responses

The potentiated tension response induced by low $[Na^+]_o$ seen in the strand preparation (Fig. 3.24) is analogous to the well documented phenomenon seen in frog cardiac muscle (Horackova and Vassort, 1976; Vassort and Rougier, 1972; Goto, Kimoto and Kato, 1971) and also in mammalian cardiac muscle from a variety of species (sheep Purkinje fibers, Gibbons and Fozzard, 1975; trabaculae or papillary muscle strips from adult cats, Trautwein, McDonald and Tripathi, 1975; and guinea pig papillary muscle strips, Ochi and Trautwein, 1971). Horackova and Vassort (1979), under voltage-clamp conditions, have proposed a model for tension

regulation suggesting two pathways whereby calcium enters the cell. One part of tension (phasic) elicited by depolarization is directly activated by Ca ions entering the cell, through slow inward calcium channels (I_{Ca}) as well as indirectly activated by entry through sodium channels; both fractions trigger further release of calcium from internal stores. The second component (tonic) of tension elicited by depolarization independent of I_{Ca} is activated by Ca^{++} entering through a sodium-calcium exchange mechanism. Calcium entering the cell through any one of the above processes could trigger the internal stores to release more calcium. This would be comparable to the calcium-induced calcium release seen in skinned cardiac fibers (Fabiato and Fabiato, 1975a). The net result is a large increase in $[Ca^{++}]_i$ and a potentiated tension response.

In frog atrial muscle under voltage-clamp conditions, Horackova and Vassort (1976; 1979) observed a triphasic potentiated tension response to reduced $[Na^+]_o$ (an initial steep increase followed by a small drop in tension to reach a steady-state), similar to Fig. 3.24 (panel b). These investigators attributed the transient increase in tension to an increased rate of Na^+ efflux and obligatory calcium influx due to a reduced sodium gradient. The slight decrease in tension following the transient increase, in transition to steady-state tension is explained by the decrease in $[Na^+]_i$ following the reduction in $[Na^+]_o$ as the

sodium-potassium pump attempted to restore the Na^+ gradient. Finally, the steady-state potentiated tension is believed to be maintained because of a decreased affinity for sodium-calcium exchange resulting from the reduced sum of Na^+ and Ca^{++} ions (Glitsch, Reuter and Schloz, 1970).

Horackova and Vassort (1976;1979) speculated that return to the standard solution, with a larger Na^+ gradient would antagonize Ca^{++} influx and lead to a transient tension decrease before recovery to control levels. When switched to low $[\text{Na}^+]_o$, the time to reach the peak of transient tension in the strand was variable; the shortest time was observed to be 1.1 min in contrast to 0.5 min, seen in frog atrial muscle voltage clamp studies (Horackova and Vassort, 1976). This apparent difference in time course may be due to the slow chamber perfusion characteristics (refer Sec. 3.6), since the exchange volume in the voltage-clamp apparatus used by Horackova and Vassort was very small.

An alternate explanation for the triphasic tension response to low $[\text{Na}^+]_o$ perfusion based on calcium flux measurements in rat ventricular cell cultures has been suggested by Langer's group (Langer, Nudd and Ricchiuti, 1976). In the first few seconds of low sodium perfusion, calcium influx increases and exceeds calcium efflux, resulting in an elevation of intracellular calcium. Hence tension increases. As $[\text{Ca}^{++}]_i$ increases calcium efflux also

increases and within a few minutes matches influx, establishing a new steady-state level at a higher asymptote during which time tension falls to its steady-state.

The spontaneous contraction rate varies proportionally with $[\text{Na}^+]_o$ (Fig. 3.29). This variation is consistent with change in the RMP predicted by constant field theory (refer Sec. 4.3.1). When all other ions were held at their standard concentration, the change in RMP and hence a change in spontaneous contraction rate is due to change in sodium concentration gradient. Based on the FF response information, if $[\text{Na}^+]_o$ were affecting only the frequency one would expect an approximately 10% decrease in isometric tension for the drop in frequency from 62 to 52 min^{-1} . However, the observed situation was the tension remained constant down to 100 mM $[\text{Na}^+]_o$ and further decrease in $[\text{Na}^+]_o$ showed prominent increase in tension. One possible explanation for the stable tension response between 146.5 and 100 mM is that the decreased inotropic response produced by the force-frequency property was compensated for by the increased contractility due to a reduced sodium gradient. Below 100 mM $[\text{Na}^+]_o$, it would appear that the effect of decreased sodium driving force on the exchange carrier are dominant, resulting in a prominent increase in active tension response.

The rate of rise of tension was proportional to tension (Figures 3.26 and 3.27) during low sodium perfusions. This parallels the observations with manipulation of $[Ca^{++}]_o$.

Time to peak tension in low Na^+ media (Fig. 3.28) was characteristically different from that observed during the manipulation of $[Ca^{++}]_o$, where it remained unaltered. In low Na^+ perfusion, time to peak tension varied inversely with $[Na^+]_o$.

From the previous discussions, it was inferred that the $[Ca^{++}]_i$ levels increase with lowering $[Na^+]_o$. The increased baseline $[Ca^{++}]_i$ level produced an increase in both the strength and duration of the active state. Furthermore, with reduced $[Na^+]_o$, an important calcium-removal mechanism (Ca-Na exchange) is impaired, leading to a prolonged active state duration. These two factors have a cumulative effect and produce an elevated and prolonged active state duration, which results in an increased time to peak tension. Because the dP/dt and t_p can be influenced by both change in the time course and in amplitude of the active state, it is not possible to make any reasonable speculation as to the changes in the time course of the rising phase of the contractile event under the low sodium conditions.

4.3.4 The Effects of Simultaneous Manipulations of $[Ca^{++}]_o$ and $[Na^+]_o$ on the Contractility of Cultured Strands

The Na-Ca exchange phenomenon at four different $[Ca^{++}]_o$ in the presence of low Na^+ perfusions is illustrated in Figures 3.30 and 3.31. At standard $[Ca^{++}]_o$ and low $[Na^+]_o$ (Fig. 3.30, panel a), the response is similar to that of Fig 3.24 (panel b).

In a perfusion medium containing $[Ca^{++}]_o$ less than or equal to 1.0 mM with 80 mM $[Na^+]_o$, a transient tension potentiation was followed by a drop in tension to a level below control (panels b and c of Fig. 3.30 and panel b of Fig. 3.31). This is not unexpected since the transient tension potentiation is due to inhibition of Ca^{++} efflux related to a sudden reduction in $[Na^+]_o$ relative to SBSS. However the potentiated tension was not maintained because of the reduced $[Ca^+]_o$ in the new perfusion media. The tension falls to a steady-state value proportional to $[Ca^{++}]_o$.

Comparison of panels b and c with panel a (Fig. 3.30) indicates that the rate of tension decrement following the tension peak was faster with lower $[Ca^{++}]_o$ (less than 1.5 mM). This rapid decay suggests that $[Ca^+]_i$ is depleted from a critical site (membrane associated pool?) at a faster rate with reduced $[Ca^{++}]_o$. One possible interpretation of this is the amount of calcium in the pool

decreases at $[Ca^{++}]_o$ below 1.5 mM, the rate of efflux being concentration dependent in a simple Fick's law relation (refer Figures 3.20 and 3.21, which also implicate 1.5 mM $[Ca^{++}]_o$ as a critical concentration).

In perfusion media containing low sodium (75 mM) and a $[Ca^{++}]_o$ of 1.5 mM and above, the elevated steady-state tension is maintained (Fig. 3.32). This suggests that tonic tension maintenance requires a critical $[Ca^{++}]_o$ level (1.5 mM) to support sustained calcium demand on the cellular pool. At concentrations greater than 1.5 mM there appears to be a graded response of steady-state tension development, reflecting the influence of $[Ca^{++}]_o$. This is what one would expect from the calcium dose-action relationship (Fig. 3.16).

For $[Ca^{++}]_o$ below 1.5 mM, transient tension potentiation occurred but the new steady-state following the transient potentiation was identical to the modified baseline tension seen with reduced calcium alone. The analysis of this data, shown in Fig. 3.33, compares the calcium dose-action relationship with in normal sodium (100% Na^+ = 146.5 mM) and low sodium (50% Na^+ = 75 mM) media. The curves differ above 1.0 mM $[Ca^{++}]_o$. This portion (above 1.0 mM) of the two curves is similar to those reported for the frog ventricular strips (Luttgau and Niederggerke, 1958). While these investigators did not examine the entire $[Ca^{++}]_o$ range, the shape and relation of

the curves are similar to those of Fig. 3.33, in the range of $[Ca^{++}]_o$ for which they used comparable values of $[Na^+]_o$ in their perfusion solution (100% and 50%). These qualitative similarities provide additional evidence that the strand preparation serves as an accurate model of the myocardium for ionic and contractility studies.

Various groups of investigators have proposed differing stoichiometry of the number of sodium ions exchanged by the exchange carrier for each calcium ion. Based upon ion flux studies, Langer and his co-workers believe that two Na^+ ions are exchanged with the influx of each Ca^{++} ion (Langer, 1976; Langer, Frank and Brady, 1976; Wendt and Langer, 1977) and that the process is electroneutral. Alternatively, investigators using voltage clamp techniques have interpreted their results to suggest that three or more sodium ions are exchanged for each calcium ion (Horackova and Vassort, 1979a; Beeler and Reuter, 1970; New and Trautwein, 1972), resulting in an electrogenic inward calcium movement. Results from the strand preparation either with reduced $[Na^+]_o$ and standard $[Ca^{++}]_o$ or with reduced $[Na^+]_o$ and reduced $[Ca^{++}]_o$ are consistent with the existence of a Na-Ca exchange phenomenon. For an electroneutral model, in which the carrier binds either one Ca^{++} or two Na^+ ions, changes in $[Ca^{++}]_o$ and $[Na^+]_o$ should not affect contractile force when

$[Ca^{++}]_o/[Na^+]_o^2$ is maintained constant (Luttgau and Niedergerke, 1958). In the strand preparation, $[Ca^{++}]_o/[Na^+]_o^2$ ratios in SBSS (0.70×10^{-4}) and low $[Na^+]_o$ (80 mM) with 0.5 mM $[Ca^{++}]_o$ (0.78×10^{-4}) were approximately equal. A biphasic tension response (Fig. 3.30, panel c) similar to that obtained from frog atrial fibers (Horackova and Vassort, 1979) was observed. This contradicts the predictions of an electroneutral model for the exchange carrier and implies the presence of an electrogenic Na-Ca exchange mechanism.

In cardiac muscle strips, from a variety of preparations, it has been widely accepted that the excitation-contraction coupling, which is highly dependent upon the $[Ca^{++}]_o$, appears to have a very significant membrane associated component and the extrusion of Ca^{++} is mediated by Na-Ca exchange mechanism. All of these properties appeared to be present in the strand preparation. Hence it appears to be a legitimate model for studying the excitation-contraction coupling process in cardiac muscle.

4.3.5 Characterization of Pharmacological Responses of the Myocardial Strand Preparation

4.3.5.1 Adrenergic receptor properties

The cultured cardiac muscle strands gave positive chronotropic (Fig. 3.37 a) and inotropic (Fig. 3.37 b) responses upon exposure to the beta-sympathomimetic drug isoproterenol (ISO) and were unresponsive to the alpha-agonist, phenylephrine. The effects produced by ISO were competitively blocked by the beta-adrenergic receptor blocking drug propranolol. These results demonstrate the presence of beta-adrenergic receptors in the strand preparation. The dose-isometric tension response is qualitatively similar to that reported for isolated right ventricular papillary muscle (fetal and newborn lamb, Friedman, 1972) and cultured cells of mouse myocardium (Boder and Johnson, 1972). However quantitative differences exist; the threshold and maximal response doses for the strand preparation are 1.0×10^{-7} M and 1.0×10^{-4} M respectively, in contrast to 1.0×10^{-9} M and 1.0×10^{-5} M respectively for both isolated papillary muscle preparation from fetal lamb and cultured mouse heart cells. It is possible that these differences are species specific.

Beta-adrenergic agonists, such as epinephrine, norepinephrine and isoproterenol, are believed to produce their effects on cardiac cells by increasing the intracellular cAMP levels (Schneider and Sperelakis, 1975). According to the current hypothesis, beta-agonists first interact with the membrane adenylate cyclase system, activating the enzyme which results in increased cAMP levels (Davoren and Sutherland, 1963). This cAMP in turn increased intracellular Ca^{++} , leading to an increased force of contraction (Robinson, Butcher, Oye, Morgan and Sutherland, 1965; Tada et al., 1975); propranolol blocks the beta-agonist stimulation of cAMP levels.

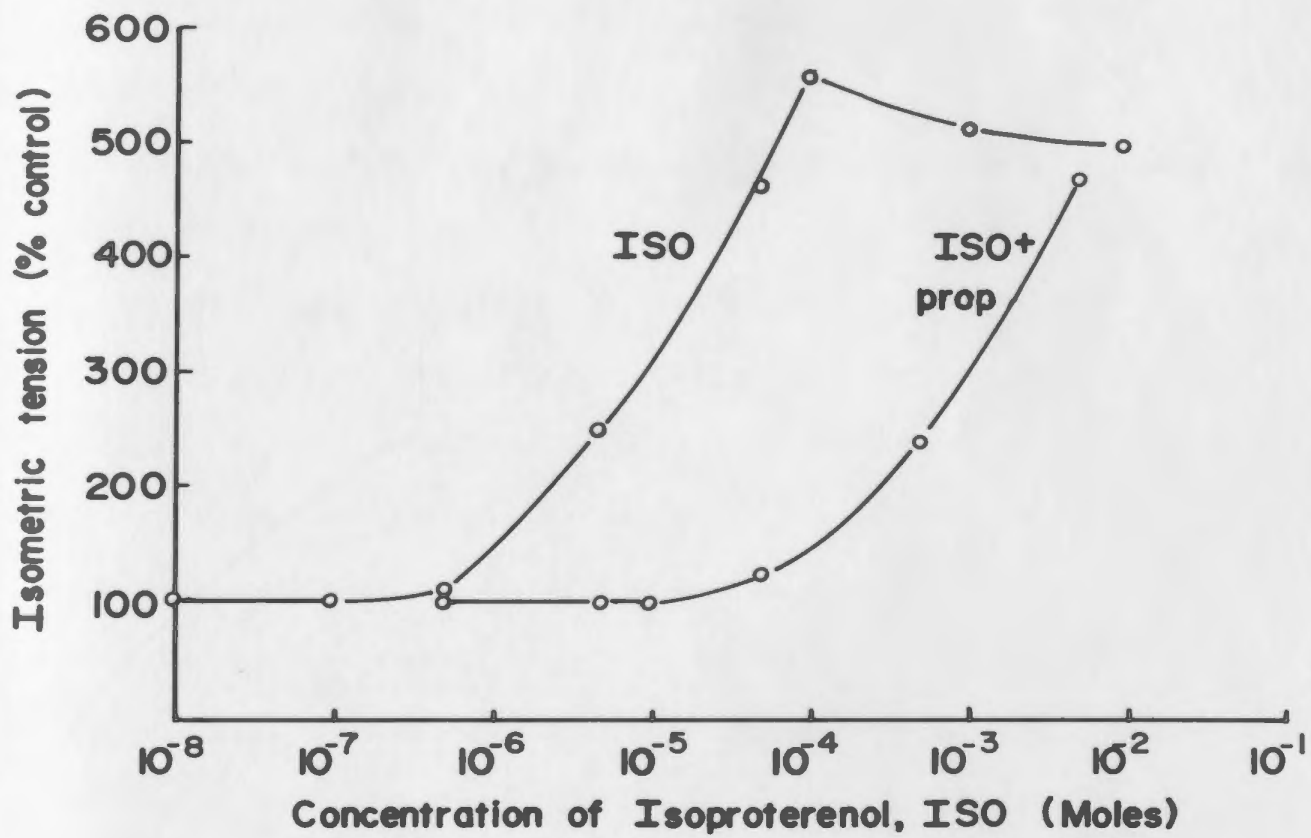
In voltage-clamped cat papillary muscle experiments, Reuter (1974) showed that the extracellular application of beta-agonists accelerated the pacemaker activity and increased slow calcium inward current (I_{Ca}). He attributed the positive inotropic effects to increased I_{Ca} . It would follow that an increased Ca^{++} -influx should also trigger a larger secondary release of calcium from the membrane associated pool. Katz (1977) has presented evidence suggesting that these reactions occur at the level of contractile proteins, leading to a positive inotropic response.

As seen in Figures 3.37 a and b, increasing concentration of ISO increases both spontaneous rate of contraction and isometric tension. The peak responses occurred at 1.0×10^{-4} M ISO. There is a clear difference in the response of the strand to increasing frequency of contraction in the presence of ISO as compared with the response during electrical stimulation. With the receptor-induced chronotropic response, there is no apparent negative inotropic response at high frequencies. This is probably due to important direct inotropic effects of ISO which are difficult to analyze precisely. A dose-isometric tension response using a rate compensated control is shown in Fig. 4.2. Compensation of the control response for increased rates of contraction is made (control for each contraction is the tension value from the force-frequency relation corresponding to the spontaneous rate achieved). The maximum potentiation of tension in relation to that of control was elevated as high as 560%.

At higher concentrations of ISO (above 1.0×10^{-4} M), both the isometric tension and the spontaneous contraction rate declined slightly. This slight negative inotropic and chronotropic effect at concentrations above 1.0×10^{-4} M, may be due to the inhibitory effects of increased $[Ca^{++}]_i$ on adenylate cyclase and its stimulatory effects on phosphodiesterase (Tada et al., 1975). It has been

Fig. 4.2 The contraction rate-corrected dose-isometric tension relationship in cultured myocardial strands responding to isoproterenol (ISO) and propranolol (prop).

The points in this figure were computed from values used in Fig. 3.38 (b) after making correction for the positive inotropic effect of increased contraction rate as derived from Fig. 3.38 (a).



suggested that cAMP mediates its response on (1) Na^+ and K^+ membrane permeability, to vary the spontaneous contraction rate (Reuter, 1974); (2) calcium channels controlling slow inward calcium currents (Reuter, 1974); and (3) the release of calcium from intracellular pools (Tada et al., 1975).

4.3.5.2 Cholinergic receptor properties

As shown in Fig. 3.35, acetylcholine (ACh) depressed both the rate of spontaneous contraction and the isometric active tension. The ACh dose-response curves were qualitatively similar to those of isolated myocardial strips from fetal lamb (Friedman, 1972). When the strand was stimulated in the presence of ACh, at its spontaneous rate of contraction in SBSS alone (Fig. 3.36), the tension returned to its earlier control value. This suggests that the influence of ACh on the myocardial strands is purely chronotropic and the apparent negative inotropic response to ACh seen in Fig. 3.35 b is simply a force-frequency effect.

Acetylcholine-mediated negative inotropic and chronotropic responses were competitively blocked by 1.0×10^{-6} M atropine. This is demonstrated by the fact that the curves were shifted by 2.5 decades to the right in the presence of atropine, but were otherwise identical.

The total pharmacological pattern demonstrates the presence of classical cholinergic-muscarinic receptors in this strand preparation.

Acetylcholine is said to modify the membrane permeabilities (to Na^+ and K^+) of excitable cell membranes (Dale, 1914; Eccles, 1964; Katz, 1966). The action of ACh to increase the potassium conductance and thereby slowing the pacemaker activity in the myocardium is well established (Katz, 1977). At a concentration of 1.0×10^{-4} M, ACh has been shown to completely stop the spontaneous beating activity of isolated single rat heart cells in culture, with recovery upon return to standard perfusion (Harary and Farley, 1960). Similar ACh-mediated negative chronotropic effects have been reported in a variety of species and preparations. These include cultured embryonic chick atrium (Fange, Persson, and Thesleff, 1956); intact embryonic chick myocardium (Barry, 1950; Fingl, Woodbury and Hecht, 1952); intact innervated frog ventricular strips (Sperelakis and Lehmkuhl, 1965). The presence of a muscarinic receptor in the cultured strand preparation appears to be consistent with the results reported for other cultured cardiac muscle preparations (chick embryo, McCarty et al., 1960; Sperelakis and Pappano, 1969a; neonatal mouse, Lane et al., 1977; rat, Harary and Farley, 1960). This is quite different from intact ventricular strips which do not

respond to ACh (Randall and Armour, 1977). It appears that the presence of innervation with its trophic influence is necessary for the selective development of only adrenergic receptors in ventricular muscle.

The evidence obtained in this study suggests that the strand preparation is an accurate model for pharmacological studies of cardiovascular drugs acting at beta-adrenergic as well as muscarinic receptors.

4.3.6 The Interaction of K^+ , Na^+ , Ca^{++} Ions Regulation and Adrenergic and Cholinergic Receptors in Cultured Cardiac Muscle Strands

The data on different ions accumulated in this research can be summarised with the help of a diagram (Fig. 4.3) to explain in the light of different mechanisms described in cardiac muscle physiology literature.

The existence of three calcium pools have been suggested: (1) an extracellular pool; (2) a membrane associated pool; and (3) an intracellular "deep" pool.

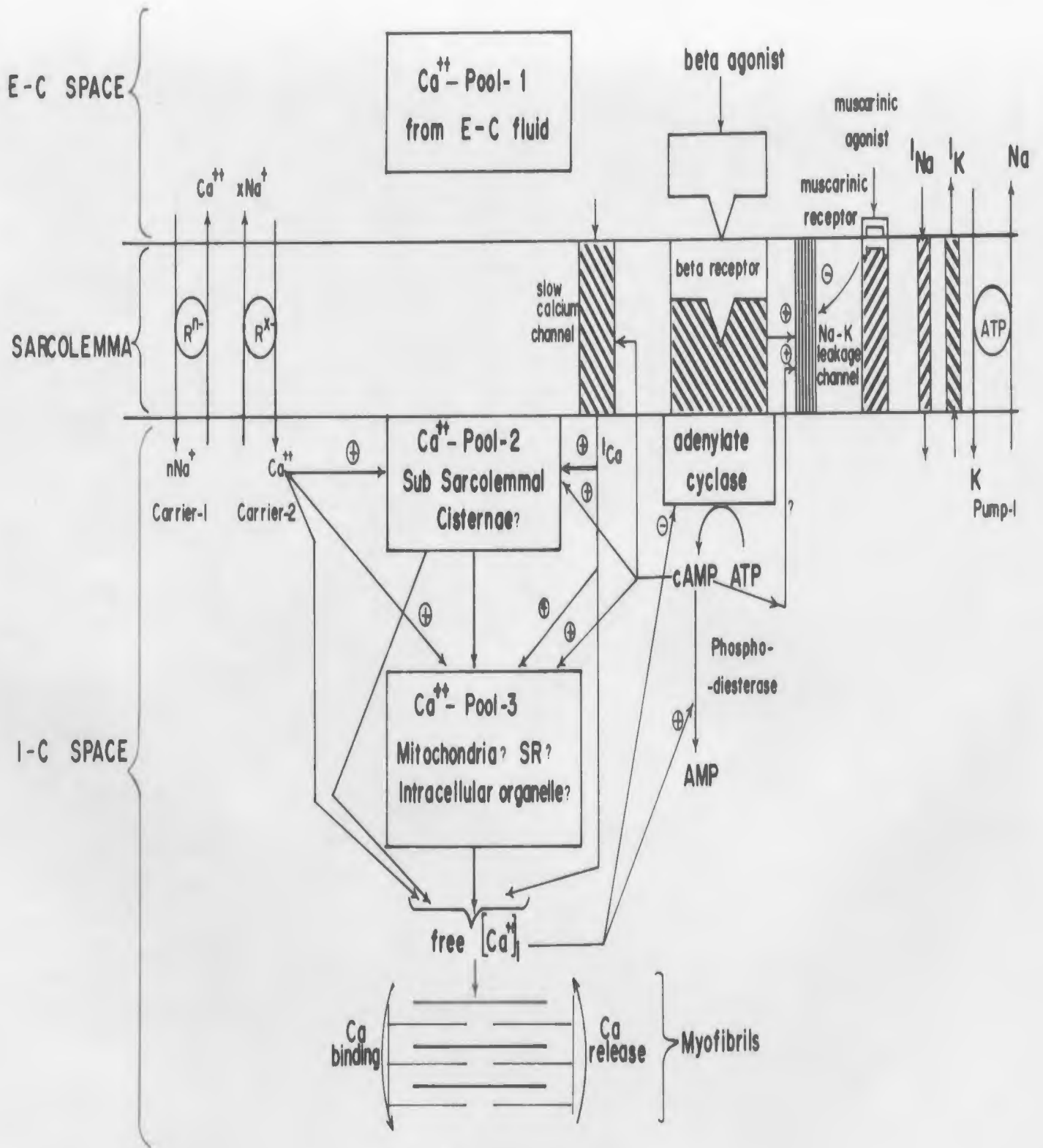
The following sequence of events is hypothesized to occur under normal conditions with standard concentrations of different ions (in SBSS) when the strand is contracting spontaneously. Spontaneous contractions result from the depolarization of the cell membrane at regular intervals,

Fig. 4.3 A schematic representation of possible mechanisms regulating the major ions involved in the contractility of cultured myocardial strands.

This figure is divided into three regions representing the extracellular (E-C) space, the sarcolemma and the intracellular (I-C) space. For a detailed explanation of this figure, refer to the text, Section 4.3.7.

Calcium ions are present in the E-C space (Pool-1) and are also believed to be stored in subsarcolemmal cisternae (Pool-2) and calcium "deep" pools (Pool-3) such as mitochondria and SR. Calcium moving from the E-C space to the I-C space via slow calcium channels triggers the release of intracellular calcium from Pools 2 and 3. Thus the level of free intracellular Ca^{++} is increased and activates tension development at the myofibrils.

The membrane is postulated to have fast sodium channels (I_{Na}); potassium channels (I_K); slow calcium channels (I_{Ca}); muscarinic and beta-adrenergic receptors; Na^+-K^+ pump; Na-Ca exchange Carriers 1 and 2.



due to a pacemaker site similar to that observed in cultured ventricular cells. During the period of depolarization, Na^+ enters the cell through the fast sodium channels (I_{Na}). The depolarization also alters the permeability of the cell membrane to calcium, which enters the cell during the plateau phase of the AP, through the slow calcium channels (I_{Ca}). This inward calcium current, I_{Ca} , may trigger further release of calcium from pools 2 and 3 (Fozzard, 1977); resulting in a transient large increase of $[\text{Ca}^{++}]_i$ (Langer, 1971). These free calcium ions are believed to activate the myofibrils to develop tension.

During the repolarization phase of the AP the muscle relaxes because Ca^{++} released from the binding sites is transported back to the extracellular space by a Na-Ca carrier mechanism. The carrier with negative charges (R^{n-}) transports 2 or more Na^+ from the extracellular space into the cytoplasm in exchange for each calcium ion (Carrier-1) (Langer, Frank and Nudd, 1979; Horackova and Vassort, 1979). According to Katz (1975), Na^+ and Ca^{++} binding occurs competitively at sites both the inside and the outside of the cell membrane. The amount of each ion binding to the carrier is determined by the ratio of $[\text{Ca}^{++}]_o/[\text{Na}^+]_o^2$ (Luttgau and Niederggerke, 1958). When the ratio is smaller (due to large $[\text{Na}^+]_o$), the predominating event is Na^+ binding on the outside and Ca^{++} on the inside;

as the ratio increases (when $[Na^+]_o$ is lowered) there is a progressive shift until the predominating event is Ca^{++} binding on the outside and Na^+ on the inside, with a net influx of calcium (Katz, 1975). The sodium entering the cell during the depolarization phase of the AP and during Na-Ca exchange are removed by a Na-K coupled ATP-dependent pump (Pump-1), which maintains the proper concentration gradients of these ions necessary for the membrane potential and provides the driving force for the exchange carrier (Mullins, 1979).

Increasing $[Ca^{++}]_o$ will augment the amount of calcium entering the cell through the slow channels during the plateau phase of the AP, and subsequently increase the related secondary release of calcium from pools 2 and 3 (Section 4.3.2). This is a consequence of the increased calcium concentration gradient across the membrane ($[Ca^{++}]_o/[Ca^{++}]_i$). This increased driving force will also tend to increase Ca^{++} influx during the resting state of the cell.

When $[Na^+]_o$ is lowered, while $[Ca^{++}]_o$ is held constant, the $[Na^+]_i/[Na^+]_o$ ratio is increased resulting in increased $[Ca^{++}]_i$ (Mullins, 1979). Under these conditions, internal sodium competes with calcium for binding sites on the carrier. This results in the change in direction of the net calcium movement to an influx. For each calcium ion entering, "X" number of Na^+ are removed (Carrier-2);

where "X" is 2 or more, the exact number being controversial (Langer, 1978; Langer et al., 1979; Horackova and Vassort, 1979). Thus $[Ca^{++}]_i$ is elevated in three ways: (1) through increased I_{Ca} , (2) through inhibition of calcium efflux and (3) through calcium influx by the Na-Ca carrier exchange mechanism (Reuter, 1975; Langer et al., 1979; Horackova and Vassort, 1979). This elevated $[Ca^{++}]_i$ results in a proportional increase in tension.

When $[Ca^{++}]_o$ is lowered below 1.5 mM in the presence of low $[Na^+]_o$, the resulting response (Figures 3.30 and 3.31) suggests that the initial transient increase in tension depends upon the release of calcium from Pool 2. If $[Ca^{++}]_o$ is below a critical level (1.5 mM?), recharging this pool to its optimal Ca^{++} content is not possible. Under these conditions, Ca^{++} available from the extracellular space becomes the sole determinant for calcium influx. The result is a flow of calcium through I_{Ca} , at a rate proportional to $[Ca^{++}]_o$ and a new reduced maxima of secondary Ca^{++} release from Pool 2. This could explain the low-level of steady-state tension seen for $[Ca^{++}]_o$ less than 1.5 mM during low sodium perfusion.

When the strand was exposed to a perfusion medium containing a beta-agonist, both spontaneous contraction rate and isometric tension amplitude increased (Fig. 3.38 a and b). In intact cardiac muscle, beta-receptors are

coupled to a membrane bound enzyme - adenylyate cyclase - which produces cyclic AMP when the receptor is activated by the beta agonist (Goldberg, 1974). Beta-agonists increase the influx of Ca^{++} into the myocardium (Grossman and Furchgott, 1964) by augmenting I_{Ca} (Trautwein, 1973; Beeler and Reuter, 1970; New and Trautwein, 1972; Reuter, 1967); this response is probably mediated by phosphorylation of membrane proteins by cAMP and a protein kinase (Woolenberger, Will, and Krause, 1975; Watanabe and Besch, 1975). Beta-agonists may also act by mobilizing calcium stores within the cell (Langer, 1973). All these changes result in an increased availability of free Ca^{++} to the contractile proteins, leading to elevated tension amplitudes. When $[Ca^{++}]_i$ is very high, adenylyate cyclase is inhibited and phosphodiesterase, which hydrolyzes cAMP to AMP, is stimulated; cAMP levels decline dramatically (Tada et al., 1975). The reduced availability of cAMP attenuates the process detailed above and reduces the freely available $[Ca^{++}]_i$.

The increased rate of contraction seen in the presence of a beta-agonist is caused by its action on leakage permeabilities (for Na^+ and K^+) which are responsible for the generator potentials (Reuter, 1974). In addition, these agents induce accelerated closure of channels which control the outward potassium current during repolarization (Katz, 1977); and increase the rate of calcium

sequestration, speeding subsequent relaxation (Langer, 1973). These properties have been studied in nodal, atrial and ventricular tissue preparations but the strand preparation appears to possess major characteristics of all these sites.

Acetylcholine appears to exert its effect via muscarinic receptors. The action is exclusively on the membrane leakage permeability as manifested in a purely chronotropic response. The associated decline in tension can be completely explained by the force-frequency relationship characteristics of the strand preparation (Sections 4.2.2 and 4.3.5.2).

CHAPTER - V
SUMMARY AND CONCLUSIONS

5.1 SUMMARY

(1) Techniques have been previously developed to produce thin preparations of spontaneously beating myocardial strands in culture from 2-3 day old rat hearts. Complete strands, terminated by glass microspheres, were formed around day 6 and were viable for over 12 days. Experimental preparations were used between 6-9 days of age.

(2) The strands were lifted by the glass microspheres from the growth substrate and suspended in the medium using a force transducer and a fixed micropipette.

(3) The force (isometric tension) generated by the spontaneously contracting strands was measured directly using a specially designed microgramme force transducer, which operates using the principle of variable capacitance in conjunction with a phase-locked loop circuit.

(4) The basic isometric mechanical properties of the strand preparation were characterized. These included:

(a) Length-tension relationship during spontaneous contractions: The strands appear to possess a length-tension relationship similar to that reported for intact isolated myocardial strips. However, the length changes required to define the entire length tension relationship were only $\pm 1\%$ of L_{\max} , a major reduction from that seen for

cardiac papillary muscle ($\pm 30\%$ of L_{\max}). The strand preparation appears to be about fifteen times stiffer than the isolated muscle strips.

(b) The length tension during electrical stimulation: Strand response to electrical stimulation was identical to that for spontaneous contractions, when rates were matched.

(c) No hysteresis was observed in the study of length-tension relationship. This implies that unlike intact papillary muscle in which the definition of full length-tension characteristics causes irreversible changes to the cell morphology and physiology, the strand operates without any such alterations. This offers significant advantages for repeated observation using the same preparation.

(d) Force-frequency relationship during electrical stimulation: Force-frequency relationship was observed to be similar to that of isolated rat cardiac muscle strip. When the strand was stimulated, the tension increased with frequency, peaked around 90 min^{-1} and showed a negative

inotropic response with further increase in frequency of stimulation.

(e) The relationship between temperature and contractile response: Temperature influenced the contractility of this preparation. The spontaneous contraction rate increased nonlinearly (similar to that of many other biological preparations) with increasing temperature. The temperature range between 15 and 37 °C was examined. The strands were not viable above 37 °C.

(5) The influence of extracellular cation concentration (K^+ , Na^+ , and Ca^{++}) manipulation upon contractility showed:

(a) When $[K^+]_o$ was varied, the rate of spontaneous contraction increased nonlinearly in proportion to $[K^+]_o$. The isometric tension magnitude was not altered by $[K^+]_o$, and the force-frequency relationship was unchanged except for spontaneous contraction rates.

(b) Manipulation of $[Ca^{++}]_o$ produced important changes in the isometric active tension response. The threshold concentration of $[Ca^{++}]_o$ for tension development was 1.0×10^{-5} M; maximal tension

occurred at 5.0×10^{-3} M. Spontaneous contraction frequency was independent of $[\text{Ca}^+]_o$ but the peak tension of the force-frequency relationship was calcium dependent. The shape of the relationship and frequency for peak tension were similar to those seen (item 4a) at standard $[\text{Ca}^{++}]_o$.

(c) Exposure to low $[\text{Ca}^{++}]_o$ (1.0×10^{-6} M) resulted in a rapid decline of tension (approximately 3.0 min) followed by a prolonged maintenance at a low value and finally abrupt termination of contractility. The time to reach zero tension was dependent upon the initial $[\text{Ca}^{++}]_o$; higher initial concentrations required longer times to reach zero tension. Conversely when returned to high $[\text{Ca}^{++}]_o$, the time required to attain the steady-state tension was inversely proportional to final concentration.

(d) The $[\text{Ca}^{++}]_o$ of 1.5 mM appears to be a critical minimum required (Refer Sec. 3.7) for maintenance of optimal contractility.

(e) Decreasing $[\text{Na}^+]_o$ produced small changes in spontaneous contraction rate in direct proportion to $[\text{Na}^+]_o$ and potentiated isometric tension as an

inverse proportion of $[\text{Na}^+]_o$ in the range of 40-100 mM. The low sodium (55 mM) induced isometric tension magnitude exceeded control values by as much as 300% (control $[\text{Na}^+]_o = 146.5$ mM). The simultaneous manipulation of $[\text{Na}^+]_o$ and $[\text{Ca}^{++}]_o$ was used to characterize the Na-Ca exchange mechanism.

(6) The myocardial strand preparation was shown to possess both cholinergic- muscarinic and beta-adrenergic receptors. There were no identifiable alpha-adrenergic receptors. Isoproterenol (beta-agonist) produced both a positive inotropic and chronotropic response. Acetylcholine elicited a negative chronotropic response and a negative inotropic response secondary to the rate changes which could be fully explained by the force-frequency relationship.

5.2 CONCLUSIONS

The isometric mechanical and ionic properties of the cultured neonatal rat myocardial strand preparation were characterized. In most major respects the preparation has characteristics analogous to intact muscle strips from the heart.

For research purposes it provides some unique advantages. The uniform cell type, simple structure and geometry of the strand provides a preparation with reduced diffusion limitations compared with intact cardiac muscle strips. In intact adult myocardium, different physiological and pharmacological functions are distributed among the differentiated structures of the heart. The spontaneous activity is controlled primarily by the SA node, which has adrenergic and cholinergic receptors; the contractility of the atrial fibers may be regulated by both cholinergic and adrenergic receptors; and ventricular fibers, which are the primary contractile tissues of the heart, lack cholinergic receptors. The cultured myocardial strand preparation possess the contractile and pharmacological properties of all three sites. Moreover, one particularly striking feature of the myocardial strand is the reproducibility of its physiological characteristics from preparation to preparation and within preparations.

At the same time, the limitations of this preparation are noted. First of all, it is a fragile preparation and the method of suspending the strand is quite cumbersome. Secondly, the cells are not differentiated (no sarcomere structures were seen under the microscope, and they possess both adrenergic and cholinergic receptors). When the

strand is used as a model for studying cardioactive drugs, one should bear in mind these differences in comparison with intact ventricular myocardium.

In spite of these limitations, the cultured myocardial strand preparation represents an accurate model for myocardial physiology and offers some important advantages for investigation of cellular physiology and the influence of ionic and drug manipulation on its basic physiology.

BIBLIOGRAPHY

- Abbott, B.C. 1971. Force-frequency relationship in heart muscle. *Cardiovasc. Res.* [Suppl I]: 51-54.
- Abbott, B.C. and Mommaerts, W.F.H.M. 1959. A study of inotropic mechanisms in the papillary muscle preparation. *J. Gen. Physiol.* 42: 533-551.
- Abbott, B.C. and Wilkie, D.R. 1953. The relation between velocity of shortening and the tension-length curve of skeletal muscle. *J. Physiol.* 120: 214-223.
- Ahlquist, R.P. 1948. A study of the adrenotropic receptors. *Am. J. Physiol.* 153: 586-600.
- Allen, D.G., Jewell, B.R., and Wood, E.H. 1976. Studies of the contractility of mammalian myocardium at low rates of stimulation. *J. Physiol.* 254: 1-17.
- Bahler, A.S., Fales, J.T. and Zierler, K.L. 1968. The dynamic properties of mammalian skeletal muscle. *J. Gen. Physiol.* 51: 369-384.
- Barry, A. 1950. The effect of epinephrine on the myocardium of the embryonic chick. *Circulation.* 1: 1362-1368.
- Barry, W.H., Pitzen, R., Protos, K. and Harrison, D.C. 1975. Inotropic effects of different Calcium ion concentration on the embryonic chick ventricle. *Circ. Res.* 36: 727-734.
- Beeler, G.W., Jr. and Reuter, H. 1970. The relation between membrane potential, membrane currents and activation of contraction in ventricular myocardial fibers. *J. Physiol.* 207: 211-229.
- Benforado, J.M. 1958. Frequency-dependent pharmacological and physiological effects on the rat ventricle strip. *J. Pharmacol. Exp. Ther.* 122: 86-100.

- Blesa, S.E., Langer, G.A., Brady, A.J and Serena, S.D.
1970. Potassium exchange in rat ventricular myocardium: Its relation to rate of stimulation. *Am. J. Physiol.* 219: 747-754.
- Blinks, J.R. and Koch-weser, J. 1963. Physical factors in the analysis of the actions of drugs on myocardial contractility. *Pharmacol. Rev.* 15: 531-599.
- Bloom, S. 1970. Spontaneous rhythmic contraction of separated heart muscle cells. *Science* 167: 1727-1729.
- Bodem, R. and Sonnenblick, E.H. 1975. Mechanical activity of mammalian heart muscle: Variable onset, species difference, and the effect of caffeine. *Am. J. Physiol.* 228: 250-261.
- Boder, G.B., Harley, R.J. and Johnson, I.S. 1971. Recording system for monitoring automaticity of heart cells in culture. *Nature.* 231: 531-532.
- Boder, G.B. and Johnson, I.S. 1972. Comparative effects of some cardioactive agents on automaticity of cultured heart cells. *J. Mol. Cell. Cardiol.* 4: 453-463.
- Brady, A.J. 1968. Active state in cardiac muscle. *Physiol. Rev.* 48: 570-600.
- Brady, A.J., Tan, S.T. and Ricchiuti, N.V. 1979. Contractile force measured in unskinned isolated adult rat heart fibres. *Nature.* 282: 728-729.
- Braunwald, E., Ross, J. and Sonnenblick, E.H. 1967. Mechanism of contraction of the normal and failing heart. *New Eng. J. Med.* 277: 794-800.

- Braunwald, E., Ross, J. and Sonnenblick, E.H. 1976. Mechanism of contraction of the normal and failing heart. 2nd Ed. Little Brown and Company, Boston.
- Buckley, N.M, Penefsky, Z.J. and Litwak, R.S. 1972
Comparative force -frequency relationships in human and other mammalian ventricular myocardium. Pflugers Arch. 332: 259-270.
- Burrows, M.T. 1910. The cultivation of tissues of the chick embryo outside the body. J. Am. Med. Assoc. 55: 2057-2058.
- Campebell, R.J. 1970. Calcium ion movements in isolated embryonic chicken heart cells. Pharmacologist. 12:267.
- Carter, S.B. 1965. Principles of cell motility: the direction of cell movement and cancer invasion. Nature. 208: 1183-1187.
- Cavanaugh, M.W. 1955. Pulsation, migration and division in dissociated chick embryo heart cells in vitro. J. Exp. Zool. 128: 573-585
- Chapman, R.A. 1971. Experimental alteration of the relationship between the external calcium concentration and the contractile force generated by auricular trabeculae isolated from the heart of the frog, *Rana Pipiens*. J. Physiol. 218: 147-161.
- Chapman, R.A and Niedergerke, R. 1970. Effects of calcium on the contraction of the hypodynamic frog heart. J. Physiol. 211: 389-421.
- Chapman, R.A. and Niedergerke, R. 1970a. Interaction between heart rate and calcium concentration in the control of contractile strength of the frog heart. J. Physiol. 211: 423-443.

- Chapman, R.A. and Tunstall, J. 1971. The dependence of the contractile force generated by frog auricular trabeculae upon the external calcium concentration. *J. Physiol.* 215: 139-162.
- Constantin, L.L. and Taylor, S.R. 1973. Graded activation in frog muscle fibers. *J. Gen. Physiol.* 61: 424-443.
- Cooley, J.W. and Dodge, Jr., F.A. 1966. Digital computer solutions for excitation and propagation of the nerve impulse. *Biophys. J.* 6: 583-599.
- Crooks, R. and Cooke, R. 1977. Tension generation by threads of contractile proteins. *J. Gen. Physiol.* 69: 37-55.
- Dale, H.H. 1906. On some physiological actions of ergot. *J. Physiol.* 34: 163-206.
- Dale, H.H. 1914. The action of certain esters and ethers of choline, and their relation to muscarine. *J. Pharmacol. Exp. Ther.* 6: 147-190.
- Dale, A.S. 1930. The relation between amplitude of contraction and rate of rhythm in the mammalian ventricle (including interpretation of the apparent indirect action of the vagus on amplitude of ventricular contraction). *J. Physiol.* 70: 455-473
- Daveron, P.R. and Sutherland, E.W. 1963. The cellular location of adenyl cyclase in the pigeon erythrocytes. *J. Biol. Chem.* 238: 3016-3023.
- Dudel, J. 1975. Excitation of nerve and muscle. In Fundamentals of neurophysiology. pp 16-64 (ed: Schmidt, R.F.) Springer Verlag, New York.
- Dudel, J., Peper, K., Rudel, R. and Trautwein, W. 1967. The effect of tetrodotoxin on the membrane current in cardiac muscle (Purkinje fibers). *Pflugers Arch.* 213: 85-93.

- Ebashi, S., Kitazawa, T., Kohama, K. and van Eerd, P.C. 1978. Calcium ion in cardiac contractility. in *Rec. Adv. Stud. Cardiac Struct. Metab.* 11: 93-101. (eds: Kobayashi, T., Sano, T. and Dhalla, N.S.) University Park Press, Baltimore.
- Eccles, J.C. 1964. The Physiology of synapses. Springer Verlag, Berlin.
- Endo, M. 1977. Calcium release from the sarcoplasmic reticulum. *Physiol. Rev.* 57: 71-108.
- Ertel, R.J., Clarke, D.E., Chao, J.C. and Franke, F.R. 1971. Autonomic receptor mechanisms in embryonic chick myocardial cell cultures. *J. Pharmacol. Exp. Ther.* 178: 73-80.
- Fabiato, A. and Fabiato, F. 1975. Contractions induced by a calcium-triggered release of calcium from the sarcoplasmic reticulum of single skinned cardiac cells. *J. Physiol.* 249: 469-495.
- Fabiato, A. and Fabiato, F. 1978. Myofilament-generated tension oscillations during partial calcium activation and activation dependance of the sarcomere length-tension relation of skinned cardiac cells. *J. Gen. Physiol.* 72: 667-699.
- Fabiato, A., Fabiato, F. and Sonnenblick, E.H. 1971. Electrical depolarization of intracellular membranes and "regenerative calcium release" in single cardiac cells with disrupted sarcolemma. *Circulation* 44(II): 90.
- Fange, R., Persson, H. and Thesleff, S. 1956. Electrophysiologic and pharmacological observations on trypsin-disintegrated embryonic chick hearts cultured in vitro. *Acta. Physiol. Scand.* 38: 173-183.
- Fawcett, D.W. and McNutt, N.S. 1969. The ultrastructure of the cat myocardium (i) ventricular papillary muscle. *J. Cell. Biol.* 42: 1-45.

- Fingl, E., Woodbury, L.A. and Hecht, H.H. 1952. Effects of innervation and drugs upon direct membrane potentials of embryonic chick myocardium. *J. Pharmacol. Exp. Ther.* 104: 103-114.
- Ford, L.E. and Podolsky, R.J. 1970. Regenerative calcium release within muscle cells. *Science* 67: 58-59.
- Forester, G.V. and Mainwood, G.W. 1974. Interval dependent inotropic effects in the rat myocardium and the effect of calcium. *Pflugers Arch.* 352: 189-196.
- Fosset, M., Barry, J.D., Lenoir, M.C. and Lazdunski, M. 1977. Analysis of molecular aspects of Na^+ and Ca^{2+} uptakes by embryonic cardiac cells in culture. *J. Biol. Chem.* 252: 6112-6117.
- Fozzard, A.F. 1977. Heart: Excitation - contraction coupling. *Ann. Rev. Physiol.* 39: 201-220.
- Friedman, W.F. 1972. The intrinsic physiologic properties of the developing heart. *Prog. Cardiovasc. Dis.* 15: 87-110.
- Frossman, N.G. and Girardier, L. 1970. A study of the T-system in rat heart. *J. Cell Biol.* 44: 1-19.
- Gettes, L.S., Surawicz, B. and Shive, J.C. 1962. Effect of high K, low K, and quinidine on QRS duration and ventricular action-potential. *Am. J. Physiol.* 203: 1135-1140.
- Ghanbari, H. and McCarl, R.L. 1976. Involvement of cyclic nucleotides in the beating response of rat heart cells in culture. *J. Mol. Cell. Cardiol.* 8: 481-488.
- Gibbons, W.R. and Fozzard, H.A. 1975. Relationship between voltage and tension in sheep cardiac Purkinje fibers. *J. Gen. Physiol.* 65: 345-365.

- Glitsch, H.G., Reuter, H. and Scholz, H. 1970. The effect of the internal sodium concentration on calcium fluxes in isolated guinea pig auricles. *J. Physiol.* 209: 25-43.
- Goldberg, N.D. 1974. Cyclic nucleotides and cell functions. *Hosp. Pract.* 9: 127-142.
- Goldman, D.E. 1943. Potential impedance and rectification in membranes. *J. Gen. Physiol.* 27: 37-60.
- Gordon, A.M., Huxley, A.F. and Julian, F.J. 1966. The variation in isometric tension with sarcomere length in vertebrate muscle fibres. *J. Physiol.* 184: 170-192.
- Goshima, K. 1973. A study on the preservation of the beating rhythm of single myocardial cells in vitro. *Exp. Cell. Res.* 80: 432-438.
- Goshima, K. 1974. Initiation of beating in quiescent myocardial cells by nonepinephrine, by contact with beating cells and by electrical stimulation of adjacent FL cells. *Exp. Cell. Res.* 84: 223-234.
- Goshima, K. 1977. Photoelectric demonstration of ouabain-induced arrhythmias in single isolated myocardial cells and in cell clusters in vitro. *Cell Struct. Funct.* 2: 329-338.
- Goss, C.M. 1931. "Slow-motion" cinematographs of the contraction of single cardiac muscle cells. *Proc. Soc. Exp. Biol. Med.* 29: 292-293.
- Goto, M., Kimoto, Y and Kato, Y. 1971. A study on the excitation-contraction coupling of the bullfrog ventricle with voltage clamp techniques. *Jpn. J. Physiol.* 21: 159-173.

- Grimm, A.F. and Whitehorn, W.V. 1968. Myocardial length-tension sarcomere relationships. *Am. J. Physiol.* 214: 1378-1387.
- Grimm, A.F., Katele, K.V., Kubota, R. and Whitehorn, W.V. 1970. Relation of sarcomere length and muscle length in resting myocardium. *Am. J. Physiol.* 218: 1412-1416.
- Grossman, A. and Furchgott, R.F. 1964. The effects of various drugs on calcium exchange in the isolated guinea pig left auricle. *J. Pharmacol. Exp. Ther.* 145: 162-172.
- Grundfest, H. 1932. Excitability of the single fibre nerve-muscle complex. *J. Physiol.* 76: 95-115.
- Halbert, S.P., Bruderer, R. and Lin, T.M. 1971. In vitro organization of dissociated rat cardiac cells into beating three dimensional structures. *J. Exp. Med.* 133: 677-695.
- Harary, I. and Farley, B. 1960. Initial studies of single isolated beating heart cells. *Science.* 131: 1674-1675.
- Harary, I. and Farley, B. 1963. In vitro studies on single beating rat heart cells: I-growth and organization. *Exp. Cell Res.* 29: 451-465.
- Harary, I and Farley, B. 1963a. In vitro studies on single beating heart cells: II-intercellular communication. *Exp. Cell Res.* 29: 466-474.
- Harrington, L. and Johnson, E.A. 1973. Voltage-clamp of cardiac muscle in a double sucrose gap: A feasibility study. *Biophys. J.* 13: 626-647.
- Harris, A. 1973. Behaviour of cultured cells on substrata of variable adhesiveness. *Exp. Cell Res.* 77: 285-297.

- Henderson, A.H., Brutsaert, D.L., Parmley, W.W. and Sonnenblick, E.H. 1969. Myocardial mechanics in papillary muscles of the rat and cat. *Am. J. Physiol.* 217: 1273-1279.
- Henry, P.D. 1975. Positive staircase effect in the rat heart. *Am. J. Physiol.* 228: 360-364.
- Hermesmyer, K. and Robinson, R.B. 1977. High sensitivity of cultured cardiac muscle cells to autonomic agents. *Am. J. Physiol.* 233: C172-C179.
- Hibberd, M.C. and Jewell, B.R. 1979. Length-dependence of the contractile system to calcium in rat ventricular muscle. *J. Physiol.* 290: 30P-31P.
- Hill, A.V. 1949. The abrupt transition from rest to activity in muscle. *Proc. Roy. Soc. B.* 136: 399-420.
- Hill, D.K. 1968. Tension due to interaction between the sliding filaments in resting striated muscle. The effect of stimulation. *J. Physiol.* 199: 637-684.
- Hodgkin, A.L. and Katz, B. 1949. The effect of sodium ions on the electrical activity of the giant axon of the squid. *J. Physiol.* 108: 37-77.
- Hoekman, T.B. 1968. A comparative study of mechanical characteristics and heat production of the Anterior and Posterior Latissimus Dorsi muscles of chicken. Ph. D. dissertation. University of Illinois, Urbana, Illinois.
- Hoekman, T.B. and Dettbarn, W.D. 1972. Neurophysiological experiments using single giant axons of the lobster. *Exp. Physiol. Biochem.* 5: 39-67.

- Hoffman, B.F. and Cranefield, P.F. 1960. Electro-physiology of the heart. McGraw Hill, New York.
- Horackova, M. and Vassort, G. 1976. Regulation of tonic tension in frog atrial muscle by voltage dependent Na-Ca exchange. J. Physiol. 258: 77P-78P.
- Horackova, M. and Vassort, G. 1979. Sodium-calcium exchange in regulation of cardiac contractility. J. Gen. Physiol. 73: 403-424.
- Horackova, M. and Vassort, G. 1979a. Slow inward current and contraction in frog atrial muscle at various extracellular concentrations of Na and Ca ions. J. Mol. Cell. Cardiol. 11: 733-753.
- Huxley, A.F. 1965. Muscle tension and the sliding filament theory. in Proceedings of the 23rd International Congress of Physiological Sciences, Tokyo, September, pp. 383-387.
- Huxley, H.E. 1965a. The mechanism of muscular contraction. Scientific American. 213: 18-27.
- Inesi, G. 1973. Active transport of calcium ion in sarcoplasmic membranes. Ann. Rev. Biophys. Bioenerget. 1: 191-210.
- Inesi, G., Ebashi, S. and Watanabe, S. 1964. Preparation of vesicular relaxing factor from bovine heart tissue. Am. J. Physiol. 207: 1339-1344.
- Jacobson, S.L. 1977. Culture of spontaneously contracting cells from adult rats. Cell. Struct. Funct. 2: 1-9.
- Jellinek, M., Sperelakis, N., Napolitano, L.M. and Cooper, T. 1968. 3,4 - Dihydroxyphenylalanine in cultured ventricular cells from chick embryo heart. J. Neurochem. 15: 959-963.

- Jewell, B.R. 1977. A re-examination of the influence of muscle length on myocardial performance. *Circ. Res.* 40: 221-230.
- Jewell, B.R. and Ruegg, J.C. 1966. Oscillatory contraction of insect fibrillar muscle after glycerol extraction. *Proc. Roy. Soc. B.* 164: 428-459.
- Jongsma, H.J. and van Rijn, H.E. 1972. Electrotonic spread of current in monolayer cultures of neonatal rat heart cells. *J. Membr. Biol.* 9: 341-360
- Julian, F.J. and Moss, R.L. 1976. The concept of active state in striated muscle. *Circ. Res.* 38: 53-59.
- Julian, F.J. and Sollins, M.R. 1975. Sarcomere length-tension relations in living rat capillary muscle. *Circ. Res.* 37: 299-308.
- Kasten, F.H. 1971. Cytology and cytochemistry of mammalian myocardial cells in culture. *Acta Histochem.* [Suppl] (Jena) 9: 775-805.
- Kasten, F.H. 1972. Rat myocardial cells in vitro: mitosis and differentiated properties. *In Vitro* 8: 128-150.
- Kasten, F.H. 1973. Mammalian myocardial cells. In: Tissue Culture. (eds: Kruse P.F. and Patterson, M.K.) Academic Press, New York.
- Kasten, F.H. and Yip, D.K. 1974. Reanimation of cultured mammalian myocardial cells during multiple cycles of trypsinization-freezing-thawing. *In Vitro* 9: 246-252.
- Katz, B. 1966. Nerve, muscle, and synapse. McGraw-Hill Book Co., New York.

- Katz, A.M. 1975. Congestive heart failure: Role of altered myocardial cellular control. *New Eng. J. Med.* 293: 1184-1191.
- Katz, A.M. 1977. Physiology of the heart. Raven Press, New York
- Kelly, J.J., Jr. and Hoffman, B.F. 1960. Mechanical activity of rat papillary muscle. *Am. J. Physiol.* 199: 157-162.
- Kitazawa, T. 1976. Physiological significance of Ca^{++} uptake by mitochondria in the heart in comparison with that by cardiac sarcoplasmic reticulum. *J. Biochem.* 80: 1129-1147.
- Koidl, B., Tritthart, H.A. and Erkingner, S. 1980. Cultured embryonic chick heart cells: Photometric measurement of the cell pulsation and the effects of calcium ions, electrical stimulation and temperature. *J. Mol. Cell. Cardiol.* 12: 165-178.
- Krueger, J.W. and Pollack, G.H. 1975. Myocardial sarcomere dynamics during isometric contraction. *J. Physiol.* 251: 627-643.
- Kruta, V. 1937. Sur l'active rythmique du muscle cardiaque; variations de la response mecanique en fonction du rythme. *Arch. Internat. de Physiol.* 45: 332-357.
- Kruta, V. 1938 - English translation. The rhythmic activity of cardiac muscle. *International Archives of Physiology.* 47: 35-62.
- Kubler, H. and Shineborne, E.H. 1971. Calcium and the mitochondria. In: Calcium and the Heart. pp 93-123 (eds: Harris, P. and Opie, L.H.) Academic Press, London.

- Lane, M.A., Sastre, A., Law, M.E. and Salpeter, M.M. 1977. Cholingeric and adrenergic receptors on mouse cardiocytes in vitro. *Dev. Biol.* 57: 254-269.
- Langendorff, O. and Nawrocki, C. 1897. Untersuchungen am uberlebenden Saugetierherzen; uber den Einfluss von warme und kalte auf das Herz der warmblutigen Tiere. *Pflugers Arch.* 66: 355-400. (reference quoted from Sumbera et al., 1966)
- Langer, G.A. 1968. Ion fluxes in cardiac excitation and contraction and their relation to myocardial contractility. *Physiol. Rev.* 48: 708-757.
- Langer, G.A. 1971. Coupling calcium in mammalian ventricle: Its source and factors regulating its quantity. *Cardiovasc. Res. Suppl.* 1: 71-75.
- Langer, G.A. 1973. Heart: Excitation-contraction coupling. *Ann. Rev. Physiol.* 35: 55-86.
- Langer, G.A. 1976. Events at the cardiac sarcolemma: Localization and movement of contractile-dependent calcium. *Fed. Proc.* 35: 1274-1278.
- Langer, G.A. 1977. Ionic basis of myocardial contractility. *Ann. Rev. Med.* 28: 13-20.
- Langer, G.A. 1978. The structure and functions of myocardial cell surface. *Am. J. Physiol.* 235: H461-H468.
- Langer, G.A. 1978a. Interspecies variation in myocardial physiology: The anomalous rat. *Environ. Health Perspect.* 26: 175-179.
- Langer, G.A., Frank, J.S. and Brady, A.J. 1976. The myocardium. In: "Cardiovascular Physiology II", International Review of Physiology 9: 191-237. (eds: Guyton, A.C. and Cowley, A.W.) University Park Press, Baltimore, MD.

- Langer, G.A., Frank, J.S. and Nudd, L.M. 1979. Correlation of calcium exchange, structure and function in myocardial tissue culture. *Am. J. Physiol.* 237: H239-H246.
- Langer, G.A., Nudd, L.M. and Ricchiuti, N.V. 1976. The effect of sodium deficient perfusion on calcium exchange in cardiac tissue culture. *J. Mol. Cell. Cardiol.* 8: 321-328.
- Langley, J.N. 1905. On the reaction of cells and nerve-endings to cation poisons, chiefly as regards the reaction of striated muscle to nicotine and to curari. *J. Physiol.* 33: 374-413.
- Legato, M.J. 1972. Ultra structural characteristics of the rat ventricular cell grown in tissue culture, with special reference to sarcomerogenesis. *J. Mol. Cell. Cardiol.* 4: 299-317.
- Lehninger, A.L. 1974. Ca^{2+} transport by mitochondria and its possible role in the cardiac contraction-relaxation cycle. *Circ. Res.* 35: 83-88.
- Levy, B. and Ahlquist, R.P. 1961. An analysis of adrenergic blocking activity. *J. Pharmacol. Exp. Ther.* 133: 202-210.
- Lieberman, M. 1967. Effects of cell density and low K on action potentials of cultured chick heart cells. *Circ. Res.* 21: 879-888.
- Lieberman, M. 1973. Electrophysiological studies of a synthetic strand of cardiac muscle. *Physiologist* 16: 551-563.
- Lieberman, M., Kootsey, J.M., Johnson, E.A. and Sawanobori, T. 1973. Slow conduction in cardiac muscle - A biophysical model. *Biophysical J.* 13: 37-55.

- Lieberman, M., Roggeveen, A.E., Purdy J.E. and Johnson, E.A. 1972. Synthetic strands of cardiac muscle: Growth and physiological implications. Science 175: 909-911.
- Lieberman, M., Sawanobori, T., Kootsey, J.M. and Johnson, E.A. 1975. A synthetic strand of cardiac muscle - its passive electrical properties. J. Gen. Physiol. 65: 527-550.
- Lieberman, M., Sawanobori, T., Shigeto, N. and Johnson, E.A. 1975. Physiologic implications of heart muscle in tissue culture. In Developmental and physiological correlates of cardiac muscle. (eds : Lieberman, M. and Sano, T.) Raven Press, New York.
- Locke, F.S. and Rosenheim, O. 1907. Contributions to the physiology of the isolated heart: The consumption of dextrose by mammalian cardiac muscle. J. Physiol. 36: 205-220.
- Loewi, O. 1921. Ueber humorale Uebertragbarkeit der Herznervenwirkung. Arch. Ges. Physiol. 189: 239-242. [reference quoted from The Pharmacological Basis of Therapeutics, 5th Ed. (eds: Goodman, L.S. and Gilman, A) pp 411. Macmillan Publishing Co., Inc. New York, 1975].
- Luttgau, H.C. and Niedergerke, R. 1958. The antagonism between Ca and Na ions on the frog's heart. J. Physiol. 143: 486-505.
- Mark, G.E. and Strasser, F.F. 1966. Pacemaker activity and mitosis in cultures of newborn rat heart ventricle cells. Exp. Cell Res. 44: 217-233.
- Martin, H.N. 1883. The direct influence of gradual variations of temperature upon the rate of beat of the dog's heart. Roy. Soc. Philos. Trans. 174: 663-688.

- Martin, G.R. and Rubin, H. 1974. Effects of cell adhesion to the substratum on the growth of chick embryo fibroblasts. *Exp. Cell. Res.* 85: 319-333.
- Maruyama, K., Kimura, S., Kuroda, M. and Handa, S. 1977. Connectin, an elastic protein of muscle: Its abundance in cardiac myofibrils. *J. Biochem. (Tokyo)* 82: 347-350.
- Matsubara, S. and Maruyama, K. 1977. Role of connectin in the length-tension relation of skeletal and cardiac muscle. *Jpn. J. Physiol.* 27: 589-600.
- McCarty, L.P., Le, W.C. and Shideman, F.E. 1960. Measurement of the inotropic effects of drugs on the innervated embryonic chick heart. *J. Pharmacol. Exp. Ther.* 129: 315-321.
- McLeod, G.K. and Koch-Weser, J. 1965. Influence of low temperature on the contractility of mammalian myocardium. *Fed. Proc. Fed. Am. Soc. Exp. Biol.* 22: 246.
- Mihalyi, E. and Szent-Gyorgyi, A.G. 1953. Trypsin digestion of muscle proteins. I. Ultracentrifugal analysis of the progress. *J. Biol. Chem.* 201: 189-196.
- Morad, M. and Goldman, Y. 1973. Excitation - contraction coupling in heart muscle: Membrane control of development of tension. *Prog. Biophys. Mol. Biol.* 27: 257-313.
- Morad, M. and Trautwein, W. 1968. The effect of the duration of the action potential on contraction in mammalian heart muscle. *Pflugers Arch.* 299: 66-82.
- Mullins, L.J. 1979. The generation of electric currents in cardiac fibers by Na/Ca exchange. *Am. J. Physiol.* 236: C103-C110.

- New, W. and Trautwein, W. 1972. The ionic nature of slow inward current and its relation to contraction. *Pflugers Arch.* 334: 24-38.
- Niedergerke, R. 1963. Movements of Ca in beating ventricles of the frog. *J. Physiol.* 167: 551-580.
- Noble, D. 1965. Electrical properties of cardiac muscle attributable to inward going (anomalous) rectification. *J. Cell. Comp. Physiol.* 66(Suppl. 2): 127-136.
- Noble, D. 1974. Cardiac action potential and pacemaker activity. In: Recent Advances in Physiology, 9: 1-50. (ed: Linden, R.J) Churchill Livingstone, London.
- Noble, D. 1979. The initiation of the heartbeat. 2nd Ed. Clarendon Press, Oxford.
- Noble, D. and Stein, R.B. 1966. The threshold conditions for initiation of action potentials by excitable cells. *J. Physiol.* 187: 129-142.
- Norwood, C.R., Castaneda, A.R. and Norwood, W.I. 1980. Heterogeneity of rat cardiac cells of defined origin in single cell culture. *J. Mol. Cell Cardiol.* 12: 201-210.
- Ochi, R. and Trautwein, W. 1971. The dependence of cardiac contraction on depolarization and slow inward current. *Pflugers Arch.* 323: 187-203.
- Ohara, P.T. and Buck, R.C. 1979. Contact guidance in vitro. A light, transmission and scanning electron microscopic study. *Exp. Cell Res.* 121: 235-249.

- Okarma, T.B. and Kalman, S.M. 1971. Photoelectric monitoring of single beating heart cells in culture. *Exp. Cell. Res.* 69: 128-134.
- Patterson, S.W., Piper, H. and Starling, E.H. 1914. The regulation of the heart beat. *J. Physiol.* 48: 465-513.
- Philipson, K.D. and Langer, G.A. 1979. Sarcolemmal-bound calcium and contractility in the mammalian myocardium. *J. Mol. Cell. Cardiol.* 11: 857-875.
- Pollack, G.H. and Huntsman, L.L. 1974. Sarcomere length-active force relations in living mammalian heart muscle. *Am. J. Physiol.* 227: 383-389.
- Prosser, C.L. 1973. Comparative Animal Physiology, 3rd Ed. p 363. H.B. Saunders, Philadelphia.
- Purdy, J.E., Lieberman, M., Roggeveen, A.E. and Kirk, R.G. 1972. Synthetic strands of cardiac muscle: formation and ultrastructure. *J. Cell Biol.* 55: 563-578.
- Randall, W.C. and Armour, J.A. 1977. Gross and microscopic anatomy of the cardiac innervation. In Neural regulation of the heart. pp 13-42. (ed: Randall, W.C.) Oxford University Press, New York.
- Rappaport, C., Poole, J.P. and Rappaport, H.P. 1960. Studies on properties of surfaces required for growth of mammalian cells in synthetic medium. I. The HeLa cell. *Exp. Cell Res.* 20: 465-510.
- Reuter, H. 1967. The dependence of slow inward current in Purkinje fibers on the extracellular calcium concentration. *J. Physiol.* 192: 479-492.

- Reuter, H. 1974. Localization of beta-adrenergic receptors, and effects of noradrenaline and cyclic nucleotides on action potentials, ionic currents and tension in mammalian cardiac muscle. *J. Physiol.* 242: 429-451.
- Reuter, H. 1975. Inward calcium current and activation of contraction in mammalian myocardial fibers. In *Rec. Adv. Cardiac Struct. Metab.* 5: 13-18, (eds: Fleckenstein, A. and Dhalla, N.S.) University Park Press, Baltimore.
- Ringer, S. 1883. A further contribution regarding the influence of different constituents of the blood on the contraction of the heart. *J. Physiol.* 4: 29-42.
- Robinson, G.A., Butcher, R.W., Oye, I., Morgan, H.E. and Sutherland, E.W. 1965. The effect of epinephrine on adenosine 3', 5'-phosphate levels in the isolated perfused rat heart. *Mol. Pharmacol.* 1: 168-177.
- Rothberger, C.J. and Sachs, A. 1938. Über den Zusammenhang zwischen Schlagfrequenz und Zuckungshöhe am Vohojstreifen des warmblütterherzens. *Pflugers Arch.* 240: 60-81.
- Rushmer, R.F. 1955. Applicability of Starling's law of the heart to intact, unanaesthetized animals. *Physiol. Rev.* 35: 138-142.
- Sarnoff, S.J. and Berglund, E. 1954. Ventricular function I: Starling's law of the heart studied by means of simultaneous right and left ventricular function curves in the dog. *Circulation* 9: 706-718.
- Scarpa, A and Graziotti, P. 1973. Mechanisms for intracellular calcium regulation in heart: I. Stopped-flow measurements of Ca^{++} uptake by cardiac mitochondria. *J. Gen. Physiol.* 62: 756-772.

- Schanne, O.F. 1970. Recording of contractile activity of cells in culture. *J. Appl. Physiol.* 29: 892-893.
- Schanne, O.F. 1972. Factors involved in the loss of spontaneous contractile and electrical activity in cluster of cultured cardiac cell. *Can. J. Physiol. Pharmacol.* 50: 523-532.
- Schanne, O.F., Rivard, C. and Doyon, G. 1975. Ionic determinants of spontaneous activity in clusters of cultured cardiac cells from newborn rats. *Can. J. Physiol. Pharmacol.* 53: 1209-1213.
- Schanne, O.F. and Bkaily, G. 1981. Explanted cardiac cells: A model to study drug actions? *Can. J. Physiol. Pharmacol.* 59: 443-467.
- Schanne, O.F., Ruiz-Cereti, E, Payet, M.D. and Deslauriers, Y. 1979. Influence of varied $[Ca^{++}]$ and $[Na^+]$ on electrical activity of clusters of cultured cardiac cells from neonatal rats. *J. Mol. Cell. Cardiol.* 11: 477-484.
- Schneider J.A. and Sperelakis, N. 1975. Slow Ca^{2+} and Na^+ responses induced by isoproterenol and methylxanthines in isolated perfused guinea pig hearts exposed to elevated K^+ . *J. Mol. Cell. Cardiol.* 7: 249-273.
- Schwartz, A. 1974. Active transport in mammalian myocardium. In: The Mammalian Myocardium. pp 81-104 (eds: Langer, G.A. and Brady, A.J.). Wiley, New York.
- Scott, A.C. 1973. Strength-duration curves for threshold excitation of nerves. *Math. Biosci.* 18: 137-152.

- Skelton, C.L., Spotnitz, W.D., Feldman, D., Serur, J.R., Mirsky, I. and Sonnenblick, E.H. 1974. Ultrastructural and functional correlates of acute cardiac distention. *Clin. Res.* 22: 304a.
- Smith, D.R. 1966. Organization and function of sarcoplasmic reticulum and T-system of muscle cells. *Prog. Biophys. Mol. Biol.* 16: 107-142.
- Sonnenblick, E.H. 1965. Determinants of active state in heart muscle: force, velocity, instantaneous muscle length, time. *Fed. Proc.* 24: 1396-1409.
- Sonnenblick, E.H. 1965a. Instantaneous force-velocity-length determinants in the contraction of heart muscle. *Circ. Res.* 16: 441-451
- Sonnenblick, E.H. 1967. Active state in heart muscle. Its delayed onset and modification by inotropic agents. *J. Gen. Physiol.* 50: 661-676.
- Sonnenblick, E.H. 1974. "General discussion III - Temperature" in "The Physiological Basis of the Starling's Law of the Heart". Ciba Foundation Symposium 24: 237.
- Sonnenblick, E.H. and Skelton, C.L. 1974. Reconsideration of the ultrastructural basis of cardiac length-tension relations. *Circ. Res.* 35: 517-526.
- Sonnenblick, E.H., Spiro, D. and Cottrell, J.S. 1963. Fine structural changes in heart muscle in relation to the length-tension curve. *Proc. Nat. Acad. Sci. U.S.A.* 49: 193-200.
- Sonnenblick, E.H., Skelton, C.L., Spotnitz, W.D. and Feldman, D. 1973. Redefinition of the ultrastructural basis of cardiac length-tension relations. *Circulation* 48, (Suppl. 4): 65.

- Sperelakis, N. 1967. Electrophysiology of cultured chick heart cells. in Electrophysiology and ultrastructure of the heart. pp 81-108. (eds: Sano. T., Mizuhira, V., and Matsuda, K.) Bunkado, Tokyo.
- Sperelakis, N. 1978. Cultured heart cell reaggregate model for studying cardiac toxicology. Environ. Health Perspect. 26: 243-267.
- Sperelakis, N. and Pappano, A.J. 1969. Increase in P_{Na} and P_K in cultured heart cells produced by veratridine. J. Gen. Physiol. 53: 97-114.
- Sperelakis, N. and Pappano, A.J. 1969a. Depolarization of cultured heart cells by a lipid-soluble acetylcholine analogue. Am. J. Physiol. 217: 625-629.
- Sperelakis, N. and Lehmkuhl, D. 1965. Insensitivity of cultured chick heart cells to autonomic agents and tetrodotoxin. Am. J. Physiol. 209: 693-698.
- Sperelakis, N. and Lehmkuhl, D. 1968. Ba^{2+} and Sr^{2+} reversal of the inhibition produced by ouabain and local anaesthetics on membrane potentials of cultured heart cells. Exp. Cell Res. 49: 396-410.
- Spiro, D. and Sonnenblick, E.H. 1964. Comparison of the ultrastructural basis of the contractile process in heart and skeletal muscle. Circ. Res. [Suppl. 2]: 14-37.
- Spurr, G.B. and Barlow, G. 1959. Influence of prolonged hypothermia and hyperthermia on myocardial sodium, potassium and chloride. Circ. Res. 7: 210-218.
- Starling, E.H. 1897. The Arris and Gale lectures. On some points in the pathology of heart disease. Lecture I: The compensating mechanism of the heart. Lancet 1: 569-572.

- Sumbera, J., Kruta, V. and Braveny, P. 1966. Influence of a rapid change of temperature on the mechanical response of mammalian myocardium. Arch. Internat de Physiol. Biochim. 74: 627-641.
- Tada, M., Kirchberger, M.A., Iorio, J.M. and Katz, A.M. 1975. Control of cardiac sarcolemmal adenylate cyclase and sodium, potassium-activated adenosinetriphosphatase activities. Cric. Res. 36: 8-17.
- Tarr, M., Trank, J.W., Leiffer, P. and Sheperd, N. 1979. Sarcomere length-resting tension relation in single frog atrial cardiac muscle. Circ. Res. 45: 554-559.
- Teiger, D.G. and Farah, A. 1967. Calcium movements in resting and isolated rabbit atria. J. Pharmacol. Exp. Ther. 157: 8-18.
- Teiger, D.G. and Farah, A. 1968. The effect of calcium and sodium on the force-frequency relationship in cardiac muscle. J. Pharmacol. Exp. Ther. 164: 1-9.
- Thompson, E.J., Wilson, S.H., Schuette, W.H., Whitehouse, W.C. and Nirenberg, M.W. 1973. Measurement of the rate and velocity of movement by single heart cells in culture. Am. J. Cardiol. 32: 162-166.
- Toll, M.O. 1973. Systems analysis of inotropic interventions in isolated heart muscle. Ph.D. Dissertation, University of London, London, U.K.
- Toll, M.O. 1979. Temperature-control system for biological preparations. Med. Biol. Eng. Comput. 17: 97-102.
- Toll, M.O. 1979a. A system for measuring cultured cardiac strand contractility. Proc. 32nd ACEMB. 21: 63.

- Trautwein, W. 1973. Membrane currents in cardiac muscle fibers. *Physiol. Rev.* 53: 793-835.
- Trautwein, W., McDonald, T.F. and Tripathi, O. 1975. Calcium conductance and tension in mammalian ventricular muscle. *Pflugers Arch.* 354: 55-74.
- Vassort, G. and Rougier, O. 1972. Membrane potential and slow inward current dependence of frog cardiac mechanical activity. *Pflugers Arch.* 331: 191-203.
- Watanabe Y. 1965. Antagonism and synergism of potassium and antiarrhythmic agents. In: Electrolytes and Cardiovascular Diseases. 1: 86-103. (ed: Bajusz, E.) The William & Wilkins Company, New York.
- Watanabe, A.M. and Besch, H.R., Jr. 1975. The relationship between adenosine 3',5'-monophosphate levels and systolic transmembrane calcium flux. In Rec. Adv. Cardiac Struct. Metab. 5: 94-102, (eds: Fleckenstein, A. and Dhalla, N.S.) University Park Press, Baltimore.
- Weidmann, S. 1955. Effects of calcium ions and local anaesthetics on electrical properties of Purkinje fibers. *J. Physiol.* 129: 568-582.
- Weidmann, S. 1956. Elektrophysiologie der herzmuskelfaser. Huber, Bern.
- Wendt, I.R. and Langer, G.A. 1977. The sodium-calcium relationship in mammalian myocardium: Effect of sodium deficient perfusion on calcium fluxes. *J. Mol. Cell. Cardiol.* 9: 551-564.
- Wildenthal, K. 1970. Factors promoting the survival and beating of intact foetal mouse hearts in organ culture. *J. Mol. Cell. Cardiol.* 1: 101-104.

- Wildenthal, K., Harrison, D.R., Templeton, G.H and Reardon, W.C. 1973. Method for measuring the contraction of small hearts in organ culture. Cardiovasc. Res. 7: 139-144.
- Winegrad, S. and McClellan, G.B. 1979. Regulation of the contractile proteins in cardiac muscle. In Cross bridge mechanism in muscle contraction pp 328-344. (eds: Sugi, H. and Pollack, G.H.) University Park Press, Baltimore.
- Woodworth, R.S. 1902. Maximal contraction, 'staircase' contraction, refractory period and compensatory pause of the heart. Am. J. Physiol. 8: 213-249.
- Woolenberger, A., Will, H. and Krause, E.G. 1975. Adenosine 3',5'-monophosphate, the myocardial cell membrane, and calcium. In: Rec. Adv. Cardiac. Struct. Metab. 5: 81-93. (eds: Fleckenstein, A. and Dhalla, N.S.) University Park Press, Baltimore.
- Yeatman, L.A., Parmley, W.W. and Sonnenblick, E.H. 1969. Effects of temperature on series elasticity and contractile element motion in heart muscle. Amer. J. Physiol. 217: 1030-1034.
- Zacchei, A.M. and Caravita, S. 1972. Observations on the ultrastructure of chick-embryo cardiac myoblasts re-aggregated in longterm cultures. J. Embryol. Exp. Morph. 28: 571-589.

APPENDICES

Appendix -I

MYOCARDIAL TISSUE CULTURING TECHNIQUES

Introduction

This appendix is essentially a duplication of a protocol prepared by the author for training a research assistant in myocardial tissue culturing to prepare cultured heart muscle strands. Because of this, the time references are based upon the working week and instructions are often explicit and very detailed.

Many of the major innovations in this technique, in particular Section 1A through 1K, were developed by Dr. Graham H. Burke in completion of his Ph.D dissertation research. The author expresses his sincere thanks to Mrs. Geetha Reddy, who patiently taught him the basic culture techniques.

I Procedures For Culturing Myocardial Single Cell Suspension

1A. Culturing procedure is preferably done on Tuesdays, since everything could be organized and kept ready on Monday for culturing on the following day.

On Monday night, keep out the following items in the incubator to defrost overnight.

- (1) One 100 ml bottle of Hanks balanced salt solution (BSS) (Gibco Cat. # 310-4170) and
- (2) an empty sterile bottle.

On Tuesday - the day of culturing - first thing in the morning put out the following in the incubator to defrost for about 90 minutes:

- (1) 10 ml Trypsin (Gibco Cat. # 610-5055)
- (2) 10 ml fetal bovine serum (FBS) (Flow laboratories Cat. # 29-101-49)
- (3) 1 ml PENSTREP (Gibco Cat. # 600-5140)
- (4) 1 ml L-Glutamine (Gibco Cat. # 320-5039)
- (5) One 100 ml bottle of Eagle's minimum essential medium (MEM) (Gibco Cat. # 380-2370)

1B. Procedures For Cleaning the Culture Hood:

- (i) Wear disposable vinyl gloves.
- (ii) Turn on the fluorescent light in the hood.
- (iii) Use 75% alcohol to clean the hood.
- (iv) If you observe yellow stains on any of the inner surfaces of the hood, use hot water to clean, followed by alcohol.
- (v) Clean all the three walls, ceiling and doors of the hood by spraying alcohol generously and wipe with cotton gauze.
- (vi) Empty the table top under the hood, spray alcohol liberally and wipe thoroughly.
- (vii) Keep a bunch of clean cotton gauze inside the hood.
- (viii) Take nine sterile polystyrene disposable centrifuge tubes with plug-seal cap (Fisher Scientific Ltd., Cat. # 05-538-51A), number them 1-9 and place them in one corner of the hood.
- (ix) If no further activity is planned under the hood, turn off the fluorescent light and turn on the ultraviolet (UV) light.

1C. Preparation of Trypsinising Solution:

- (i) Turn on the fluorescent light of the hood. The following steps must be carried out under the hood.
- (ii) Mix 10 ml of the trypsin into the 100 ml Hanks BSS (refer item 1A).
- (iii) Add 2.5 ml of HEPES buffer (Gibco Cat. # 845-1344), stored in the refrigerator all the time, using a 3 cc syringe.
- (iv) Hold the cap of the bottle with left palm and small finger. Never place the cap on the surface. At any time if the syringe touches the surface of the table or bottle or any unsterilised surface, dispose it immediately and use a new one. This procedure should be followed for any glassware used during culturing.
- (v) Fit a millipore filter (pore diameter 0.22 μm ; Millipore Inc., Cat. # SLGS 025 OS) on to a syringe. The plunger of the syringe must be removed before attaching the filter. Pour the trypsin mixture (step iii) into the syringe, place back the plunger and filter the mixture into the empty sterile bottle that was kept in the incubator.

- (vi) Inside the sterile cover, first remove the filter, then remove the plunger, fit the filter back again on to the syringe, and follow step v if more filtering is to be done.
- (vii) All the time, hold the cap of the bottle in your left palm and close as soon as filtering is completed. At the end of filtering, dispose syringe, Hanks BSS bottle and the millipore filter.
- (viii) Keep the trypsin solution thus prepared in the incubator (at 37°C).
 - (ix) Clean the table top under the hood with alcohol.
- (x) If no further activity is planned, turn off the fluorescent light and turn on the UV light.

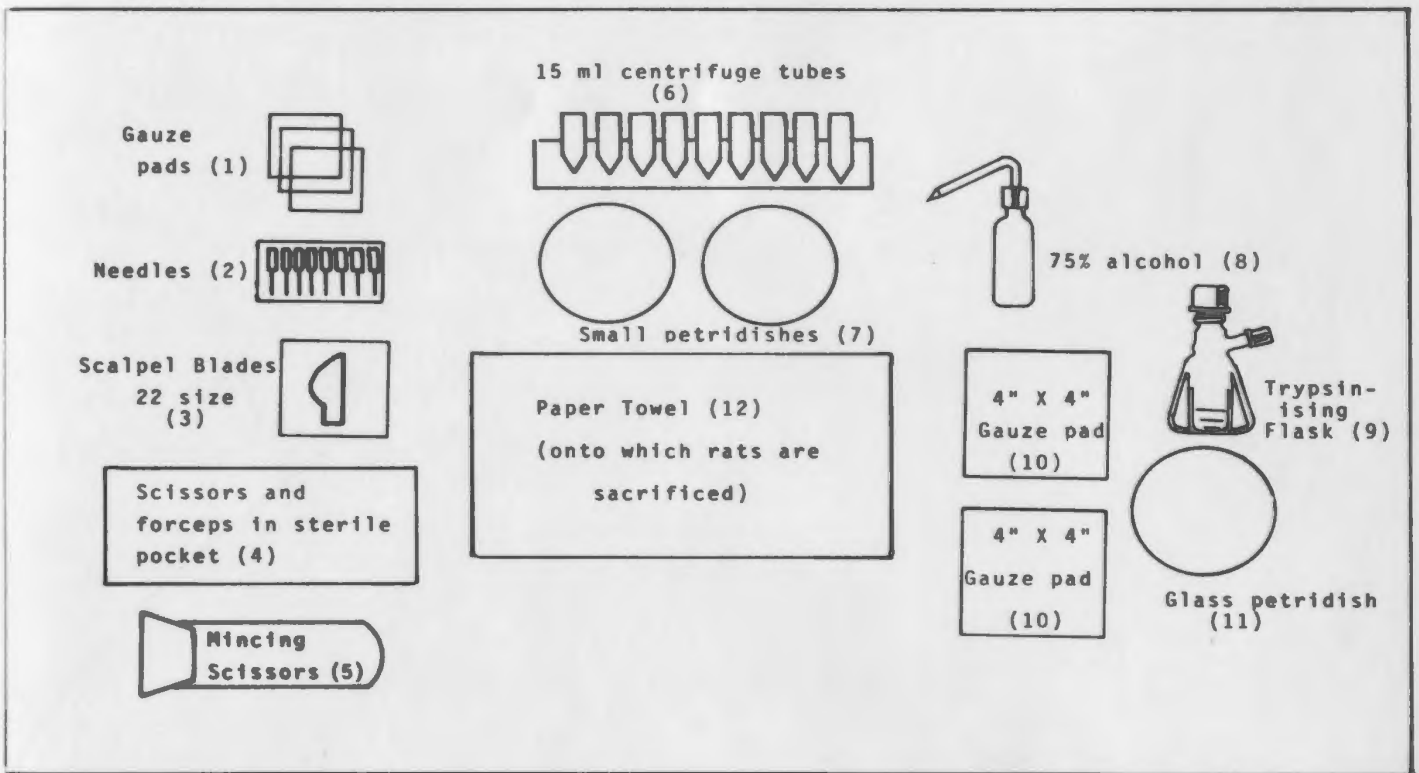
1D. Preparing the Layout For Culturing:

The suggested layout for culturing is diagrammatically indicated in Fig. A1. Various item used are indicated as well as numbered for further reference in the text.

- (i) Pour warm trypsin in the two disposable polystyrene petri dishes⁷ (Fisher Scientific, Cat.# 08-772B).
- (ii) Peel the gauze pad wrap and remove both the gauze pads¹⁰ and lay the one below the other in the same position.

Fig. A1. Layout for culturing.

Various items used are indicated as well as numbered for reference in the text.



- (iii) Open the sterile pocket⁴, take out the pair of scissors and a pair of forceps and place them on one gauze pad. Leave the remaining pair of forceps in the sterile pocket itself; close and leave it aside.
- (iv) Take out a 22 size scalpel blade³ and place it on the other gauze pad.

1E. Extraction of Hearts:

- (i) Insert paper towels¹² on the bench on which rats are sacrificed.
- (ii) Handle the rats with left hand only.
- (iii) Wipe the neck of the rats with alcohol.
- (iv) Aseptically remove the heart. Use the sterile scalpel blade to decapitate the newborn rat. With the sterile scissors make a cut through the chest towards the stomach. Using a small amount of pressure spread the chest; the heart should pop up. (The skin of the rat is not sterile, therefore try to avoid any instrument contact with the skin. Also, try to hold the scissors the same way for each cut so that the same blade cuts from the outside of the rat).

- (v) Using one pair of small forceps pluck the beating heart and place it immediately in trypsin in one petri dish⁷.
- (vi) When hearts are extracted from all rats (usually 8-9 rats), wrap up the wastes on the paper towel and keep out of the hood. Clean the scissors and forceps with alcohol. Keep the waste and all used gauze pads in a plastic bag and leave outside. Dispose the used scalpel in a syringe disposer.
- (vii) Clean the table with alcohol and wash your hands. If necessary change the pair of vinyl gloves.
- (viii) Take another pair of gauze pads.
- (ix) Lay down the other pair of scissors⁴ and the mincing scissors⁵ on one gauze pad.
- (x) Hold each heart in the petri dish with forceps. Using mincing scissors cut out the ventricle (about 1/3 from the apex) and place it in the other petri dish with trypsin solution.
- (xi) Take off as much blood clots as possible from the ventricles. Cut the ventricles into four pieces using mincing scissors and transfer all of them into a glass petri dish¹¹.
- (xii) Mince the ventricles thoroughly and remove blood clots if any.

- (xiii) Use a fresh scalpel blade³ and transfer the minced ventricles into the trypsinising flask⁹ (Fisher Scientific, Cat. # 6-426 A) through the side pour-out.
- (xiv) Dispose the polystyrene petri dishes into the plastic bag (step vi), tie it up and throw it into the incinerator.
- (xv) Immerse the used instruments in distilled water.

1F. Preparation of Modified Medium:

- (i) To the bottle containing the Eagle's MEM, add the following:
 - * 1 ml L Glutamine
 - * 1 ml PENSTREP
 - * 10 ml FBSAll these four constituents are already defrosted and available in the incubator (refer Sec. 1A).
- (ii) Shake well.
- (iii) Make sure the bottle cap was never placed on the table top any time.
- (iv) Mark the bottle as "Modified MEM" and label the date, using a glass marking pen.
- (v) Leave the bottle containing the modified MEM in the refrigerator.
- (vi) Dispose the tubes that contained the chemicals and FBS (refer step i).

1G. Digestion of Minced Cardiac Tissues:

- (i) Add 20 ml of trypsin solution to the ventricular tissue in the digestion flask.
- (ii) Set the flask on the magnetic stirrer in the incubator at a speed of approximately 1 revolution per minute (rpm). Spin very gently.
- (iii) Spin the mixture for 20 minutes. Use a timer.
- (iv) When the alarm rings, take out the flask and pour out as much supernatant as possible through the side opening into the centrifuge tube numbered 1.
- (v) Repeat steps i through iv two more times (supernatants poured into centrifuge tubes 2 & 3).
- (vi) Now, add 15 ml of trypsin solution to the digestion flask. Return to be spun for 15 minutes.
- (vii) After 15 minutes, take out the flask and pour approximately 8 ml of the supernatant through the side opening into centrifuge tube marked number 4 and subsequent numbered tubes for subsequent iterations.
- (viii) Add cold medium to the centrifuge tubes (about 4 ml) to bring the level to 12 ml. Close the tube. Turn it upside down twice to mix. This will stop trypsinising action.

- (ix) Repeat steps vi through viii five more times.
- (x) The first three digestions contain large amounts of debris (blood cells, damaged tissues, epithelial cells, etc.) and are therefore discarded. The remaining six tubes contain sufficient viable cardiac cells.

1H. Centrifugation:

- (i) When the digestion procedure is completed, place the 6 tubes (numbered 4 through 9) and 2 dummies (filled with distilled water exactly up to 12 ml) inside the centrifuge.
- (ii) Switch on "Power" followed by "Brake".
- (iii) Set the timer at 5 minutes and run the centrifuge at 1000 rpm.
- (iv) Pour off the fluid above the sediment in each tube into a clean beaker.
- (v) Add 1-2 ml of cool medium to the tubes.
- (vi) Resuspend the cells by drawing the sediments into a pasteur pipette and gently releasing them into one of the centrifuge tubes. Fill this tube with fresh medium to make up a volume of exactly 12 ml.
- (vii) Place it in the centrifuge along with 3 other dummies and run it for another 5 minutes at 1000 rpm.

- (viii) Pour off the supernatant quickly and fill it with 2 ml of fresh medium.
- (ix) Using a new pasteur pipette, agitate gently.
- (x) Fill it with fresh medium to raise the volume to exactly 6 ml.
- (xi) Place it in the centrifuge with 3 other dummies (which also have exactly 6 ml of distilled water) and run it for 5 minutes at 1000 rpm.

1I. Filtering the Final Suspension to Isolate Single Myocardial Cells:

- (i) This follows Sec. 1H. Pour off the supernatant and fill it with 2 ml of fresh medium.
- (ii) Using a new pasteur pipette agitate gently.
- (iii) Add fresh medium to bring the content up to 6 ml.
- (iv) Turn the tube upside down twice.
- (v) Take a 10 ml syringe and remove its plunger. To this plungerless syringe fit a millipore filter marked "Filter" (which contains a lens paper inside).
- (vi) Slit the arrangement over a sterile centrifuge tube.
- (vii) Pour the final suspension into the syringe body.
- (viii) Allow the suspension to freely drip through.
- (ix) Pour the suspension into a canted-neck disposable plastic tissue culture flask (Fisher Scientific, Cat. # 10-126-30) and close with the cap.

- (x) Place the flask on its flat side in the incubator (at 37 °C) for 90 minutes.
- (xi) Take out the flask and tap it gently twice on the table.
- (xii) Pour the suspension into a graduated centrifuge tube and record the resulting volume. Following steps ix through xi, the final suspension obtained contains chiefly myocardial cells since all other cell types (such as fibroblasts and epithelial cells) adhere to the bottom of the flask within 90 minutes.

1.J. Cell Count

- (i) Have the hemacytometer [Spencer "Bright Line" hemacytometer, Cat. #. A-2440/B(4011)] clean and dry (i.e. soak in alcohol, wash in hot sudsy water, rinse in distilled water, and let it dry by evaporation).
- (ii) When it is dried, place it on the microscope stage and above it keep a hemacytometer coverglass (Hellige, Inc. standard grade, 20 x 20 mm; Cat. #. 146-0).
- (iii) Using a 1 cc syringe, draw out 0.5 ml of cultured suspension and transfer into a centrifuge tube.

- (iv) Using another 1 cc syringe, draw 0.1 ml of trypan blue and mix into the cultured suspension in the centrifuge tube.
- (v) Mix it thoroughly and let it remain between 6 and 15 minutes.
- (vi) This liquid sample is now ready for cell count.
- (vii) Using a clean, dry pasteur pipette (not necessarily sterile) transfer a quantity of the fluid to the hemacytometer. Discard the first two drops of the fluid. Load one section of the hemacytometer by placing the tip of the pipette against the coverglass and slowly releasing the pressure. Discard the fluid left in the pipette and repeat the procedure to fill the other section.
- (viii) Allow the cells to settle for 2 minutes. Living cells will not take up the trypan blue dye, but the dead cells absorb it. Hence the live cells will appear green in colour and the dead ones are blue in colour.
- (ix) Using the 10X objective of the Nikon M inverted microscope count the total number of viable and nonviable cells in large squares (four corner sequences and the centre square) of the counting chamber grid.

- (x) To obtain the cell count of viable cells per cubic centimeter (cells/ml) add the number of live cells from each of the two grids and multiply by a factor of 10^3 (i.e. each square is 1 mm^2 and $1/10 \text{ mm}$ in depth giving a cubic content of $1/10$ cubic mm. The total count of the two grids is therefore 1 mm^3 . A factor of 10^3 will thus give a concentration of viable cells per ml).

1K. Preparation of Final Cell Dilution

- (i) The cell count will give a concentration per ml (C).
 (ii) The volume of culture suspension (V_1) is known.
 (iii) The desired concentration (C_d) is

$$1.5 \times 10^5 \text{ cells/ml.}$$

- (iv) Hence to obtain C_d , the volume of suspension must be modified.

- (v) The final volume (V_f) will be

$$V_f = \frac{V_1 \times C}{C_d} \quad (\text{ml})$$

- (vi) Add fresh medium to the centrifuge tube to make up a new volume of the desired concentration.
 (vii) This diluted solution would be used in preparing the final culture chambers (see Section 2G).

1L. Cleaning Up

- (i) During the process of culturing once the dissection procedures are over soak the instruments in distilled water for 2 hours.
- (ii) About 2 hours, before completing the day's schedule, take out the instruments, throw off the water and leave the instruments in the plastic tray for wash up on the Wednesday. DO NOT soak the instruments in distilled water overnight.
- (iii) Throw away all the used pipettes and corning tubes in a disposable bag which should be autoclaved before disposing.
- (iv) Break the needles and dispose them in the needle disposing box.
- (v) Throw the medium into the sink and leave the beaker and rubber caps for washing.
- (vi) Clean the hemacytometer and coverglass with distilled water and soak them in 95% alcohol.
- (vii) Mark the date on the bottle containing the remaining medium after culturing. Close it tight and keep it in the refrigerator.
- (viii) Clean the hood with alcohol and follow wash up procedures (see Section 1B).

II Culture Chamber Preparation

2A. Preparation of 2% Agar

- (i) Weigh exactly 2 g of Agar.
- (ii) Transfer into a conical flask. Add 100 ml distilled water.
- (iii) Close the flask.
- (iv) Place it in the autoclave for 40 minutes (20 min + 20 min + 0 dry time) and run the autoclave in "LIQUID CYCLE" mode.
- (v) Use asbestos hand gloves to remove the flask from autoclave.

2B. Preparation for Agar Coating Procedures

- (i) Take out glass cover slips from the incubator (which were previously cleaned with 75% alcohol and placed between tissue papers).
- (ii) Clean the working area on the table top with alcohol.
- (iii) Lay 3 to 4 tissue paper towels on the table.
- (iv) Lay the cover slips (approximately 4 per row and 4 rows in each tissue paper).
- (v) Cover the layout with another set of paper towels.
- (vi) Keep an empty glass beaker and glass spreader (Y shaped glass rod) ready for agar coating.

2C. Agar Coating Procedures

- (i) Keep hot distilled water ready all the time.
- (ii) Place asbestos sheets (at least 4) on the table.
- (iii) Place Bunsen burner and tripod on the asbestos sheets.
- (iv) Place a wire gauze over the tripod.
- (v) Take approximately 40 ml of 2% agar in a beaker
(marked at least 140 ml).
- (vi) Turn on the Bunsen burner.
- (vii) Take approximately 200 ml of hot water in a separate
beaker.
- (viii) Heat the agar until it bubbles.
- (ix) Dip the glass spreader into the foam, place it on the
left side of the coverglass and gently, with light
pressure, pull down towards the right. (Don't stop
in between, avoid streaks and air bubbles).
- (x) Place the glass spreader into the hot water beaker.
For the next time, take out the glass rod, wipe it
thoroughly with facial tissue and then dip it into
the foam and repeat step ix.
- (xi) After coating all the cover slips, pour back the
remaining agar into the agar flask.
- (xii) Turn off the Bunsen burner and close the gas outlet.
- (xiii) Examine the glass cover slips and make sure that they
are properly coated with agar. A good coating
makes the coverslip appear opaque.

(xiv) Open a few plastic petri dishes. Place cotton gauze on each petri dish.

(xv) Place one glass coverslip in each petri dish, such that the noncoated side of the coverslip is in contact with the cotton gauze.

(xvi) Wait for the agar to dry (about one hour).

(xvii) When it is completely dried, close the petri dishes and store them.

After 24 hr, palladium lines were deposited on the agar coated glass coverslips using the "Mask" in the high vacuum coating machine.

2D. Microsphere Placement

(i) Use glass micropipette puller and prepare half a dozen glass microtool pointers. (Use 20 λ micropet).

(ii) Keep them on a thermocool, with the pointers projecting upward.

(iii) Use "Wild" light microscope.

(iv) Open the glass cover slip coated with agar and palladium.

(v) Use silicone grease.

(vi) Using the microtool, touch the silicone grease and put a dot of grease on appropriate locations on the

palladium lines as shown. . . .

With two dots on both top

and bottom lines and 4 dots

in the remaining 5 lines with

approximately equal

spacing between microspheres on the

horizontal line. . . .

(vii) Take 100 μm glass microspheres in a petri dish.

(viii) Using an hypodermic needle pick up microspheres and place them exactly above the grease spots.

(ix) View through the microscope and remove excess microspheres in and near the grease spots.

(x) Good microsphere placement should not leave any excess grease spots or stray microspheres lying in the field.

(xi) After placing the microspheres, carefully leave the coverslip in the petri dish and store it aside.

(xii) This arrangement is now ready for preparing empty culture chambers.

2E. Preparation of Empty Culture Chambers

(i) By now the glass cover slips coated with agar and palladium followed by placement of microspheres should be ready.

- (ii) Take out the rings from the bottle marked #4, wash it in distilled water and leave it to dry for 2 hours, preferably under U-V light inside the culturing hood.
- (iii) Evenly coat silicone grease on the bottom of the ring.
- (iv) Place the ring on the coverglass with microspheres.
Care should be taken to see that the ring does not sit on a microsphere.
- (v) Turn the arrangement upside down.
- (vi) Press coverglass lightly followed by heavy pressure using a rubber weight.
- (vii) Press with thumb around the areas of contact to make sure no air bubble is present in sealing.
- (viii) Turn it upside down. Evenly coat silicone grease on the top of the ring.
- (ix) Leave the whole arrangement in a petri dish.
- (x) Close the petri dishes. Tape both sides with small pieces of gas sterilizing tapes (green).
- (xi) Make at least 7 chambers each time.
- (xii) Wrap the chambers with green cloth and put a small piece of gas sterilizing tape at the edge of the wrap to seal it.
- (xiii) Place all the wrapped chambers in the gas sterilizing box, such that they all face upwards.

- (xiv) Wrap the box tight with the appropriate green cloth and leave it for sterilization with ethylene dioxide gas.
- (xv) This package could be picked up from the gas sterilization unit on the next day.
- (xvi) Once you brought this, open the package in the cupboard to dissociate from gas at least for 24 hours. DO NOT open the petri dishes.

2F. Final Culture Chamber Preparation

- (i) The final diluted purified cell suspension, upon completion of the preparatory culturing procedures (Section 1K, step vii), are used to inoculate the final culture chambers
- (ii) Use a sterile pipette - do not pour! Draw off enough of the suspension to fill the chamber.
- (iii) Gently transfer the suspension to the chamber through the side walls.
- (iv) Seal the chamber by pressing a sterile coverslip onto the face of the stainless steel ring previously coated with silicone grease.
- (v) Ensure that there is an air bubble in each chamber.
- (vi) Label each chamber with concentration, date and chamber number.
- (vii) Keep all the chambers in the incubator.

III Post-Culture Maintenance Procedures

3A. Wash Up (Wednesday)

- (i) Use only distilled water for washing the labware.
- (ii) Distilled water could be obtained from "glass wash" room.
- (iii) Spray 4 spoons ofalconox over the glassware.
- (iv) Pour hot distilled water on the glassware and let it soak for 15 minutes.
- (v) Spray one spoon ofalconox in a beaker, pour hot distilled water and soak the instruments for 15 minutes.
- (vi) Use appropriate brushes to clean the glassware and hang them on the glassware holder.
- (vii) Wash the rubber caps, filters and instruments and leave them on a tissue paper to dry and cover with another tissue paper.
- (viii) Wash the plastic tray with distilled water and leave it to dry.

3B. Cleaning the Rings and Discarding the Old Cultures

- (i) Use disposable hand gloves.
- (ii) Remove the top coverglass and put it into a glass disposer.

- (iii) Pour off the culture into an empty glass which is to be autoclaved.
- (iv) Peel off the bottom coverglass and put it into the glass disposer.
- (v) Wipe the rings with paper towel and soak into xylene (bottle marked #1) for 24-48 hours.
- (vi) Dispose of the gloves, paper towels, etc., into an envelope that can be autoclaved.

3C. Transferring Rings to Subsequent Numbered Bottles

- (i) After 48 hours remove the rings from xylene (bottle #1), using the stainless steel prongs.
- (ii) Peel off the glass particles using a stainless steel scraper.
- (iii) Wash it with distilled water and clean the bottom thoroughly.
- (iv) Wash it with distilled water and soak in xylene bottle marked #2.
- (v) After 24 hours take them out of bottle, wash in distilled water and soak in 95% Ethanol (marked bottle #3).
- (vi) After 24 hours take them out of bottle #3, wash in distilled water and soak in 70% alcohol (marked bottle #4) for 24 hours.

3D. Preparing Materials for Autoclaving

I. Autoclaving box contains:

- (i) Three empty bottles. Close the bottle cap loosely and wrap it with aluminum foil and bit of autoclave tape.
- (ii) Three packages of Pasteur pipettes - 6 pipettes per package. Seal the mouth of the package with autoclave tape.
- (iii) One mincing scissor tube.
- (iv) Two millipore filters marked "FILTER".
- (v) One trypsinising flask. Put in the little magnet, loosely close both caps and wrap them with aluminum foil and autoclave tape.
- (vi) One pack of cleaned coverglass slips. Insert lens papers in between coverglasses and keep in a glass petri dish. Wrap the petri dish with autoclave tape.
- (vii) Six rubber caps. Close the mouth of the rubber cap with aluminum foil.
- (viii) One package of dissecting instruments. Wrap 1 pair of scissors and 2 pairs of forceps in a double layered aluminum foil. Wrap this package again in another double layered aluminum foil. Use autoclave tape to secure the wrapping tightly.

- (ix) One glass petri dish. Wrap it up completely with aluminum foil. Use autoclave tape if necessary.

II. Auxiliary box contains:

- 3 bottles
- 3 packages of pasteur pipettes
- 3 millipore filters marked "MEDIUM"
- 4 rubber caps

Leave both autoclaving box and auxiliary box for autoclaving.

3E. Autoclaving Procedure

- (i) Set heating/cooling suited to 15 minutes
 - "sterile" switch to 15 minutes
 - "drying" switch to 15 minutes
- (ii) Press "manual reset"
- (iii) Press "with dry time"
- (iv) Close the door. Turn the handle upward. Rotate the wheel clockwise until you hear a click sound.
- (v) After 55 minutes you hear an alarm.
- (vi) Press "manual reset"

- (vii) Press "off"
- (viii) Turn the wheel counterclockwise until it is completely released.
- (ix) Turn the handle downward and open the door.
- (x) Be careful! Sometimes steam can blast out.
- (xi) Collect the autoclaved containers and leave them in the cupboard in the culture room.

IV Microscopic Examination and Photography of Cultures

4A. Microscope Examination of Cultures

- (i) Use Nikon M. inverted microscope for viewing the cultures.
- (ii) Switch on the fan by turning on the switch to position 2.
- (iii) Increase the illumination to 9V.
- (iv) Make sure the three filters are placed in the path of the light beam.
- (v) Carefully open the petri dish, take out the culture chamber and place it on the platform.
- (vi) Set the magnification at 20X.
- (vii) Do not open the culture chamber.
- (viii) Adjust the phase and contrast to get a nice orange background.

- (ix) Move the platform left to right, top to bottom and view the whole field.
- (x) To view through TV monitor turn the illumination down to 6V; pull the knob for cine.

(Make sure TV camera just touches the lens on the right hand side; videotape is switched on and in record mode, the cables are hooked up to the monitor, and the mat gain control is switched on).

4B. Microscope Photography

Full knowledge of pages 4 to 19 of the booklet "Nikon, Microflex Model AFM, Automatic Photomicrographic Attachment" is required. This booklet can be found in the black folder marked, "Microscope Operating Manuals".

With the camera set-up on the vertical tube, the following procedure is followed to take pictures:

- (i) The switch on the back of the vertical tube is switched to the center position, so that the image is transmitted up the vertical tube.
- (ii) Push "Auto" mode on the control box.
- (iii) Set ASA and D.ADJ. to required settings for the film speed. (Example: film speed 125, ASA = $1/2 \times 100$, and D.ADJ. = $1/3$ over).

- (iv) Connect the connecting cord from the Control Box to the Shutter Housing.
- (v) Screw cable release in the side of Shutter Housing.
- (vi) Set the light intensity to 9V.
- (vii) Load film into the camera.
- (viii) With dark slide left in camera, release the shutter to check for correct operation of the signal lamp.
- (ix) Draw out the dark slide.
- (x) Take a picture of the scale at the beginning of each roll.
- (xi) Bring the finder image in sharp focus and compose the picture.
- (xii) Release the shutter and wait for signal lamp to go out.
- (xiii) Cock the shutter on the camera body.
- (xiv) Move the microscope stage from right to left.
- (xv) Repeat steps ix to xii.
- (xvi) When finished taking pictures close the dark slide.

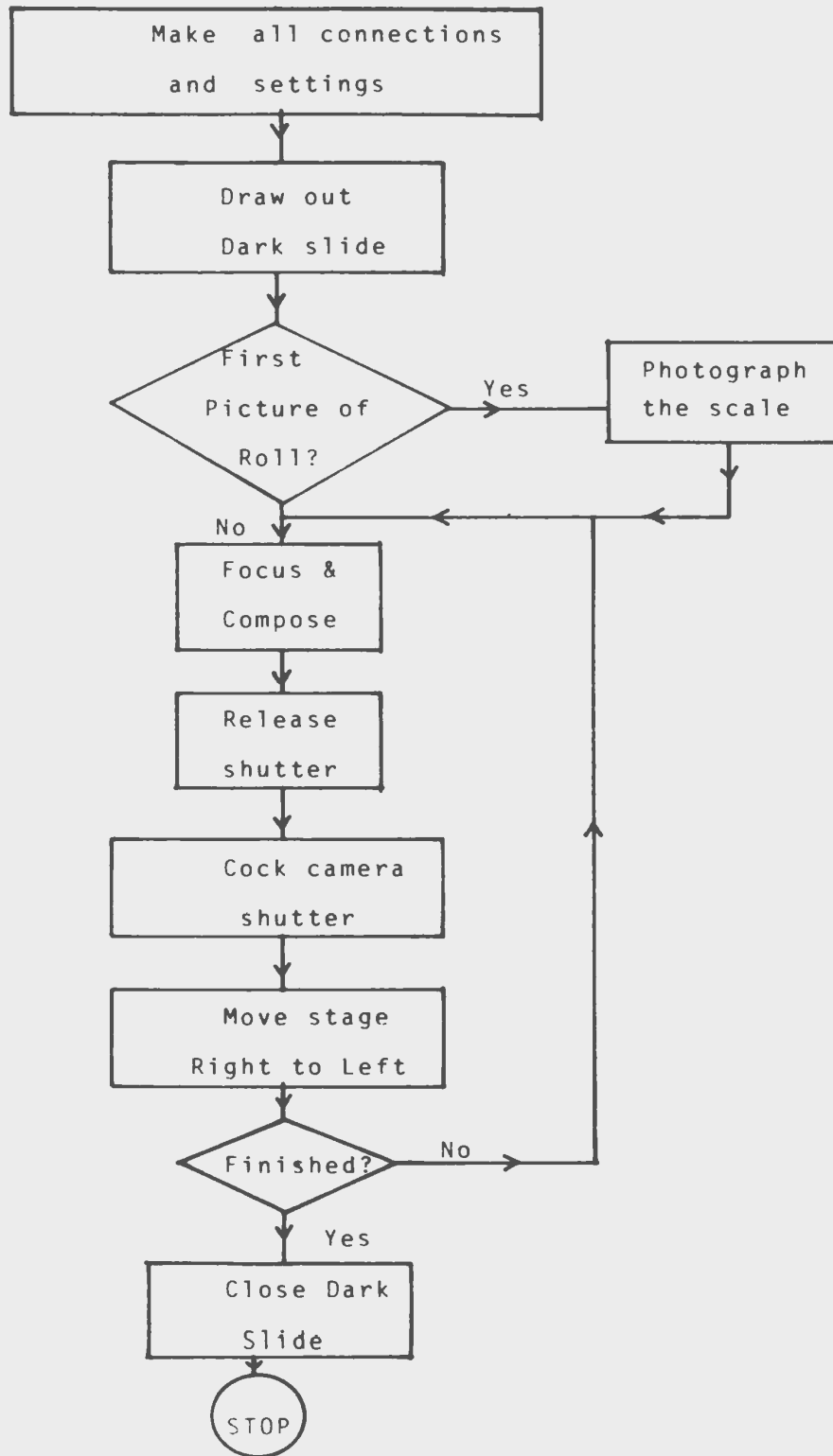
These steps are diagrammatically illustrated in the flow chart, Fig. A2.

4C. Camera Alignment

- (i) Open camera back.
- (ii) Place smoked glass over guide rail.
- (iii) Set control box to "Manual" and Shutter speed of "T".

Fig. A2. Flow diagram for microscope photography.

Microscope Photography - Procedure



- (iv) Draw the dark slide out of the camera.
- (v) Switch on the back of the vertical tube, is switched to right position, so that image is transmitted up the vertical tube and the eye pieces.
- (vi) Place the scale on the microscope stage and compose and focus picture through the eye pieces.
- (vii) The image should now be viewed in the smoked glass (this might have to be done in a dark room).
- (viii) To focus the image move the vertical photo tube up and down until the image is in focus. This is usually at the red line.
- (ix) The eyepiece sleeve lock screw is now used to move the viewfinder to a position where it can be used with ease.
- (x) The 35 mm projection lens, is loosened from the Lech type mount and the camera is moved around until the composed and aligned picture is viewed through the smoked glass. The 35 mm projection lens is then tightened.
- (xi) Two screws next to the lock nut for AFM main body on the ocular finder are used to adjust the finder mask to see the same picture as that in the smoked glass.
- (xii) The alignment is now complete.

V. Procedure for Changing the Medium

- (i) Make sure enough fresh modified medium is available.
- (ii) If not, prepare medium (see Section. 1F).
- (iii) Clean the hood (refer Section. 1B).
- (iv) Get the following things ready:
 - a) 2 Corning tubes
 - b) a glass beaker
 - c) a packet of Pasteur pipettes
 - d) 2 rubber bulbs (caps)
 - e) rubber weight
 - f) modified medium
- (v) Open the sterile pipette packet, fit the rubber bulbs on two pipettes and leave one in each of the Corning tubes.
- (vi) Keep the beaker on the left-hand side and medium on the right-hand side.
- (vii) Use one pipette to draw out the medium from the chambers and the other pipette to deliver fresh medium to the chambers.
- (viii) Do not alter during the procedure. At any time, during the procedure, if any of the pipettes touch either the glass walls or the surface of any sort, immediately change the pipette (with a new one from the sterile packet).

- (ix) Open a chamber. Keep the top cover glass just above the chamber as a protection.
- (x) Keep a pipette near the inside culture chamber wall, slowly and gently draw out the medium. Gently pump it in and out twice. Then draw out completely. Close the chamber.
- (xi) Pour this into the beaker and leave the pipette in the Corning centrifuge tube in the left hand side.
- (xii) With the next pipette, draw out fresh medium.
- (xiii) Open the chamber. Slowly and gently deliver the fresh medium through the side walls. Fill just half the chamber. Close the chamber and leave the pipette (with leftover medium) in the next Corning tube in the right-hand side.
- (xiv) Using the other pipette, repeat Steps x and xi. Periodically rotate the chamber, such that the same side is not used often for withdrawal and delivery.
- (xv) On the first medium change, repeat step xiv twice.
- (xvi) Fill the chamber with fresh medium.
- (xvii) Close the chamber with coverslip. Make sure the same grease points are used again.
- (xviii) Press the coverslip with rubber weight.
- (xix) Leave the bottle containing medium in the refrigerator.

- (xx) When all the chambers are done, place them back in the incubator.
- (xxi) Leave the bottle containing medium in the refrigerator.
- (xxii) Wipe the table top with alcohol.
- (xxiii) Throw away the old medium in the sink. Leave the beaker and rubber caps for washing. Dispose the pipettes in the pipette disposer bottle. Dispose the Corning tubes in a plastic disposer bag which should be autoclaved before disposing.
- (xxiv) Turn off the fluorescent light and turn on the UV light. Close the doors of the Culture hood.

Appendix - II

THE MICROGRAMME FORCE TRANSDUCER.

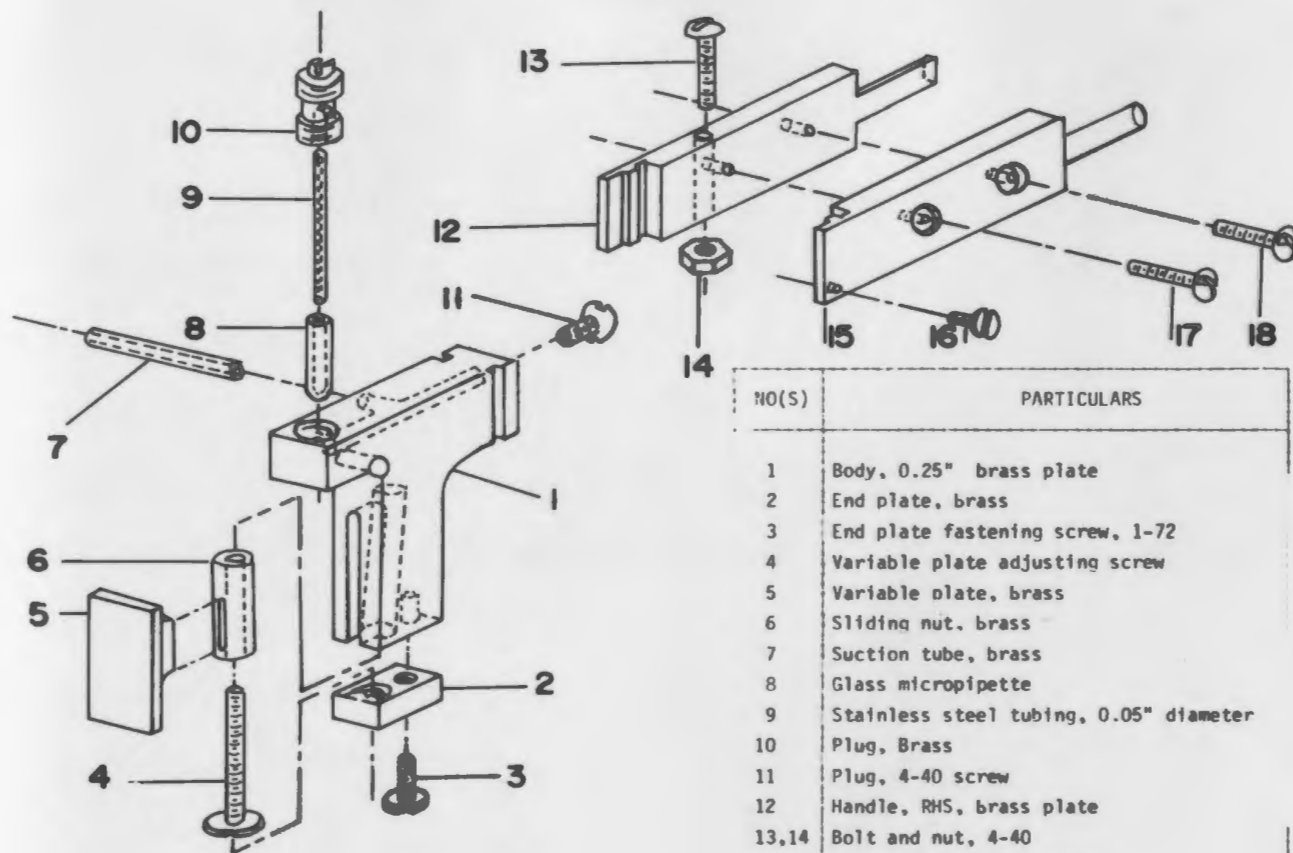
The construction and calibration of the force transducer used in the study of cultured myocardial strand contractility are described in this appendix.

A: Construction:

1. Mechanical Assembly: The mechanical assembly of the force transducer is illustrated in Fig. A3. The body (1) of the assembly contains two main features. First a variable brass plate (5) whose position can be adjusted by a sliding nut (6) and an adjusting screw (4), and second a composite cantilever beam (8,9, and 10). This composite beam is made up of a glass micropipette (8) (3.8 cm long, 20 λ Yankee Disposable Micropet) with a tip diameter of 60 μm ; a 5.0 cm length of 24 gauge (type 304) thin-walled hypodermic stainless steel tubing (9) and a brass plug (10). There is a 1.0 cm overlap between the glass and steel tubings. The lumen acts as a vacuum passage starting from the suction inlet (7) through the body (1), the brass plug (10), the steel tubing (9) and the glass micropipette (8). Thus the suction at the inlet (7) is transmitted to the tip of the cantilever beam (8).

Fig. A3. Mechanical assembly of the force transducer.

(Figure redrawn from the report of Kryski, January 1977).

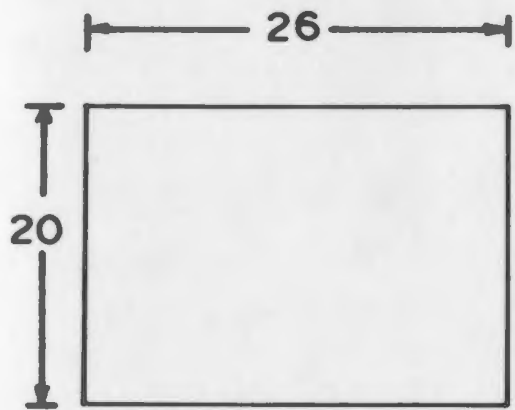


NO(S)	PARTICULARS
1	Body, 0.25" brass plate
2	End plate, brass
3	End plate fastening screw, 1-72
4	Variable plate adjusting screw
5	Variable plate, brass
6	Sliding nut, brass
7	Suction tube, brass
8	Glass micropipette
9	Stainless steel tubing, 0.05" diameter
10	Plug, Brass
11	Plug, 4-40 screw
12	Handle, RHS, brass plate
13,14	Bolt and nut, 4-40
15	Handle, LHS, brass plate
16	Tightening screw, 1-72
17,18	Handle screws, 4-40

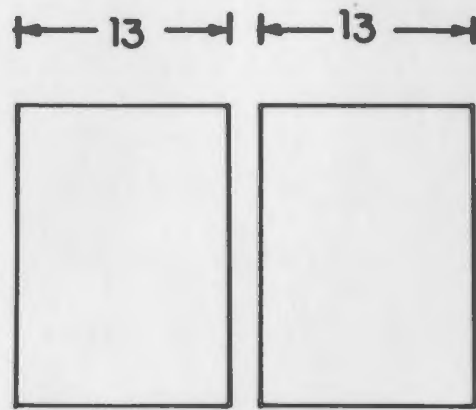
2. Capacitance Plates: The functional element of the transducer is a variable capacitance plate. Various steps in preparing the capacitance plates are diagrammatically represented in Fig. A4. A rectangular (20 X 26 X 0.4 mm) hemacytometer cover glass (a) was divided into two pieces (20 X 13 X 0.4 mm) (b) and the left hand corner of each (4 mm from the corner) was cut at a 45° angle (c). These two plates were positioned such that the cut corners face each other in an opposite direction (d). Using a high vacuum coating machine the facing sides of these two plates were coated first with chromium followed by aluminium. Electrical continuity throughout the plate surface was checked and a thin flexible wire was attached to the corners (e) of the plates using a drop of silver conducting paint (SPI supplies, division of Structure Probes Inc., Westchester, PA; SPI Cat. # 5001). When the plates dried they were dipped in a solution containing clear nail polish and acetone in a ratio of 1:10, for a fraction of a second and then dried on a flat surface. This coating protects the plates from short circuiting.

One of the plates was firmly attached to the variable plate (5 in Fig. A3), while the other plate was attached to the steel tubing of the cantilever beam (9 in Fig. A3) with a drop of molten wax (refer Fig. 2.3 for physical arrangement of the plates). The positioning of the two

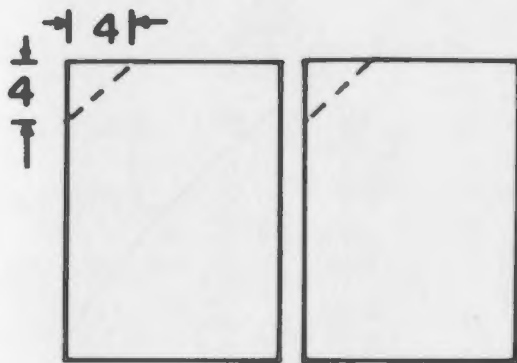
Fig. A4. Different stages in the preparation of capacitor plates used in the force transducer.
(refer text for description)



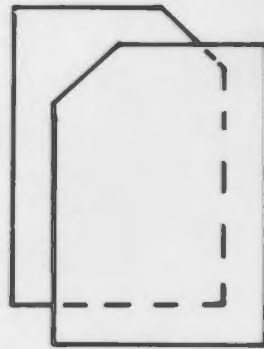
(a)



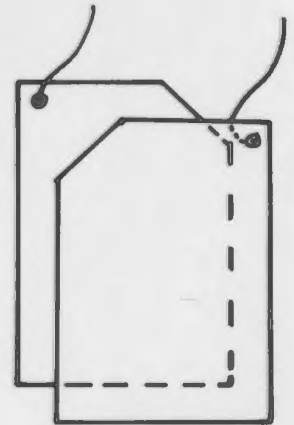
(b)



(c)



(d)



(e)

All dimensions in mms.

plates was such that they face each other. The distance (or the air gap) between these two plates can be precisely adjusted using an adjusting screw (4 in Fig. A3).

A force applied at the tip of the beam (8 in Fig. A3) causes it to deflect and thereby changes the distance between the two plates resulting in a change of capacitance.

3. Phase-Locked Loop (PLL): The change in capacitance modulated the voltage controlled oscillator (VCO) of the PLL (Fig. A5). In this unconventional use of the PLL, the modulated VCO signal was compared to an external reference signal by the phase detector of the PLL. The change in VCO frequency generated an output error signal in the phase detector, which was filtered to produce a d.c. signal proportional to the change in capacitance and hence the applied force. This d.c signal was also used to drive the VCO to keep the loop in lock with the 5 MHz reference signal.

Actual circuits used for the PLL and the 5 MHz reference signal are shown in Fig. A6. The variable capacitance plates were connected to the PLL at its terminals 2 and 3 as shown in Fig. A6(a) marked by "transducer". In Fig. A6 the ports A, B and C refer to the

Fig. A5. Block diagram of the phase-locked loop (PLL) circuit.

Note the unconventional use of the PLL.

(Figure, courtesy of Dr. M.O. Toll)

Fig. A6. Circuit configurations of (a) the PLL and (b) the 5 MHz crystal oscillator.

The values of resistors (in ohms) and capacitors (in μF , unless specified) used are indicated.

In circuit (a):

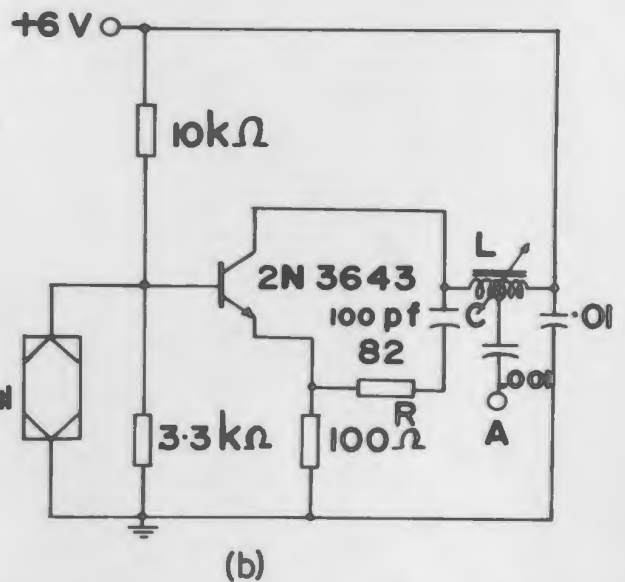
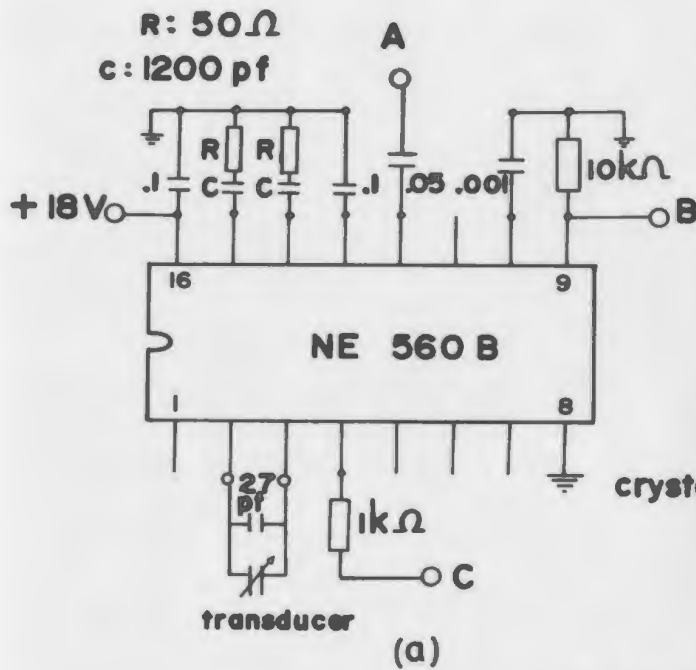
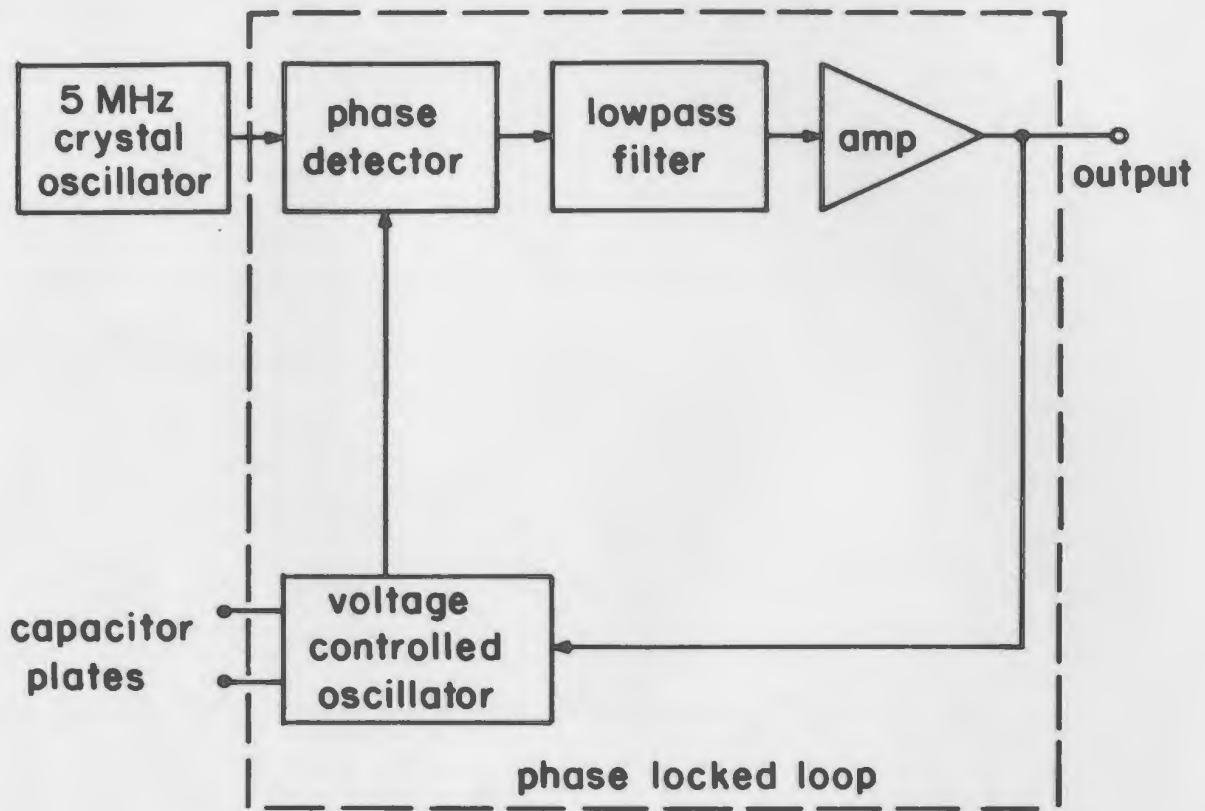
'A' : Crystal oscillator reference frequency input.

'B' : Transducer's voltage output.

'C' : Transducer VCO frequency output.

NE 560 B : Phase-locked loop circuit (Signetics, Inc.)

In circuit (b) the reference frequency was determined by the combination of L,C and R in conjunction with the crystal.



all capacitors in μF, unless specified

5 MHz reference signal, PLL voltage output and the VCO frequency output respectively. In the reference oscillator the combination of the crystal, resistance R, capacitance C and inductance L provided the 5 MHz signal. This circuit was assembled using the kit obtained from International Crystal Manufacturing Company.

B. Calibration Procedures:

1. Static displacement calibration: The displacement sensitivity (S_d) of this transducer was characterized by moving the tip of the transducer in 10 μm increments, using a precision micrometer, while recording the transducer output. The relationship (Fig. A7) observed was linear up to 120 μm ; at larger displacements the transducer PLL was driven out of lock and the output decreased (as indicated by the dotted line). The useful displacement range of this transducer was 0-120 μm . The displacement sensitivity, obtained by measuring the slope of the curve, was 30 mV/ μm .

2. Static force calibration: Because the forces involved were small, a special calibrator (Fig. A8 a) was devised for measuring the force sensitivity. This device was a simple lever, using the edge of a razor blade as the fulcrum which was counterbalanced by an adjusting nut so

Fig. A7. Static displacement sensitivity characteristics of the force transducer.

Displacement (in μm) along the abscissa and the transducer output (in Volts) along the ordinate is plotted. At displacements greater than 120 μm , the transducer PLL was driven out of lock and the output decreased (shown by dotted line).

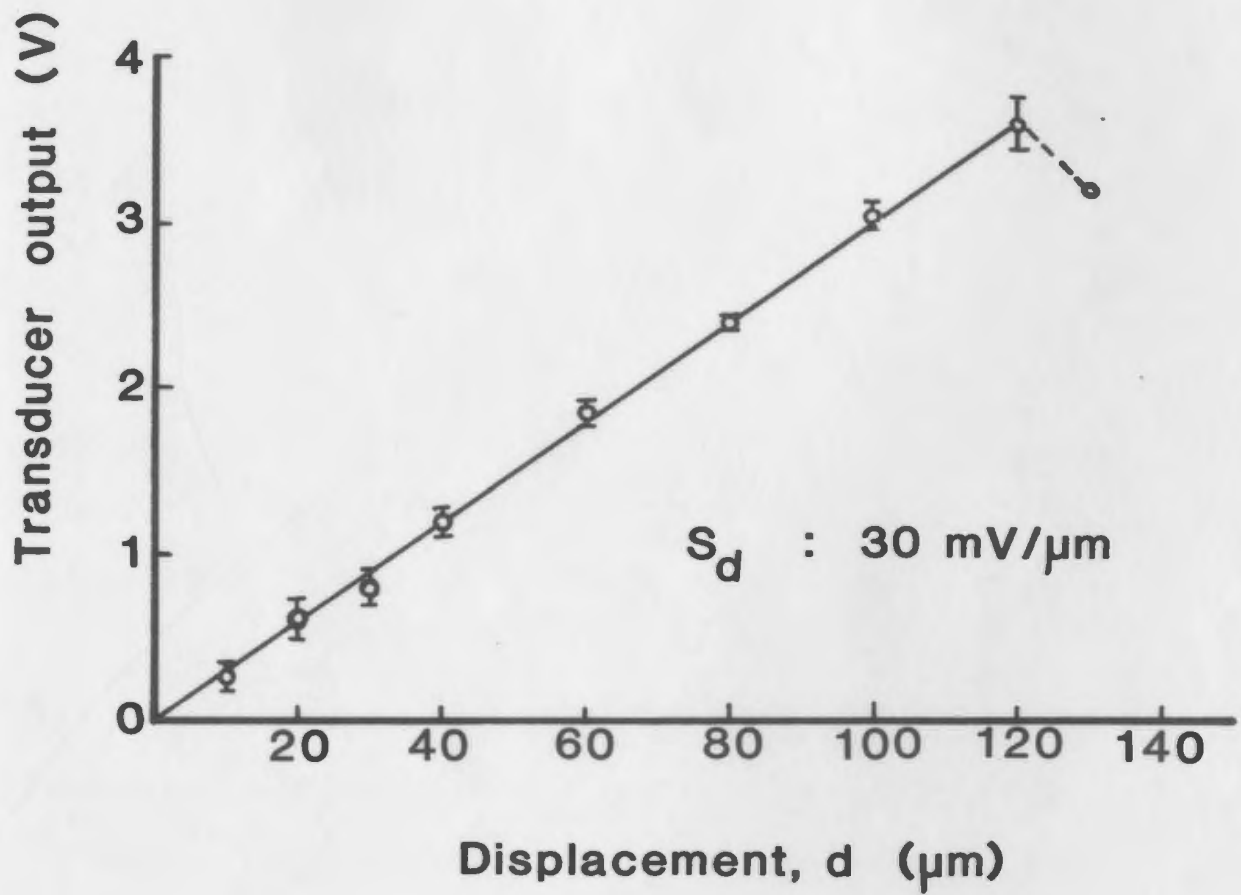


Fig. A8. Transducer force calibrator.

(a) Specialised calibrator devised for measuring the transducer's force-sensitivity.

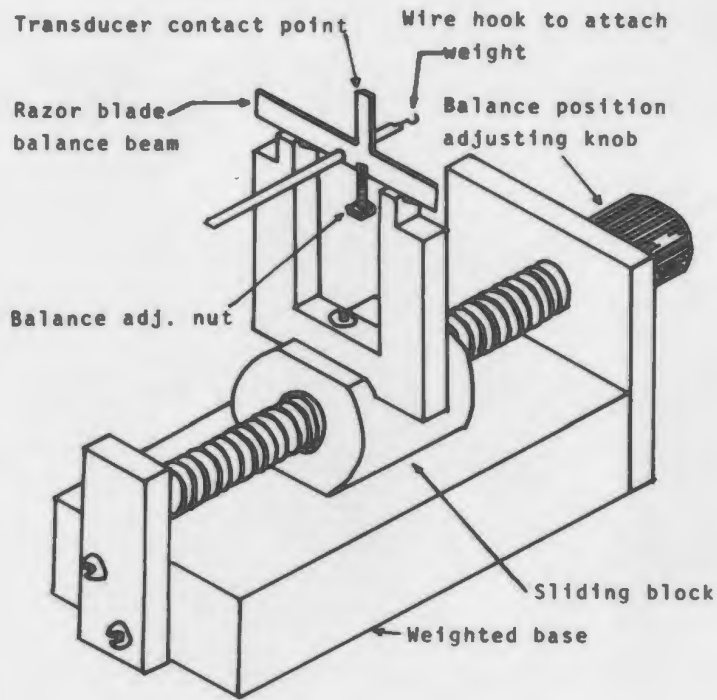
(Figure redrawn from the report of Kryski, January 1977)

(b) Principle of operation of the calibrator.

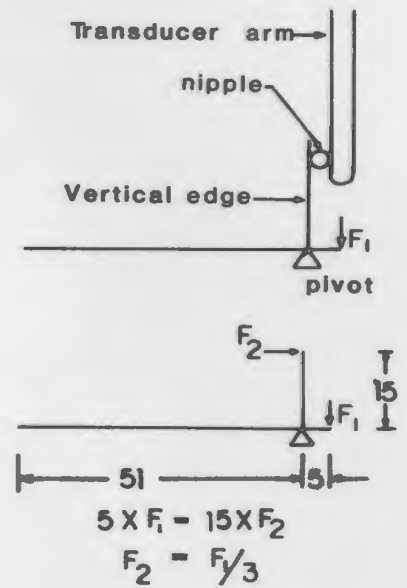
Fig. A9. Static force sensitivity characteristics of the force transducer.

Force (in mg) along the abscissa and the transducer output (in mV) along the ordinate is plotted. When the applied force exceeds 18 mg, the transducer PLL was driven out of lock and the output decreased (shown by dotted line).

Transducer Calibrator

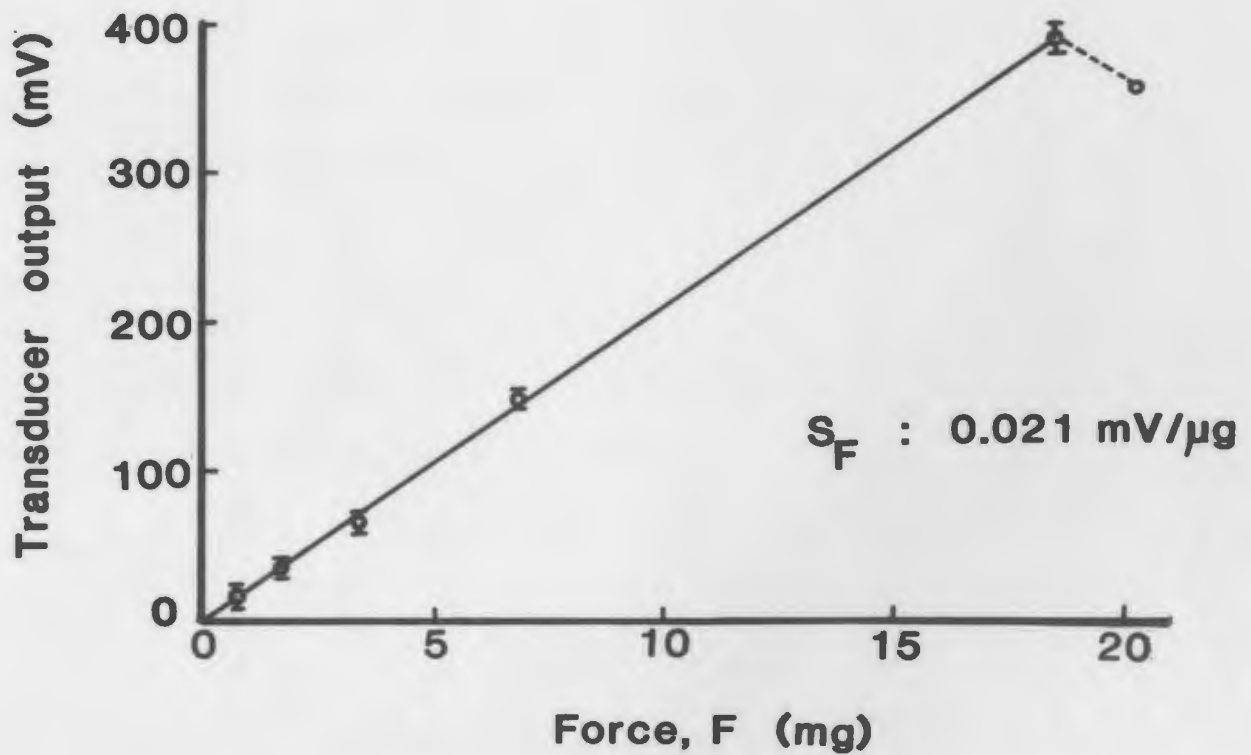


(a)



All dimensions in mms.

(b)



that the beam was horizontal with no load attached. A thin vertical beam was used to apply the force against the composite beam of the transducer.

A glass microsphere was attached to the glass micropipette end of the transducer as a reference marker, so that the force was applied against that point every time. Based on the principle of simple momentum (Fig. A8 b), when a force F_1 is applied at the horizontal end of the calibrator, a related force F_2 , which is $F_1 \times 1/3$, is applied to the tip of the transducer.

The force sensitivity (S_F) of the transducer was calibrated up to 18.0 mg, the transducer output was linear with the applied force (Fig. A9). Above 18 mg, the transducer PLL was driven out of lock and the output fell (as indicated by the dotted line). The force sensitivity, computed in the linear range of the curve, was 0.021 mV/ μ g.

3. Compliance: The compliance of the transducer [$(0.021 \text{ mV}/\mu\text{g}) / (30 \text{ mV}/\mu\text{m}) = 0.0007 \mu\text{m}/\mu\text{g}$] was measured indirectly by taking the ratio of S_F to S_d .

4. Dynamic calibration; frequency response: A special calibrator was devised (Fig. A10) to study the dynamic characteristics of the transducer system. The loudspeaker diaphragm displacement was proportional to the amplitude and frequency of its input signal. A thin lightweight rod was attached to the diaphragm of the speaker. A wedge-shaped film, with a clear wedge area surrounded by black area (as shown in the insert of Fig. A10), was attached to the push rod. When the rod was stationary the black area of the film was in the light path between a fixed light source and a photo detector. During displacement as the rod moves, the wedge portion enters the path, allowing light to pass through and change the resistance of the photocell.

The photo detector output had a linear relationship with the amplitude of the input signal driving the loudspeaker.

The frequency response of the transducer was evaluated by varying the frequency of the signal input to the test system and measuring the transducer output. The transducer response was flat up to about 35 Hz, and had a natural resonant frequency at 120 Hz (Fig. A11).

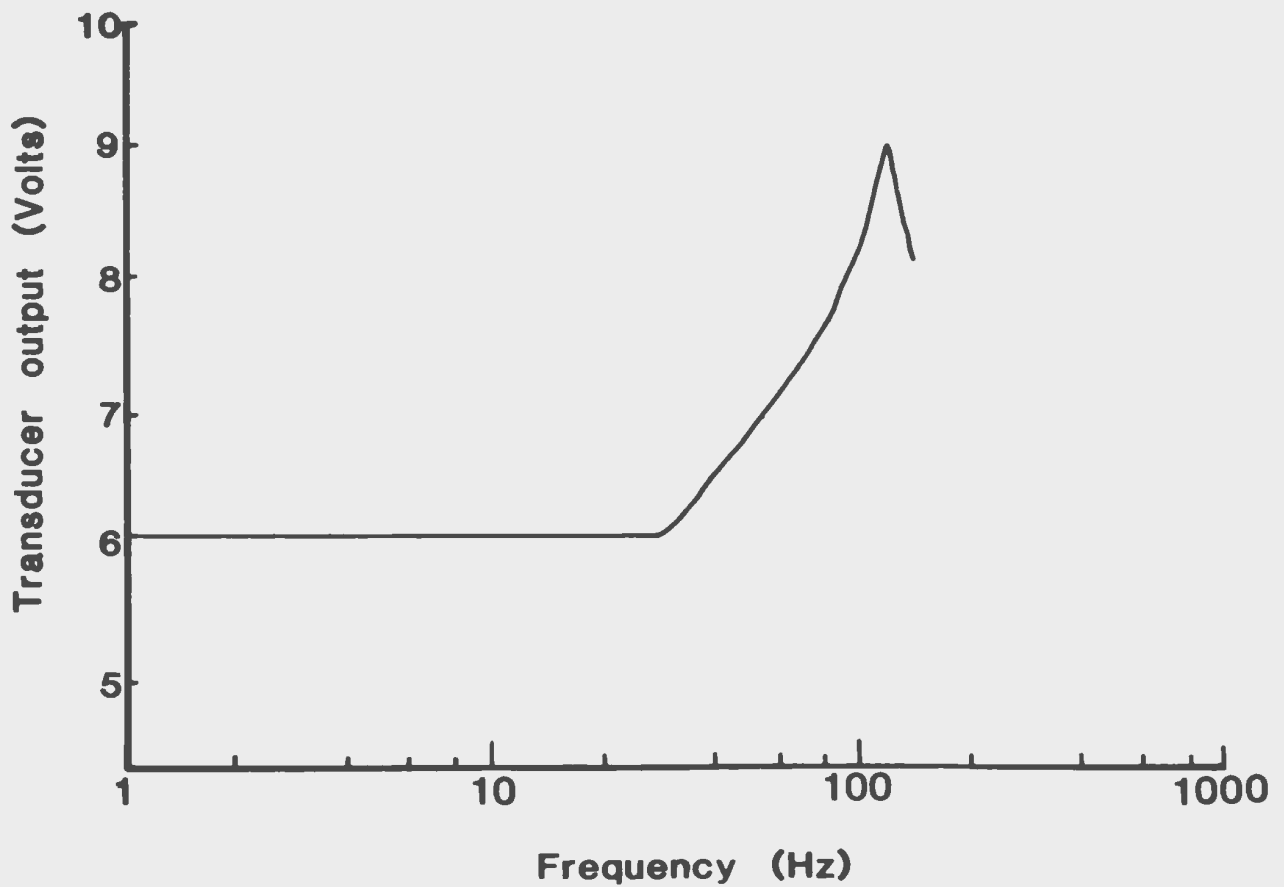
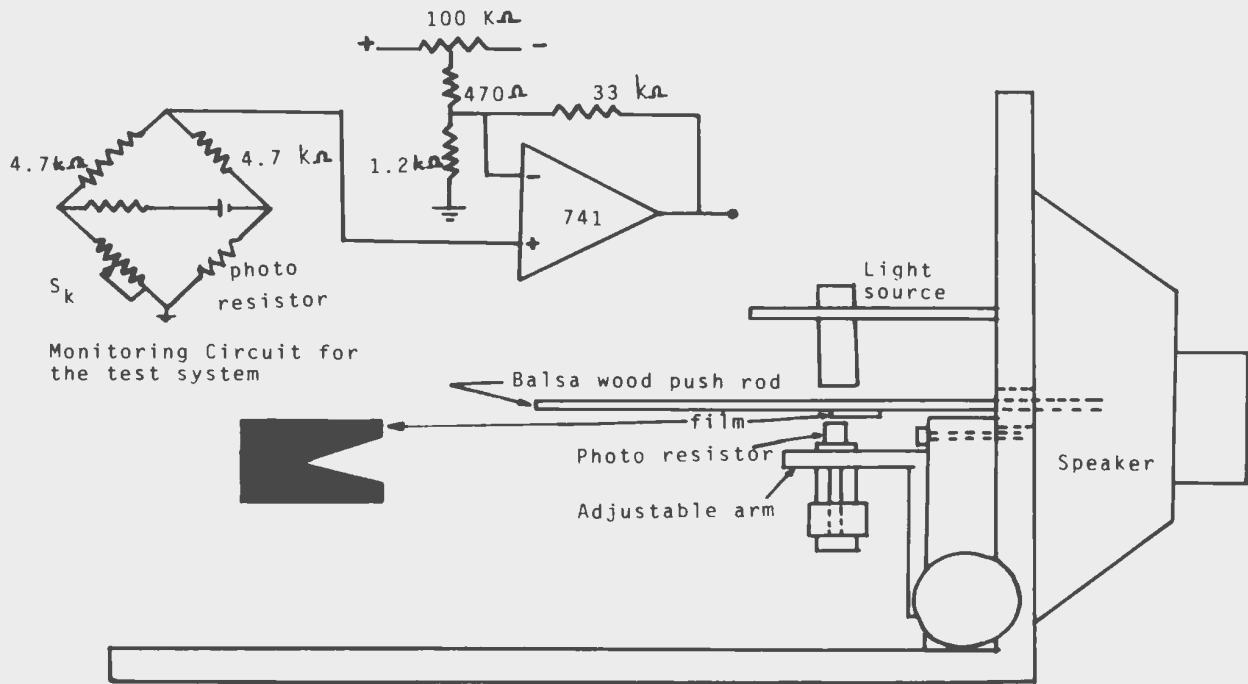
Fig. A10. Specialised calibrator used in the study of dynamic characteristics of the force transducer.

(Figure, redrawn from the report of Jacobs, 1979).

Fig. A11. Frequency response of the force transducer.

Frequency (in Hz) along the abscissa versus the transducer output (in Volts) along the ordinate is plotted.

(Figure, redrawn from the report of Jacobs, 1979).



To summarize the characteristics of the transducer, the specifications are:

Force sensitivity	:	0.021	mV/ μ g
Displacement sensitivity	:	30.00	mV/ μ m
Compliance at the tip	:	0.0007	μ m/ μ g
Resonant frequency	:	120	Hz.
damping ratio	:	0.085	

Acknowledgements: This transducer was developed by Dr. M.O Toll with the technical assistance of Mr. L. Kryski. Transducer modification and static calibrations were done by the author and Mr. M. Sullivan. The dynamic characteristics of the transducer were obtained by Mr. W. Jacobs.

References:

- Kryski, L. January 1977. Work term report entitled "Construction of a Micro Force Transducer", submitted to Dr. M.O. Toll, Faculty of Engineering and Applied Sciences, Memorial University of Newfoundland.
- Kryski, L. September 1977. Work term report entitled "Refinement of a Micro Force Transducer", submitted to Dr. M.O. Toll, Faculty of Engineering and Applied Sciences, Memorial University of Newfoundland.
- Jacobs, W.K. May 1979. Report entitled "Characterization of the Micro Force Transducer", submitted to Dr. M.O. Toll, Faculty of Engineering and Applied Sciences, Memorial University of Newfoundland.

Appendix - III

CONSTANT CURRENT STIMULATOR

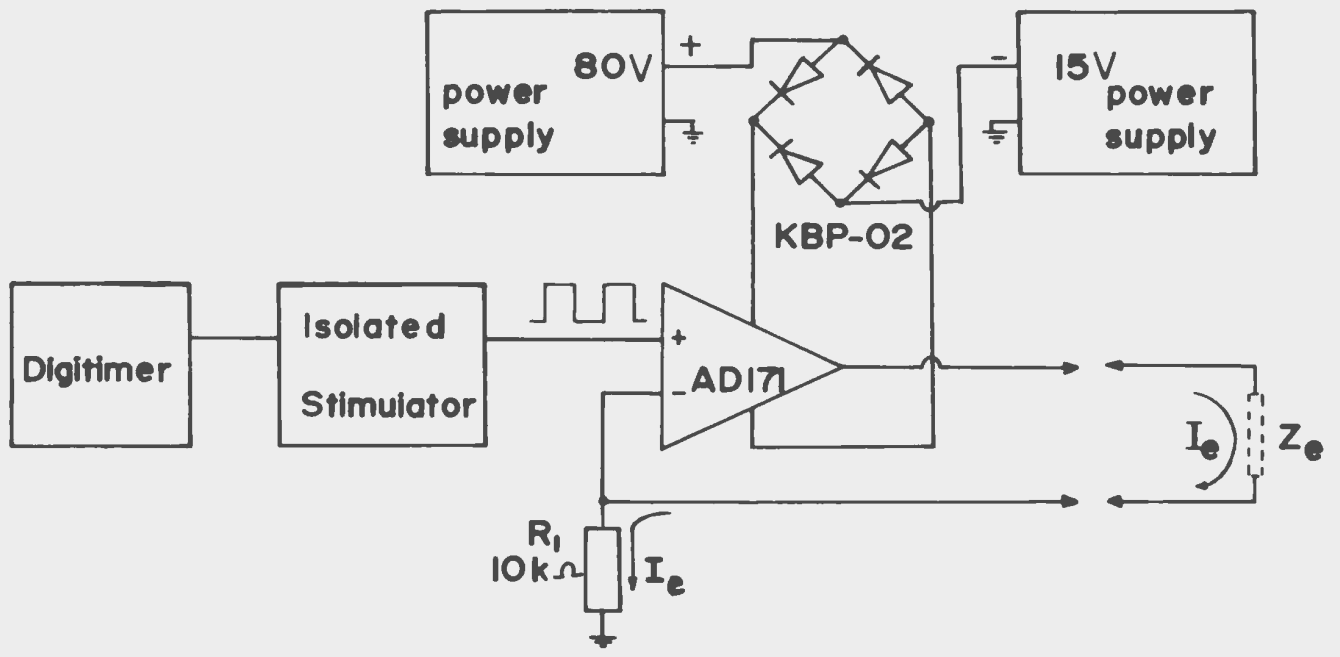
The constant current stimulator was a circuit that converted a voltage into a current. A voltage pulse was fed into the circuit from the isolated stimulator (Digitimer Limited, type 2533) as shown in Fig. A12. This circuit adjusted the output voltage to the electrodes so that the current passing between them was constant and proportional to the input voltage. In the cultured strand study, this ratio was 100 μ A per Volt but its value can be changed by changing the single resistor R_1 .

In the figure Z_e represents the impedance of the stimulating electrodes (Ag/AgCl active electrode and platinum return electrode) and the solution in the bath.

Fig. A12. Constant-current stimulator circuit arrangement.

The output of the isolated stimulator, driven by the Digitimer, was fed into the constant-current stimulator circuit shown in this figure.

The current output of this circuit was adjustable by varying the value of R_1 .



Appendix - IV

BACK-OFF AMPLIFIER AND DIFFERENTIATOR CIRCUITS

While measuring the force generated by the strands, it would be convenient if the force sensitivity were $1 \text{ mV}/\mu\text{g}$. Hence a custom configured amplifier was developed to produce a d.c. offset to remove the reference d.c. output of the transducer and with a low pass filter to eliminate unnecessary high frequency components in the signal. The actual circuit employed is shown in Fig. A13.

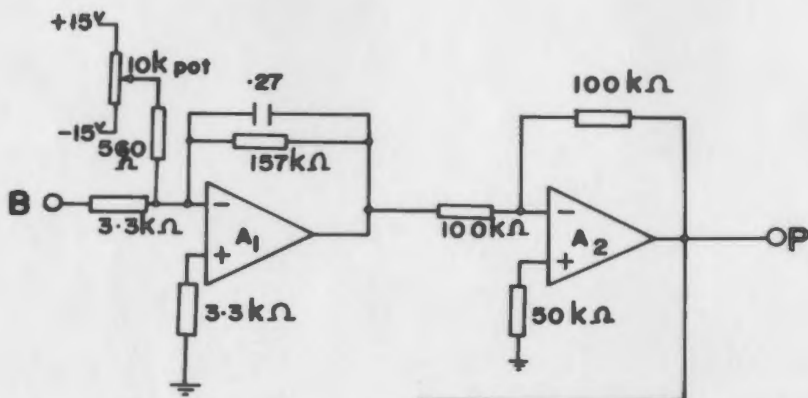
The output of the transducer is applied to this circuit at port B, through a resistor to the negative input of the operational amplifier A_1 . A d.c. signal is also fed to the same input of amplifier A_1 through a voltage-divider network. When the transducer is static, the $10 \text{ k}\Omega$ potentiometer was adjusted to provide a back-off signal such that the output of A_1 was zero and thus to eliminate the reference d.c. signal produced by the transducer. The output of A_1 with a low pass filter was passed through a unity gain inverter A_2 to remove the 180° phase shift introduced by A_1 . The output of A_2 , designated as P, was a measure of force equivalent to $1 \text{ mV}/\mu\text{g}$.

Fig. A13. Electrical circuit arrangement of the back-off amplifier and differentiator.

In this circuit, four operational amplifiers ($A_1 - A_4$) are used. Their functions are:

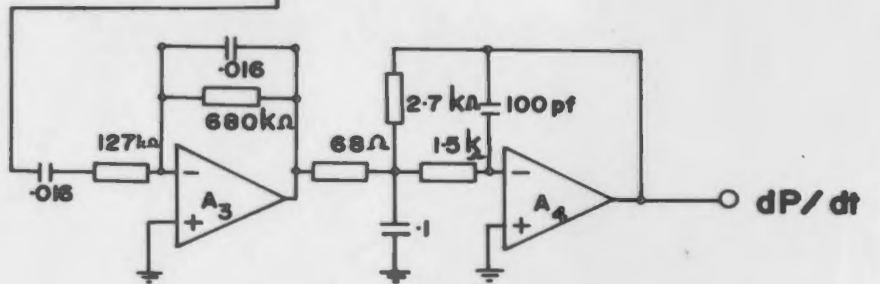
- A_1 : Back-off amplifier with an amplification factor of 47.8
- A_2 : Unity gain inverter.
- A_3 : Differentiator.
- A_4 : Low-pass filter.

The input to this circuit (B) is the transducer output from the PLL (refer Fig. A6 a).



All capacitors in μF ,
unless specified

$A_1 - A_4$: $\mu\text{A} 741\text{C}$



The output P was also connected to a differentiator (A_3) and a low pass filter (A_4) to monitor the rate of change of force, dP/dt . The polarity of the differentiated signal is correct, since it has been passed through two amplifiers (A_3 and A_4).

The differentiator was calibrated using a 1 Volt amplitude triangular-wave applied to the input of A_3 . The output measured at A_4 was a rectangular-waveform with + 1 Volt amplitude during the positive-going phase of the triangular-wave input and a - 1 Volt amplitude during the negative-going phase. The components shown in the differentiator circuit of Fig. A13 represent the values chosen during calibration. The input and output were recorded on the chart recorder. After calibration, the chart recorder's gain- and position-sensitivity controls were not altered.

Appendix - V

SOLUTION EXCHANGE CHARACTERISTICS OF THE PERFUSION SYSTEM

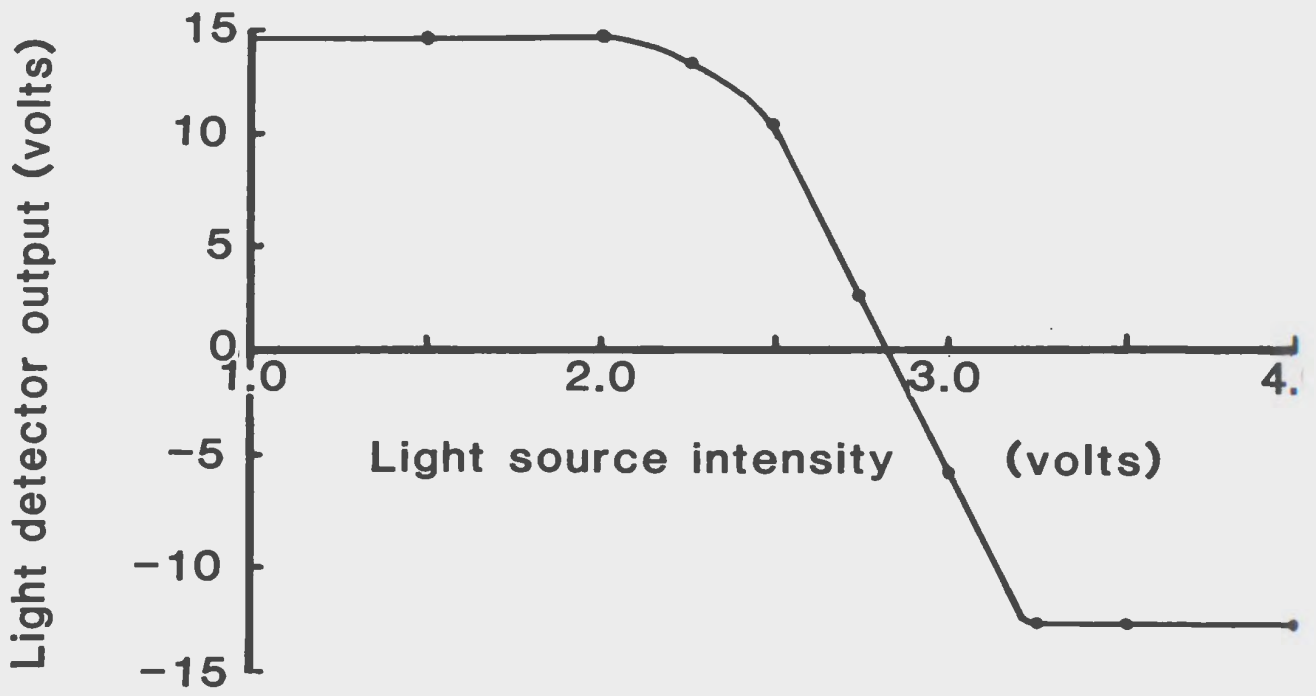
The perfusion arrangement consisted of a pump with a delta head which carried the input tube. By varying the speed of the pump the flow rate was altered. The optimum flow rate was 2.56 ml min^{-1} . The input and output ports were placed at the surface of the chamber fluid such that the level of the medium in the chamber remained constant (refer Sec. 2.10).

The microscope light from the bottom of the chamber passed through the chamber medium and impinged upon a photocell light detector. Detector output was a measure of the depth of solution in the chamber. To study the depth of a dye solution at different locations, the detector was positioned at five different points above the chamber and the flow characteristics were recorded for mixing of dye solution.

The photocell itself has nonlinear characteristics. The linear region of the detector was first identified in the absence of any media in the chamber. The detector output was linear in the region of 2.50-3.25 V of the input light signal (Fig. A14). The intensity of the light source was set at 2.75 V and was not disturbed until the calibration was completed.

Fig. A14. Characteristics of the photocell used in this study.

An index of light source intensity (in Volts) is represented in the abscissa. The amplified output of the photocell (in Volts) is plotted along the ordinate. The linear region of the photocell response is obtained from this graph.



For different depths of water and a dye solution of thionin acetate (at a concentration of 3 cc of dye in 1 liter of distilled water), which is blue in colour, the output of the photocell was recorded. The depth of the chamber was 8 mm. The relations are as shown in Fig. A15.

From these two curves a composite relationship for different depths of dye solution with the remaining filled by water can be computed as shown in Fig. A16. From this curve, knowing the photocell output, the depth of dye in the chamber can be computed.

The light detector was set up at 5 different locations (as shown in the insert of Fig. A17) and for each location the perfusion experiment was carried out until the output reached a steady-state (Figures A17 and A18). As seen from these measurements, the time to reach equilibrium is shorter at location 1, followed by 2 and 3, and is largest at 4 and 5. The depth of dye solution is marked on the right hand side.

The flow was laminar. Hence, because of the location of inlet and outlet ports at the surface, the concentration gradient extended downward from the surface. From Figures A17 and A18, the depth of dye solution at different times along and transverse to the flow axis can be computed. For analysis only Fig. A17 is chosen, however this analysis also holds for Fig. A18.

Fig. A15. The output of the photocell when the chamber was filled with different depths of water and the dye solution.

Fluid depths (in mm) of the chamber along the abscissa is plotted versus the normalized value for light absorption (along the ordinate). 100% light absorption corresponds to the photocell response when the chamber was completely filled with the dye solution.

Fig. A16. Light absorption in the chamber for constant fluid depth (8 mm) with varying ratios of dye and water. This relation was computed using the data shown in Fig. A15.

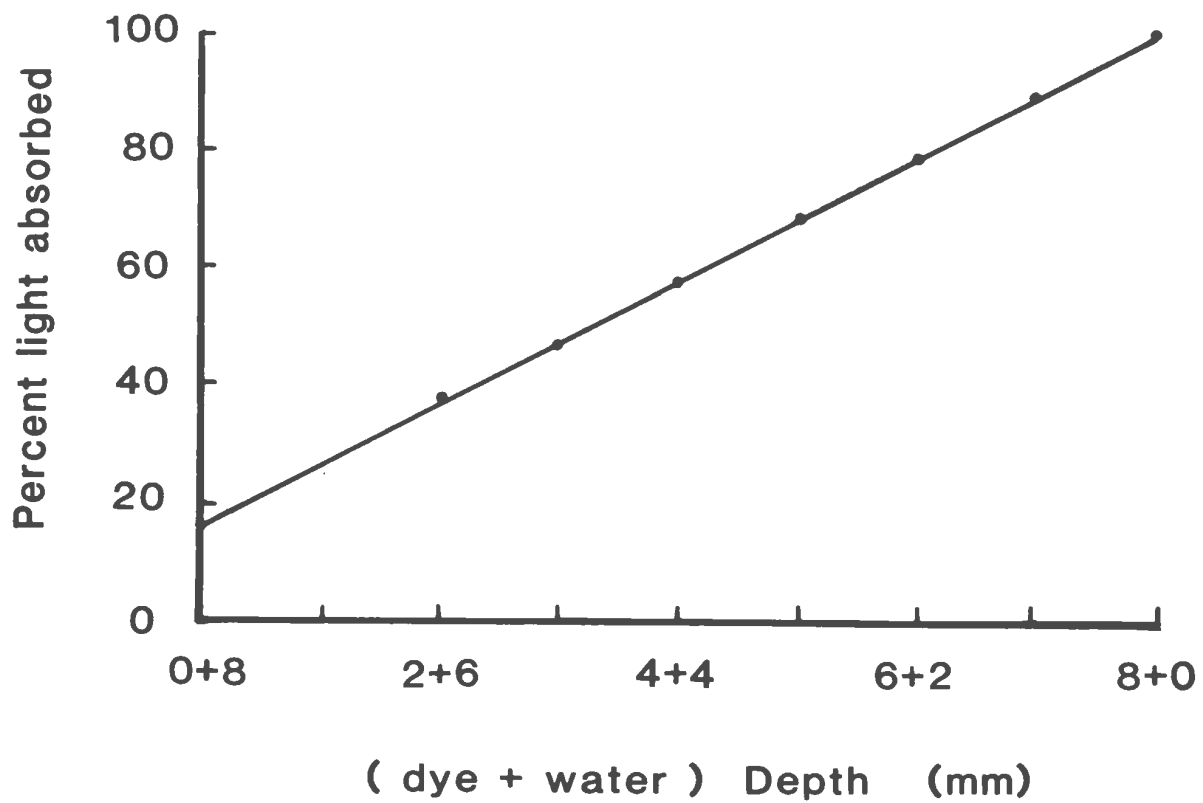
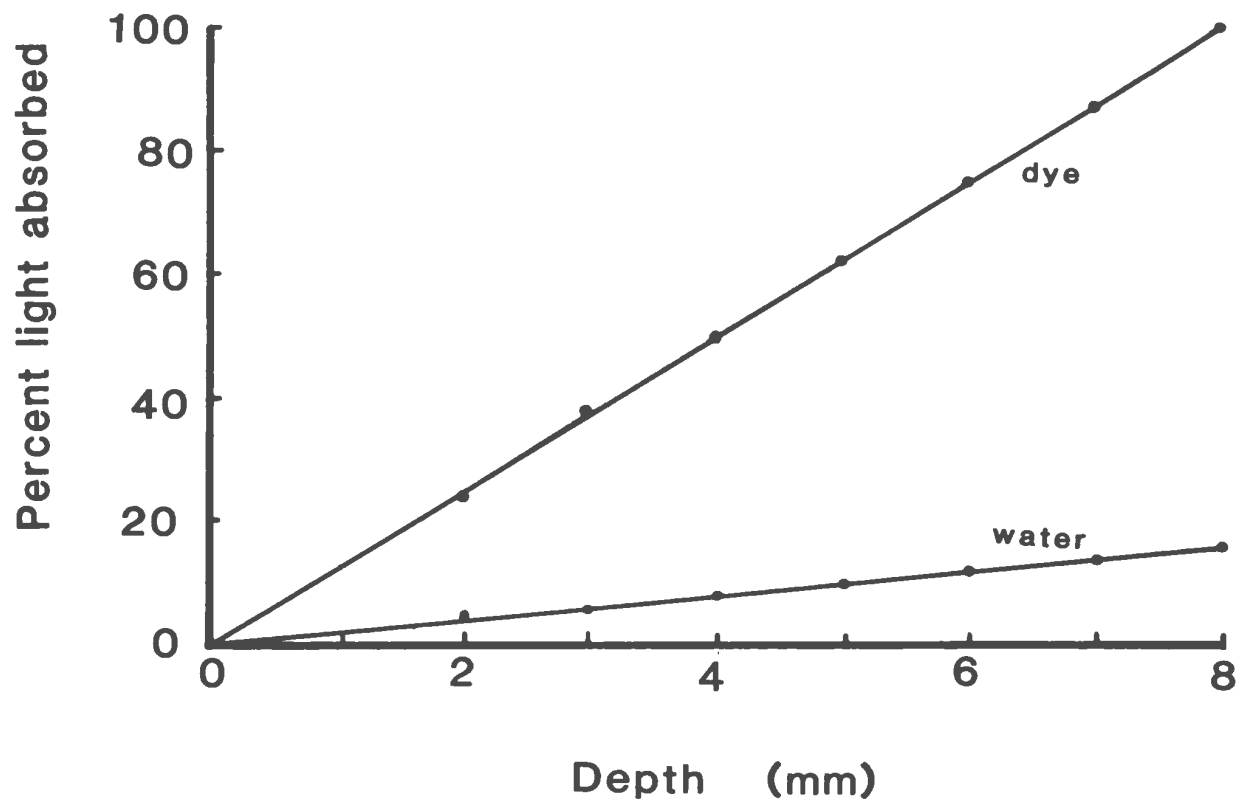


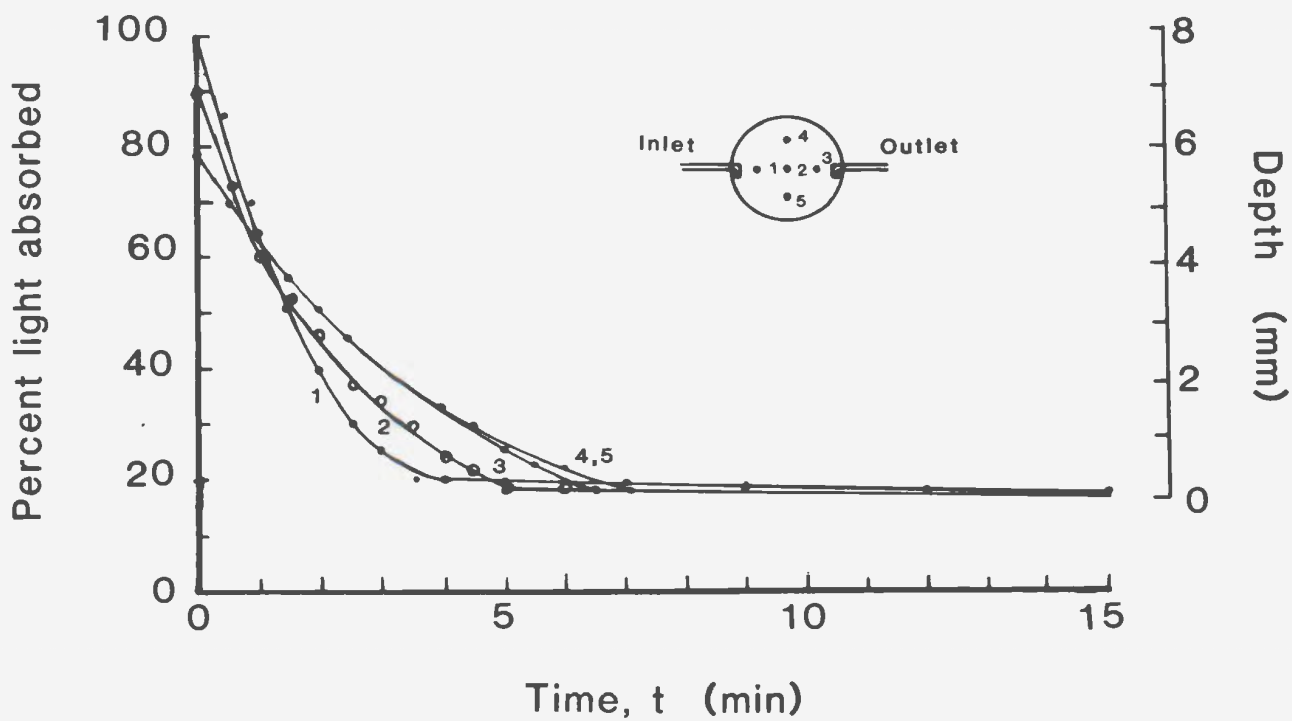
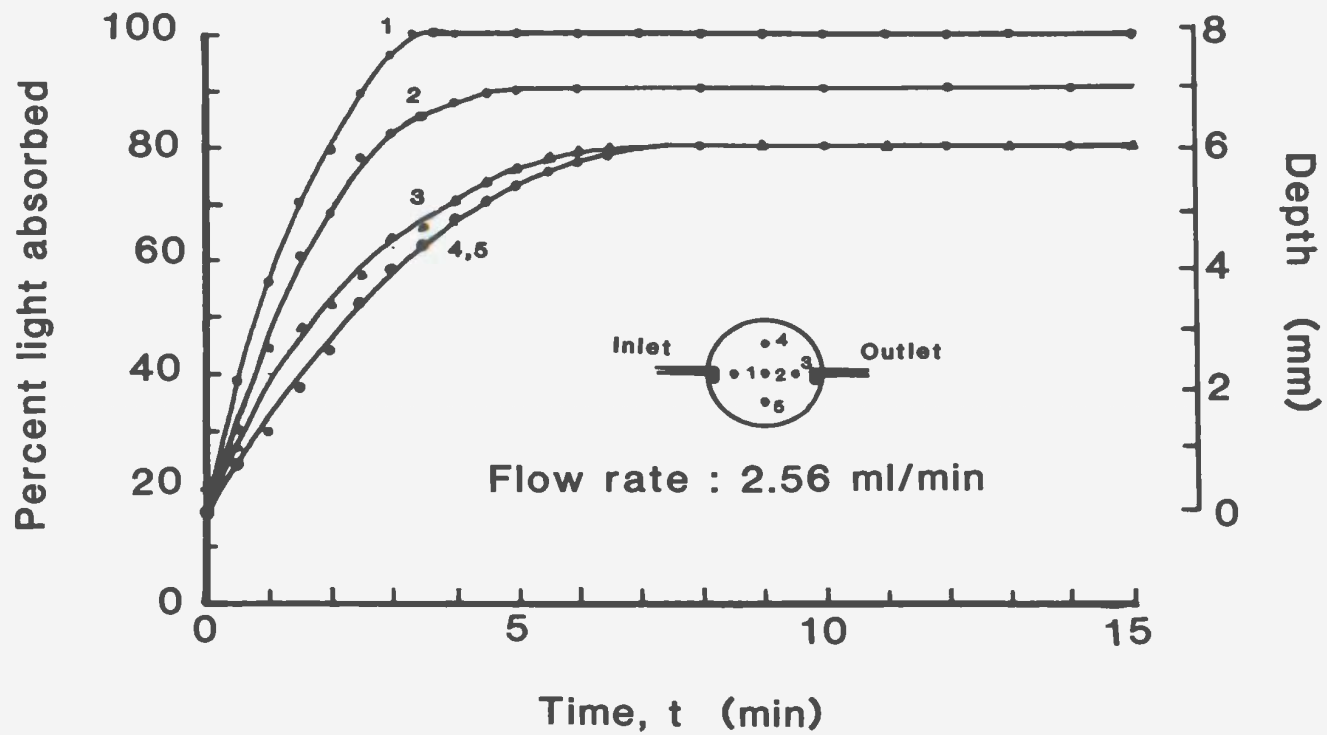
Fig. A17. Equilibration characteristics of the chamber during dye perfusion.

Light absorption was measured at 5 different locations which are indicated in the inset of this figure.

Time (in min) is represented along the abscissa and normalized light absorption along the ordinate (legend on the left-hand side). The corresponding depth of dye with respect to the top surface of the chamber is also indicated along the ordinate (right-hand side legend). Laminar flow characteristics were assumed.

Fig. A18. Chamber washout characteristics of an equilibrated dye solution by perfusion with water.

Light absorption was measured at 5 different locations which are indicated in the inset of this figure.



The depth of the dye along the flow axis at different times is as marked by labels in Fig. A19. The top 1 mm of the chamber volume was replaced with the new solution within 0.5 min and by 1.0 min the top 2 mm had exchanged with the new solution. As illustrated in Fig. A20, measurements along the transverse axis, showed that dye solution occupied the top 1 mm within 0.5 minute. In other words the central region of the top 1 mm of the chamber is mixed within 0.5 min and the top 2 mm within 2 minutes.

From these limited data points, the depth contours could be estimated. The approximate depth contours at two different times are shown in Fig. A21. At 45 s, the area under the contour is mixed to 1.9 mm depth and at 2 min the depth reached is 3 mm. Thus a strand suspended in the top 1 mm of the chamber receives the steady-state concentration of a new solution within 45 seconds.

A rough analysis of the chamber-perfusion system was attempted using these data in a Fourier analyser. If the input and output functions of a system are known, its transfer function and impulse response can be computed using Fourier analysis. In the first 45 s, top 1 mm of the chamber fluid volume was mixed with a new perfusion fluid (refer Fig. A17 and A18). The dye concentration appeared to increase in an approximately linear relationship with time. For the purposes of this analysis, a 'ramp' function

Fig. A19. Depth of dye solution along the flow-axis, at different times.

The inset represents the detector positions.

Fig. A20. Depth of dye solution along the transverse-axis, at different times.

Both Figures A19 and A20 were computed from Fig. A17.

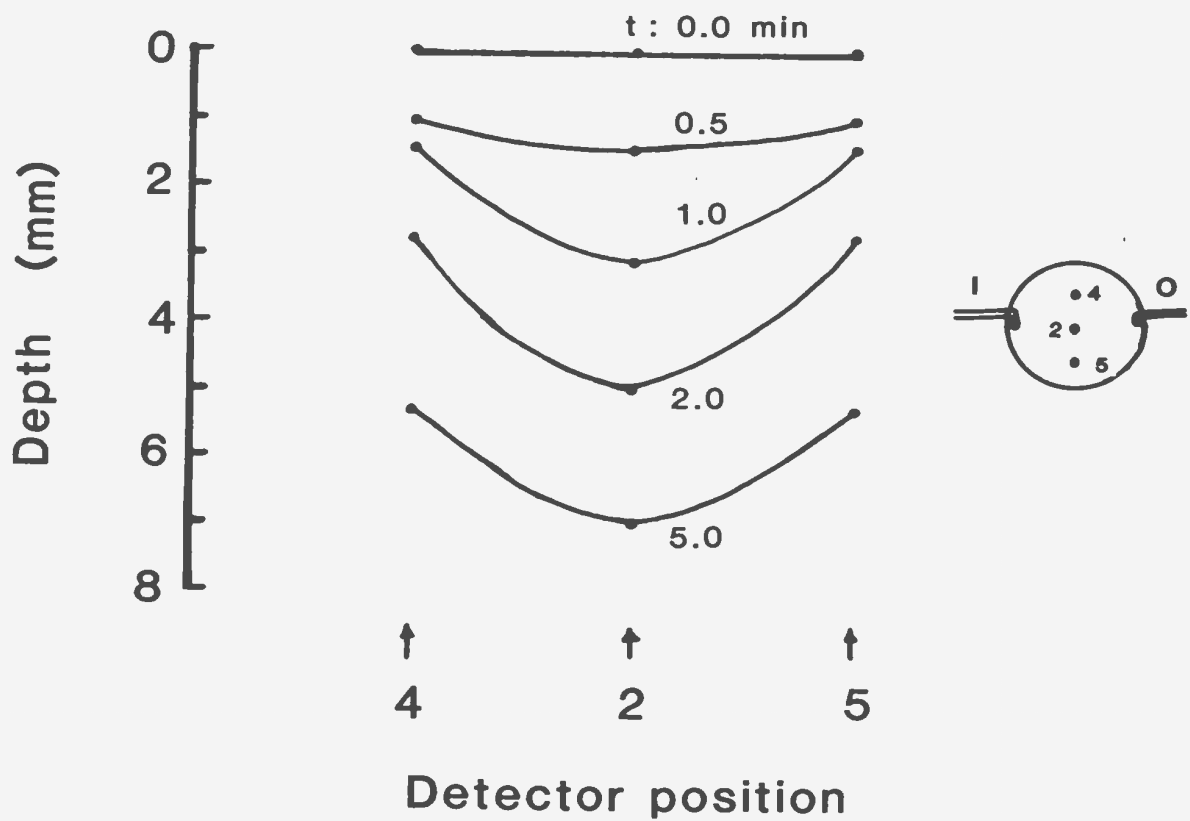
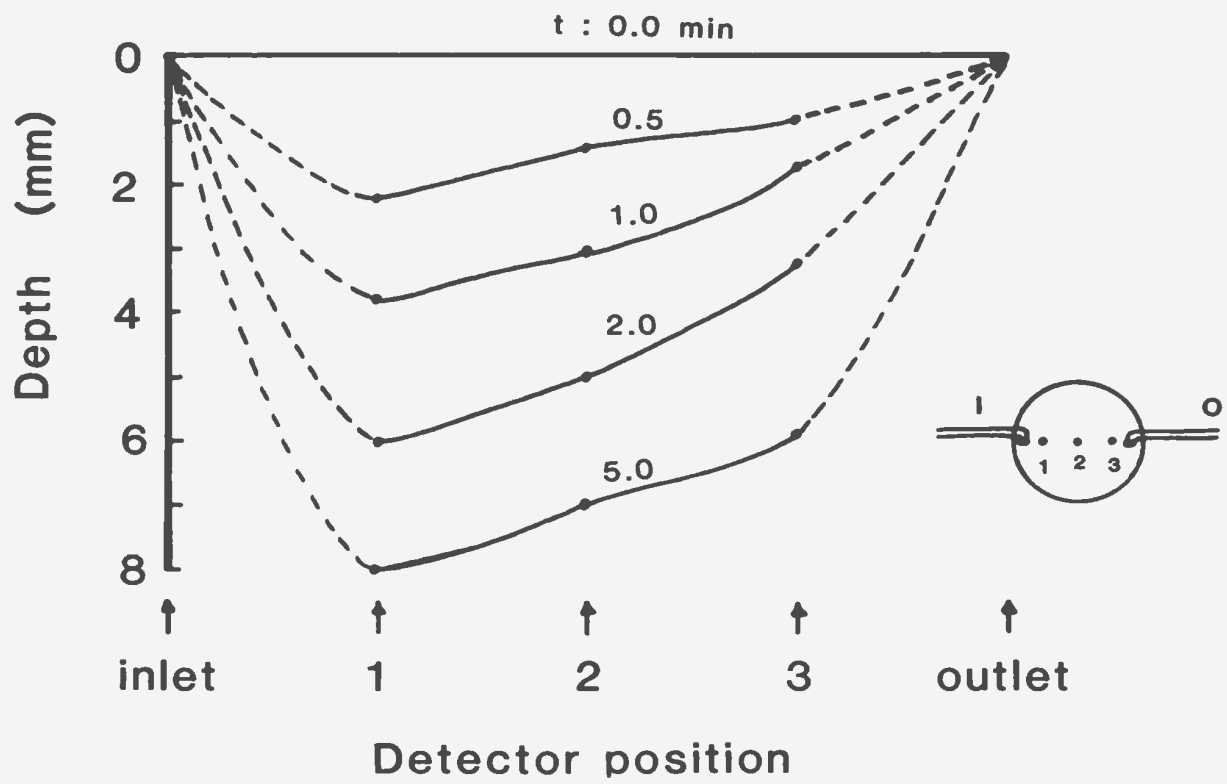
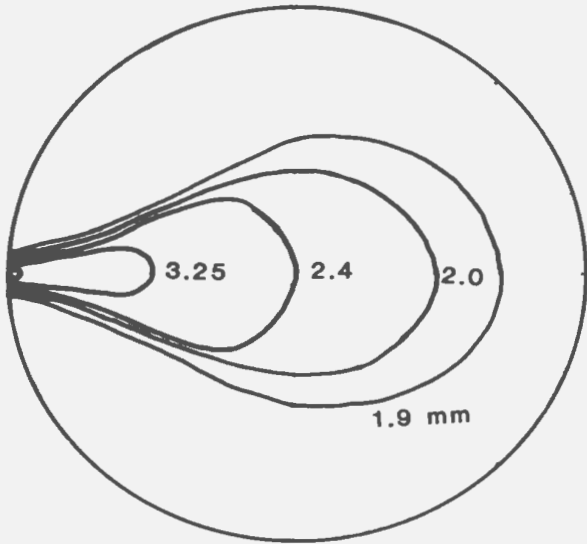


Fig. A21. Depth contours of dye concentrations at two different times after initiation of perfusion.

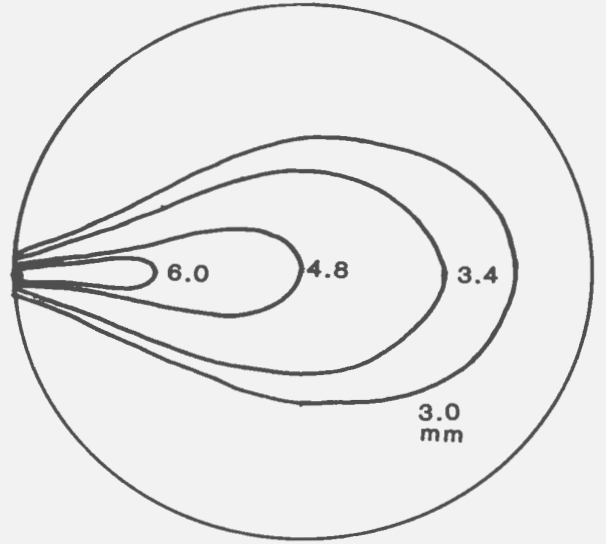
The area enclosed in each contour has mixed with the dye solution to the depth indicated in mm by 45 s and 2.0 min respectively. Depths are referenced to the top surface of the chamber.

t:45 sec.



↑
Inlet

t: 120 sec.



↑
Outlet

↑
Inlet

↑
Outlet

was assumed. For a step change as the input function and the chamber fluid mixing (ramp function) as the output, the transfer function of the chamber alone was obtained. Next, using chamber mixing as the input and the tension response of the strand to a step change in calcium concentration as the output, the transfer function of the strand was computed. This analysis showed that the impulse response of the strand was instantaneous while a considerable delay existed in the chamber-perfusion system.

Thus it was concluded that this perfusion arrangement was suitable for steady-state measurements only and that dynamic analysis was not possible. When suspended in the central portion of the chamber within the top 1 mm, the strand received the new concentration within 45 seconds. To assure that a true steady-state response was attained the perfusion was maintained for at least 4 times the mixing time for top 1 mm of the chamber (3.0 minutes).





